NASA/TP–2005-213150

Arc Jet Screening Tests Of Phase 1 Orbiter Tile Repair Materials and Uncoated RSI High Temperature Emittance Measurements

Engineering Directorate
Structural Engineering Division

June 2005

THE NASA STI PROGRAM OFFICE … IN PROFILE

Since its founding, NASA has been dedicated to the advancement of aeronautics and space science. The NASA Scientific and Technical Information (STI) Program Office plays a key part in helping NASA maintain this important role.

The NASA STI Program Office is operated by Langley Research Center, the lead center for NASA's scientific and technical information. The NASA STI Program Office provides access to the NASA STI Database, the largest collection of aeronautical and space science in the world. The Program Office is also NASA's institutional mechanism for disseminating the results of its research and development activities. These results are published by NASA in the NASA STI Report Series, which includes the following report types:

- TECHNICAL PUBLICATION. Reports containing completed research or major significant phases of research. Also presents the results of NASA programs (including extensive data or theoretical analysis). Includes compilations of significant scientific and technical data and information deemed to be of continuing reference value. This is the NASA equivalent of peer-reviewed, formal, professional papers, but has less stringent limitations on manuscript length and extent of graphic presentations.

- TECHNICAL MEMORANDUM. Scientific and technical findings that are preliminary or of specialized interest. For example, quick release reports, working papers, and bibliographies that contain minimal annotation. Does not contain extensive analysis.

- CONTRACTOR REPORT. Scientific and technical findings by NASA-sponsored contractors and grantees.

- CONFERENCE PUBLICATION. Collected papers from scientific and technical conferences, symposia, seminars, or other meetings sponsored or cosponsored by NASA.

- SPECIAL PUBLICATION. Scientific, technical, or historical information from NASA programs, projects, and missions, often concerned with subjects having substantial public interest.

- TECHNICAL TRANSLATION. English-language translations of foreign scientific and technical material pertinent to NASA's mission.

Specialized services that complement the STI Program Office's diverse offerings include creating custom thesauri, building customized databases, organizing and publishing research results, and even providing videos.

For more information about the NASA STI Program Office, see the following:

Access the NASA STI Program Home Page at **http://www.sti.nasa.gov**.

E-mail your question via the Internet to help@sti.nasa.gov.

Fax your question to the NASA STI Help Desk at (301) 621-0134.

Telephone the NASA STI Help Desk at (301) 621-0390.

Write to:

NASA Access Help Desk
NASA Center for AeroSpace Information
7121 Standard Drive
Hanover, MD 21076-1320

NASA/TP–2005-213150

Arc Jet Screening Tests Of Phase 1 Orbiter Tile Repair Materials and Uncoated RSI High Temperature Emittance Measurements

Engineering Directorate
Structural Engineering Division

June 2005

Available from:

NASA Center for AeroSpace Information
7121 Standard Drive
Hanover, MD 21076-1320

National Technical Information Service
5285 Port Royal Road
Springfield, VA 22161

This report is also available in electronic form at http://ston.jsc.nasa.gov/collections/TRS

TABLE OF CONTENTS

TABLES

NUMBER **PAGE**

FIGURES

NUMBER **PAGE**

1.0 SUMMARY

Arc jet tests of candidate tile repair materials and baseline Orbiter uncoated reusable surface insulation (RSI) were performed in the Johnson Space Center's (JSC) Atmospheric Reentry Materials and Structures Evaluation Facility (ARMSEF) from June 23, 2003, through August 19, 2003. These tests were performed to screen candidate tile repair materials by verifying the high temperature performance and determining the thermal stability. In addition, tests to determine the surface emissivity at high temperatures and the geometric shrinkage of bare RSI were performed. In addition, tests were performed to determine the surface emissivity at high temperatures and the geometric shrinkage of uncoated RSI.

The tile repair specimens consisted of two types of silicone ablators; pre-cure (MB0130-199 Type 1) and cure-in-place (MA-25S) (MB0130-199 Type 2). A total of two (2) pre-cure specimens from Boeing and five (5) and two (2) cure-in-place specimens from Boeing and Lockheed Martin respectively were tested at nominal surface temperature conditions of 1800°F, 2000°F, 2300°F and 2700°F surface temperatures on reaction cured glass (RCG) coated RSI. These specimens were tested in a stagnation "puck" configuration where the plasma flow impacts the model face perpendicularly. Qualitative evaluation of the materials was made based on geometric stability, erosion rate, and backface temperature through video coverage and thermocouple data.

The uncoated RSI specimens consisting of LI-900, densified LI-900, LI-2200, FRCI-12 were subjected to conditions that produced 1600°F, 1700°F, 1800°F, 2000°F, and 2300°F surface temperatures on RCG coated RSI. Later during the test program MA-25S and LI-900 with a silicon carbide emittance wash was added to the test matrix. At each condition a scanning spectroradiometer was used that measures the spectral intensities at 423 discrete wavelengths between 0.6μm and 8μm. From this data it is possible to determine the directional emittance of the specimen at the elevated temperature. For some of the specimens (LI-900 in particular) it was not possible to determine conclusively what the surface temperature is from the spectral data, which is the critical variable for emissivity calculation. Although there is considerable scatter in the data acquired from this technique, the primary test objectives for this phase of the test program were satisfied. Emittance data at high temperatures was obtained which will be a critical input for all future thermal assessments of damaged TPS tiles and for the development of thermal math models.

2.0 INTRODUCTION

Prior to the first Shuttle flight, efforts were undertaken to understand the damage sensitivity of TPS tile materials and methods/materials to perform on-orbit repair if needed. The ablator repair approach that evolved from this effort was not carried through to completion and the activity was terminated. The loss of STS-107 on February 1, 2003, demonstrated a serious need for an on-orbit repair capability for thermal protection system (TPS) materials. This has lead to intensive efforts to fully understand the damage sensitivity of the TPS tile materials and develop a tile repair kit prior to return to flight (STS-114). Along with a repair concept an accurate thermal analysis tool is needed in order to determine if a repair is required. The level of conservatism employed should be well understood since it could lead to an unnecessary extravehicular activity (EVA) that

places an astronaut at risk and consumes time and resources. Thus, accurate material properties are required with the optical properties of uncoated (i.e., damaged) reusable surface insulation (RSI) tile being one of them.

3.0 TEST OBJECTIVES

The objectives of this test program are to:

- Evaluate the high temperature thermal performance of candidate TPS tile repair materials.
- Evaluate the thermal stability characteristics of TPS tile repair materials.
- Determine the surface emissivity of the baseline Orbiter uncoated RSI materials at elevated temperatures.
- Obtain high temperature shrinkage data for uncoated RSI materials.

4.0 TEST SPECIMENS

All test articles received are assigned a facility model ID number (Table 1). This number is used for tracking purposes and documentation and will be the model reference used for the remainder of this test report. All of the tile repair specimens had bondline thermocouples with a subset having instrumented plugs (Figure 1). The bare tile specimens were not instrumented.

Model #1835 was tested in two configurations. First, the densified side was tested and scanned. Then the undensified side was treated with an emittance wash and the model was re-identified as #1835A. The emittance wash is an on-orbit repair concept which would be used if the tile coating is damaged significantly and/or a limited volume of the uncoated substrate material would be exposed to the flow. This concept consists of silicon carbide powder suspended in diffusion pump oil which could be easily applied to the damage site. The oil would vaporize over time under vacuum leaving only the silicon carbide which would increase the emittance. For the arc jet specimen the emittance wash was brushed onto the bare tile surface and the oil was then baked out in an oven at 2250°F.

Supplier	Instrumentation	Substrate	Model ID
Boeing	Bondline	MB0130-199 Type 1 Cure-in-place	1805
			1806
		MB0130-199 Type 2 Pre-cure	1807
			1808
	Plug and Bondline	MB0130-199 Type 1 Cure-in-place	1809
			1810
			1811
		MB0130-199 Type 1 Cure-in-place (Long duration vacuum degas – vacuum cure)	1817
		MB0130-199 Type 1 Cure-in-place (Long duration vacuum degas – air cure)	1818
		MB0130-199 Type 2 Pre-cure	1812
			1813
			1814
Lockheed Martin	Bondline	MB0130-199 Type 1 Cure-in-place	1815
			1816
			1821
JSC	None	Uncoated LI-900	1833
			1834
			1835
			1836
			1837
		Uncoated FRCI-12	1828
			1829
			1830
			1831
			1832
		Uncoated LI-2200	1838
			1839
			1840
			1841
			1842

Table 1: Specimen and Model ID Matrix

5.0 TEST FACILITY

This test program was performed in Test Position #2 (TP2) of the ARMSEF. The test gasses (23% O_2 and 77% N_2 by mass) were heated by a segmented constricted arc heater that is powered by a 10MW power supply regulated by four silicon rectifiers (SCRs). The heater configuration utilized during this test program is shown in Appendix A. The

heated gas was accelerated through a convergent/divergent water-cooled nozzle with a 2.25-inch diameter throat and a 5 or 15-inch nozzle exit into the test chamber. The test chamber was evacuated by a four stage steam ejector system supplied by a boiler operating at 80,000 lb/hr that kept the static pressure below 300 microns. The test specimens were mounted on remotely actuated sting arms. These arms positioned the test articles at distances from 15 to 20 inches from the nozzle exit plane (z-distance) depending on the desired conditions.

6.0 TEST PROCEDURES

All test specimens were photographed, front, back, and oblique, before and after the test program with the trackable NASA photo ID summarized in Table 7 and Table 8 in Appendix C. The specimens were handled with clean nitrile gloves at all times. The models were stored in an isolated area of the model preparation area and maintained under the supervised control of the NASA Test Program Manager and quality assurance personnel.

Test management and control were implemented by formal documentation (e.g., Standard Operating Procedures (SOP), Test Preparation Sheets (TPS) Discrepancy Reports (DR), and Anomaly Logs). A Test Readiness Review was held prior to test and the NASA/Contractor test team maintained proper control during the entire test program. Quality assurance representatives witnessed required specimen preparations, monitored test system configurations, and participated as test observers.

After each run the tile repair specimens were left under vacuum for at least 20 minutes to allow the temperature to drop below 500°F to prevent oxidation.

7.0 TEST MATRIX AND CALIBRATION

The test matrix for this program is summarized in Table 4. The test conditions summarized in Table 2 were established by an RCG coated RSI calibration model that had a thermocouple embedded underneath the coating. Adjustments to the power (i.e., current) and mass flow were required at some test conditions to maintain the desired surface temperature conditions established during the calibration runs. This can be attributed to instability in the arc when operating at low current conditions and/or minor degradation of the coating in the calibration models due to repeated test cycling.

RCG Surface Temperature (F)	Calibrated Condition		Actual Run Condition	
	Current (amps)	Mass Flow (lb/sec)	Current (amps)	Mass Flow (lb/sec)
1800	140	0.08	180	0.08
2000	200	0.15	220	0.13
2300	330	0.20	330	0.20
2700	620	0.30	620	0.30

Table 2: Test Conditions with a 5in Nozzle Exit

RCG Surface Temperature (F)	Current (amps)	Mass Flow (lb/sec)
1600	230	0.10
1700	280	0.15
1800	370	0.15
2000	500	0.25

Table 3: Test Conditions with a 15in Nozzle Exit

Date	Run #	Model ID	Time (sec) at Equivalent RCG Surface Temperature (F)			
			1800	2000	2300	2700
06/24/2003	2-2530-3	1805				900
		1807				900
06/25/2003	2-2532-3	1806	60	120	120	600
		1816	60	120	120	141 (1)
06/26/2003	2-2533-3	1809	180	180	600	
		1812	180	180	431 (2)	
07/01/2003	2-2536-3	1821	180	180	600	
07/01/2003	2-2537-3	1817	180	180	600	
		1818	180	180	600	

(1) Test aborted 459 sec early due to specimen shedding a large amount of material

(2) Test aborted 169 sec early due to backface thermocouple reaching 600F

Table 4: Tile Repair Screening Test Summary

8.0 TEST RESULTS OF TILE REPAIR MATERIAL

The first test of the candidate tile repair material (pre-cure and cure-in-place) on run # 2-2530-3 demonstrated two significant results. The first was that the 2700°F condition was too severe and the material could not form a stable char layer resulting in a large amount of erosion. The second was the material swelled considerably prior to the erosion.

The second test (run # 2-2532-3) was modified to allow a char layer to form on the cure-in-place ablators by beginning at the 1800°F condition and gradually increasing the conditions through 2000°F and 2300°F before reaching 2700°F. A good char layer did form, however, the 2700°F condition was still too severe and rapid erosion occurred again. Model #1816 (Lockheed Martin cure-in-place) was terminated early when a large portion of the specimen broke off. Again, a large amount of swelling was observed during the test.

The rest of the tests (run # 2-2533-3 through 2-2537-3) began at 1800°F and stopped at 2300°F with 2000°F as an intermediate condition. The cure-in-place specimens formed a good stable char and did not erode under this profile. The pre-cure specimen (model #1812) test was terminated early because the bond-line thermocouple reached the 600°F abort limit. Later observations of this model revealed that the interior was eroded leaving only a charred shell. This result was most likely caused by the presence of the instrumented plug that allowed the hot gas to penetrate below the model surface.

Models #1809 and #1812 had in-depth thermocouples and the temperature responses during the tests are shown in Figure 2 and Figure 3, respectively. For model #1812 the failures of the thermocouples are evident as the interior of the specimen eroded.

9.0 TEST RESULTS OF UNCOATED RSI

The emissivity values from this test are compared to the data from TPSX in Figure 4 through Figure 6 for each substrate. The data in TPSX was determined by measuring the spectral emittance at room temperature and the extrapolating to higher temperatures[1]. The major assumption for this data is that there is no temperature dependence on the spectral emittances.

For determining the emissivity of uncoated RSI a scanning spectroradiometer is used that measures the spectral intensity at 423 discrete wavelengths between 0.689μm and 8.025μm. Scans (see Appendix C for all spectroradiometer scans) were made at 5 test conditions that produced 1600°F, 1700°F, 1800°F, 2000°F, and 2300°F (Table 5) surface temperatures on an RCG over TUFI specimen with a thermocouple embedded in the RCG. The 1600°F, 1700°F, and 1800°F conditions were obtained using a 15 inch nozzle exit. The 2300°F condition was obtained using a 5 inch nozzle exit. The 2000°F condition was obtained with both the 5 inch and 15 inch nozzle exits and scans were taken using both nozzles. In addition to using the RCG over TUFI model for defining the test conditions, they were also used for confirmation of the scanner alignment (Figure 15 through Figure 30). Since the emissivity of RCG is well known, a misalignment of the scanner would have manifested as a lower than expected emissivity from the scan data.

Determining the emissivity of a test specimen from the spectroradiometer data is straightforward for well-behaved materials[2]. Well-behaved in this context is defined as:

- Having a gray-body behavior (i.e., the emittance being wavelength independent).
- Having an opaque surface.
- Having a constant surface temperature across the specimen surface and throughout the duration of the scan (approximately 32 seconds.)

For well behaved materials the scan data can be curve-fit to a theoretical gray-body Planck function (EQUATION 1). The curve fit results in the surface temperature and the directional emittance of the test specimen.

$$I_{\lambda,BLACKBODY} = \frac{C_1}{\pi\lambda^5\left[\exp\left(\frac{C_2}{\lambda T}\right)-1\right]}$$

where:

$$C_1 = 3.7417\times10^8\left(\frac{W\cdot\mu m^4}{m^2}\right)$$

$$C_2 = 1.4389\times10^4\ (\mu m\cdot K)$$

λ = Wavelength (μm)

T = Temperature (K)

$$I_{\lambda,BLACKBODY} = \text{Spectral Intensity}\left(\frac{W}{m^2\cdot sr\cdot\mu m}\right)$$

EQUATION 1

RCG, MA-25S and LI-900 with an emittance wash are examples of well behaved materials. The other materials (i.e., densified LI-900, FRCI-12, and LI-2200) exhibited gray-body behavior over a much smaller subset of the total wavelength range. Determining the surface temperature and directional emittance of these materials is done in two steps. First a curve fit using EQUATION 1 is applied to the gray-body wavelength range in order to get the surface temperature. Once the temperature is known then the directional emittance is a ratio of the measured emissive power to the maximum theoretical (blackbody) emissive power at that temperature (EQUATION 2). It should be noted that spectral scan data can be noisy; however, the impact on the emittance value is minimal because of the smoothing effect from the integration procedure.

$$\varepsilon_D = \frac{\int_{0.689}^{8.025} I_{\lambda,DATA}\, d\lambda}{\int_{0.689}^{8.025} I_{\lambda,BLACKBODY}\, d\lambda}$$

where:

ε_D = Directional Emittance $(0 \le \varepsilon_D \le 1)$

EQUATION 2

Bare LI-900 required a unique method for determining the surface temperature and directional emittance. Gray-body behavior is exhibited in the short (~1.5mm to ~2.5mm) and long (~6.5mm to ~8mm) wavelength ranges. However, these data ranges could not be used for curve fitting due to the noise in the data. In the shorter wavelength range a large amount of noise is present making the curve fit unreliable. In the longer wavelength range there is little noise, however, the Planck function is very sensitive to the noise producing physically unrealistic results (i.e., an emittance greater than 1.) Therefore, at longer wavelengths it was assumed that LI-900 has the same optical properties of glass, i.e., an emittance of 0.93. This allows for the determination of the surface temperature. The directional emittance is then found by using EQUATION 2.

Determining the total hemispherical emittance from a directional emittance value requires some knowledge of the material itself. Diffuse emitters have a constant emittance over all

incident angles to the surface. However, real materials are rarely diffuse. Non-conductors (i.e., glass) typically have a constant emissivity from 90 to approximately 50 degrees off normal and rapidly drops to zero beyond 50 (see Figure 7.) Thus, for 40 degrees off normal, which is the JSC ARMSEF configuration, the measured emittance values can be assumed to be the normal emittance values. A factor of 0.95 can be used to convert the measured directional emittance to the total hemispherical emittance[3,4].

Assumptions have to be made using the data generated during this test program and the following factors have to be considered in the interpretation of the results:

1. Constant temperature – Bare RSI is a volumetric emitter due to its porous nature. This means that the spectroradiometer is receiving radiant energy from material below the surface which more than likely is at a lower temperature. Therefore, EQUATION 2 is considered an ideal situation where the sample is emitting at a single temperature.
2. Diffuse emitter – During testing machine marks were visible on the specimen face. This is a concern because the machining process itself can induce a bias in the orientation of the silica fibers. Random fiber orientation is essential to the assumption that the bare RSI behaves as a diffuse emitter. Otherwise the emittance is not constant between 0 and 50 degrees off normal as stated earlier. Also, and more importantly, the actual orientation of the specimen relative to the scanning spectroradiometer becomes a factor (see Figure 8.)
3. Geometric stability – Post-test inspection of the specimens revealed that the uncoated LI-900 undergoes a morphological change during the test. Only LI-900 only exhibited this effect. As shown in Figure 9 the silica fibers melt and coalesce into a porous glassy substrate. As this change occurs the surface of the specimen recedes or slumps into localized pits (see Appendix C, photos JSC2003E50261, JSC2003E54524, and JSC2003E55041). These pits would generate temperature gradients across the model surface and change the viewing angle of the spectroradiometer into an unknown value.

All of these factors lead to the considerable scatter seen in the calculated emittance of the bare RSI from the test data.

A comparison was made of all the results from each condition to estimate any catalytic effects. Figure 10 through Figure 14 demonstrate how the emittance of RCG would have to change with temperature to maintain a constant heat flux according to EQUATION 3 with the dashed lines indicating the measured RCG data. The constant heat flux is a radiation equilibrium value. The error bars denote the potential effect of catalytic heating for the arc jet conditions as calculated by Bouslog[5]. Non-catalytic heating can be 30-40% lower than the RCG value and fully catalytic heating can be 60-110% higher. LI-900 is consistently demonstrating lower catalytic heating than RCG while LI-900 with an emittance wash and MA-25S has higher catalytic heating. All of the data points are bounded by the catalytic heating region (from non to fully catalytic) indicating reasonable results.

$$\varepsilon_H = \frac{\varepsilon_{H,DATA} T_{DATA}^{\ 4}}{T^4} \qquad \text{EQUATION 3}$$

10.0 TEST CONCLUSIONS AND RECOMMENDATIONS

This test program was successful in that all of the test objectives were satisfied. Thermal performance data was acquired for silicone type ablator materials for potential on-orbit TPS tile repair applications. Initial test results of the pre-cure and MA-25 ablators were positive. Subjecting the material to a steadily increasing thermal environment similar to re-entry allows a stable char layer to form which dramatically improves the performance of the material. Initial measurements of the emittance of the char layer of the MA-25S show it to be approximately equivalent to RCG. A higher surface temperature indicates that the catalycity is higher than RCG and this should be investigated further. A significant concern, however, is the amount of swelling seen in the specimens. Further tests should be performed to investigate how the material behaves when imbedded within a tile and characterize the amount of swelling versus the exposed environment. Excessive swelling may create a protrusion that will cause early transition during re-entry.

Adequate data, with limitations, were acquired that characterize the emittance of uncoated RSI at elevated temperatures. LI-2200 and FRCI-12 exhibited gray-body behavior although there is considerable scatter among the specimens. LI-900 did not behave as a gray-body and additional assumptions were required to allow calculation of the emittance from the test data. It is apparent that further enhancements in equipment and environmental simulation techniques would be required to fully characterize the optical properties of the low density, highly porous materials that comprise the TPS tiles. However, the test data that was acquired from this arc jet test program represents a significant improvement in the acquisition of emittance data at the high temperatures experienced by the TPS tiles during entry heating. This data will definitely enhance the understanding of the failure modes of damaged TPS tiles and be used as part of the thermophysical property database as inputs for thermal math modeling purposes.

11.0 REFERENCES

[1] Ridge, J. and Marschall, J., "Estimation of Temperature Dependent Emissivities from Room Temperature Spectral Reflectance Measurements on Coated and Uncoated TPS Tiles", Thermal Science Institute, ELORET, September, 1996.

[2] De Witt, D. P., and Incropera, F.P., "Fundamentals of Heat and Mass Transfer", 3rd Edition, John Wiley & Sons, 1990

[3] Donabedian, M., "Reflectance and Emittance of Selected Materials and Coatings," SAMSO-TR-75-24, Space and Missile Systems Organization, Los Angeles Air Force Station, 1975.

[4] Bouslog, S. and Cunnington, G., "Emittance Measurements of RCG-Coated Shuttle Tiles," NASA JSC-25794, April 1992.

[5] Bouslog, S., "Catalytic Effects on Heating to a 5-inch Flat-Faced Cylinder in the Arc-jet", Lockheed Martin, Houston, TX, SAB-01102003, October, 2003.

DATE	RUN #	MODEL	TEST CONDITION (F)	SCAN	T (F)	ε_D (1)	ε_H (2)	RAD EQ (3)	RECESSION (in)
July 23 2003	2-2551-3	RCG OVER TUFI	2000	1843-1	1980	0.807	0.767	12.9	0.109
		LI-900	2000	1833-1	2700	0.201	0.191	9.1	
				1833-2	2700	0.201	0.191	9.1	
				1833-3	2700	0.204	0.194	9.2	
				1833-4	2650	0.215	0.204	9.1	
				1833-5	2630	0.220	0.209	9.1	
July 24 2003	2-2552-3	RCG OVER TUFI	2000	1843-2	1950	0.842	0.800	12.8	NONE
				1843-3	1930	0.846	0.804	12.5	
			2300	1843-4	2310	0.867	0.824	23.1	
		LI-2200	2000	1838-1	2610	0.349	0.332	14.0	0.001
				1838-2	2600	0.370	0.352	14.7	
				1838-3	2600	0.366	0.348	14.5	
				1838-4	2550	0.402	0.382	14.9	
				1838-5	2600	0.382	0.363	15.1	
July 28 2003	2-2554-3	FRCI-12	2000	1828-1	2850	0.261	0.248	14.2	0.026
				1828-2	2830	0.269	0.256	14.2	
				1828-3	2870	0.278	0.264	15.5	
				1828-4	2810	0.290	0.276	15.0	
				1828-5	2800	0.288	0.274	14.7	
		LI-900	2300	1834-1	MODEL EXPERIENCED SEVERE RECESSION. DATA UNUSABLE.				2.011
				1834-2					
				1834-3					
				1834-4					
				1834-5					
July 29 2003	2-2555-3	LI-2200	2300	1839-1	2910	0.441	0.419	25.7	0.034
				1839-2	2740	0.544	0.517	25.8	
				1839-3	2740	0.547	0.520	25.9	
				1839-4	2740	0.543	0.516	25.7	
				1839-5	2740	0.535	0.508	25.4	
July 30 2003	2-2557-3	LI-900 DENSE	2000	1835-1	2170	0.734	0.697	15.9	.092
				1835-2	2350	0.580	0.551	16.3	
				1835-3	2390	0.536	0.509	16.0	
				1835-4	2410	0.509	0.484	15.6	
				1835-5	2400	0.503	0.478	15.2	
			2300	1835-21	2630	0.639	0.607	26.3	
				1835-22	2640	0.636	0.604	26.6	
				1835-23	2610	0.674	0.640	27.1	
				1835-24	2600	0.686	0.652	27.2	
				1835-25	2600	0.674	0.640	26.7	

Table 5: Bare Tile and MA-25S Emittance Summary

DATE	RUN #	MODEL	TEST CONDITION (F)	SCAN	T (F)	ε_D (1)	ε_H (2)	RAD EQ (3)	RECESSION (in)
July 31 2003	2-2558-3	FRCI-12	2300	1829-1	3000	0.379	0.360	24.6	0.056
				1829-2	2940	0.417	0.396	25.2	
				1829-3	2860	0.464	0.441	25.5	
				1829-4	2860	0.463	0.440	25.4	
				1829-5	2860	0.458	0.435	25.2	
		MA-25S	2000	1810-1	Temperature unsteady				-.241
				1810-2	2110	0.825	0.784	16.3	
				1810-3	2100	0.804	0.764	15.6	
				1810-4	2100	0.821	0.780	15.9	
			2300	1810-21	2460	0.887	0.843	29.2	
				1810-22	2460	0.889	0.845	29.2	
				1810-23	2470	0.877	0.833	29.2	
Aug 8 2003	2-2559-3	RCG OVER TUFI	2000	1844-1	SCANNER PARTIALLY BLOCKED BY LEFT ARM. DATA UNUSABLE				NONE
				1844-2					
			1800	1844-3					
				1844-4					
				1844-5					
			1700	1844-6					
				1844-7					
			1600	1844-8					
				1844-9					
Aug 14 2003	2-2560-2	RCG OVER TUFI	1800	1844-21	1790	0.822	0.781	9.5	NONE
				1844-22	1780	0.831	0.789	9.5	
			1700	1844-23	1690	0.805	0.765	7.8	
				1844-24	1690	0.835	0.793	8.1	
			1600	1844-25	1600	0.802	0.762	6.5	
				1844-26	1590	0.827	0.786	6.6	
				1844-27	1600	0.813	0.772	6.6	
			2000	1844-28	1970	0.812	0.771	12.8	
				1844-29	1970	0.810	0.770	12.8	
Aug 15 2003	2-2561-3	RCG OVER TUFI (2.65 FACTOR)	2000	1844-31	1970	0.768	0.730	12.1	NONE
				1844-32	1980	0.777	0.738	12.5	
				1844-33	1970	0.772	0.733	12.2	
		LI-900 (2.65 FACTOR)	1600	1836-1	2500	0.146	0.139	5.1	0.172
				1836-2	2500	0.154	0.146	5.3	
			1700	1836-3	2650	0.164	0.156	6.9	
				1836-4	2600	0.172	0.163	6.8	
			1800	1836-5	2730	0.176	0.167	8.2	
				1836-6	2700	0.181	0.172	8.2	
			2000	1836-7	2900	0.190	0.181	10.9	
				1836-8	2800	0.211	0.200	10.8	
				1836-9	2750	0.222	0.211	10.7	

Table 5: Bare Tile and MA-25S Emittance Summary (Cont.)

DATE	RUN #	MODEL	TEST CONDITION (F)	SCAN	T (F)	ε_D (1)	ε_H (2)	RAD EQ (3)	RECESSION (in)
Aug 18 2003	2-2562-3	FRCI-12 (2.65 FACTOR)	1600	1830-1	2170	0.229	0.218	5.0	0.023
				1830-2	2180	0.266	0.253	5.8	
				1830-3	2180	0.266	0.253	5.8	
			1700	1830-4	2350	0.269	0.256	7.6	
				1830-5	2320	0.281	0.267	7.6	
			1800	1830-6	2500	0.286	0.272	9.9	
				1830-7	2480	0.295	0.280	10.0	
			2000	1830-8	2640	0.332	0.315	13.9	
				1830-9	2580	0.351	0.333	13.6	
		LI-2200 (2.65 FACTOR)	1600	1840-1	2100	0.292	0.277	5.7	0.004
				1840-2	2100	0.317	0.301	6.2	
				1840-3	2150	0.302	0.287	6.3	
			1700	1840-4	2320	0.302	0.287	8.2	
				1840-5	2320	0.301	0.286	8.1	
			1800	1840-6	2500	0.311	0.295	10.8	
				1840-7	2500	0.309	0.294	10.7	
			2000	1840-8	2700	0.337	0.320	15.2	
				1840-9	2700	0.333	0.316	15.0	
Aug 19 2003	2-2563-3	LI-900 DENSE (2.65 FACTOR)	1600	1836-21	1820	0.540	0.513	6.6	.286
				1836-22	1810	0.556	0.528	6.7	
			1700	1836-23	1950	0.546	0.519	8.3	
				1836-24	1950	0.555	0.527	8.5	
			1800	1836-25	2130	0.507	0.482	10.3	
				1836-26	2140	0.499	0.474	10.3	
			2000	1836-27	2400	0.453	0.430	13.7	
				1836-28	2440	0.420	0.399	13.4	
		MA-25S (2.65 FACTOR)	1600	1845-1	1860	0.654	0.621	8.6	-.566
				1845-2	1850	0.678	0.644	8.7	
			1700	1845-3	1980	0.678	0.644	10.9	
				1845-4	1970	0.678	0.644	10.7	
			1800	1845-5	2100	0.685	0.651	13.3	
				1845-6	2070	0.730	0.694	13.5	
			2000	1845-7	2290	0.704	0.669	18.2	
				1845-8	2320	0.681	0.647	18.4	

Table 5: Bare Tile and MA-25S Emittance Summary (Cont.)

DATE	RUN #	MODEL	TEST CONDITION (F)	SCAN	T (F)	ε_D (1)	ε_H (2)	RAD EQ (3)	RECESSION (in)
Aug 20 2003	2-2564-3	LI-900 (2.65 FACTOR)	2000	1837-1	2820	0.223	0.212	11.7	0.265
				1837-2	2750	0.243	0.231	11.7	
				1837-3	2720	0.251	0.238	11.6	
				1837-4	2700	0.254	0.241	11.5	
				1837-5	2700	0.252	0.239	11.4	
		LI-900 W/ EMITTANCE WASH (2.65 FACTOR)	1600	1835A-1	1760	0.727	0.691	8.0	NONE
				1835A-2	1750	0.750	0.713	8.1	
			1700	1835A-3	1880	0.753	0.715	10.2	
				1835A-4	1870	0.757	0.719	10.1	
			1800	1835A-5	2000	0.759	0.721	12.6	
				1835A-6	2010	0.750	0.713	12.6	
			2000	1835A-7	2220	0.734	0.697	17.1	
				1835A-8	2220	0.734	0.697	17.1	

(1) ε_D = Measured directional emittance

(2) ε_H = Total hemispherical emittance ($\varepsilon_H = 0.95\ \varepsilon_D$)

(3) Radiation Equilibrium (BTU/ft^2-sec) = $\varepsilon_H \sigma T^4$

Table 5: Bare Tile and MA-25S Emittance Summary (Cont.)

Model #	Pre-Test Weight	Post-Test Weight	Delta	Pre-Test Centerline Thickness	Post-Test Centerline Thickness	Delta	Pre-Test Diameter	Post-Test Diameter	Delta
	(grams)			(inches)			(inches)		
1805	297.221	176.680	-120.541	2.090	1.070	-1.020	3.869	3.969	0.100
1806	294.691	161.628	-133.063	2.098	1.439	-0.659	3.873	3.888	0.015
1807	181.040	142.227	-38.813	2.098	1.964	-0.134	3.860	3.850	-0.010
1808	179.131			2.090			3.868		
1809	319.228	274.033	-45.195	2.091	2.287	0.196	3.861	4.085	0.224
1810	291.584	272.397	-19.187	2.093	2.334	0.241	3.867	3.799	-0.068
1811	278.018			2.092			3.870		
1812	188.897	141.138	-47.759	2.083	1.967	-0.116	3.857	N/A	
1813	188.636			2.090			3.862		
1814	189.891			2.089			3.864		
1815	384.237	236.464	-147.773	2.118	1.729	-0.389	3.830	3.930	0.100
1816	384.071	318.007	-66.064	2.126	2.084	-0.042	3.814	3.713	-0.101
1817	281.928	189.879	-92.049	2.030	2.315	0.285	3.788	3.924	0.136
1818	381.549	341.202	-40.347	2.071	2.398	0.327	3.844	3.941	0.097
1821	383.315	350.324	-32.991	2.113	2.843	0.730	3.833	3.982	0.149
1828	84.755	84.466	-0.289	2.014	1.988	-0.026	3.862	3.856	-0.006
1829	86.539	87.258	0.719	2.001	1.945	-0.056	3.861	3.855	-0.006
1830	86.333	86.077	-0.256	2.000	1.987	-0.013	3.864	3.853	-0.011
1831	86.367			2.010			3.868		
1832	87.542			2.005			3.859		
1833	69.678	69.291	-0.387	1.995	1.886	-0.109	3.862	3.848	-0.014

Model #	Pre-Test Weight	Post-Test Weight	Delta	Pre-Test Centerline Thickness	Post-Test Centerline Thickness	Delta	Pre-Test Diameter	Post-Test Diameter	Delta
	(grams)			(inches)			(inches)		
1834	68.361	70.079	1.718	2.011			3.865	3.873	0.008
1835	66.238	64.442	-1.796	2.005	1.913	-0.092	3.862	3.847	-0.015
1836	65.966	65.404	-0.562	1.996	1.710	-0.286	3.853	3.845	-0.008
1837	68.459	68.211	-0.248	1.990	1.725	-0.265	3.856	3.837	-0.019
1838	158.339	158.089	-0.250	1.998	1.997	-0.001	3.862	3.860	-0.002
1839	154.125	153.593	-0.532	2.000	1.966	-0.034	3.867	3.849	-0.018
1840	154.229	153.892	-0.337	1.999	1.995	-0.004	3.864	3.861	-0.003
1841	151.908			2.002			3.870		
1842	142.997			1.999			3.867		
1845	377.529	360.323	-17.206	2.064	2.630	0.566	3.851	3.825	-0.026
1846	376.027			2.062			3.854		

Table 6: Pre- and Post-Test Weights and Measures

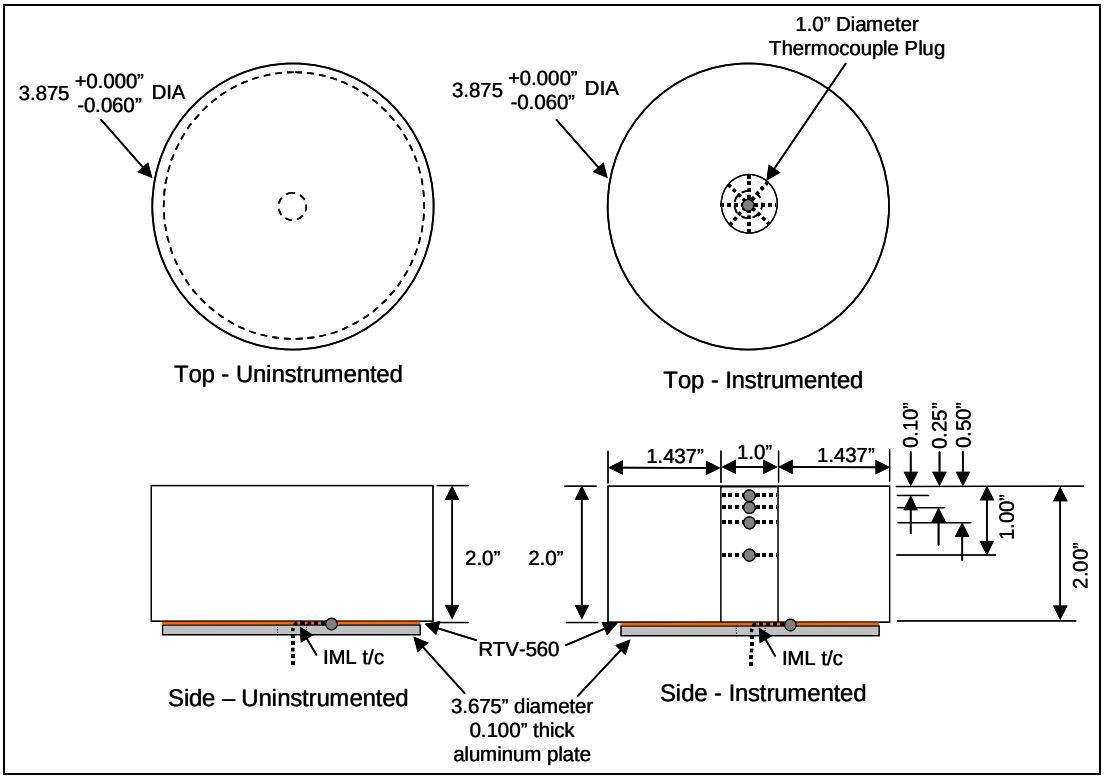

Figure 1: Tile Repair Specimen Configuration

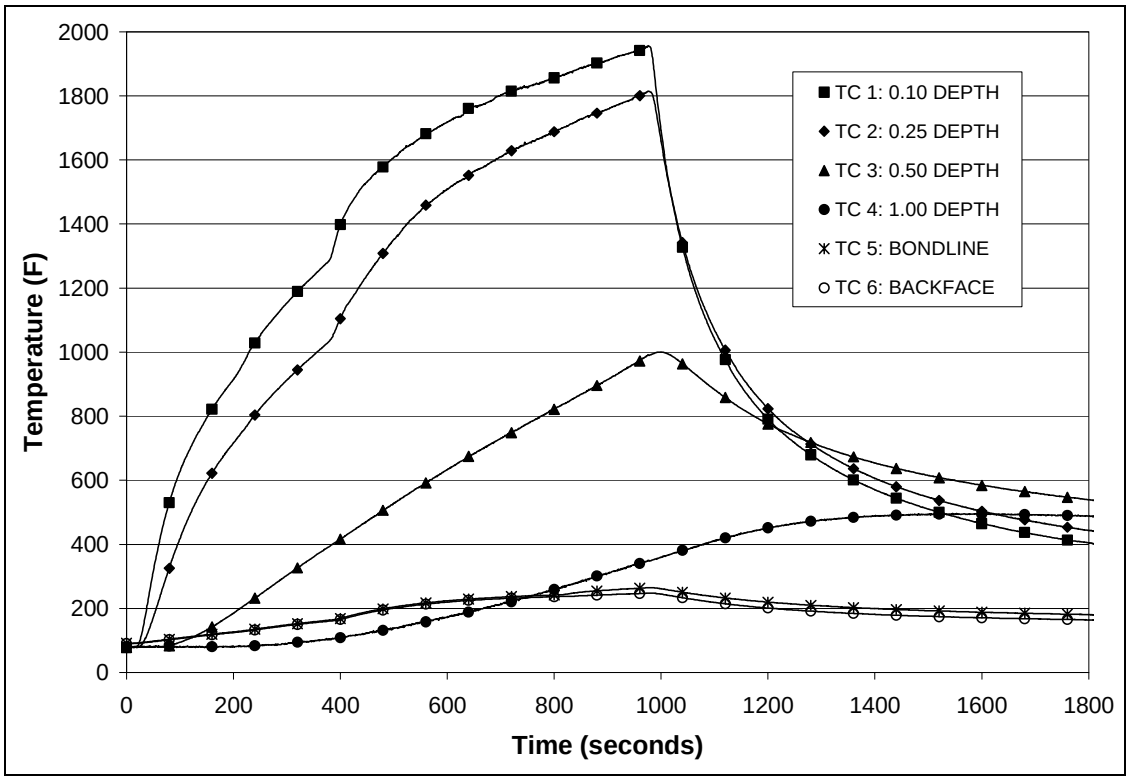

Figure 2: Model #1809 Thermocouple Test Data

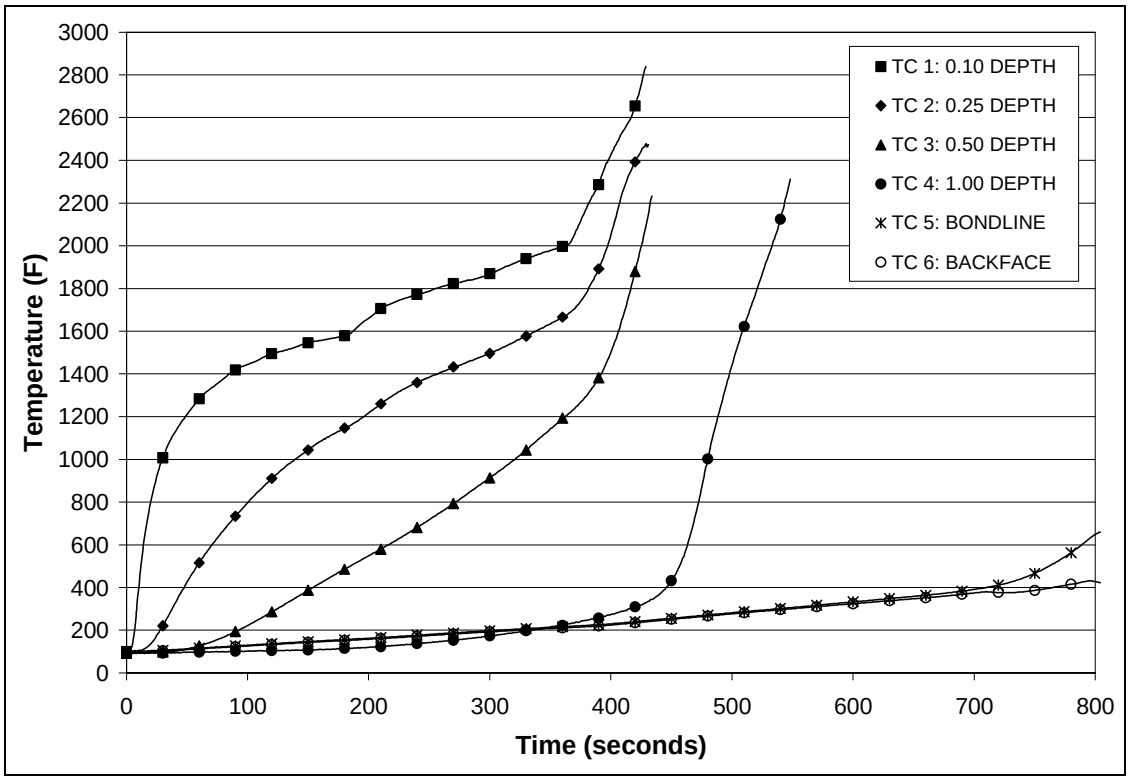

Figure 3: Model #1812 Thermocouple Test Data

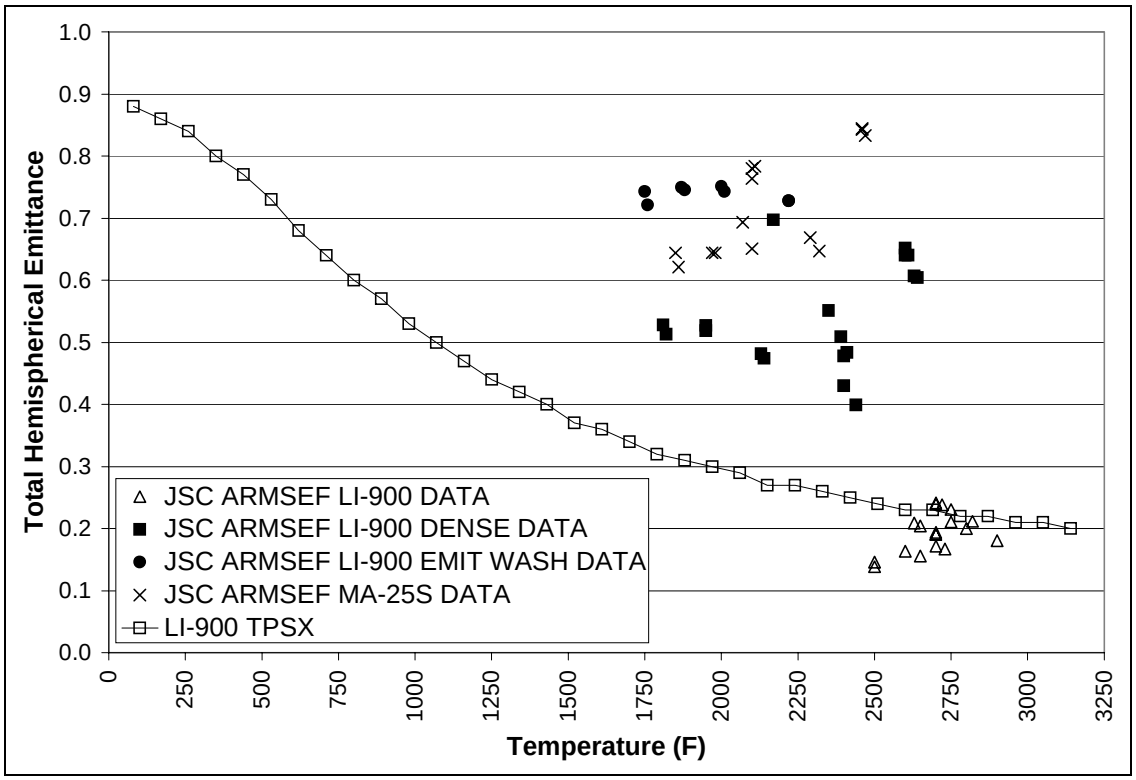

Figure 4: Bare and Repaired LI-900 Total Hemispherical Emittance vs. Temperature

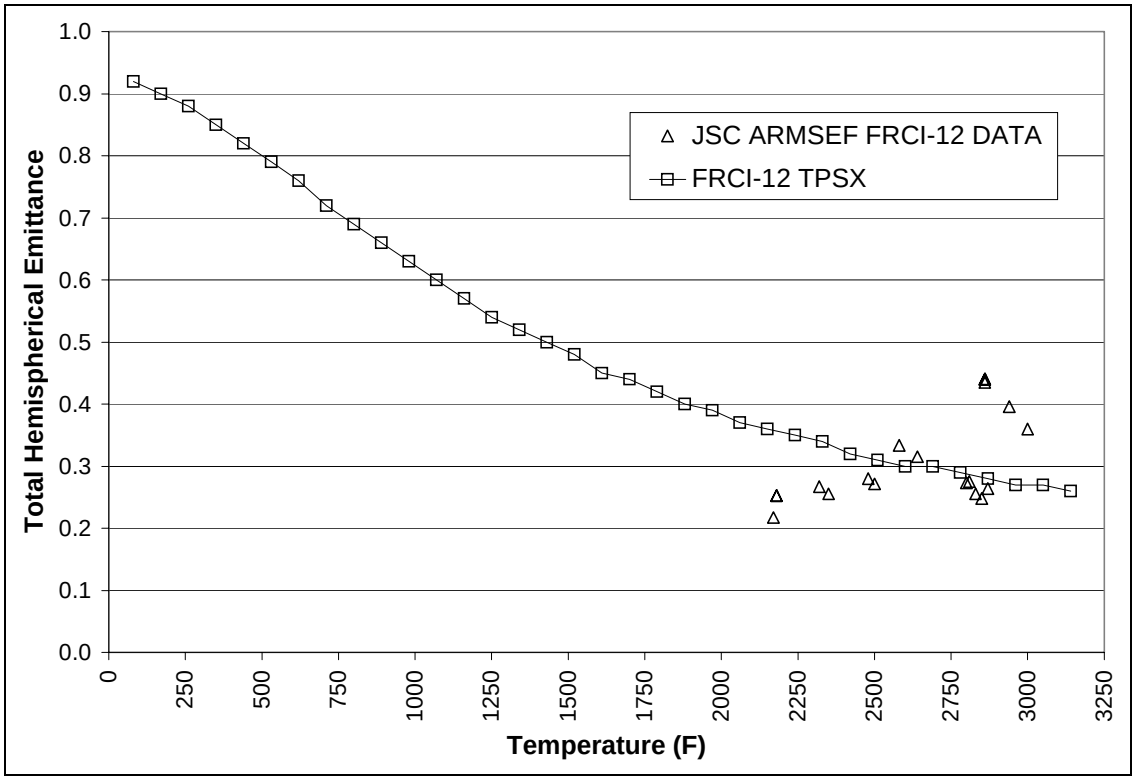

Figure 5: Bare FRCI-12 Temperature vs. Total Hemispherical Emittance

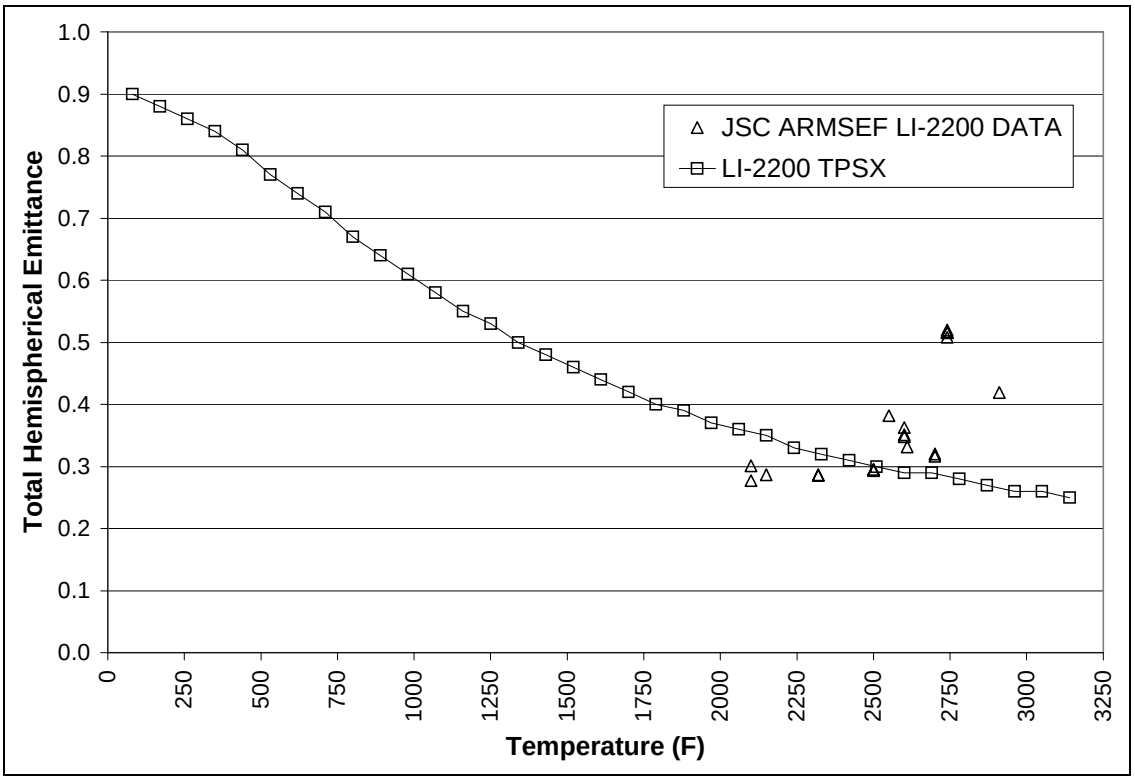

Figure 6: Bare LI-2200 Temperature vs. Total Hemispherical Emittance

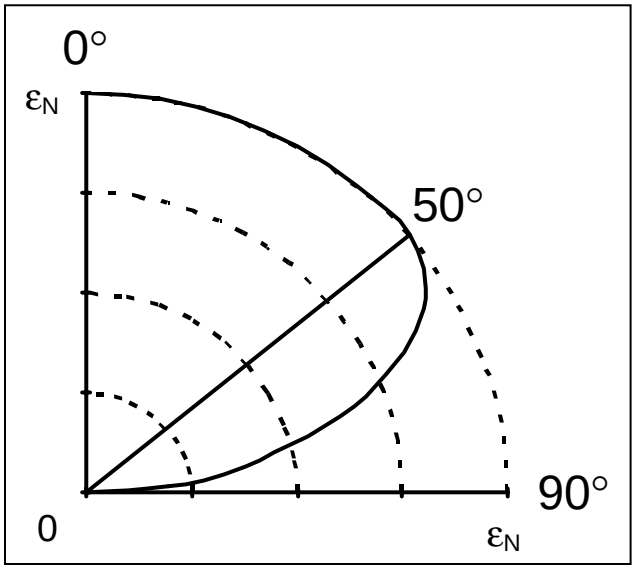

Figure 7: Directional Emittance vs. Incident Angle

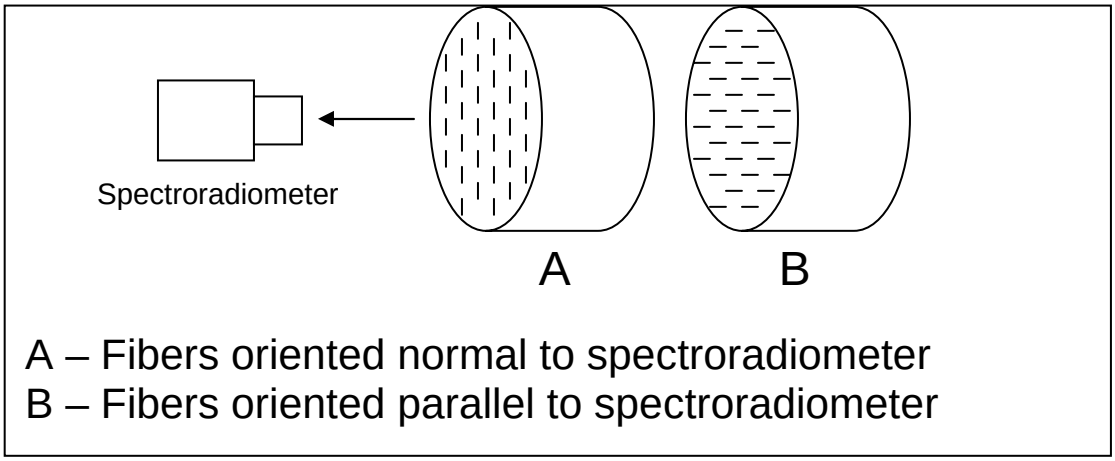

Figure 8: Fiber orientation schematic

Figure 9: Model #1836 Post Test Photo at 10X Magnification

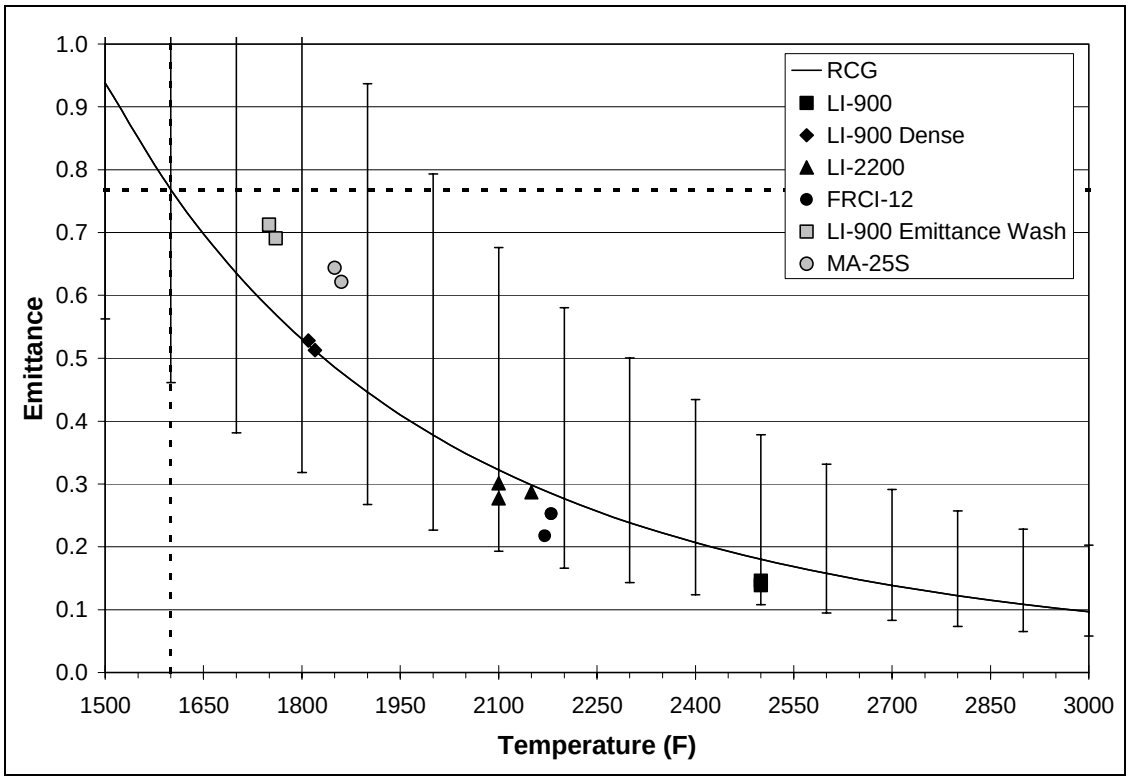

Figure 10: Constant Heat Flux Comparison for 1600°F Condition

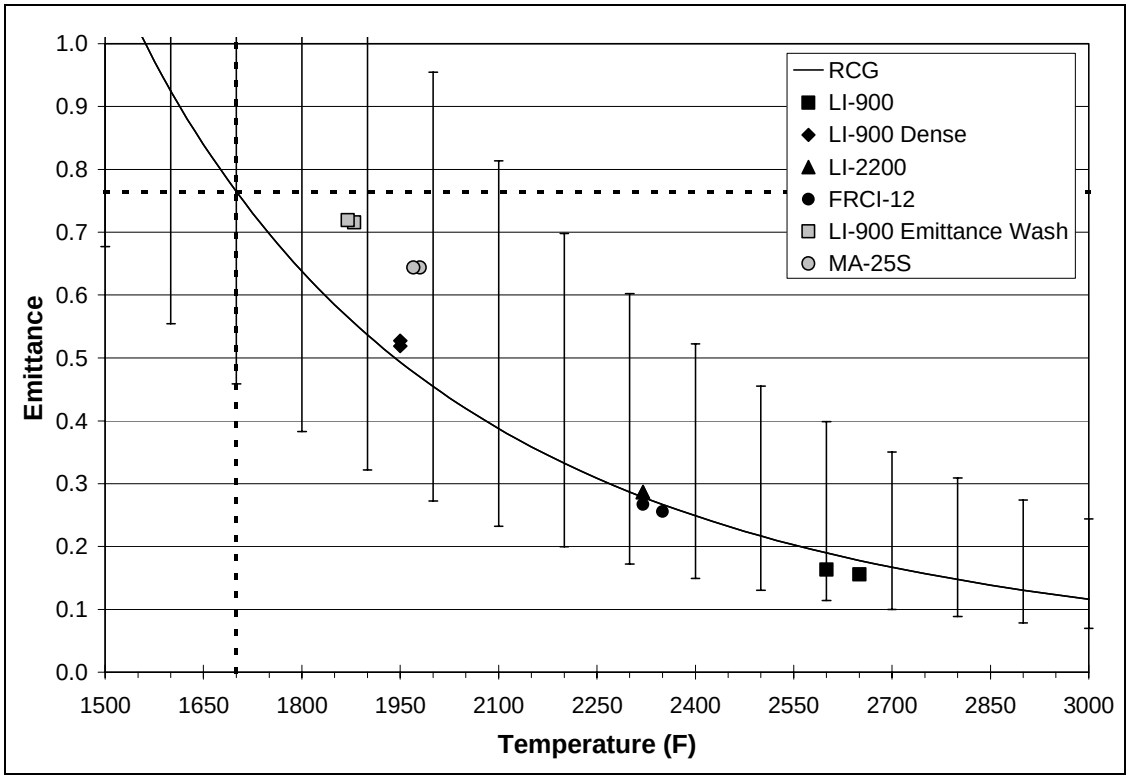

Figure 11: Constant Heat Flux Comparison for 1700°F Condition

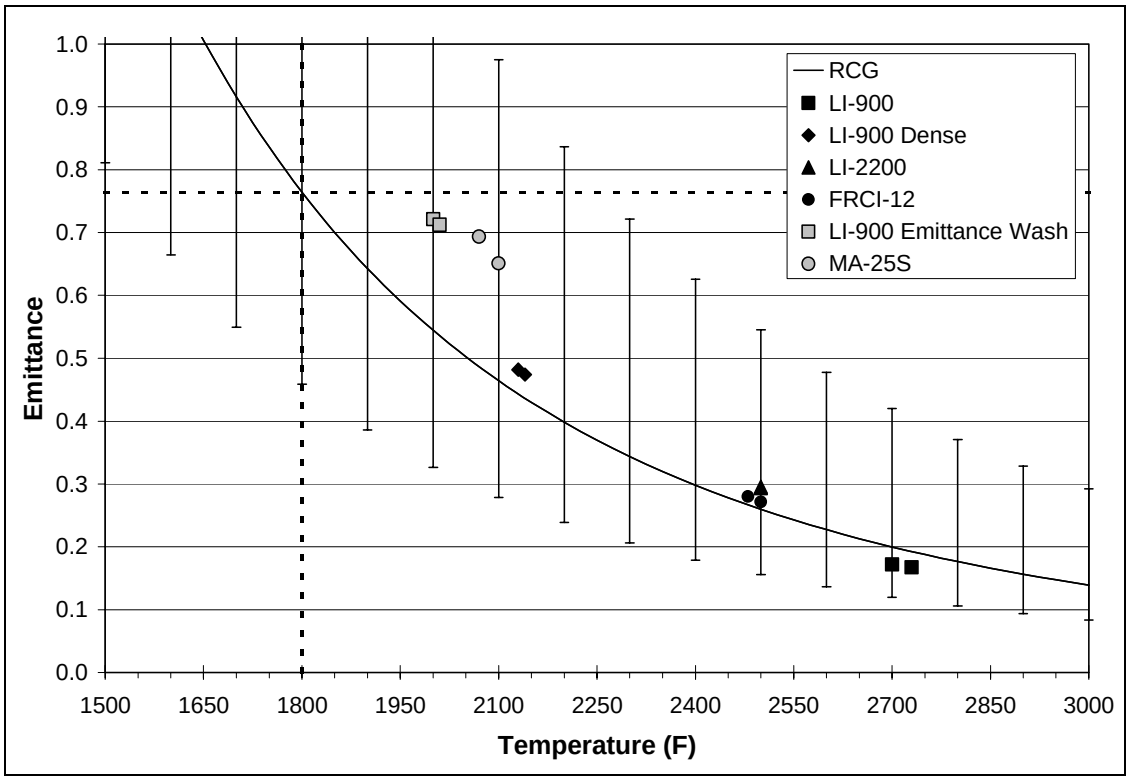

Figure 12: Constant Heat Flux Comparison for 1800°F Condition

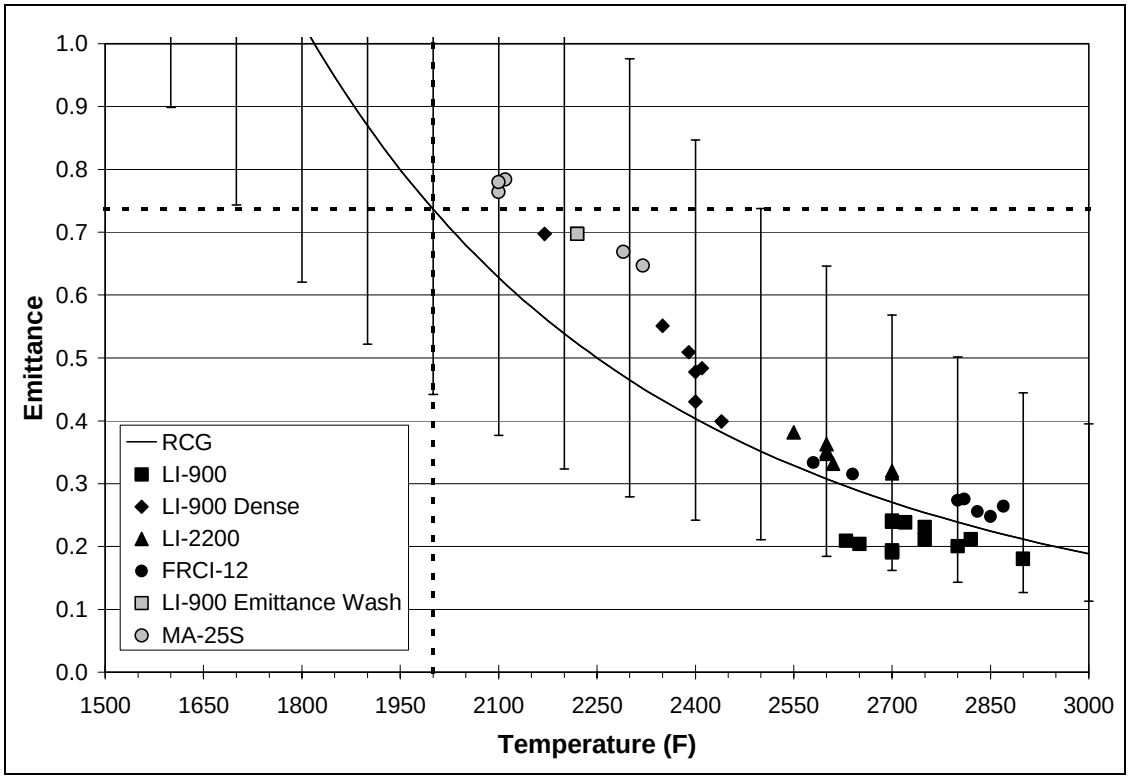

Figure 13: Constant Heat Flux Comparison for 2000°F Condition

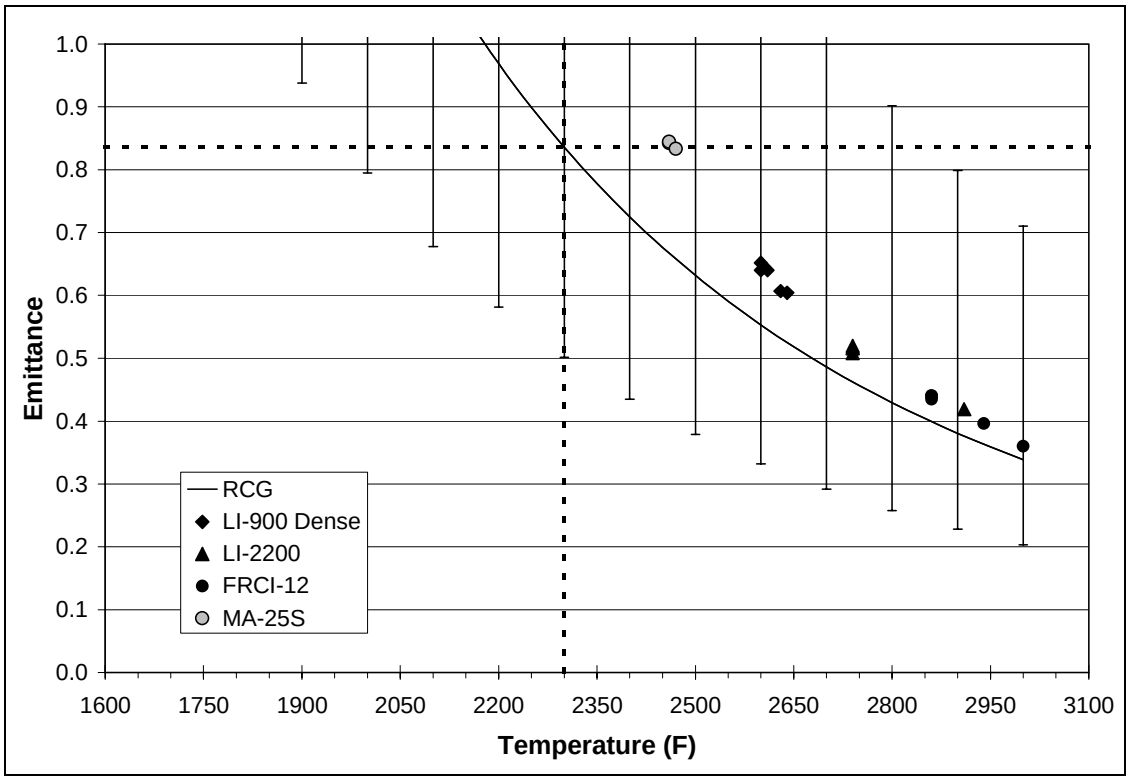

Figure 14: Constant Heat Flux Comparison for 2300°F Condition

APPENDIX A – ARC JET HEATER CONFIGURATION

Heater Configuration Number 10DDC03P0
(P0 = 4 plenum gas valves in the closed position)

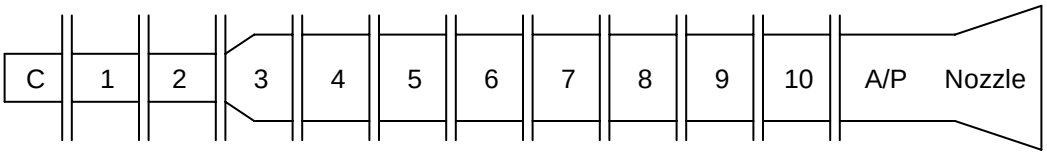

	HARDWARE CONFIGURATION											
Cathode	1	2	3	4	5	6	7	8	9	10	Throat	Nozzle
Tungsten Button	1.5	1.5	Trans 4,5,6	2.36	2.36	2.36	2.36	2.36	2.36	2.36	2.25	5/15

	GAS INJECTION CONFIGURATION										
Pack No.	1	2	3	4	5	6	7	8	9	10	Plenum
GN_2	2,2 4,4 6,6			3,3 13,13	3,3					3,3 8,8 13,13 18,18	
GO_2						3,3 8,8 13,13 18,18	3,3 8,8				

	INSTRUMENTATION CONFIGURATION										
Pack No.	1	2	3	4	5	6	7	8	9	10	Plenum
6 ohms										20-A	
Pressure	10				8						Gas Segment
Voltage										17-18 18-19 19-20 20-A	

Notes:
Gas injection lines have no restriction (no orifices at the manifolds)
For the 5” Nozzle – 50” Adapter inside/5” Adapter outside/5” Nozzle outside
For the 15” Nozzle – 50” Adapter inside/15” Adapter outside/15” Nozzle outside
Vent orifices: GN_2 = 0.515” DIA GO_2 = 0.625” DIA
(8) 0.1085” DIA orifices in anode gas injection segment

APPENDIX B – SPECTRORADIOMETER SCAN DATA

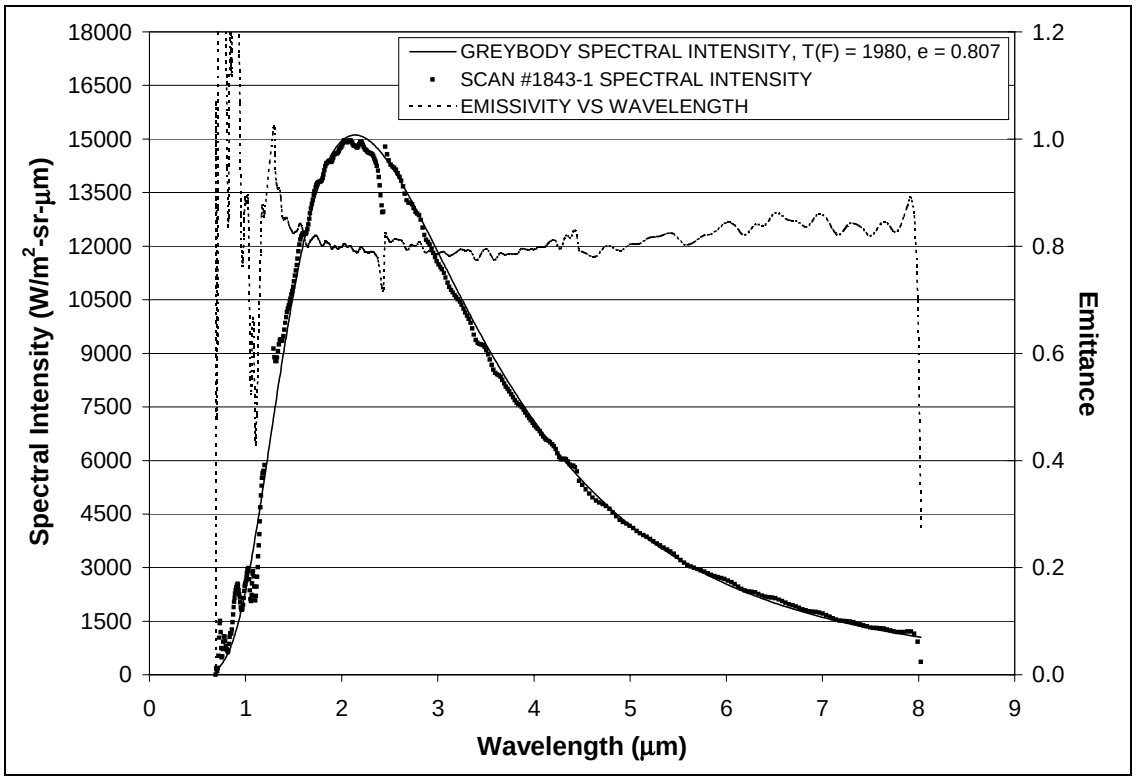

Figure 15: #1843-1, RCG Over TUFI, 2000°F Condition, 5in Nozzle

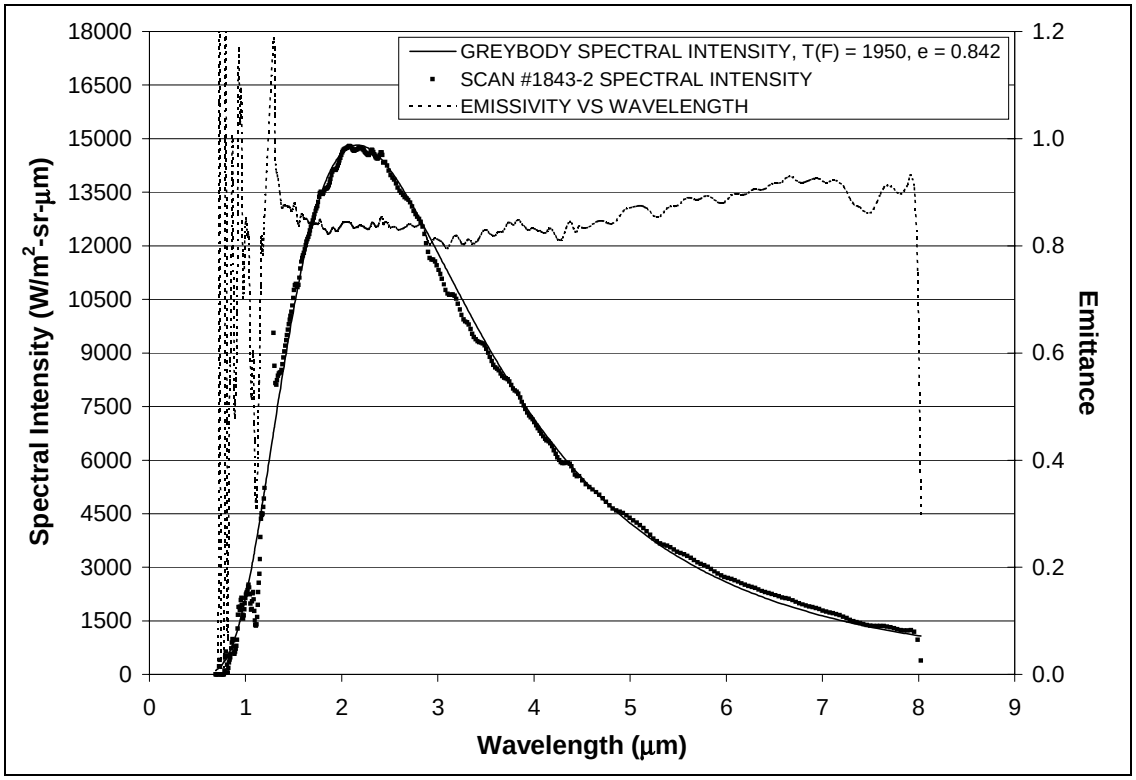

Figure 16: #1843-2, RCG Over TUFI, 2000°F Condition, 5in Nozzle

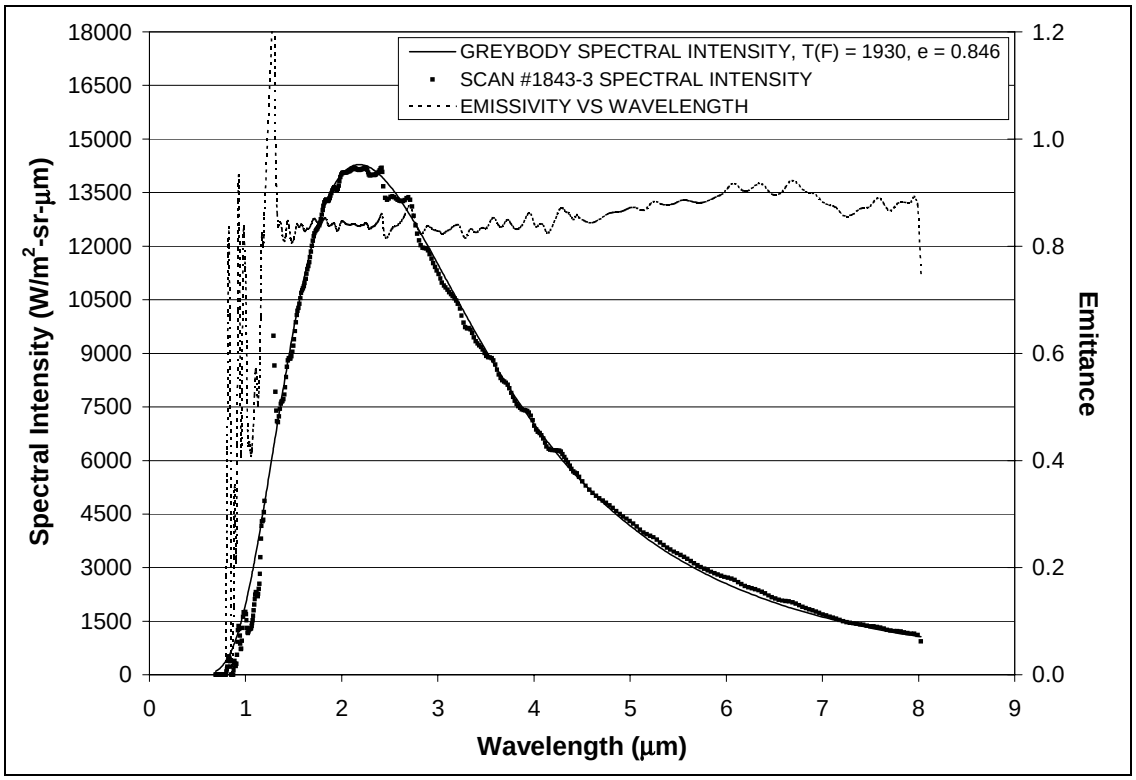

Figure 17: #1843-3, RCG Over TUFI, 2000°F Condition, 5in Nozzle

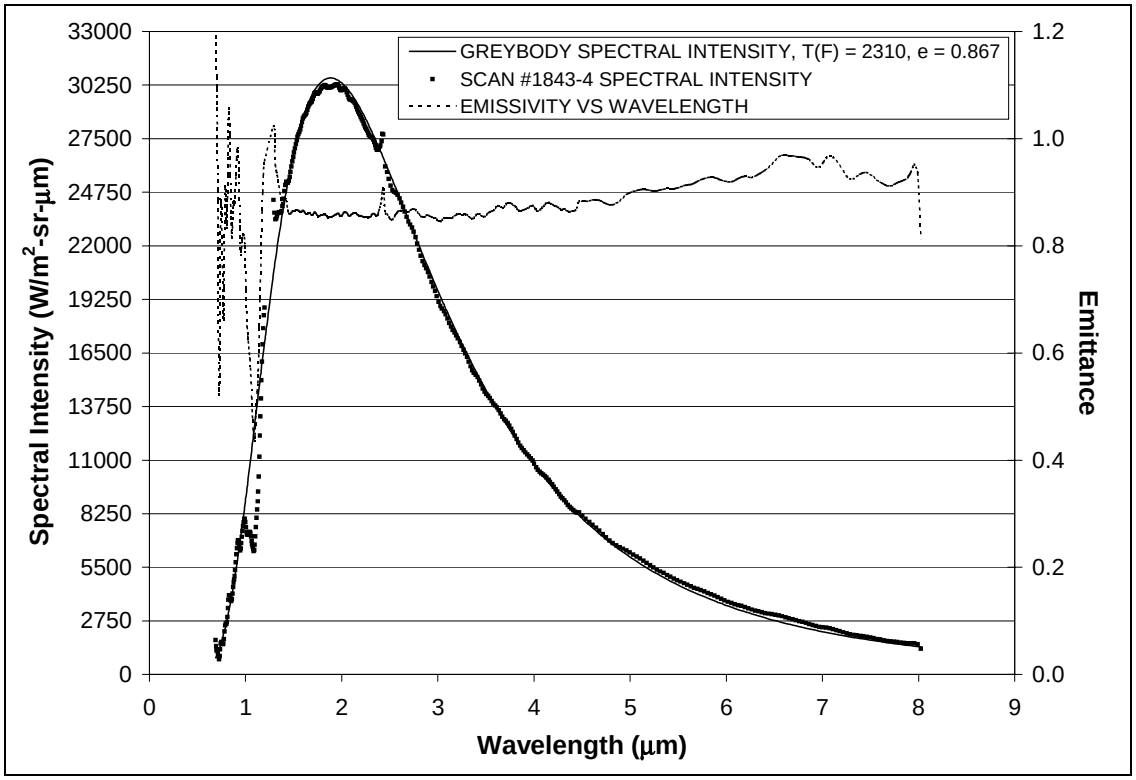

Figure 18: #1843-4, RCG Over TUFI, 2300°F Condition, 5in Nozzle

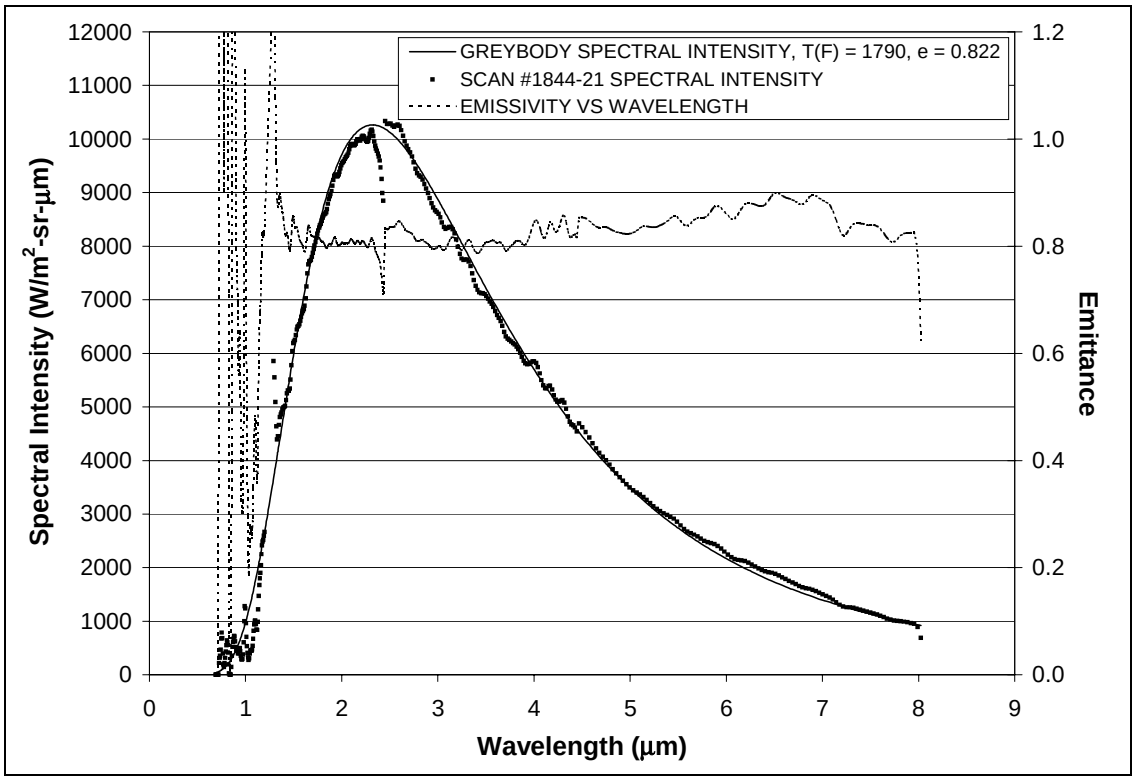

Figure 19: #1844-21, RCG Over TUFI, 1800°F Condition, 15in Nozzle

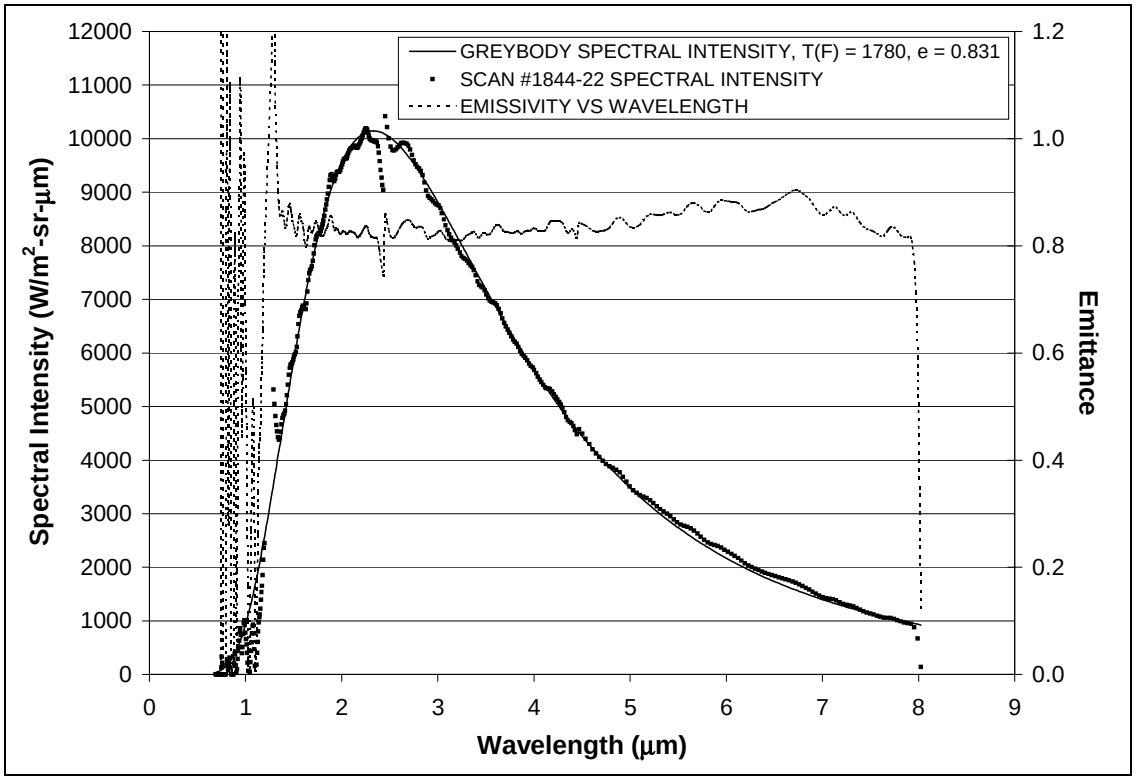

Figure 20: #1844-22, RCG Over TUFI, 1800°F Condition, 15in Nozzle

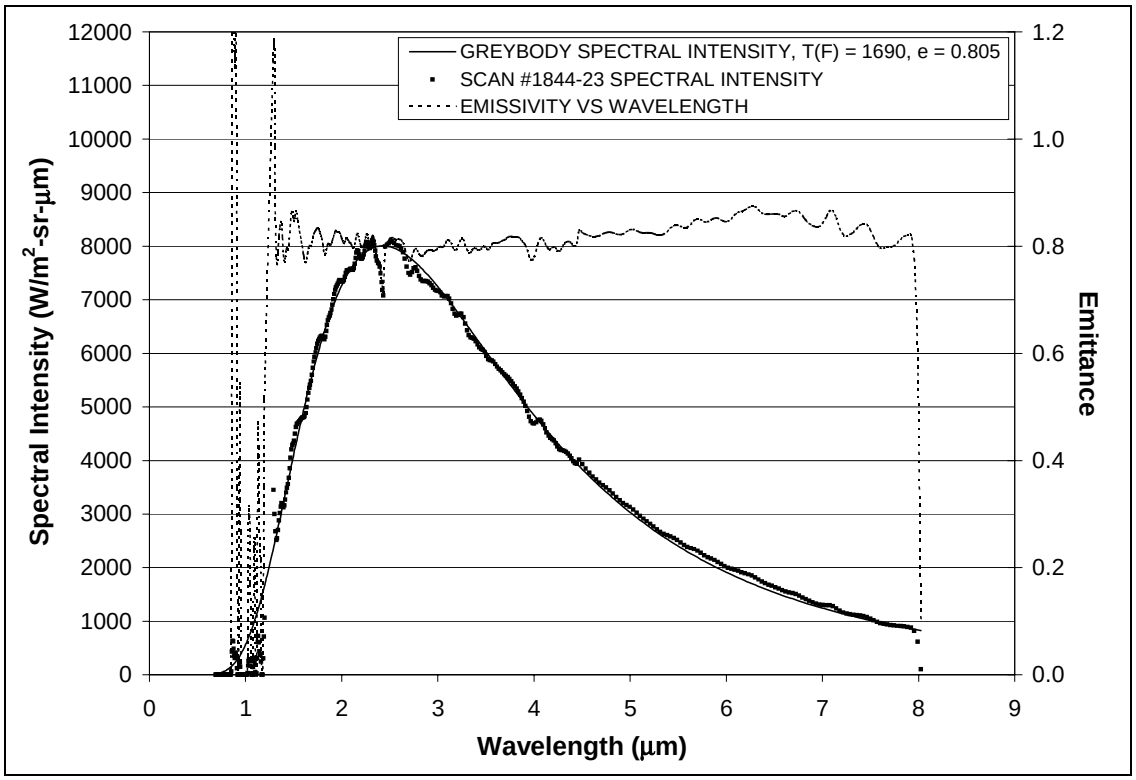

Figure 21: #1844-23, RCG Over TUFI, 1700°F Condition, 15in Nozzle

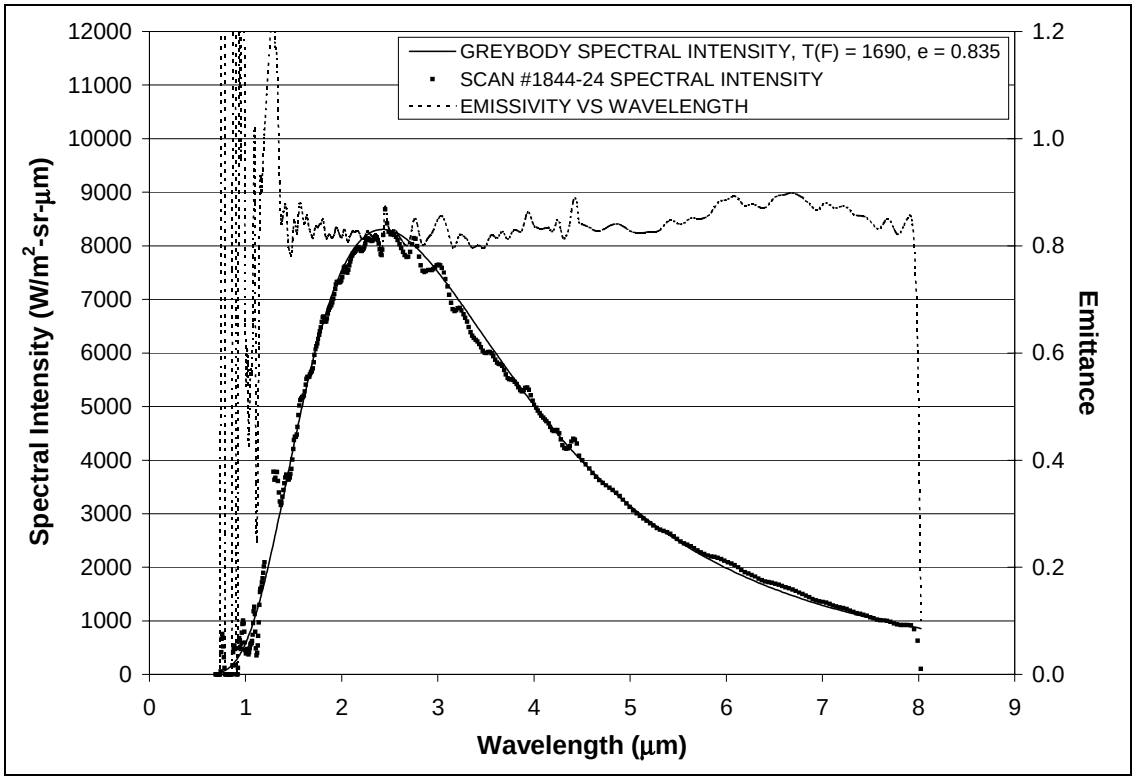

Figure 22: #1844-24, RCG Over TUFI, 1700°F Condition, 15in Nozzle

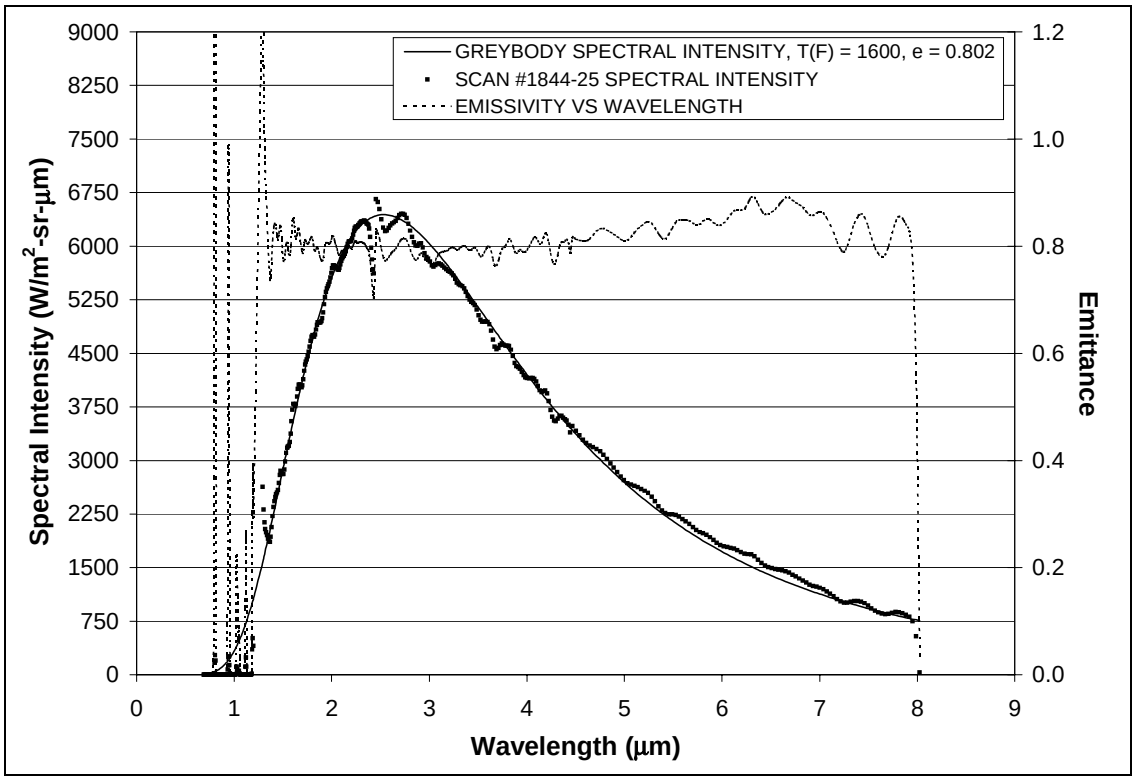

Figure 23: #1844-25, RCG Over TUFI, 1600°F Condition, 15in Nozzle

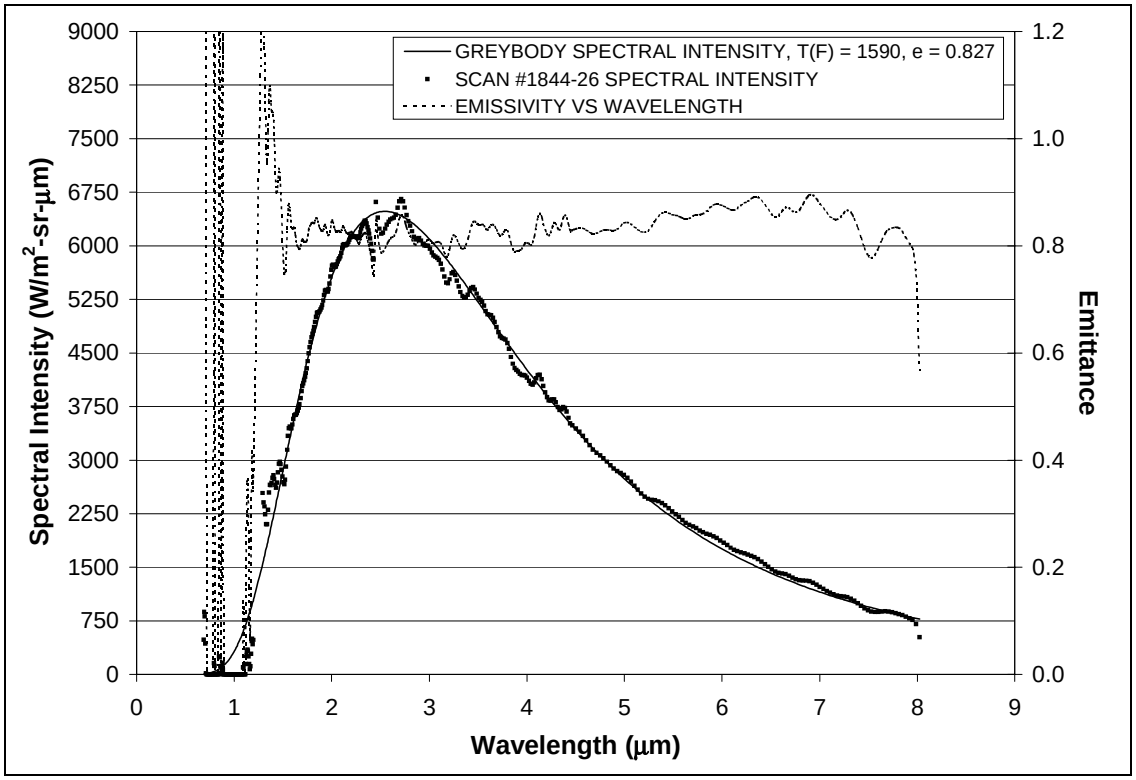

Figure 24: #1844-26, RCG Over TUFI, 1600°F Condition, 15in Nozzle

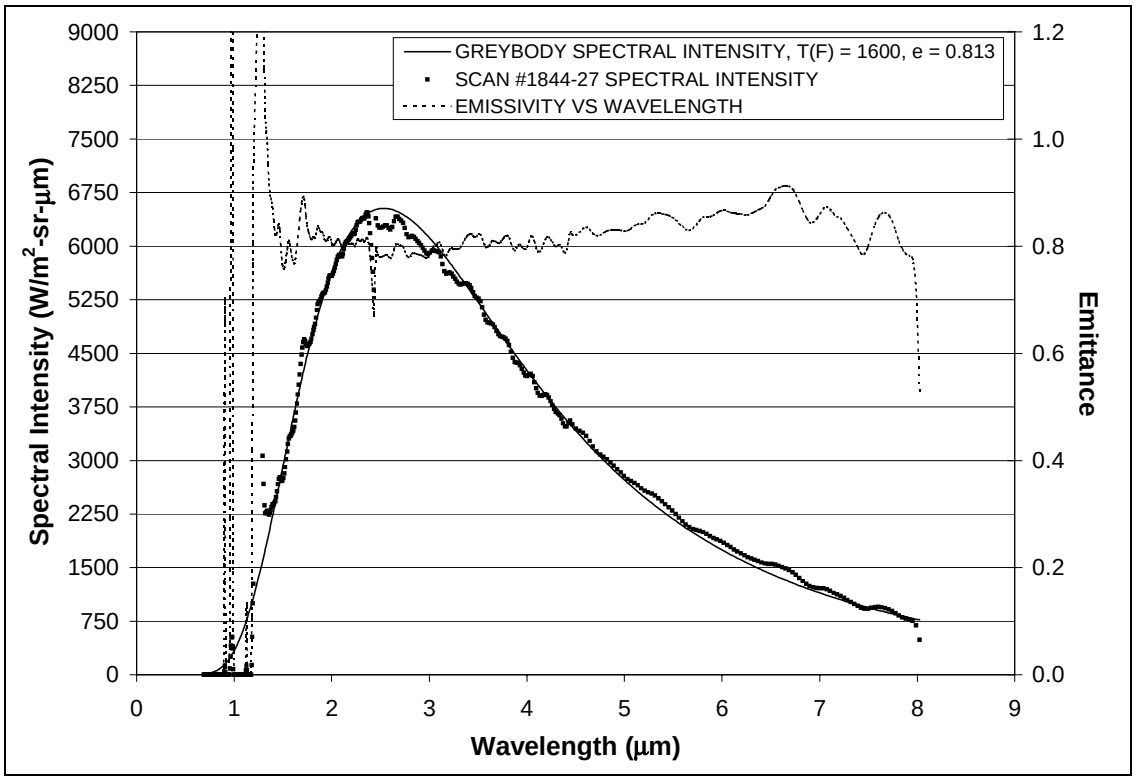

Figure 25: #1844-27, RCG Over TUFI, 1600°F Condition, 15in Nozzle

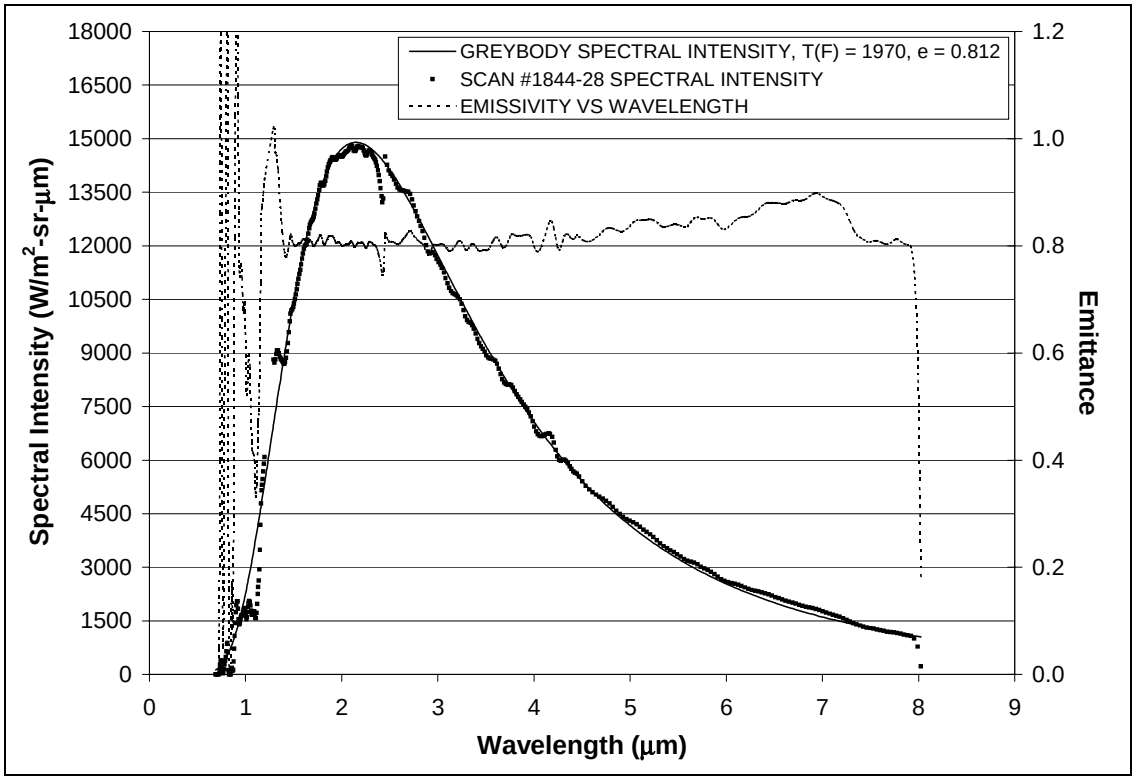

Figure 26: #1844-28, RCG Over TUFI, 2000°F Condition, 15in Nozzle

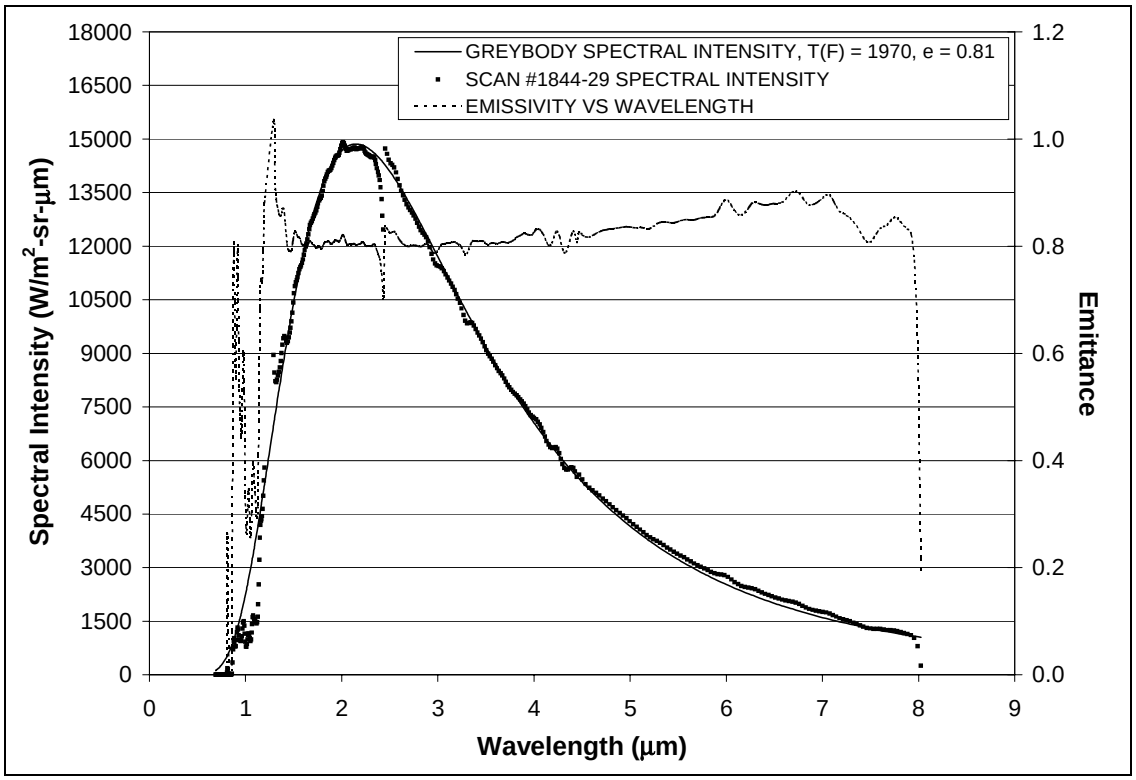

Figure 27: #1844-29, RCG Over TUFI, 2000°F Condition, 15in Nozzle

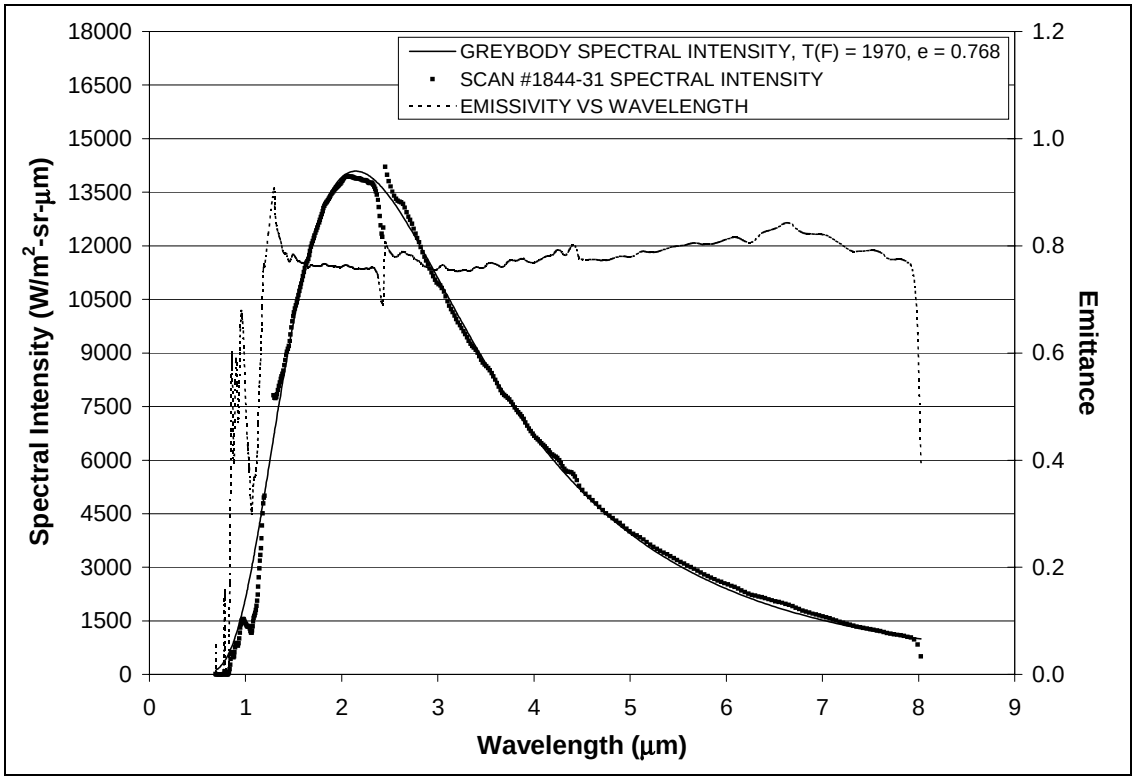

Figure 28: #1844-31, RCG Over TUFI, 2000°F Condition, 15in Nozzle

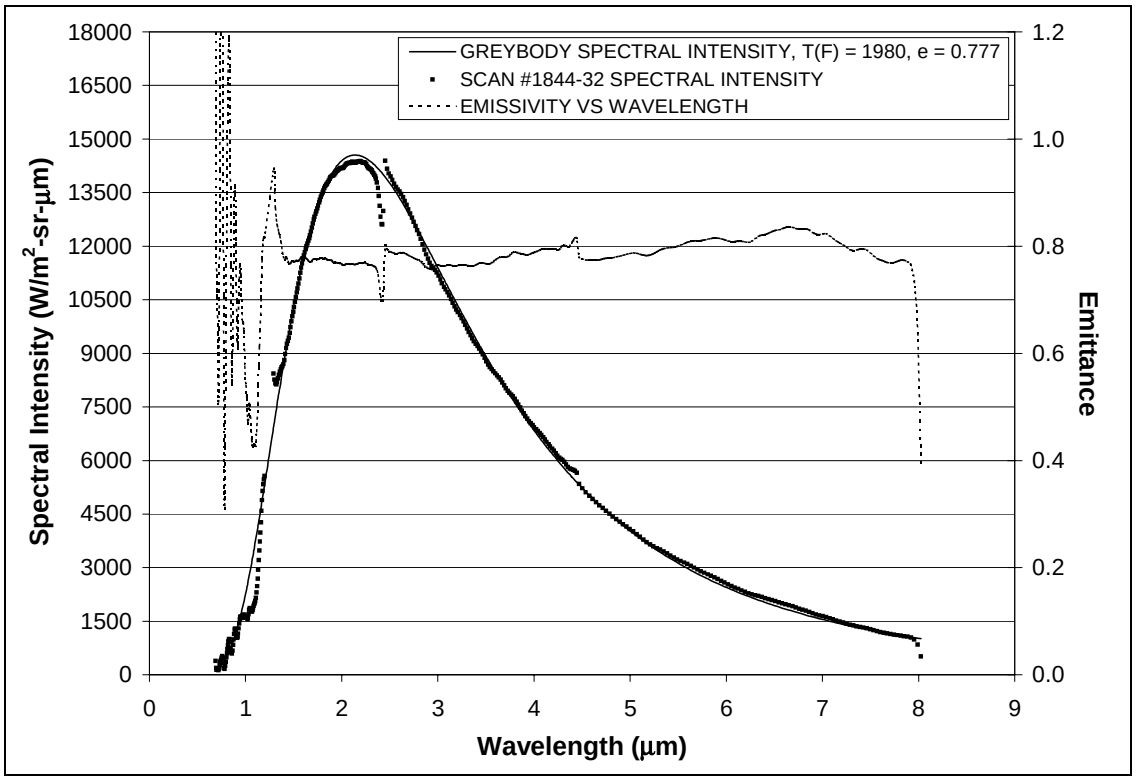

Figure 29: #1844-32, RCG Over TUFI, 2000°F Condition, 15in Nozzle

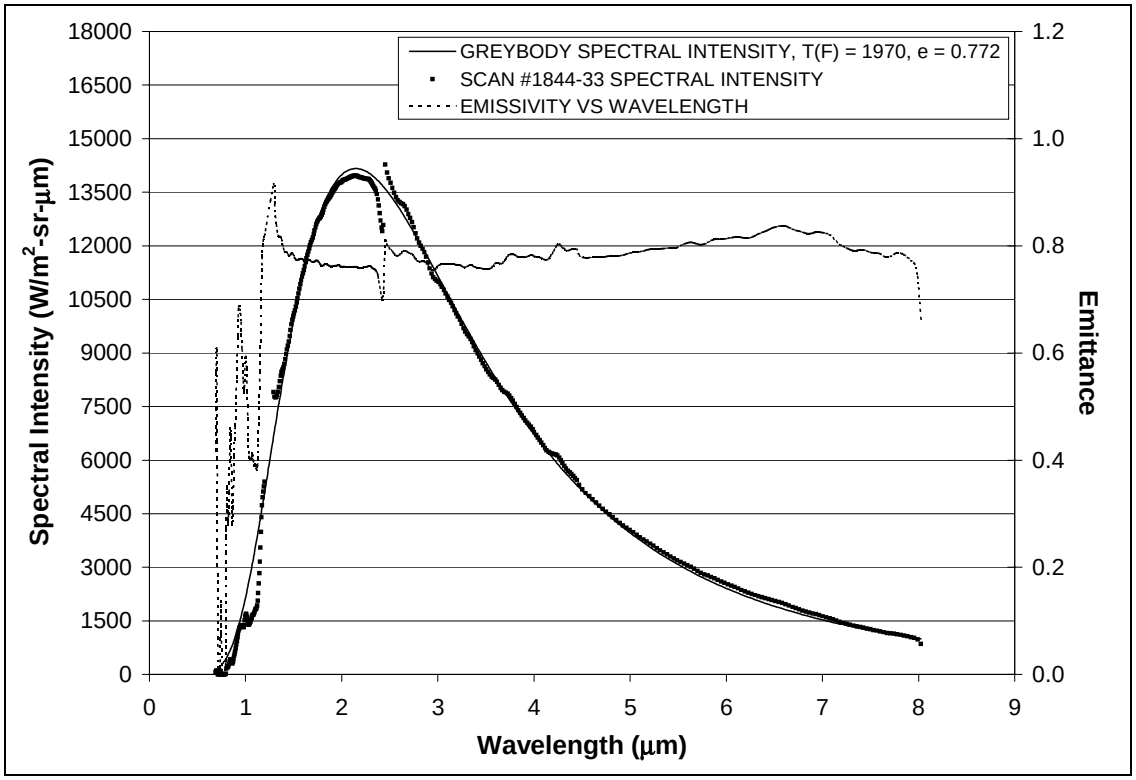

Figure 30: #1844-33, RCG Over TUFI, 2000°F Condition, 15in Nozzle

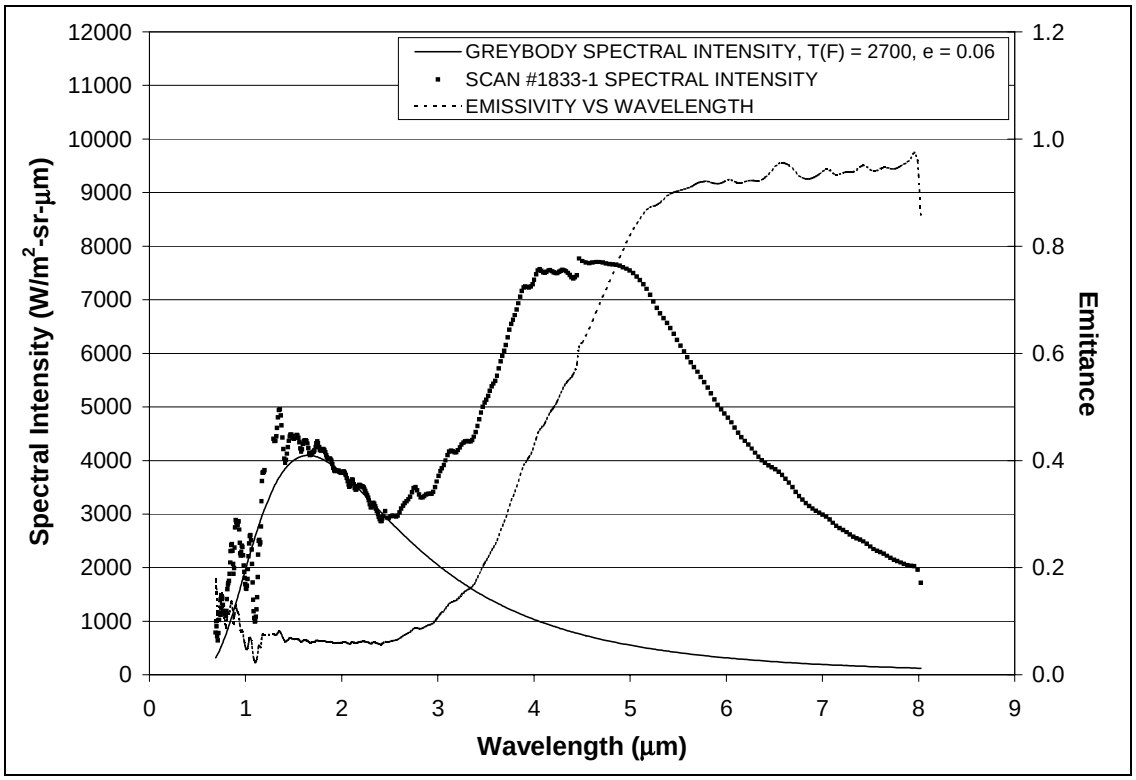

Figure 31: #1833-1, Bare LI-900, 2000°F Condition, 5in Nozzle

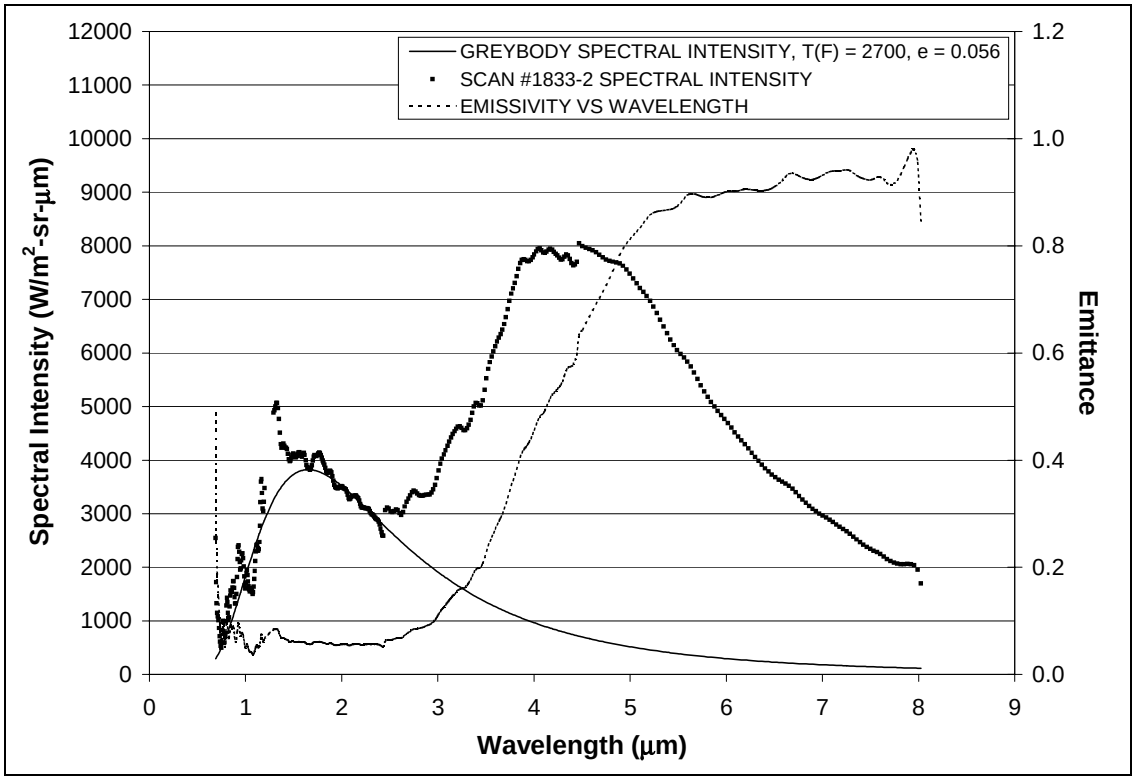

Figure 32: #1833-2, Bare LI-900, 2000°F Condition, 5in Nozzle

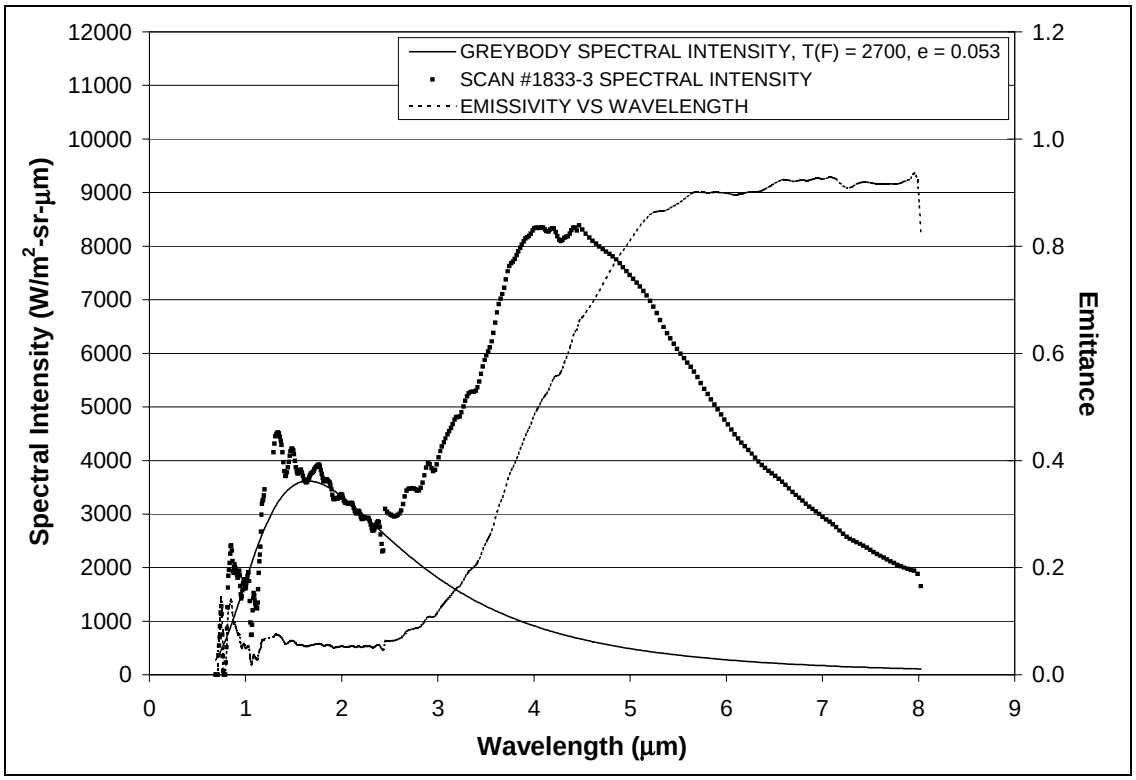

Figure 33: #1833-3, Bare LI-900, 2000°F Condition, 5in Nozzle

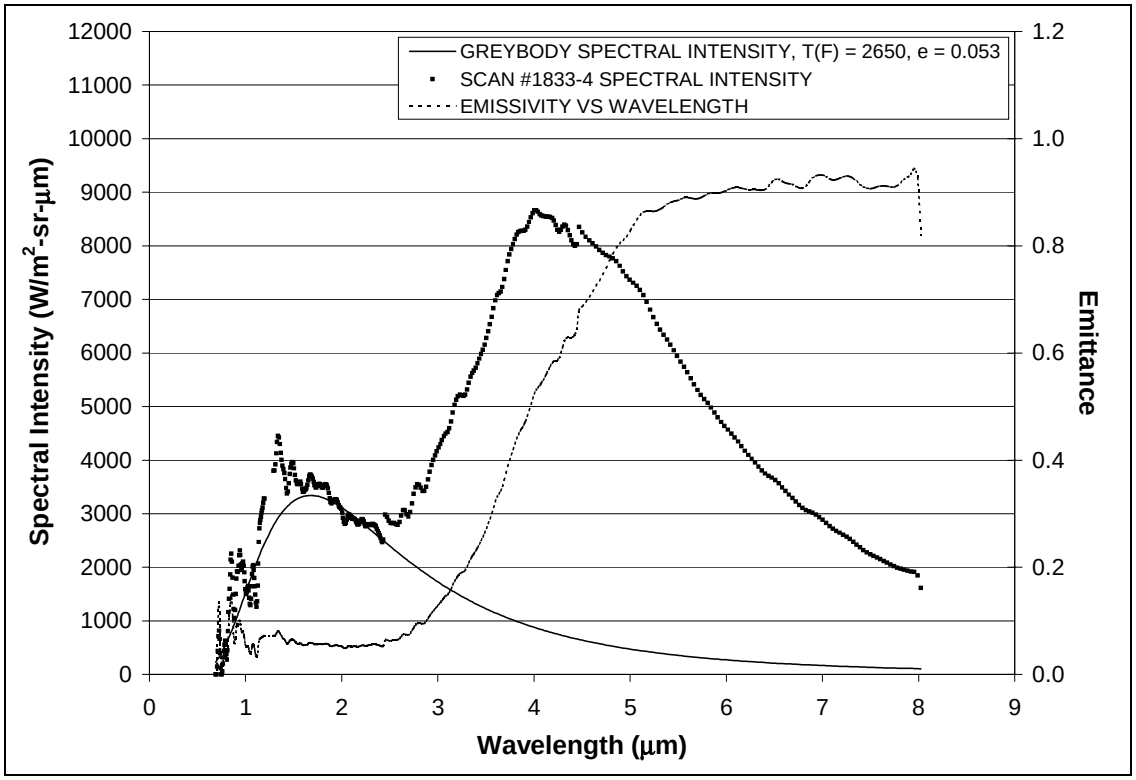

Figure 34: #1833-4, Bare LI-900, 2000°F Condition, 5in Nozzle

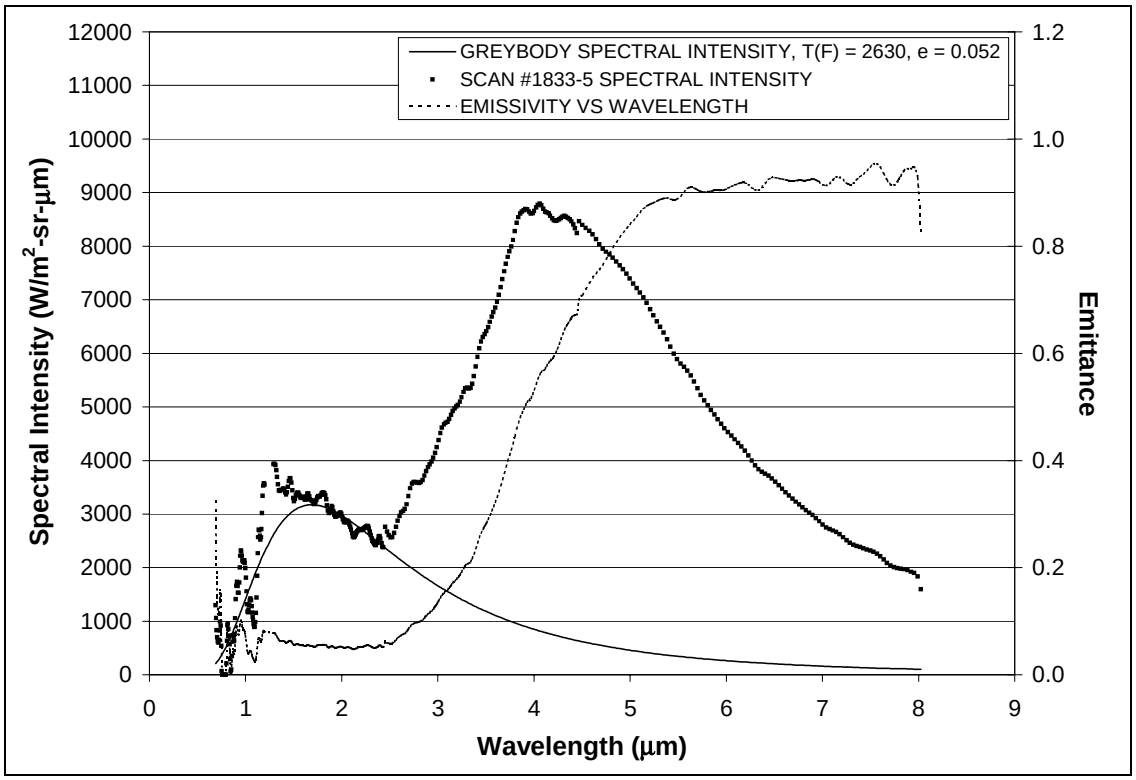

Figure 35: #1833-5, Bare LI-900, 2000°F Condition, 5in Nozzle

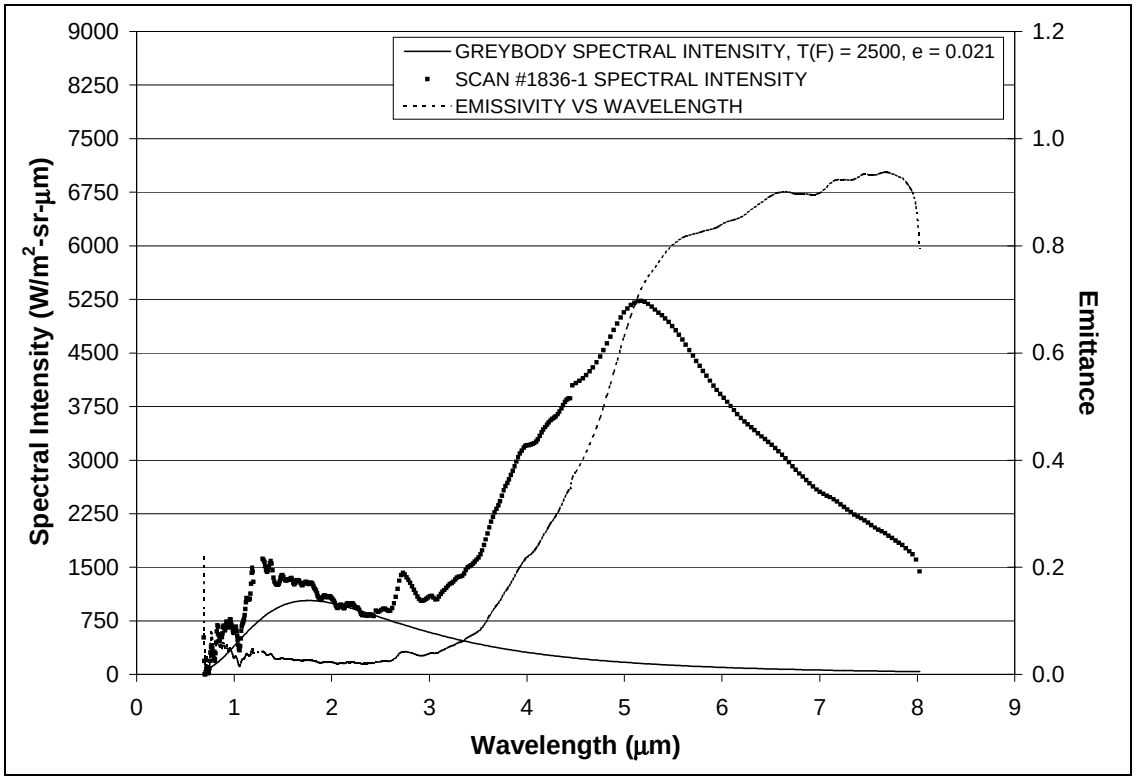

Figure 36: #1836-1, Bare LI-900, 1600°F Condition, 15in Nozzle

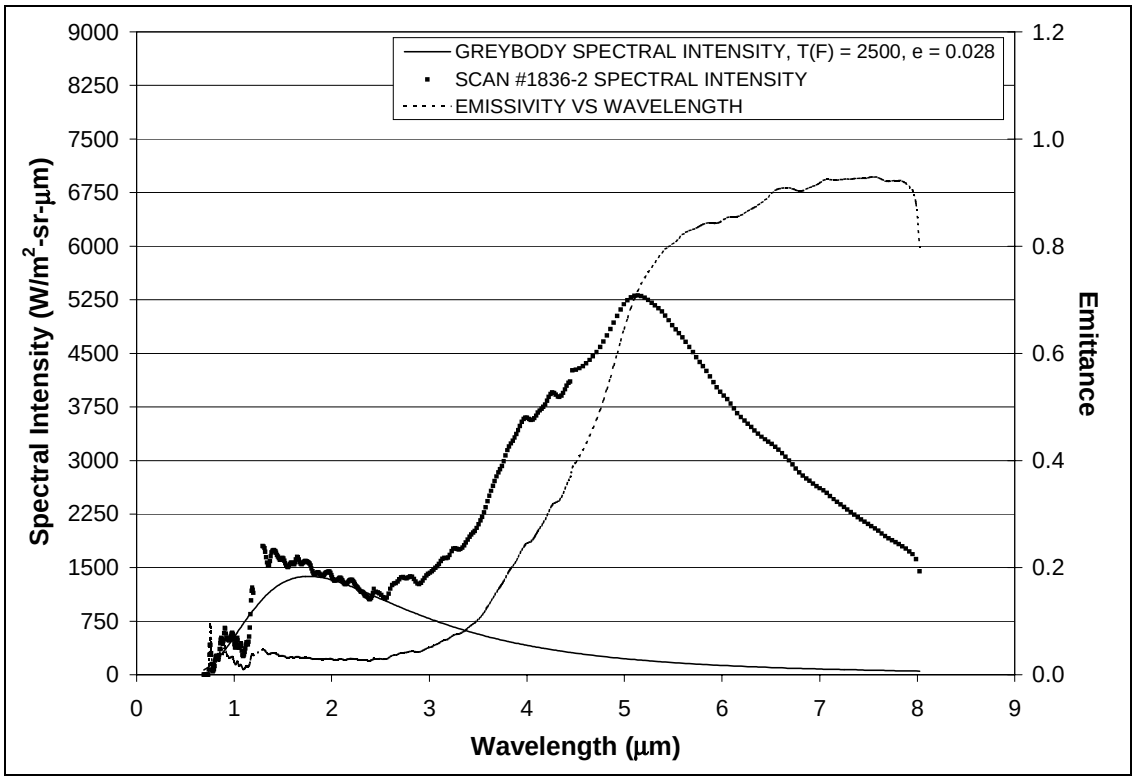

Figure 37: #1836-2, Bare LI-900, 1600°F Condition, 15in Nozzle

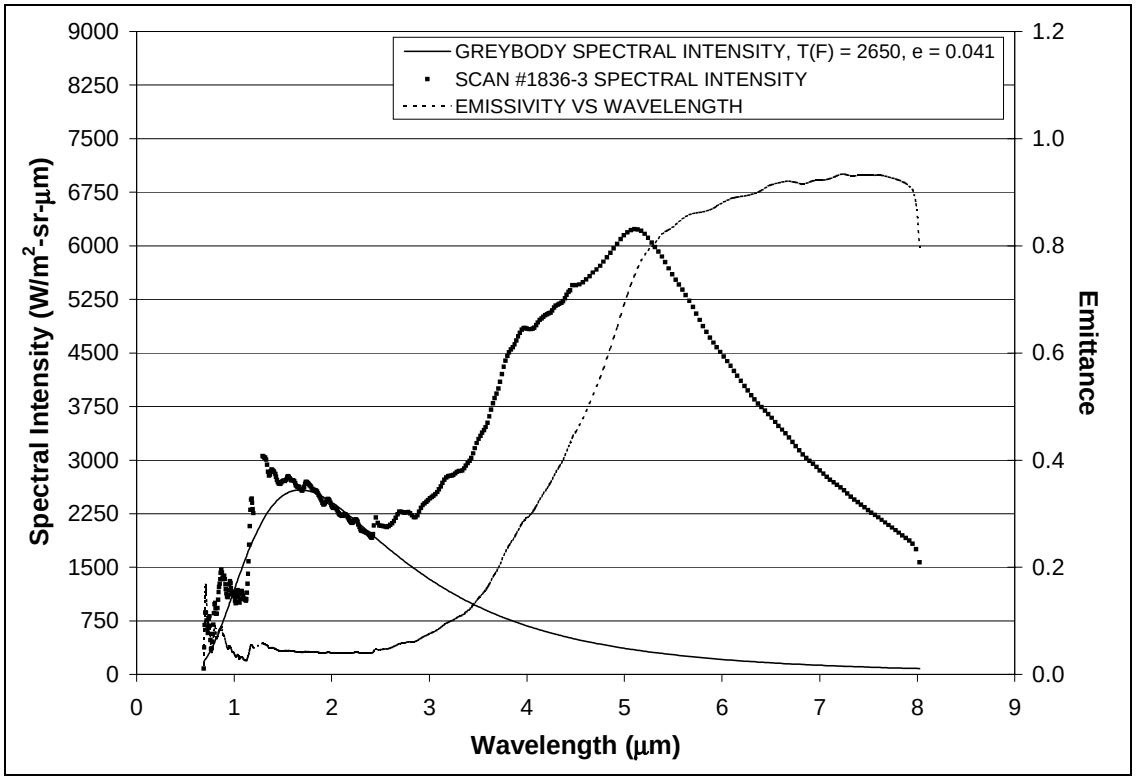

Figure 38: #1836-3, Bare LI-900, 1700°F Condition, 15in Nozzle

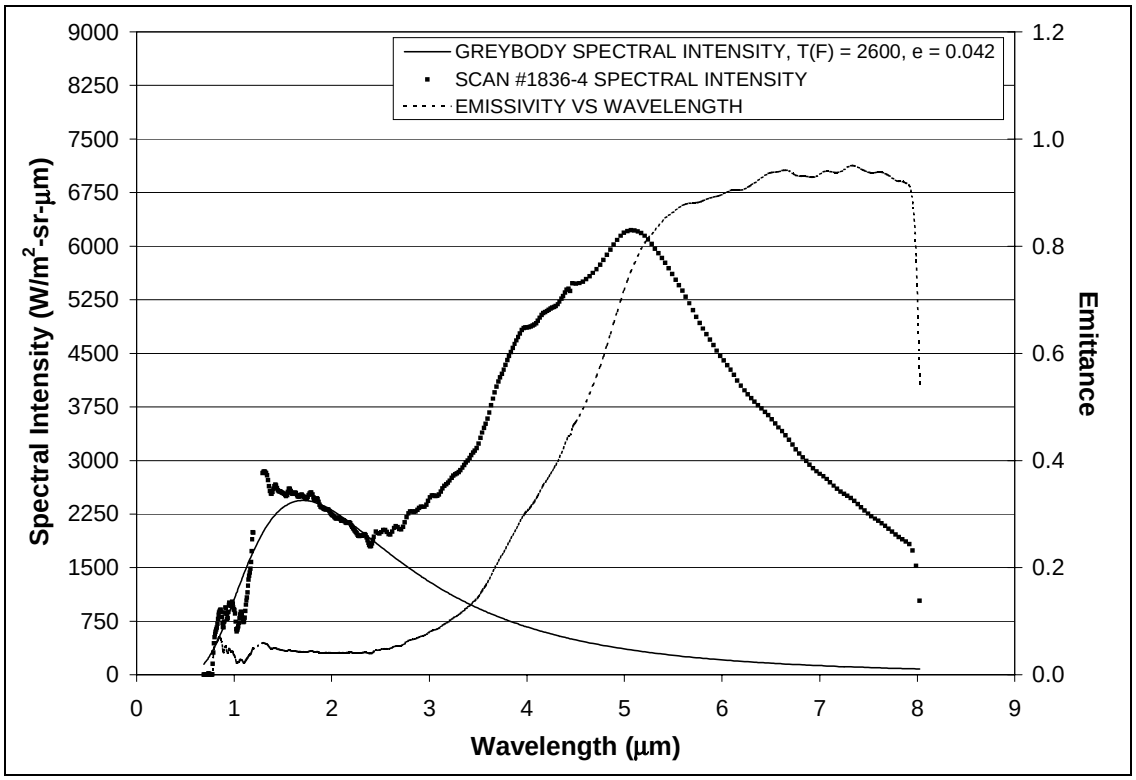

Figure 39: #1836-4, Bare LI-900, 1700°F Condition, 15in Nozzle

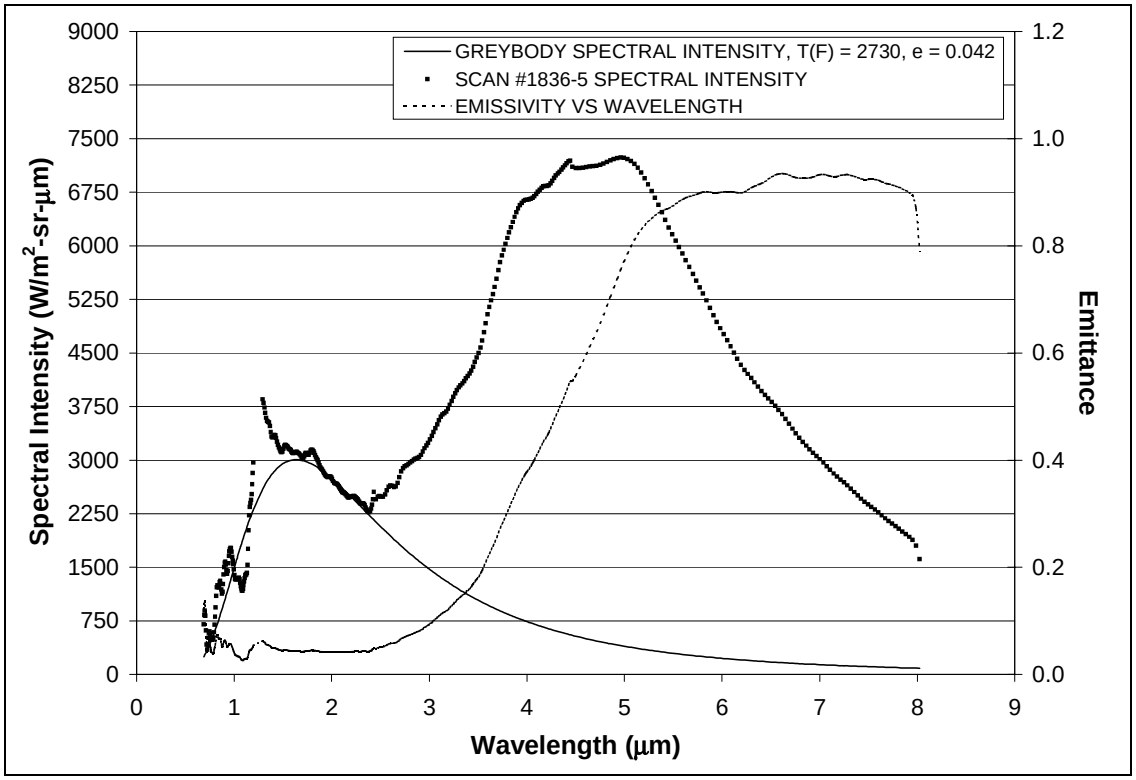

Figure 40: #1836-5, Bare LI-900, 1800°F Condition, 15in Nozzle

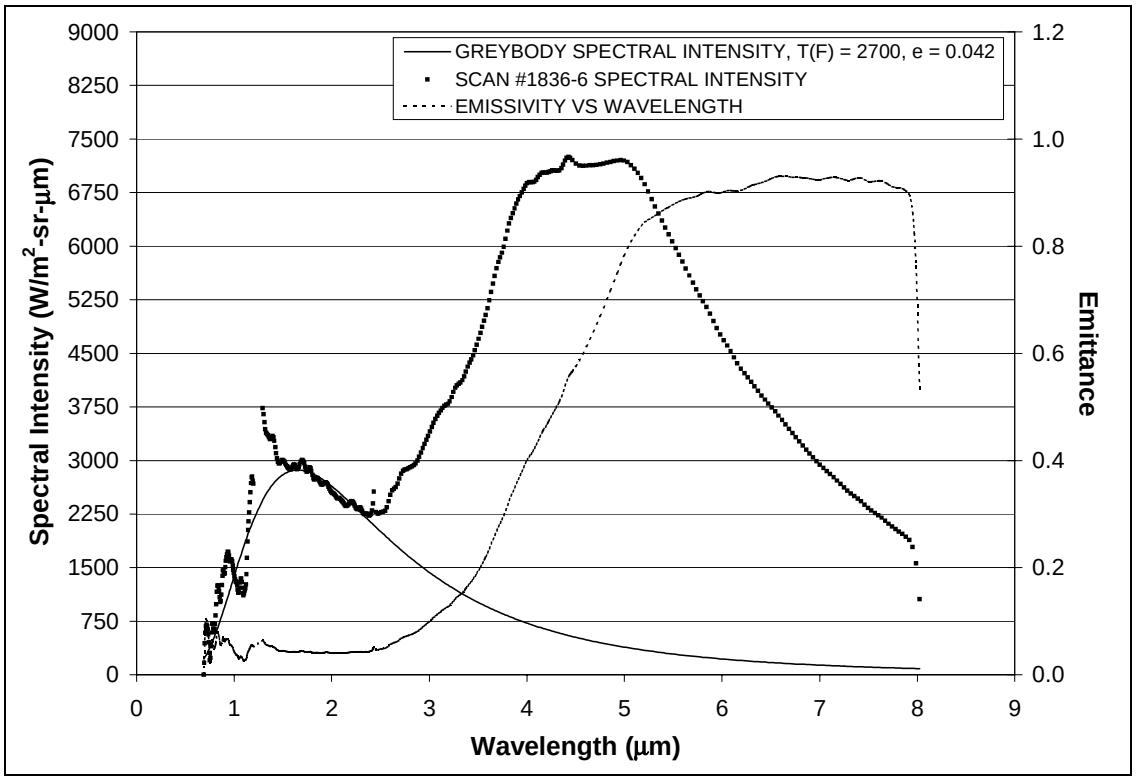

Figure 41: #1836-6, Bare LI-900, 1800°F Condition, 15in Nozzle

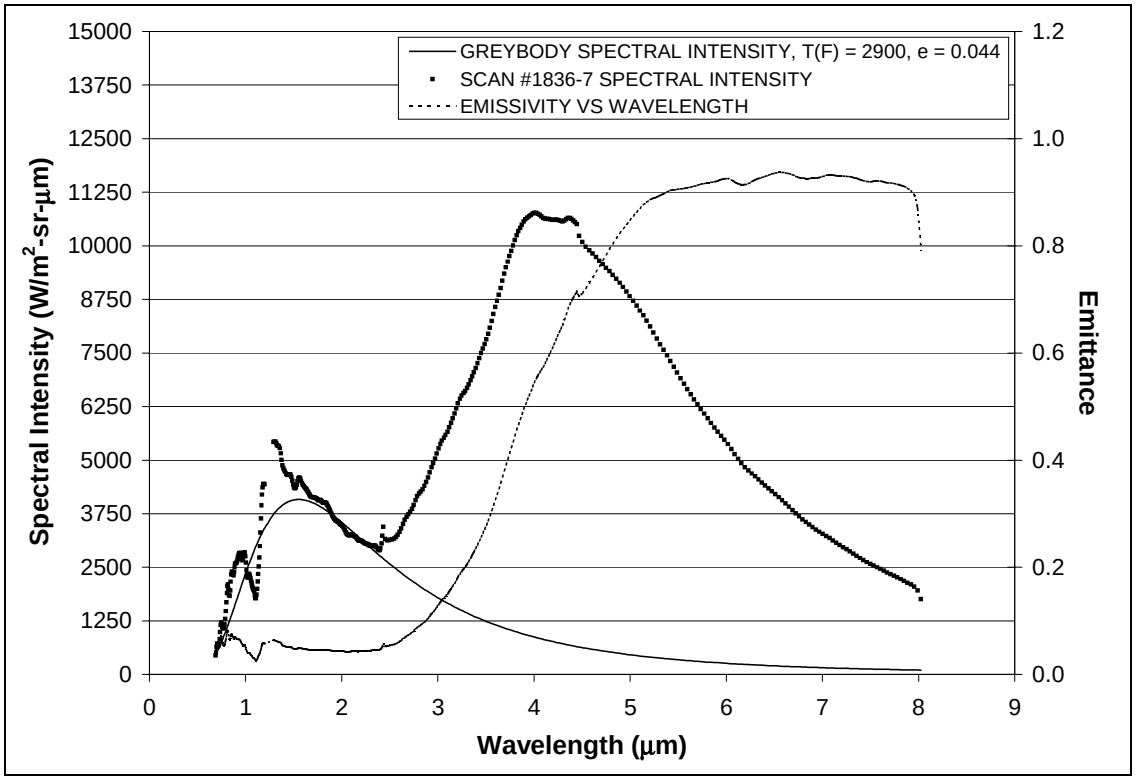

Figure 42: #1836-7, Bare LI-900, 2000°F Condition, 15in Nozzle

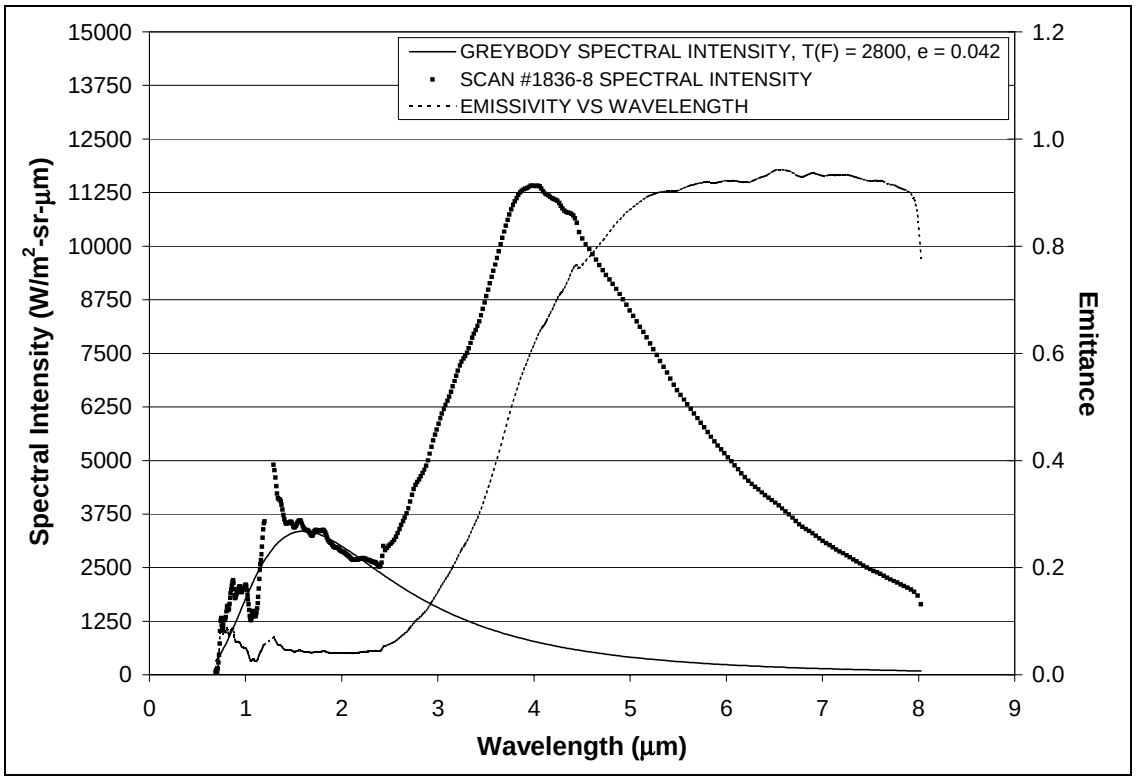

Figure 43: #1836-8, Bare LI-900, 2000°F Condition, 15in Nozzle

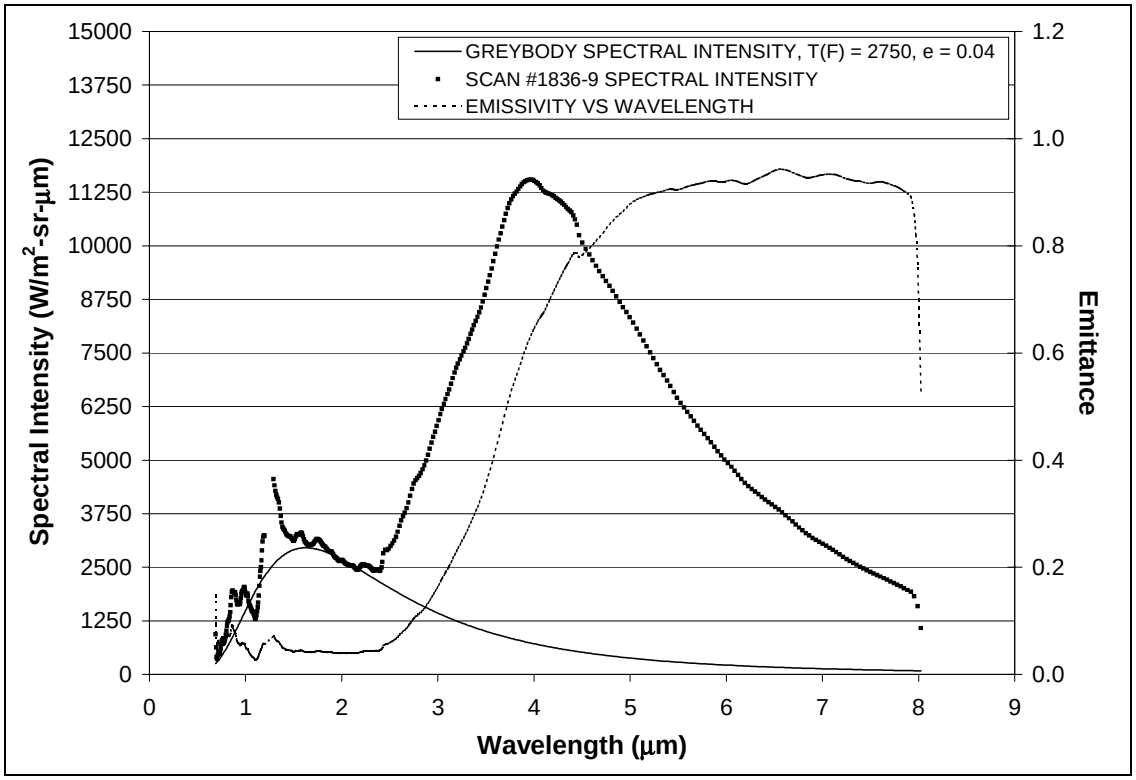

Figure 44: #1836-9, Bare LI-900, 2000°F Condition, 15in Nozzle

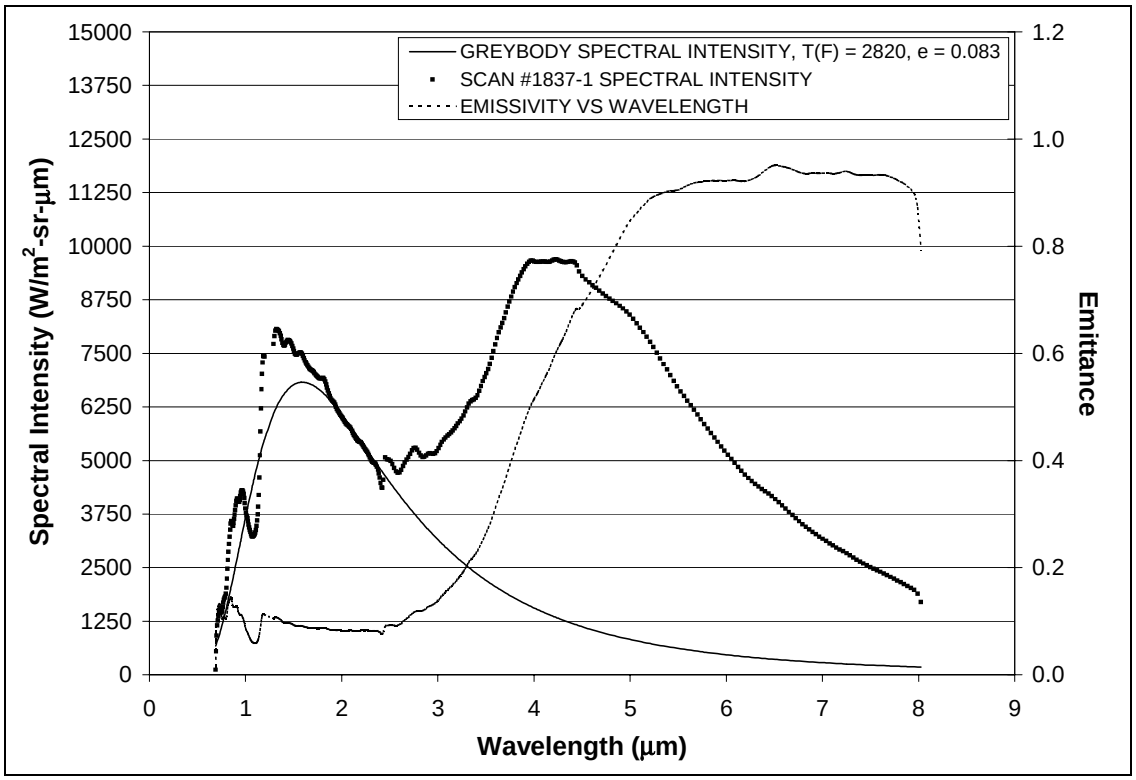

Figure 45: #1837-1, Bare LI-900, 2000°F Condition, 15in Nozzle

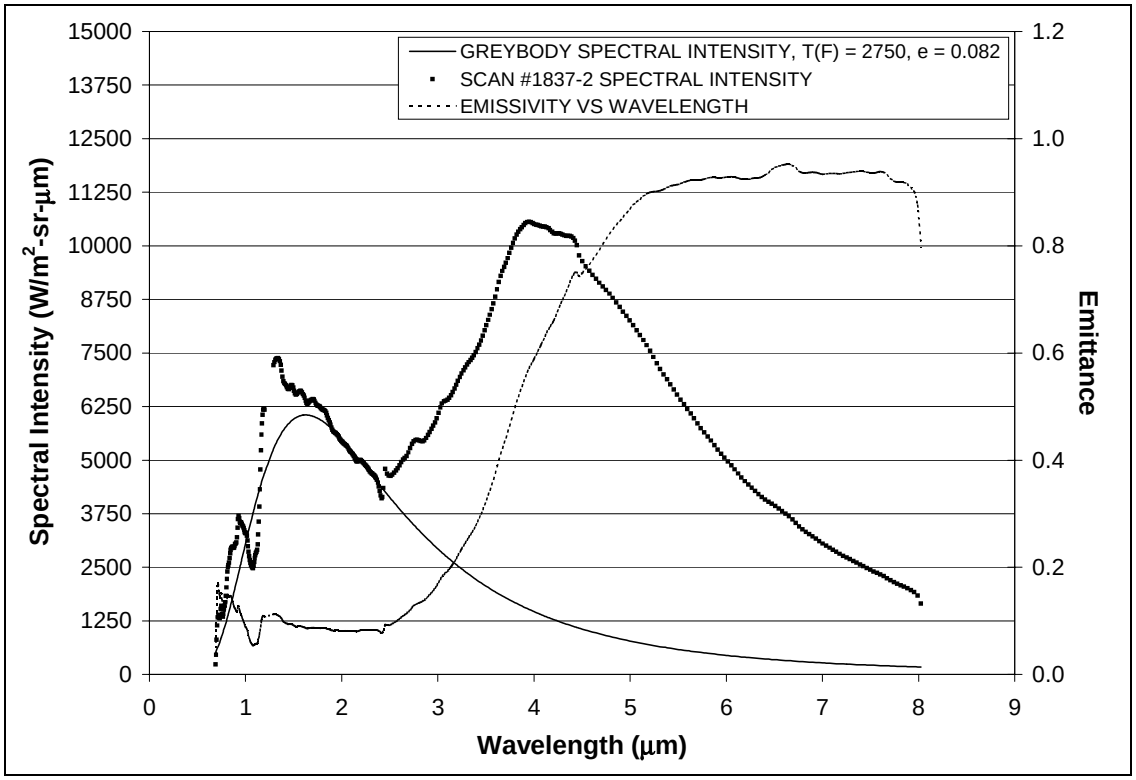

Figure 46: #1837-2, Bare LI-900, 2000°F Condition, 15in Nozzle

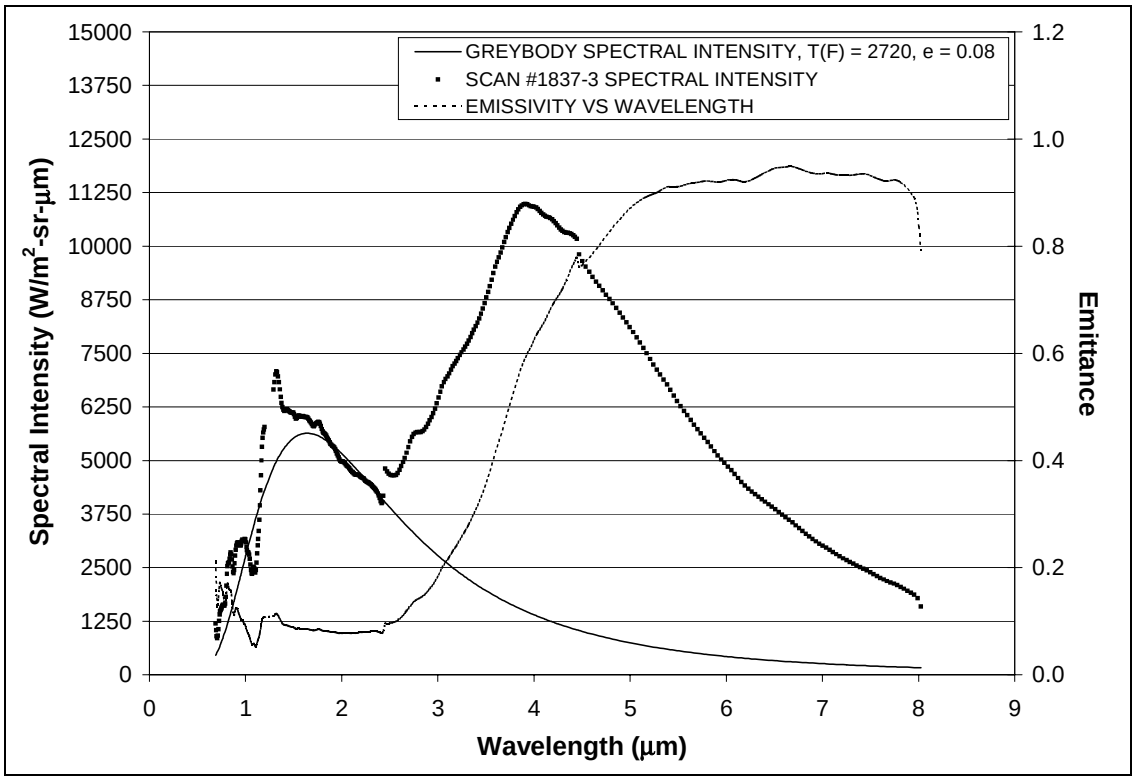

Figure 47: #1837-3, Bare LI-900, 2000°F Condition, 15in Nozzle

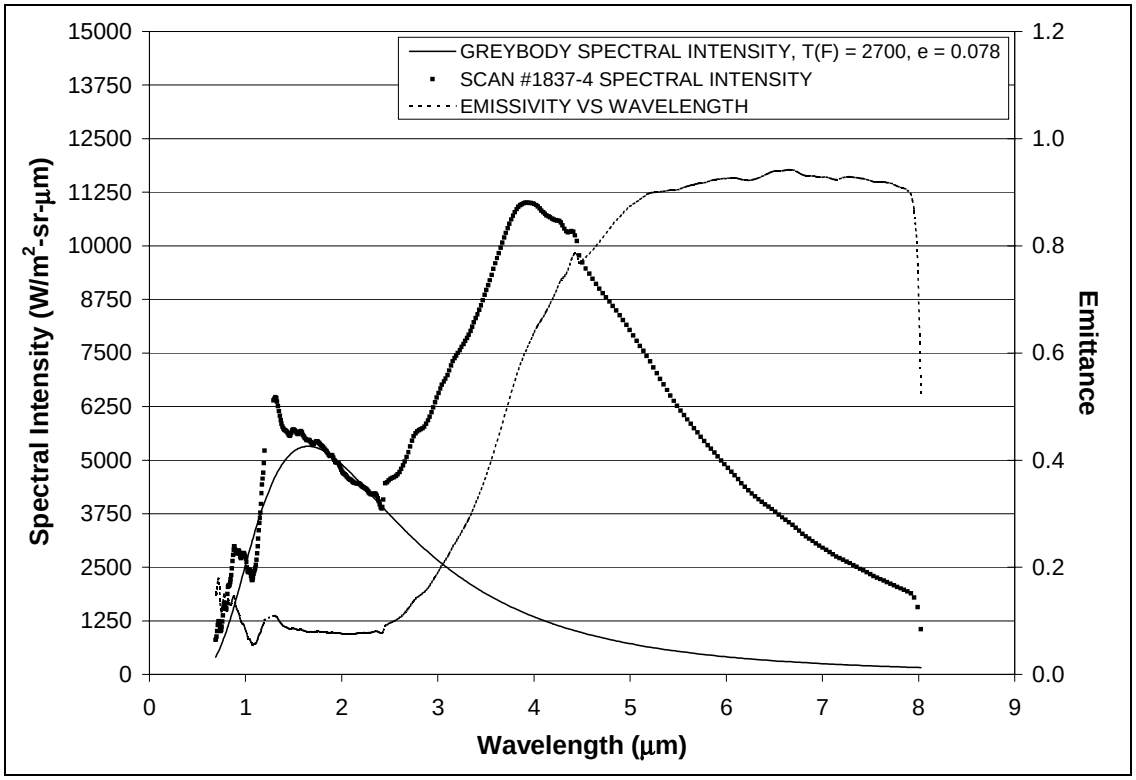

Figure 48: #1837-4, Bare LI-900, 2000°F Condition, 15in Nozzle

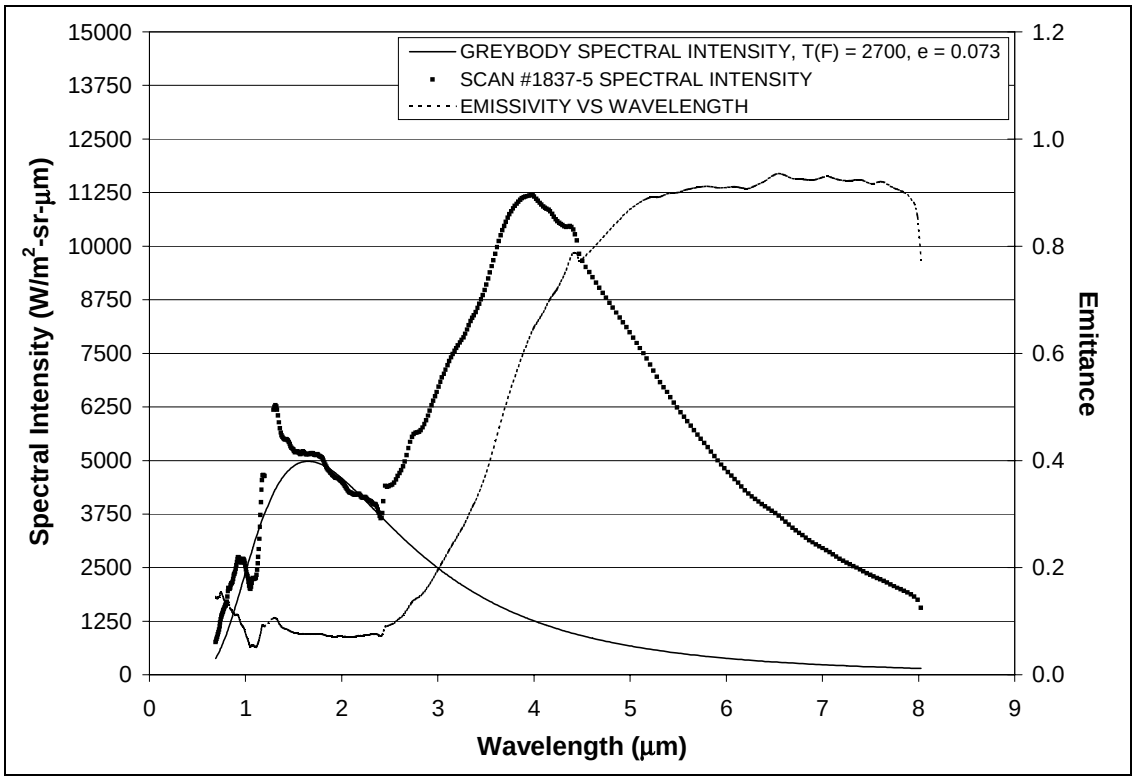

Figure 49: #1837-5, Bare LI-900, 2000°F Condition, 15in Nozzle

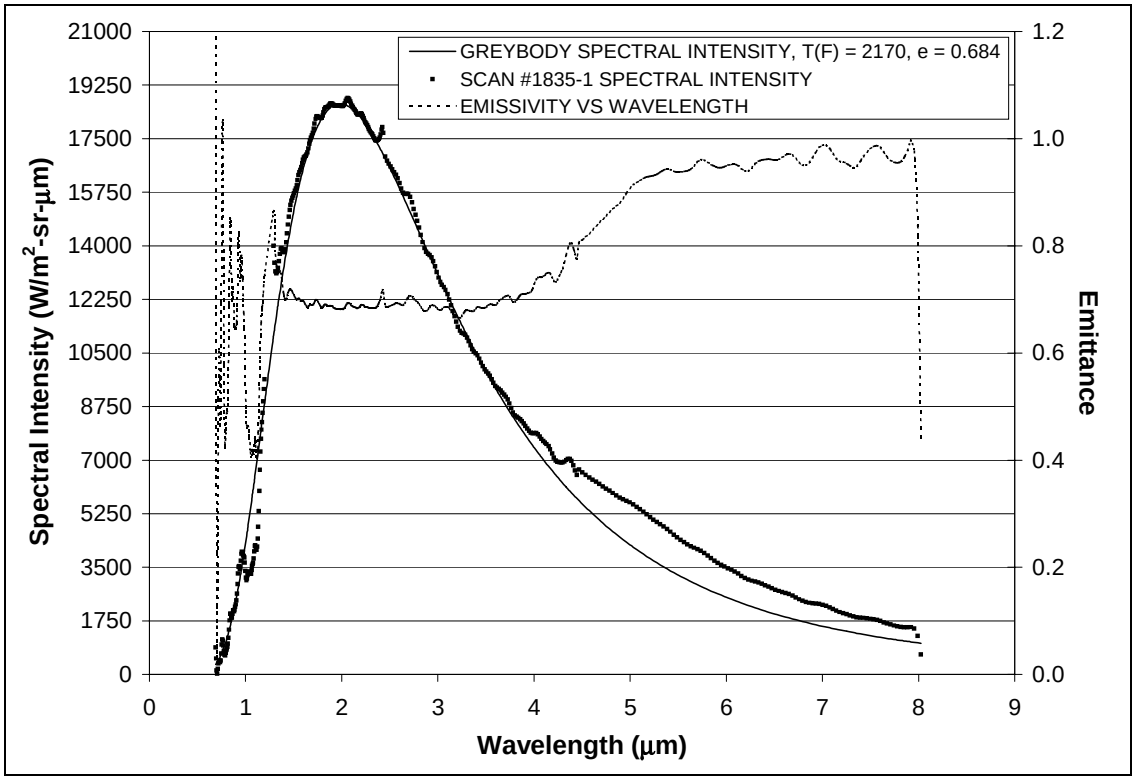

Figure 50: #1835-1, Bare Densified LI-900, 2000°F Condition, 5in Nozzle

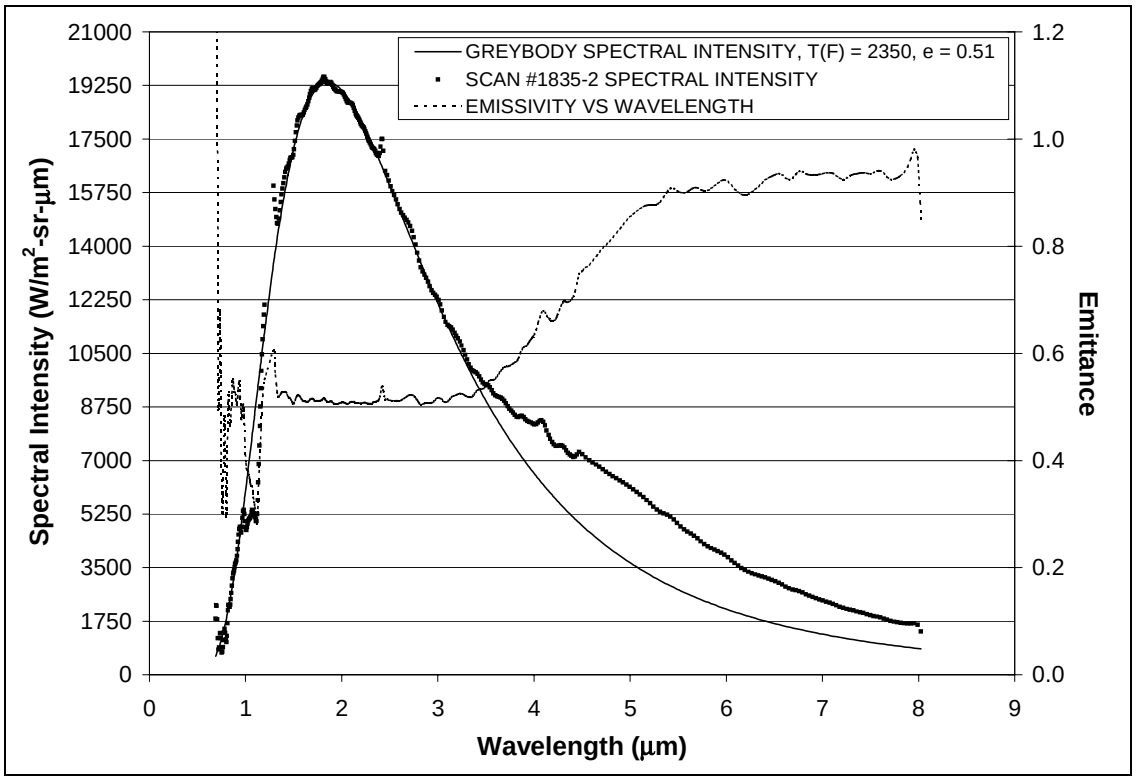

Figure 51: #1835-2, Bare Densified LI-900, 2000°F Condition, 5in Nozzle

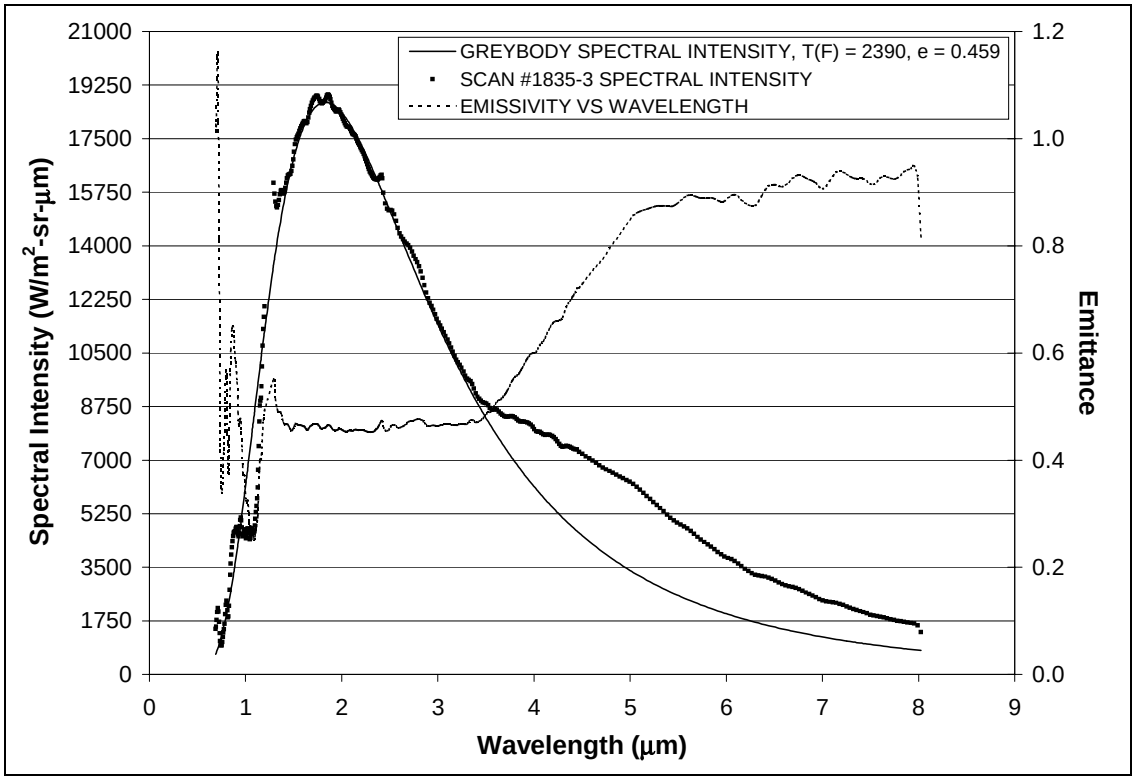

Figure 52: #1835-3, Bare Densified LI-900, 2000°F Condition, 5in Nozzle

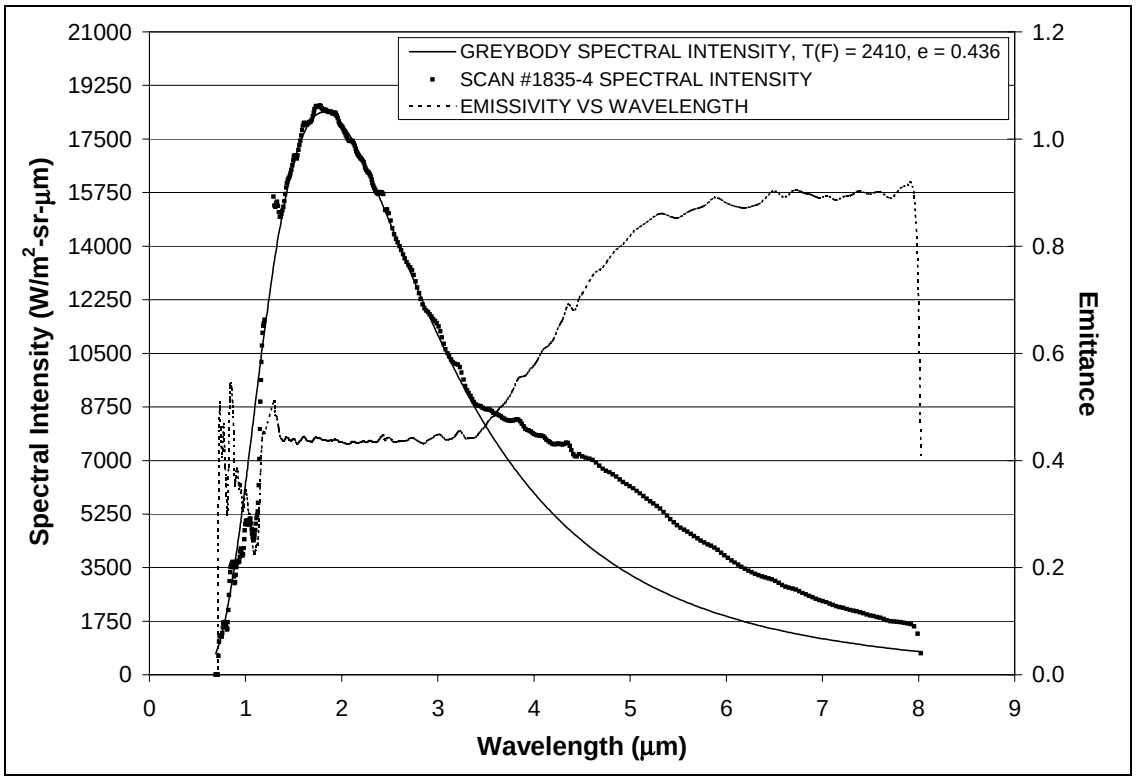

Figure 53: #1835-4, Bare Densified LI-900, 2000°F Condition, 5in Nozzle

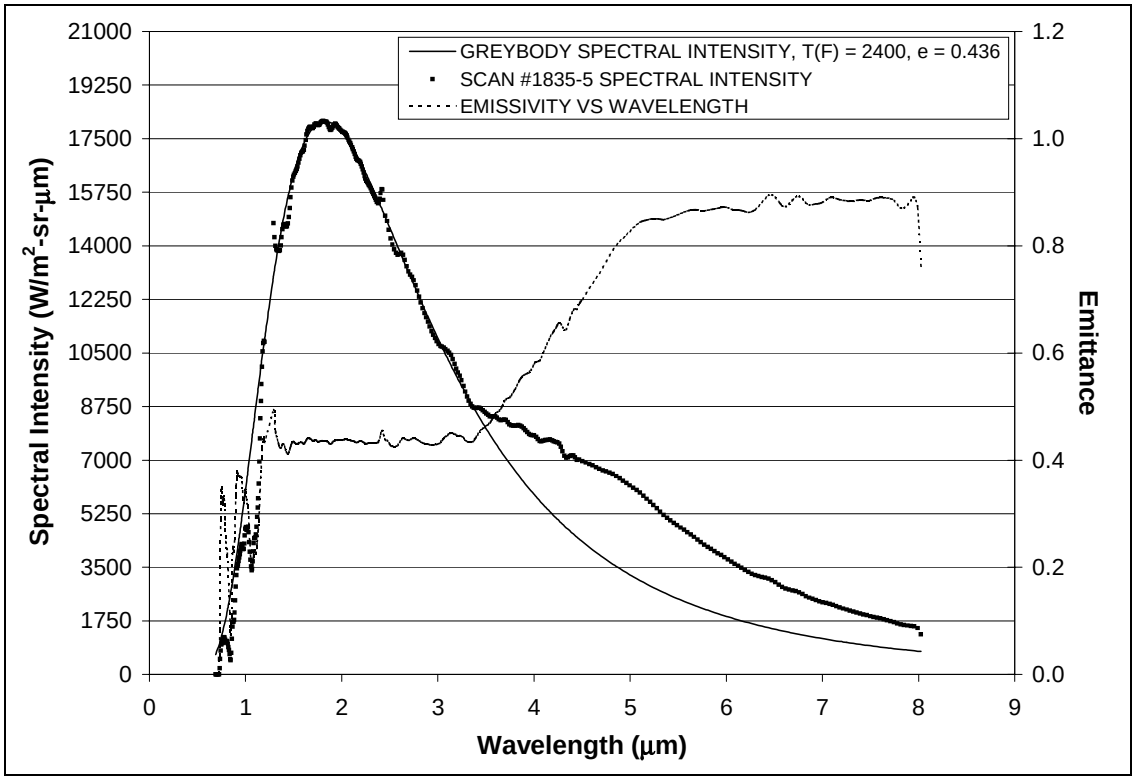

Figure 54: #1835-5, Bare Densified LI-900, 2000°F Condition, 5in Nozzle

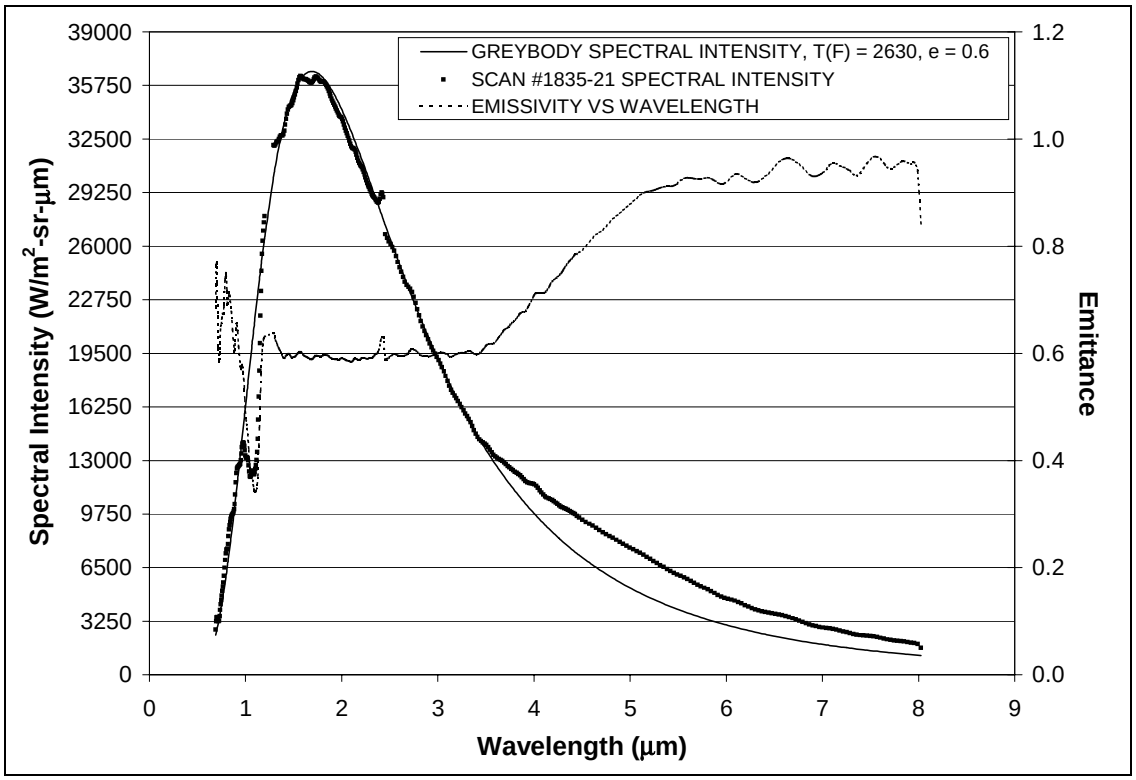

Figure 55: #1835-21, Bare Densified LI-900, 2300°F Condition, 5in Nozzle

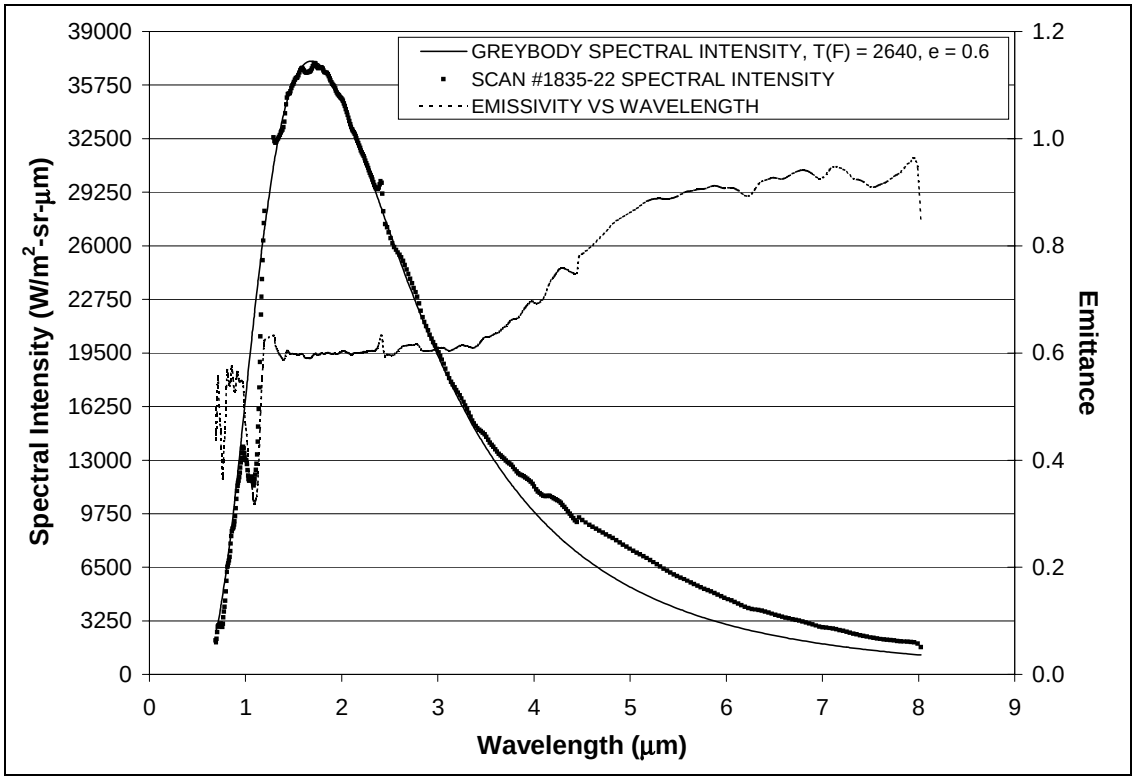

Figure 56: #1835-22, Bare Densified LI-900, 2300°F Condition, 5in Nozzle

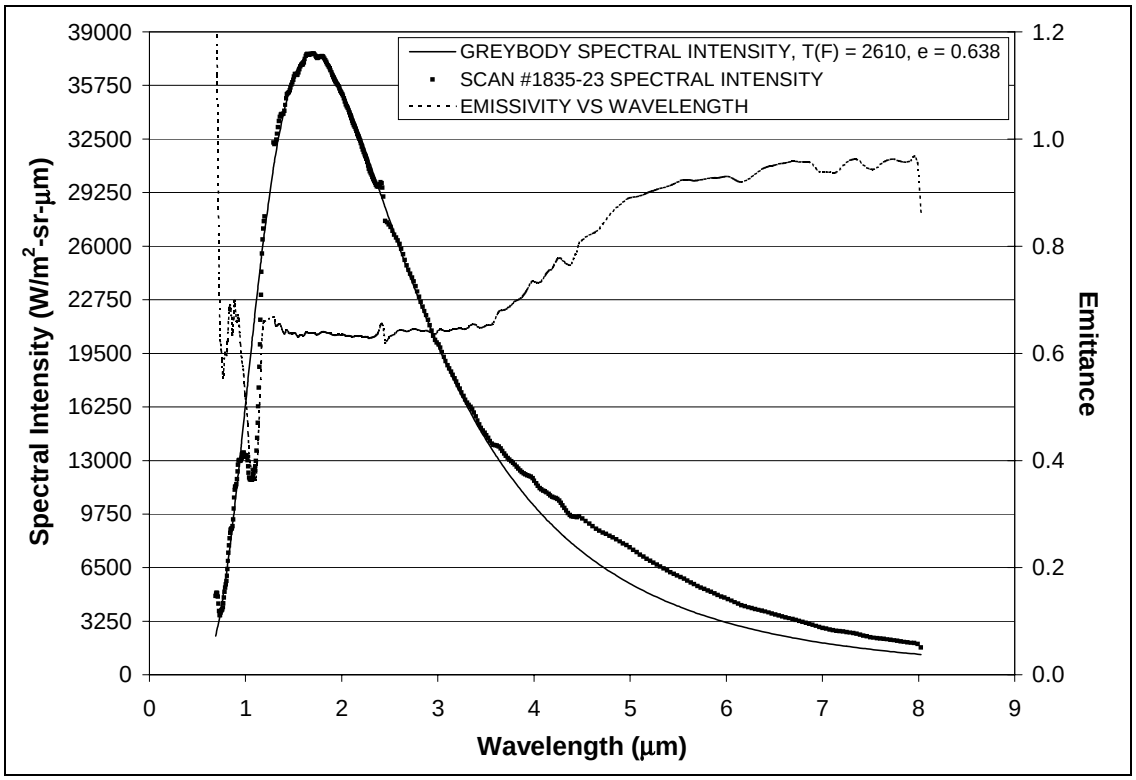

Figure 57: #1835-23, Bare Densified LI-900, 2300°F Condition, 5in Nozzle

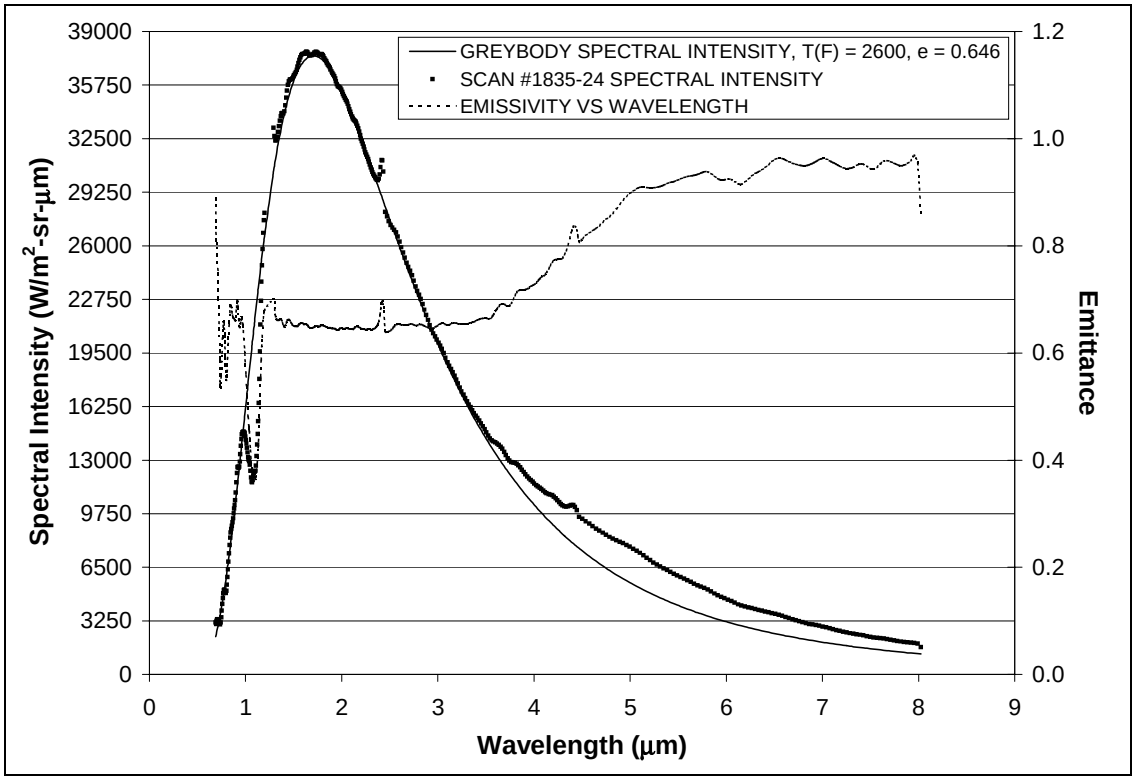

Figure 58: #1835-24, Bare Densified LI-900, 2300°F Condition, 5in Nozzle

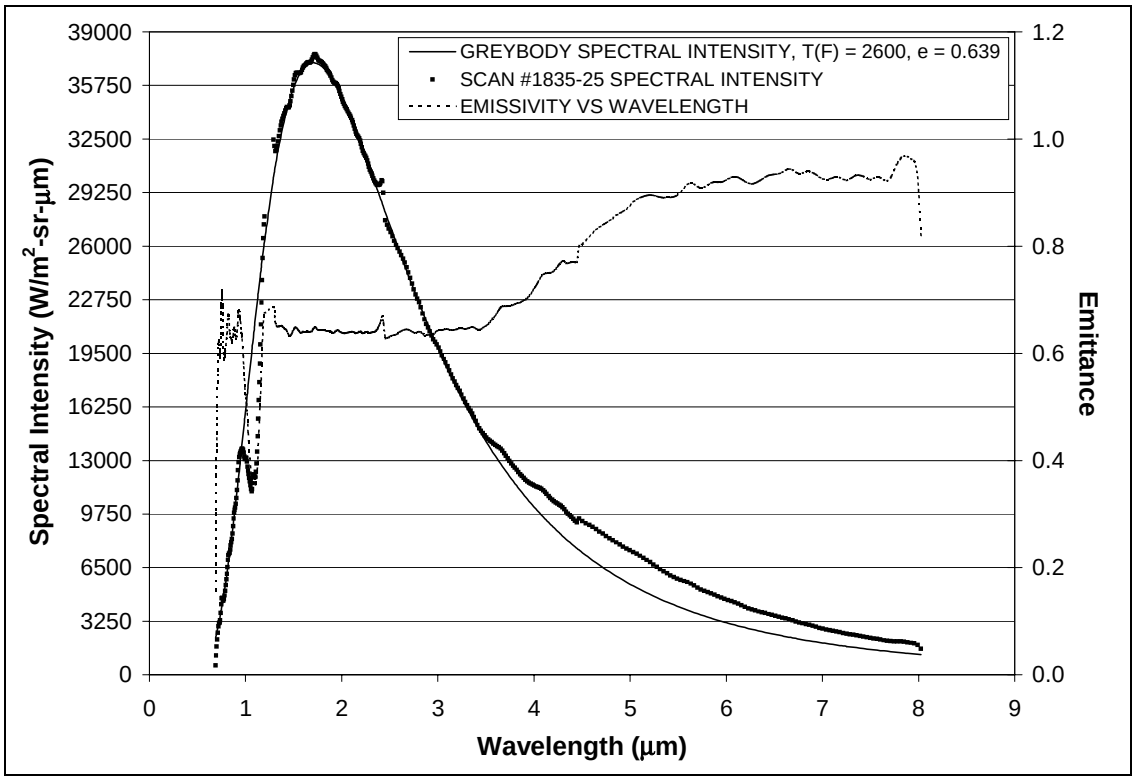

Figure 59: #1835-25, Bare Densified LI-900, 2300°F Condition, 5in Nozzle

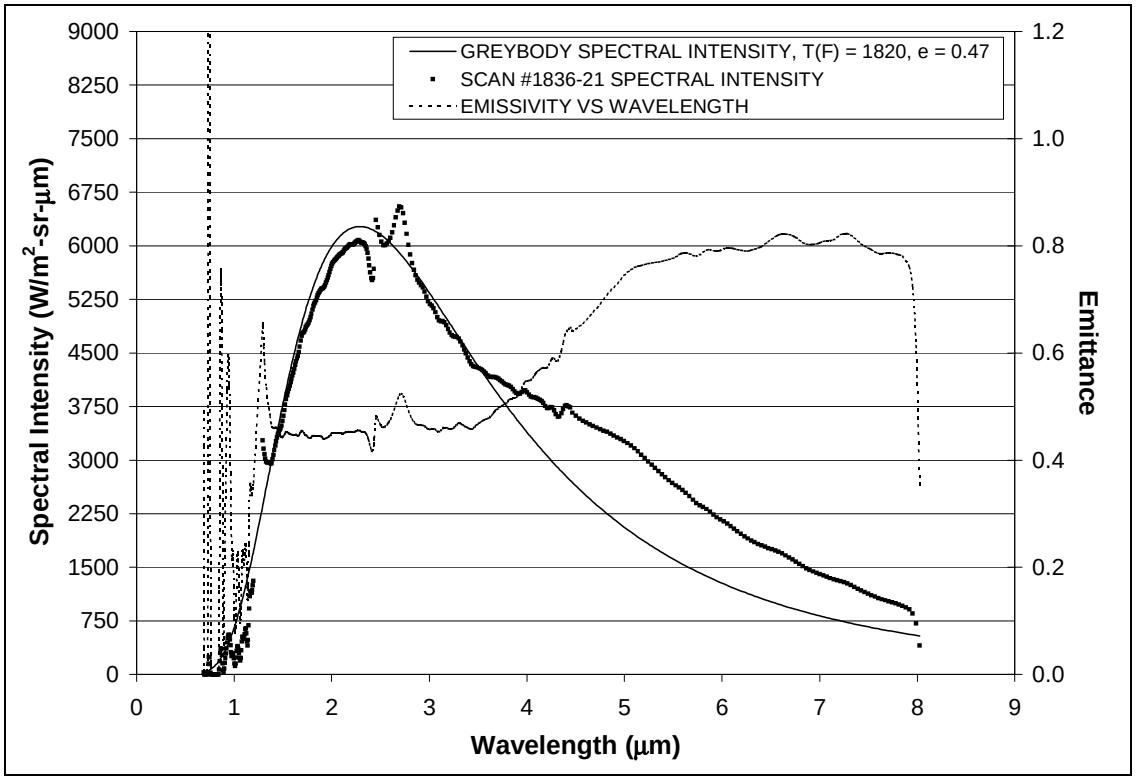

Figure 60: #1836-21, Bare Densified LI-900, 1600°F Condition, 15in Nozzle

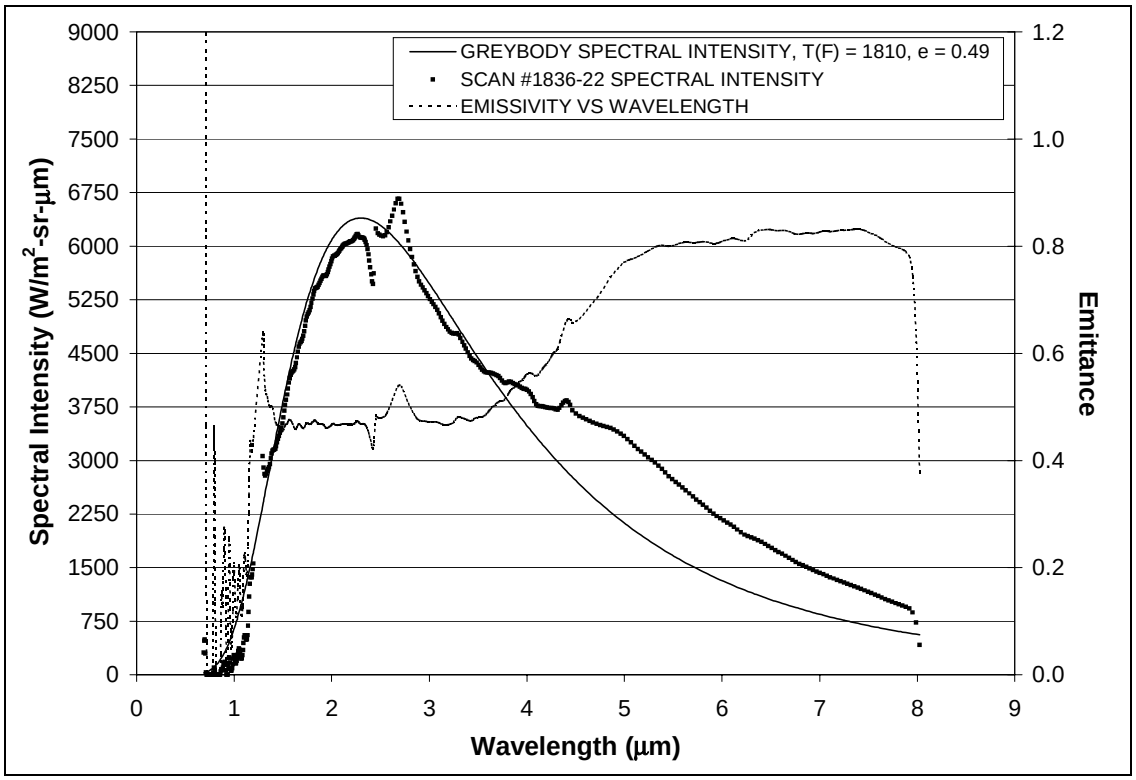

Figure 61: #1836-22, Bare Densified LI-900, 1600°F Condition, 15in Nozzle

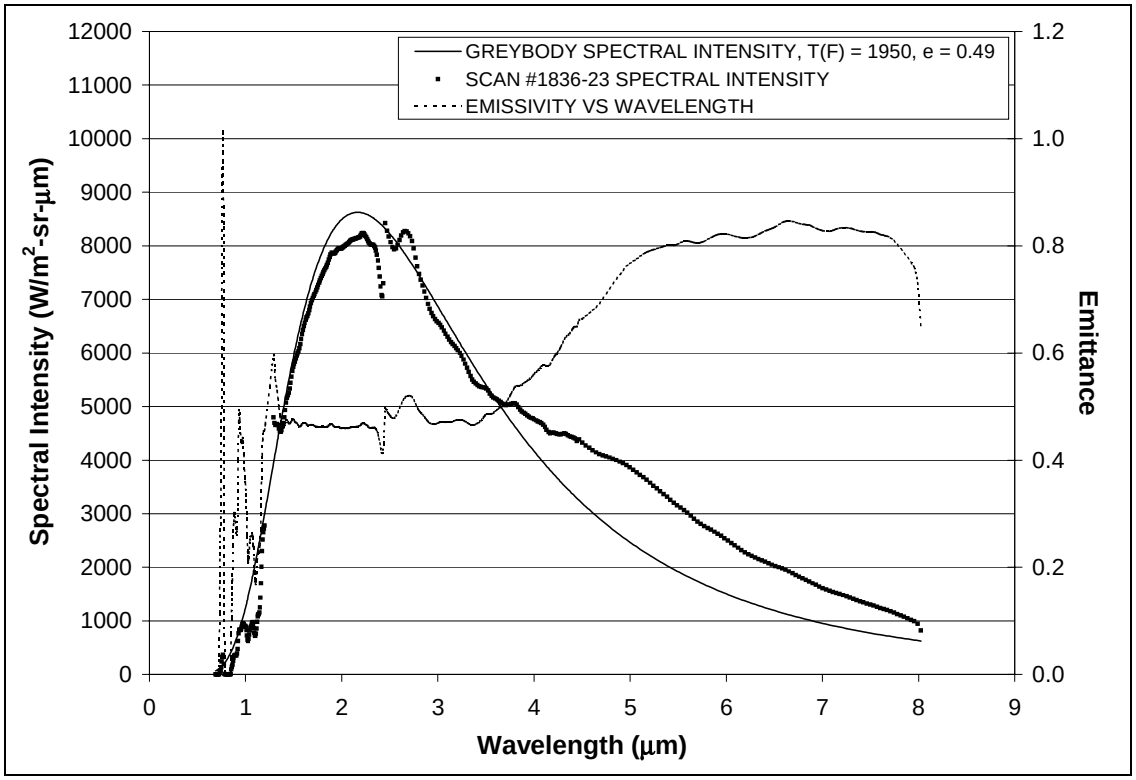

Figure 62: #1836-23, Bare Densified LI-900, 1700°F Condition, 15in Nozzle

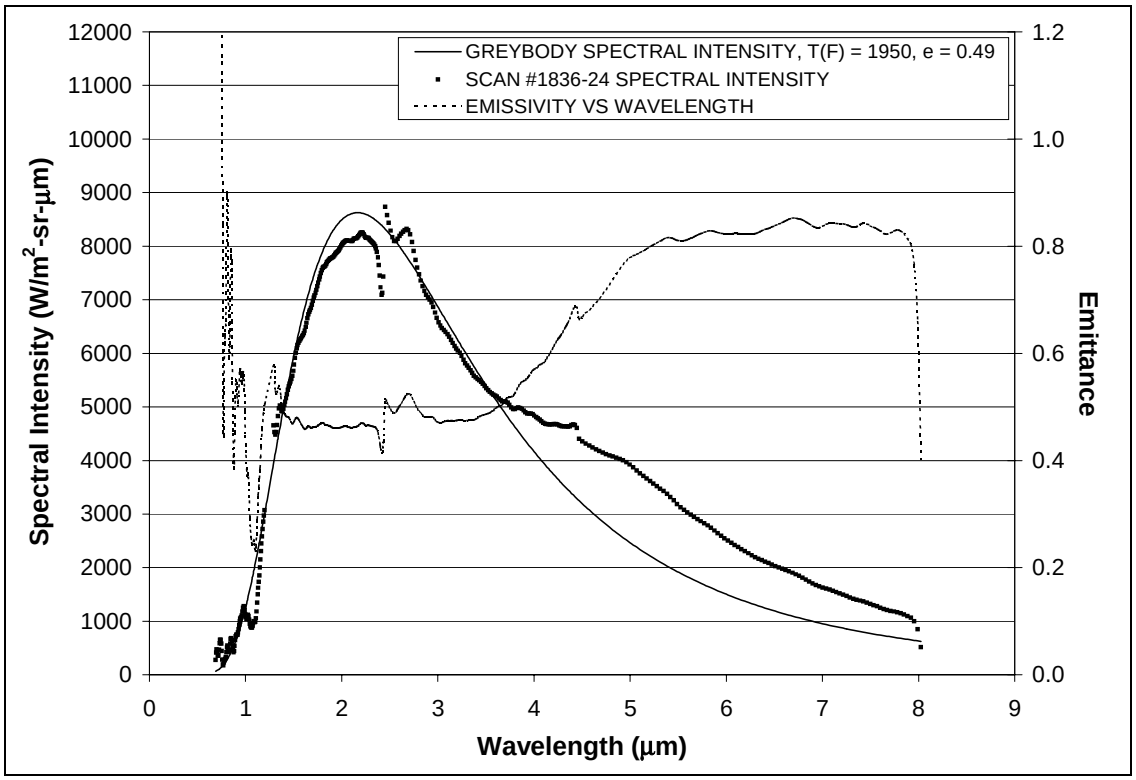

Figure 63: #1836-24, Bare Densified LI-900, 1700°F Condition, 15in Nozzle

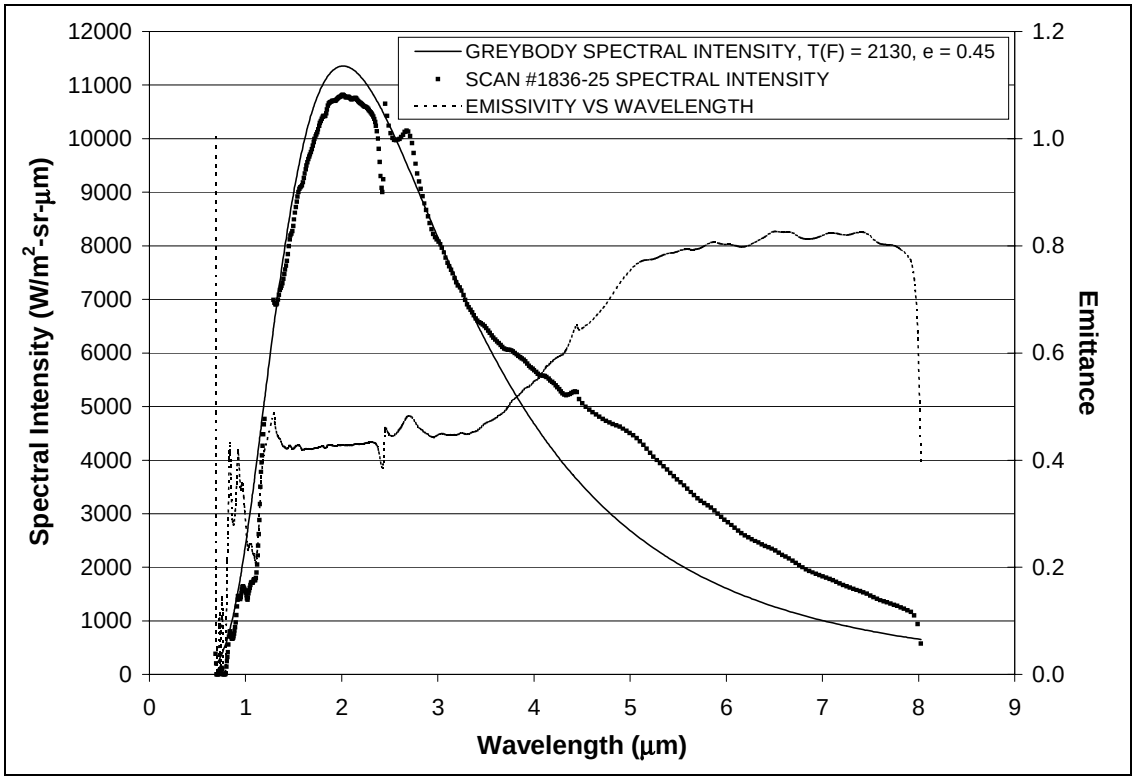

Figure 64: #1836-25, Bare Densified LI-900, 1800°F Condition, 15in Nozzle

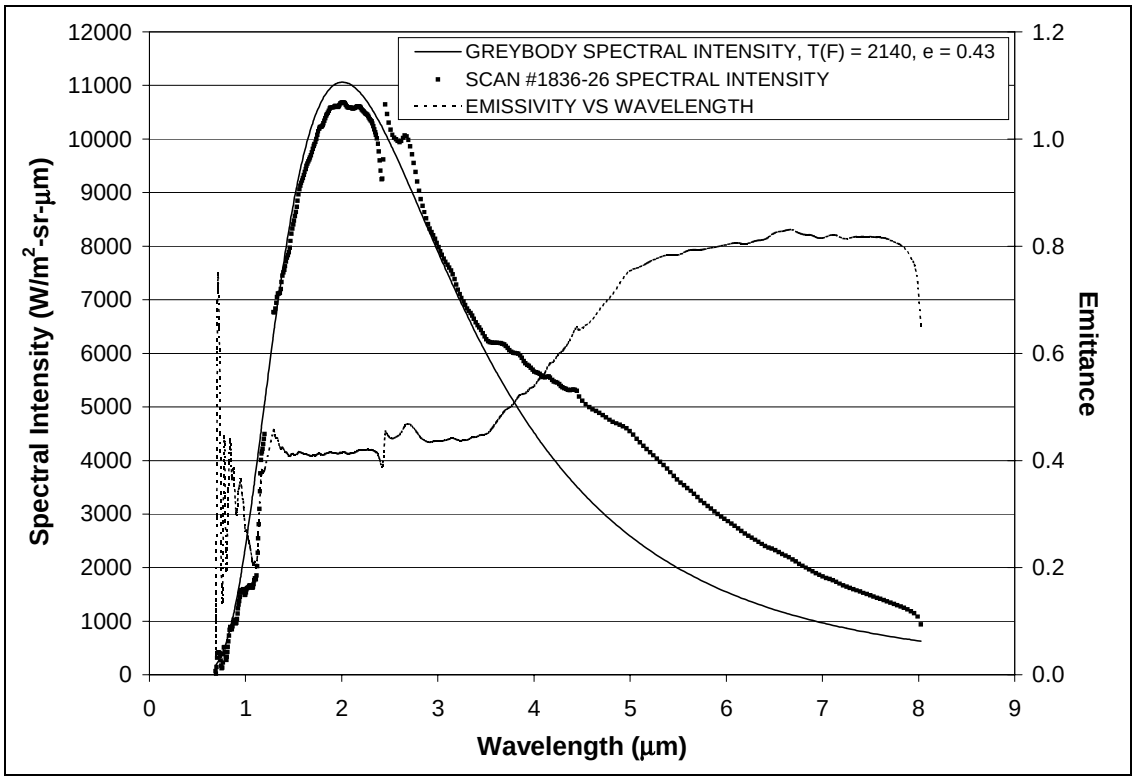

Figure 65: #1836-26, Bare Densified LI-900, 1800°F Condition, 15in Nozzle

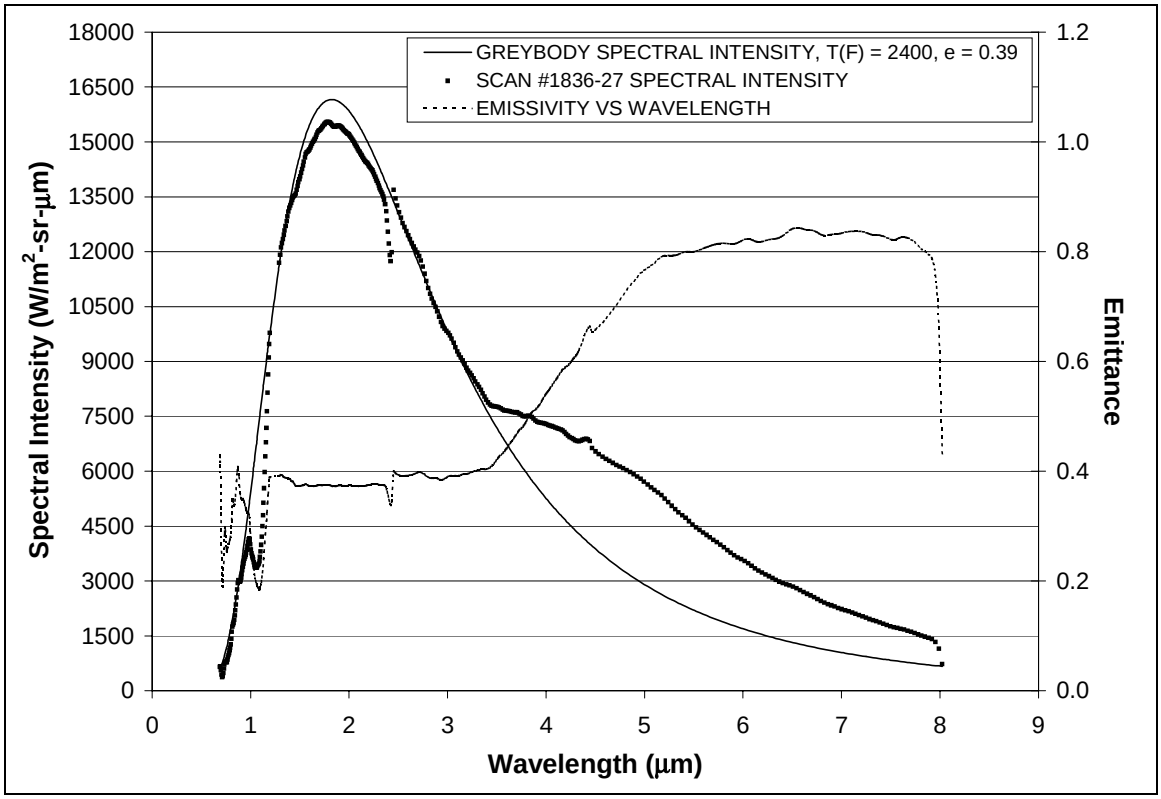

Figure 66: #1836-27, Bare Densified LI-900, 2000°F Condition, 15in Nozzle

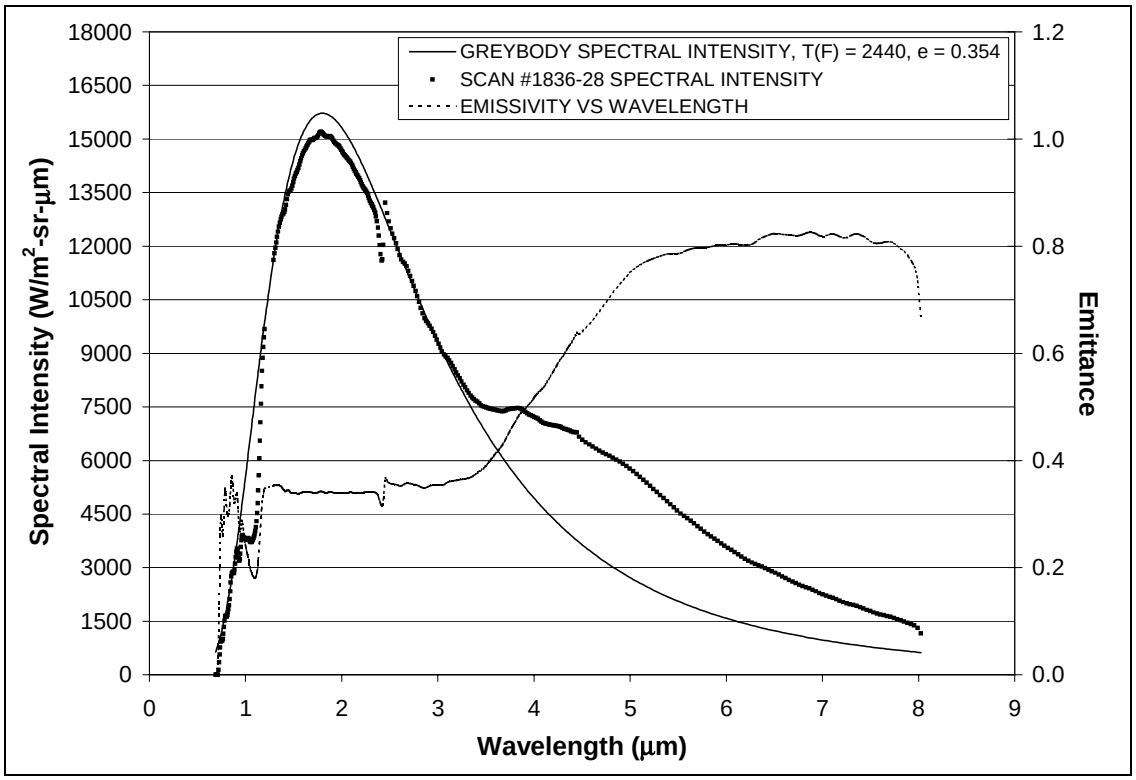

Figure 67: #1836-28, Bare Densified LI-900, 2000°F Condition, 15in Nozzle

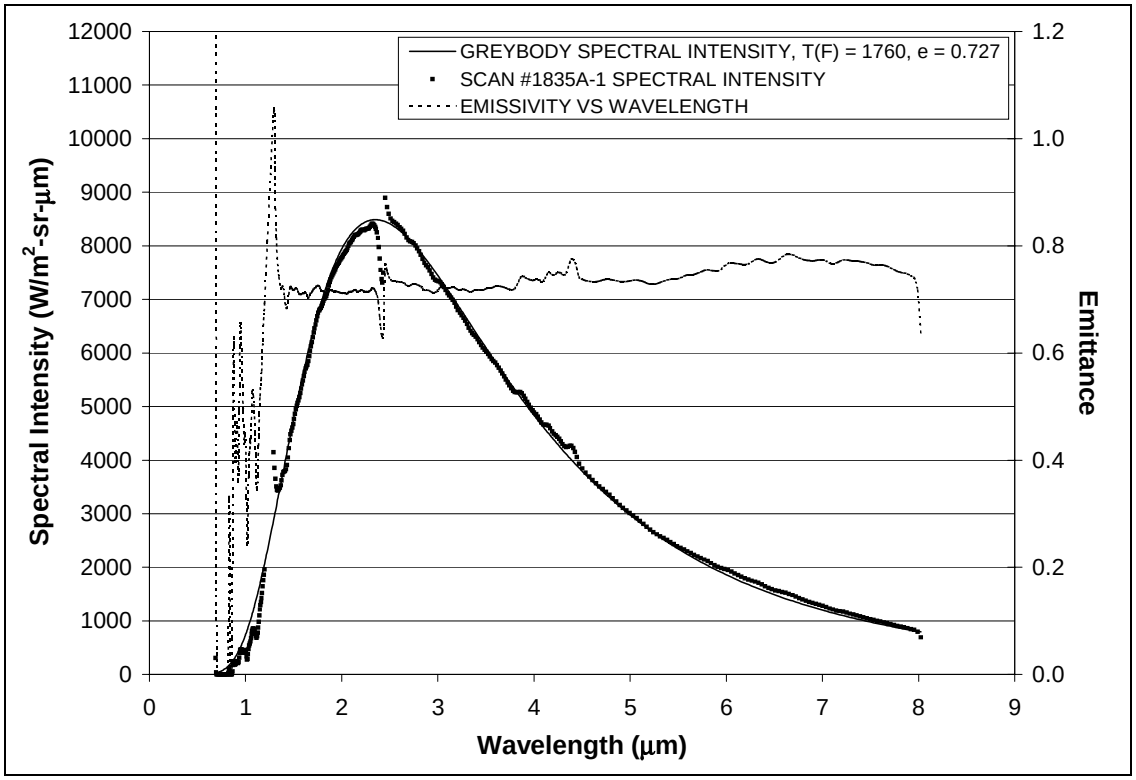

Figure 68: #1835A-1, Bare LI-900 with Emittance Wash, 1600°F Condition, 15in Nozzle

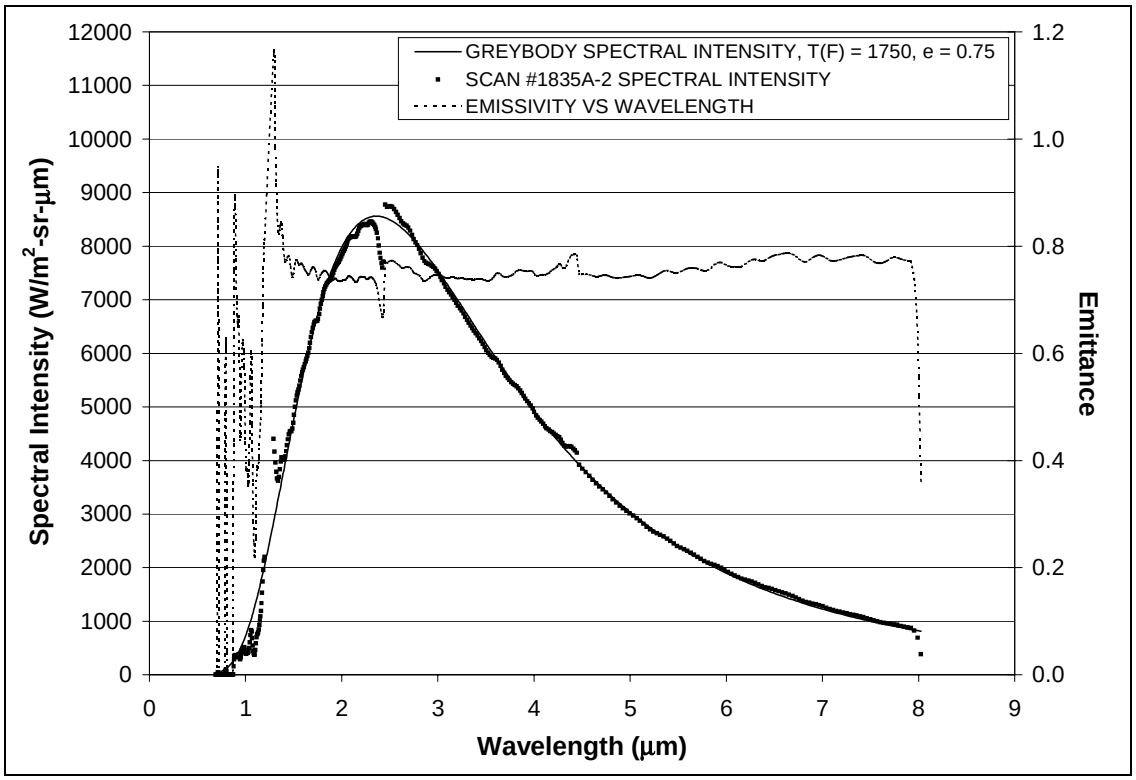

Figure 69: #1835A-2, Bare LI-900 with Emittance Wash, 1600°F Condition, 15in Nozzle

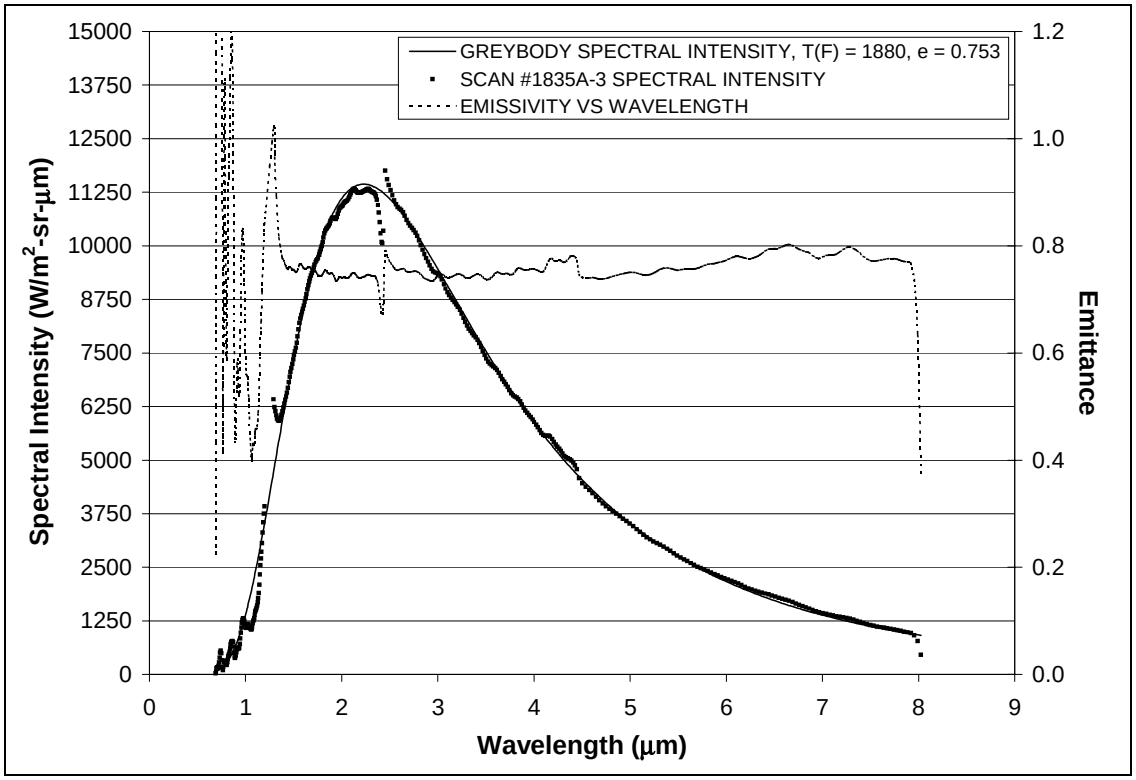

Figure 70: #1835A-3, Bare LI-900 with Emittance Wash, 1700°F Condition, 15in Nozzle

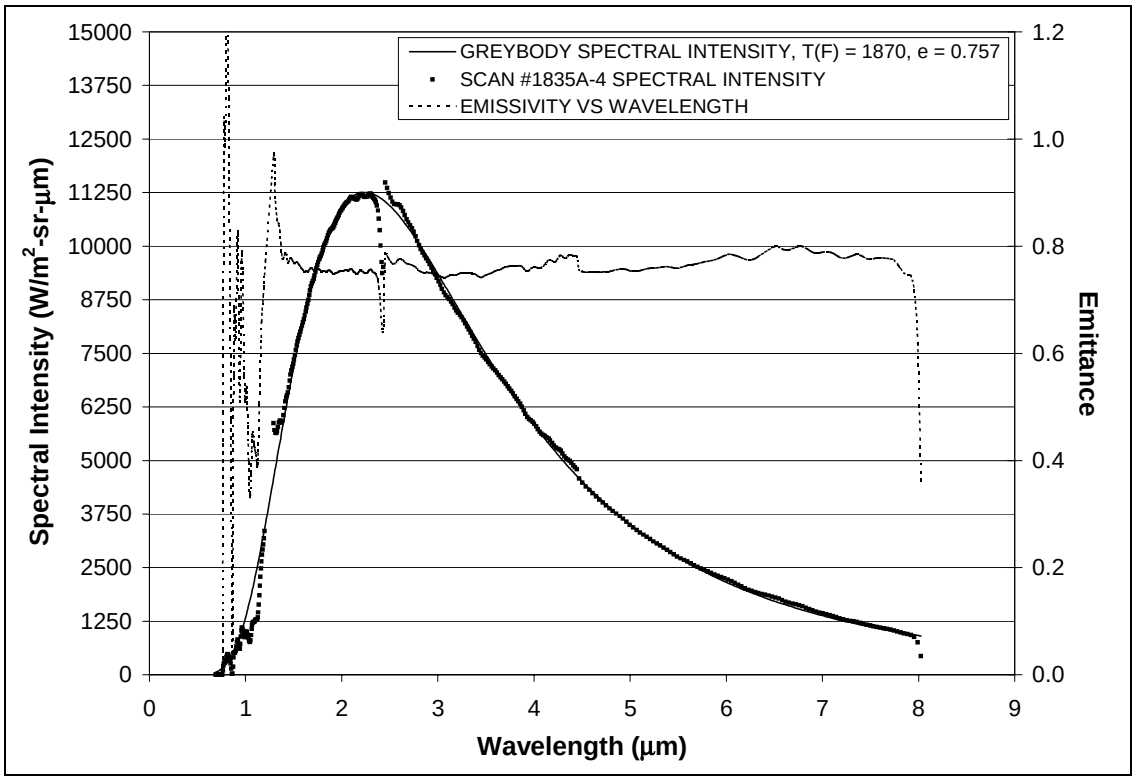

Figure 71: #1835A-4, Bare LI-900 with Emittance Wash, 1700°F Condition, 15in Nozzle

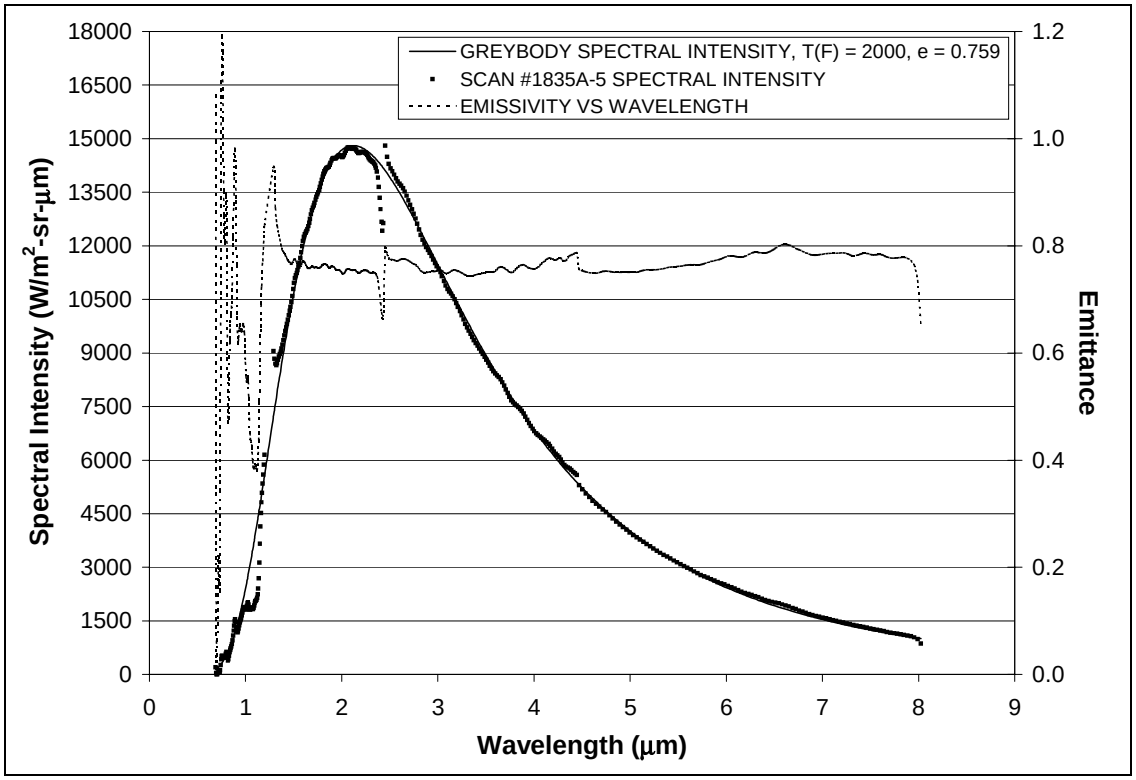

Figure 72: #1835A-5, Bare LI-900 with Emittance Wash, 1800°F Condition, 15in Nozzle

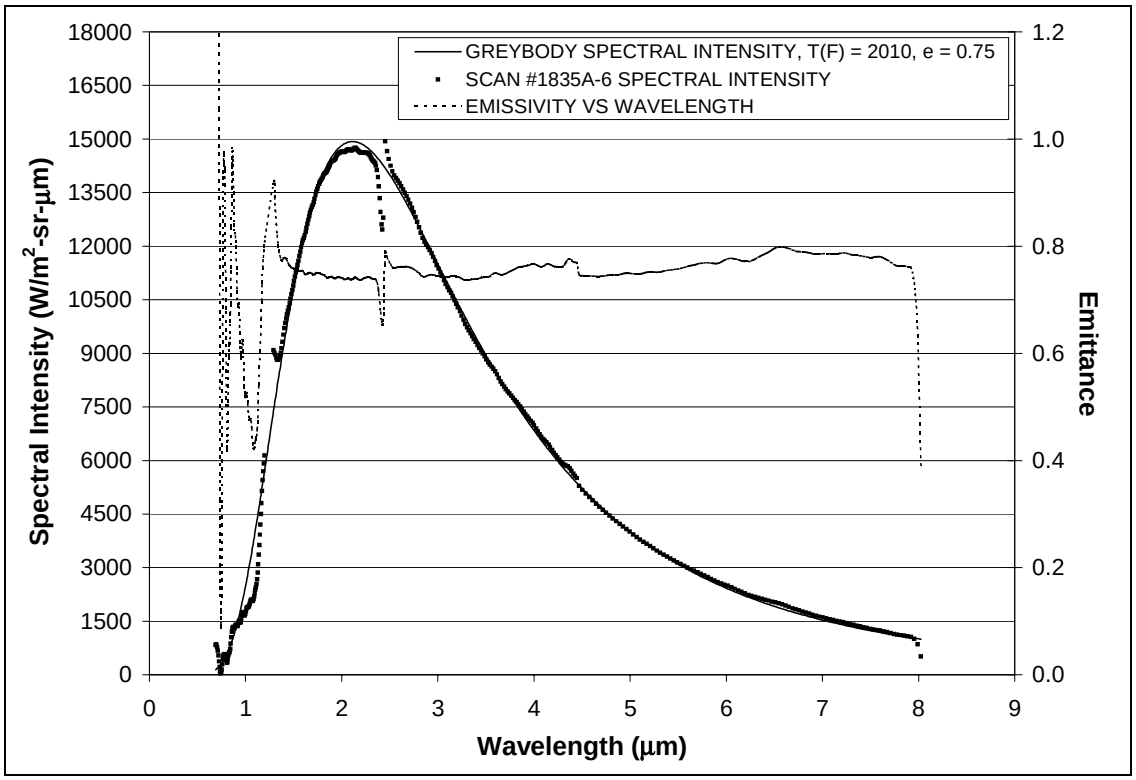

Figure 73: #1835A-6, Bare LI-900 with Emittance Wash, 1800°F Condition, 15in Nozzle

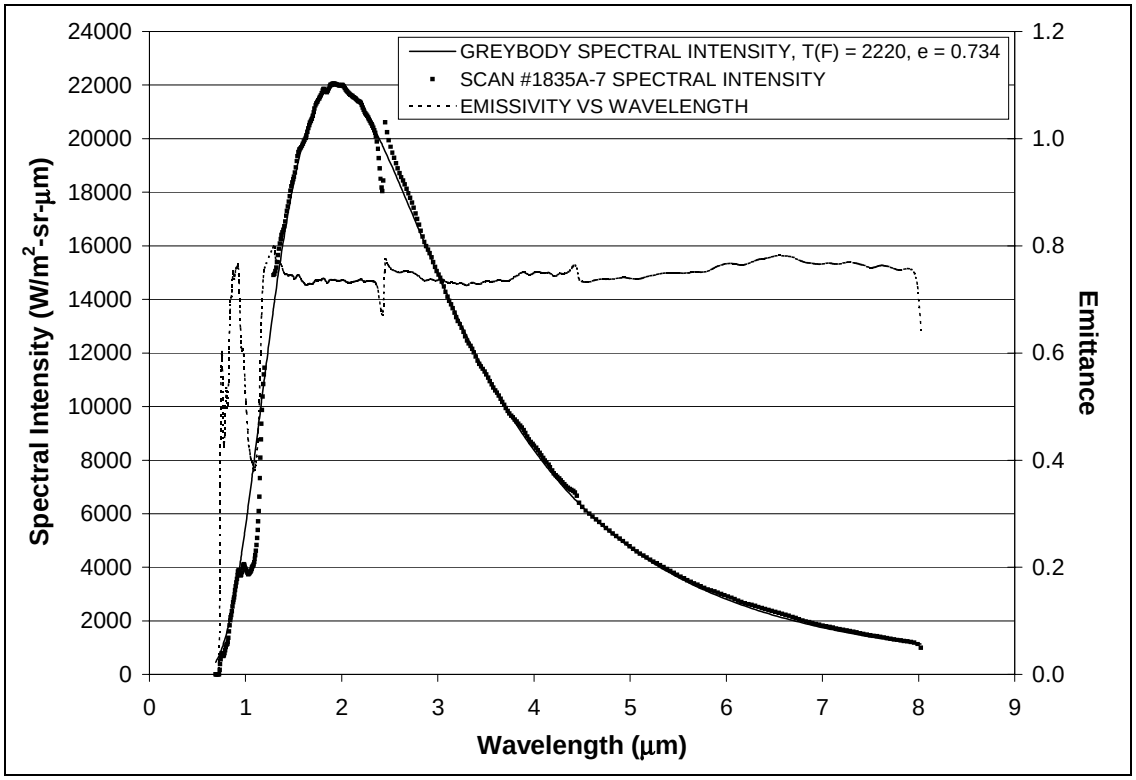

Figure 74: #1835A-7, Bare LI-900 with Emittance Wash, 2000°F Condition, 15in Nozzle

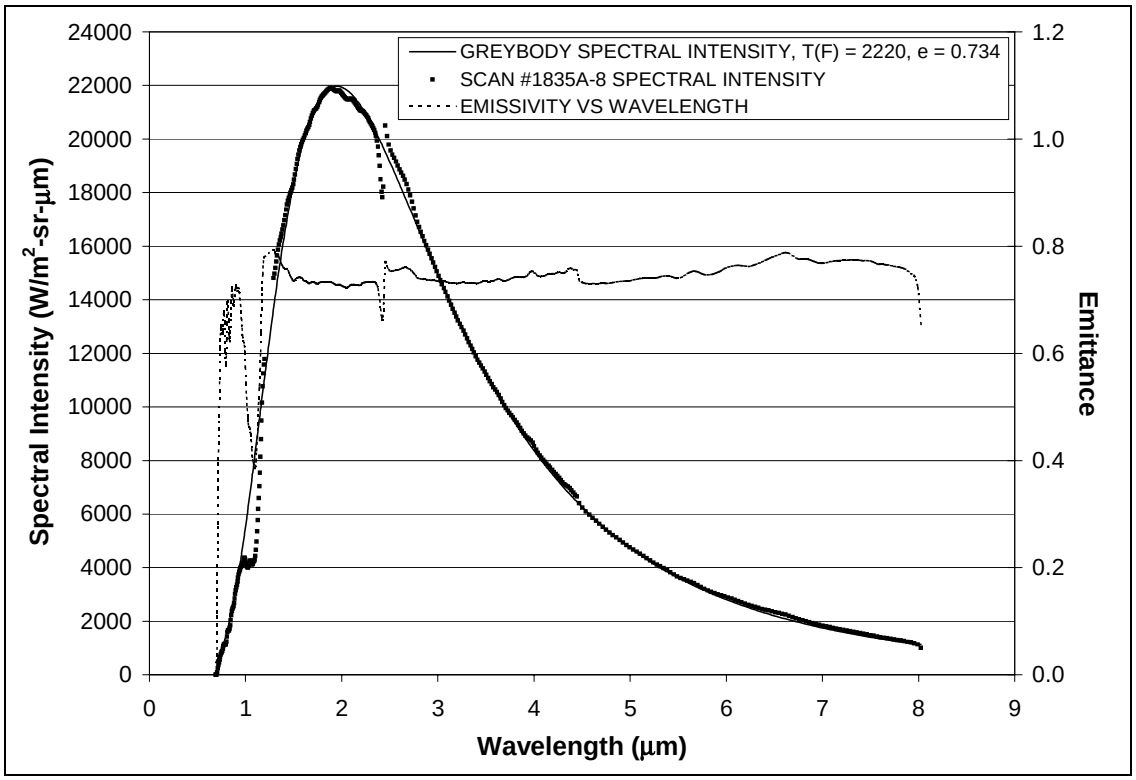

Figure 75: #1835A-8, Bare LI-900 with Emittance Wash, 2000°F Condition, 15in Nozzle

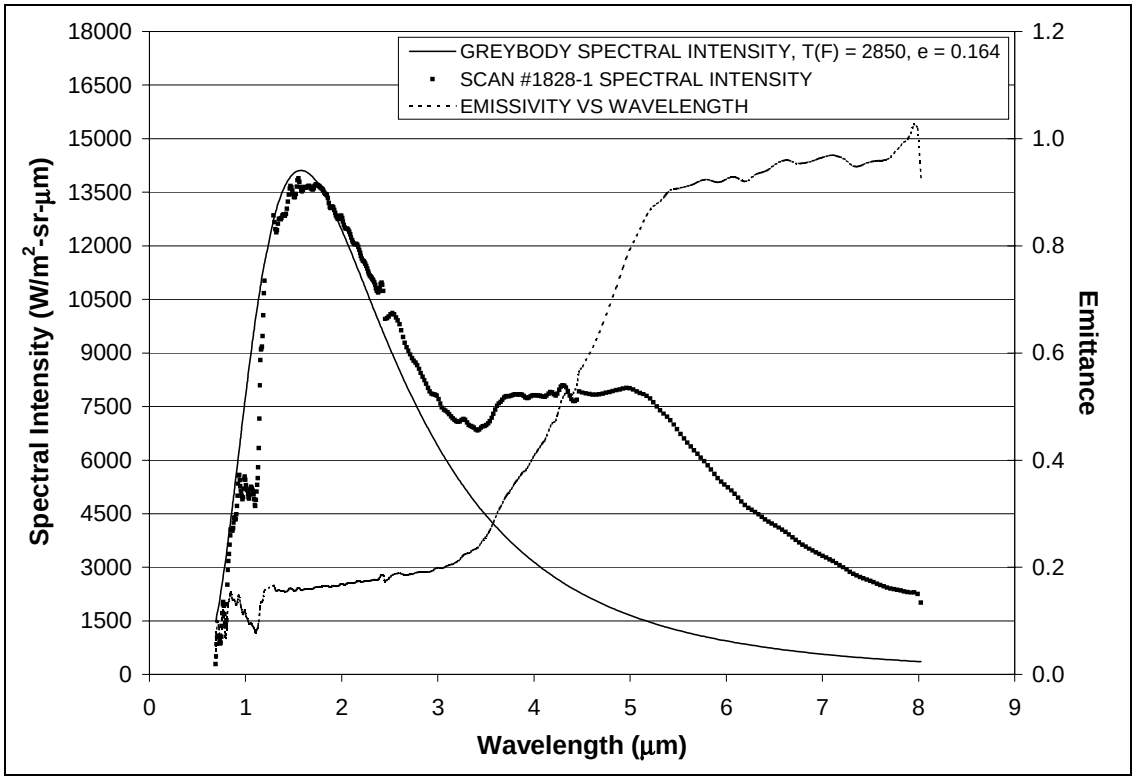

Figure 76: #1828-1, Bare FRCI-12, 2000°F Condition, 5in Nozzle

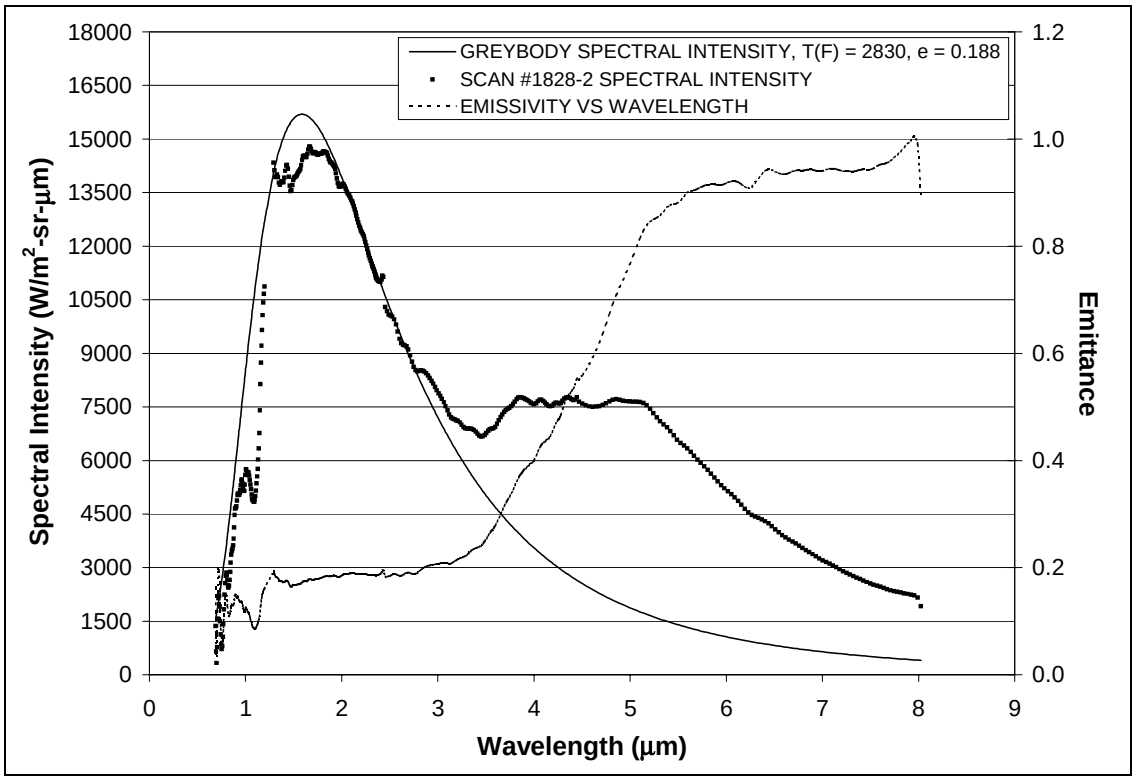

Figure 77: #1828-2, Bare FRCI-12, 2000°F Condition, 5in Nozzle

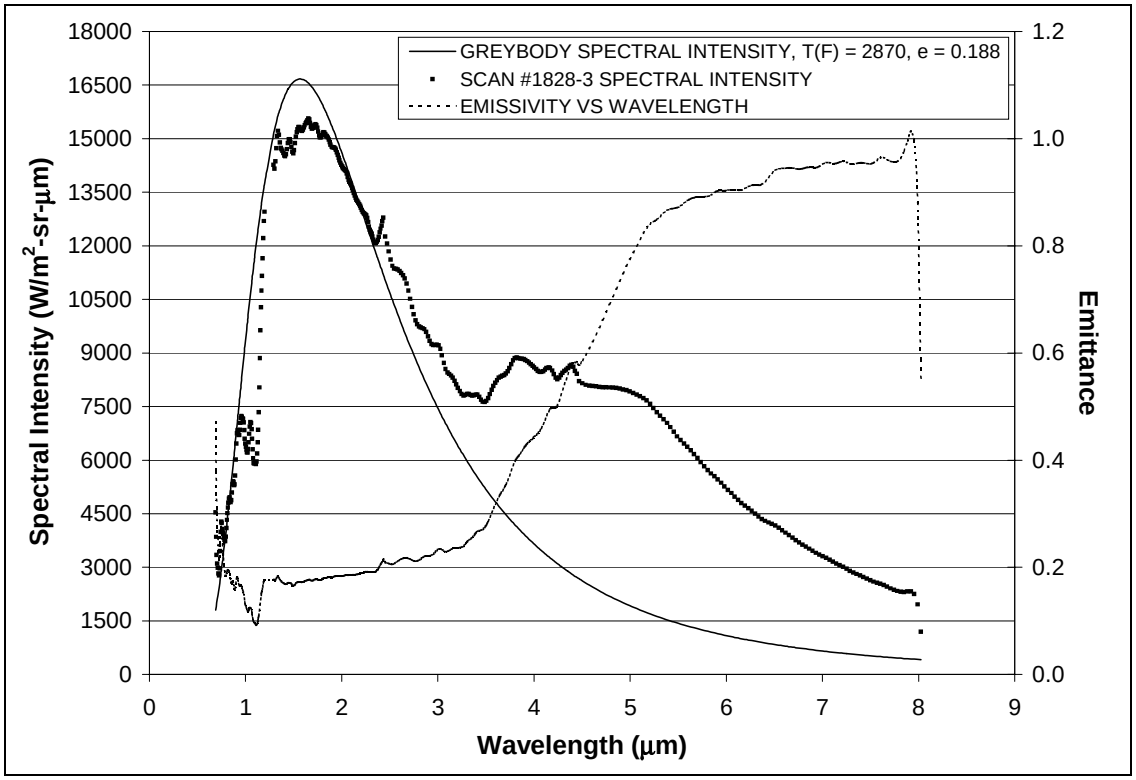

Figure 78: #1828-3, Bare FRCI-12, 2000°F Condition, 5in Nozzle

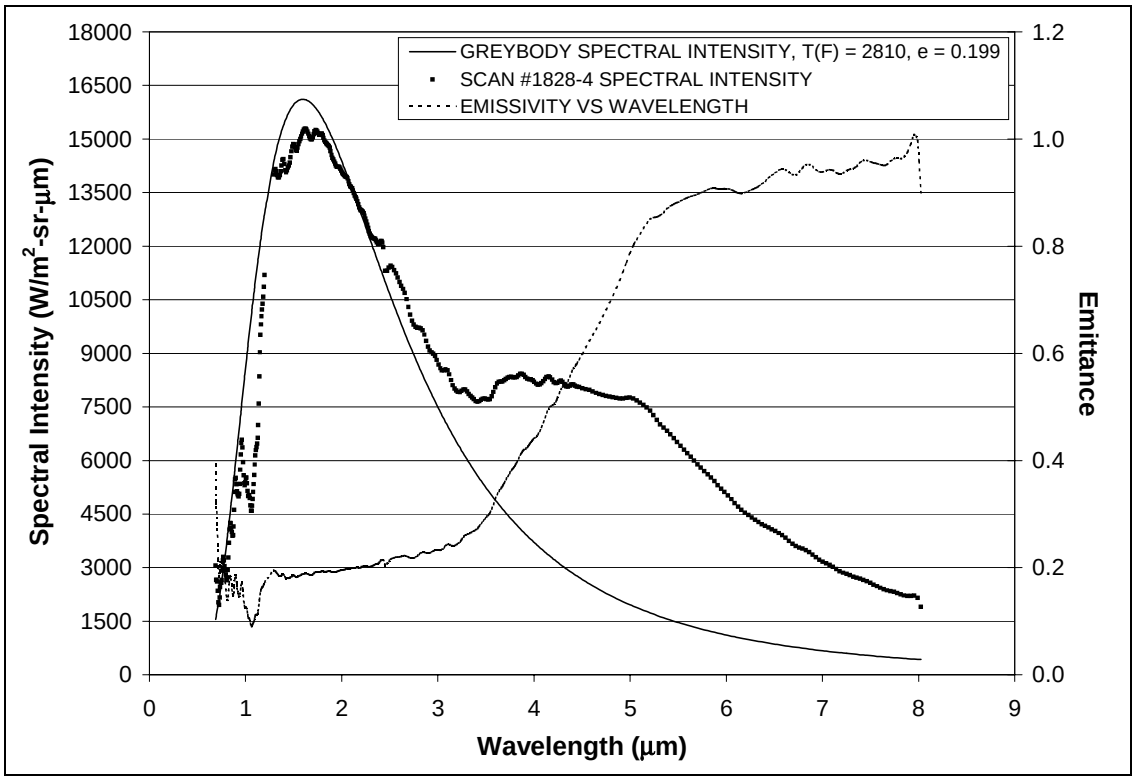

Figure 79: #1828-4, Bare FRCI-12, 2000°F Condition, 5in Nozzle

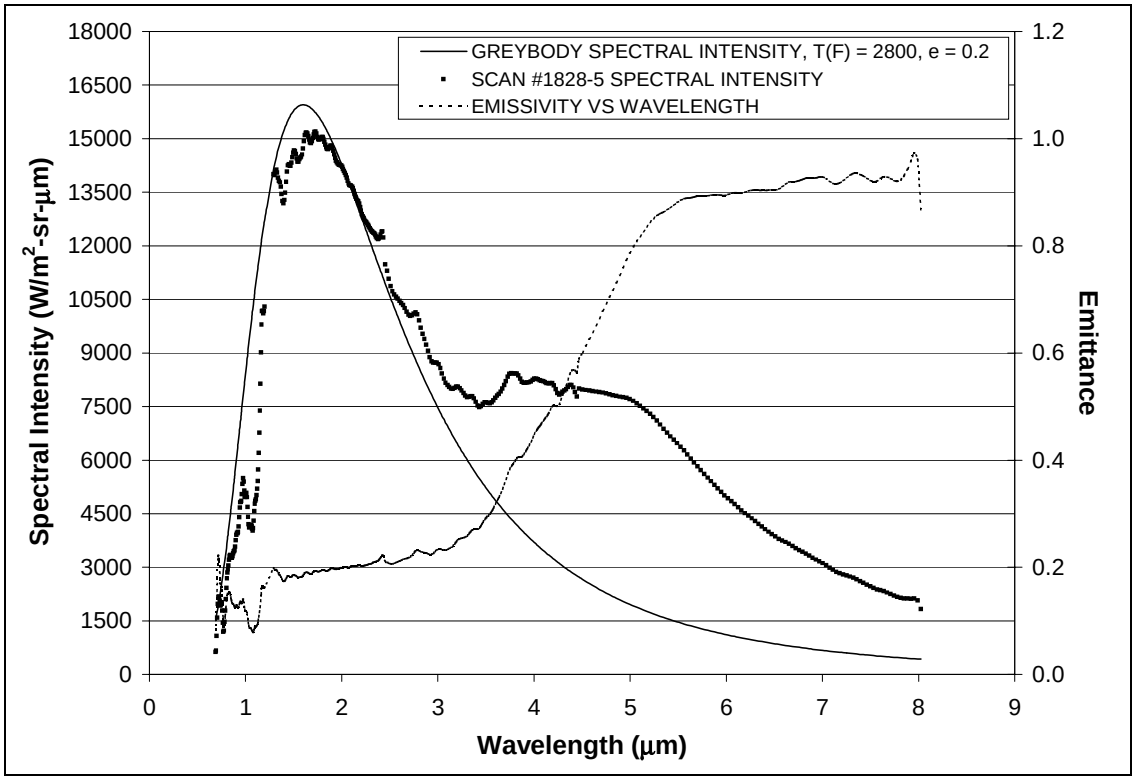

Figure 80: #1828-5, Bare FRCI-12, 2000°F Condition, 5in Nozzle

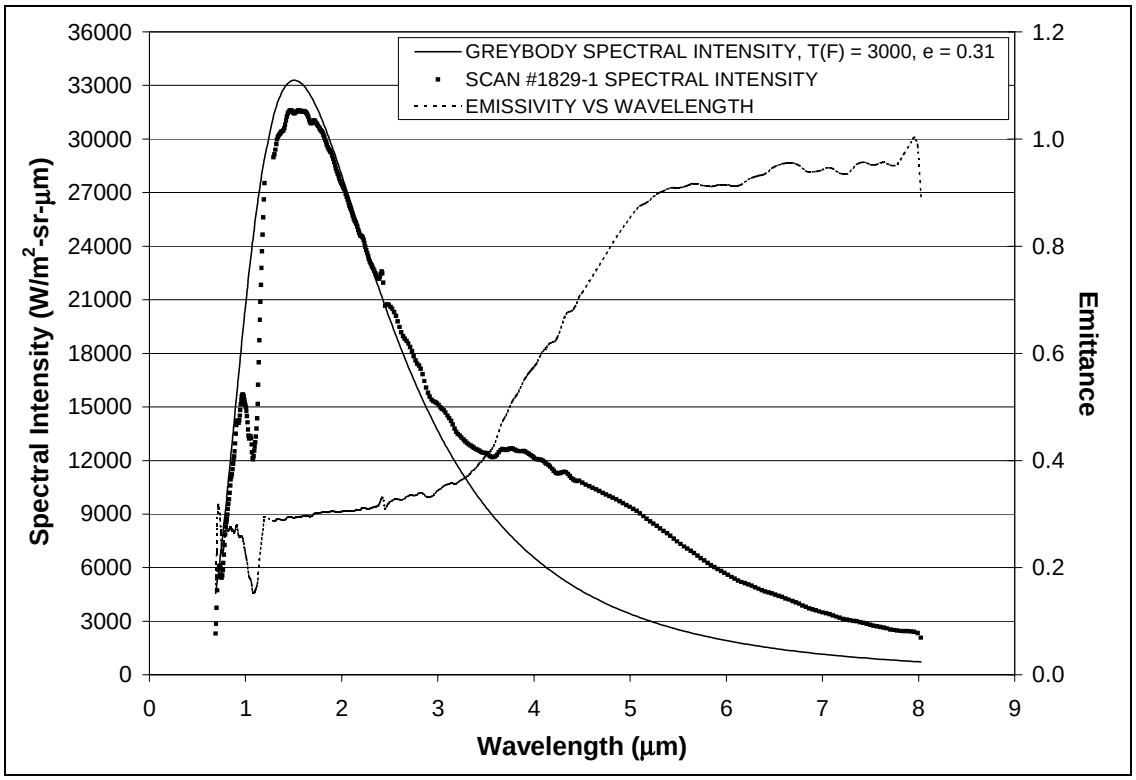

Figure 81: #1829-1, Bare FRCI-12, 2300°F Condition, 5in Nozzle

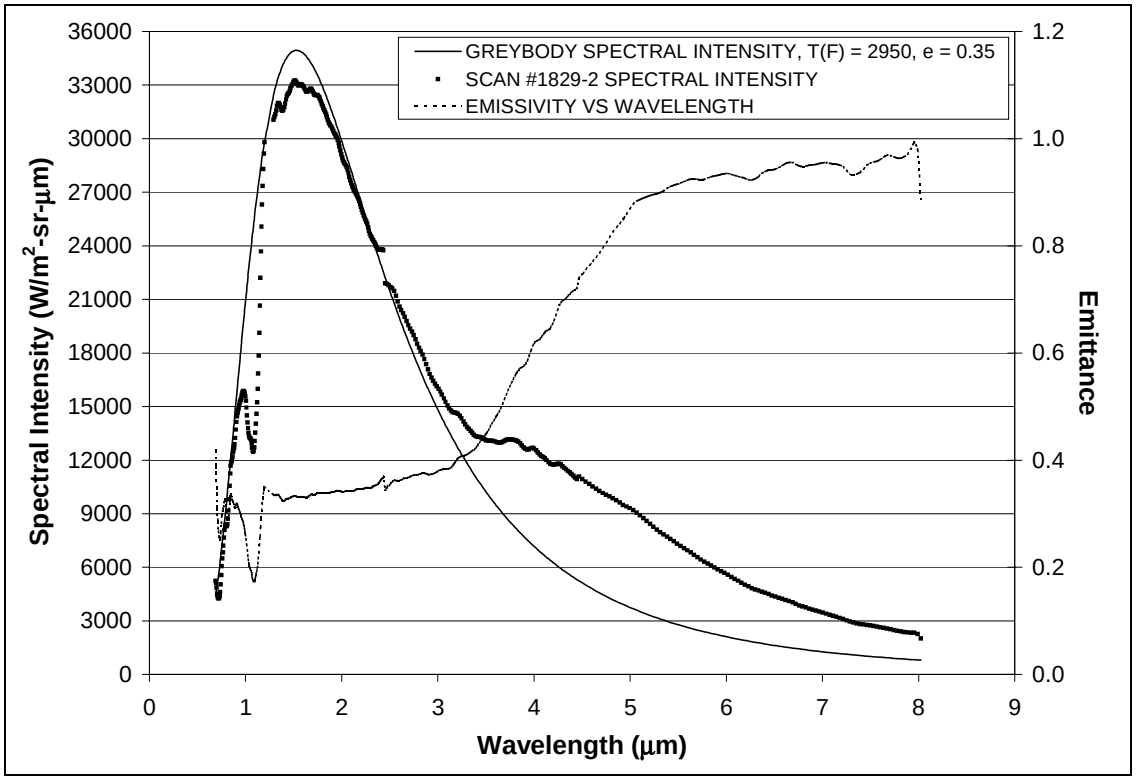

Figure 82: #1829-2, Bare FRCI-12, 2300°F Condition, 5in Nozzle

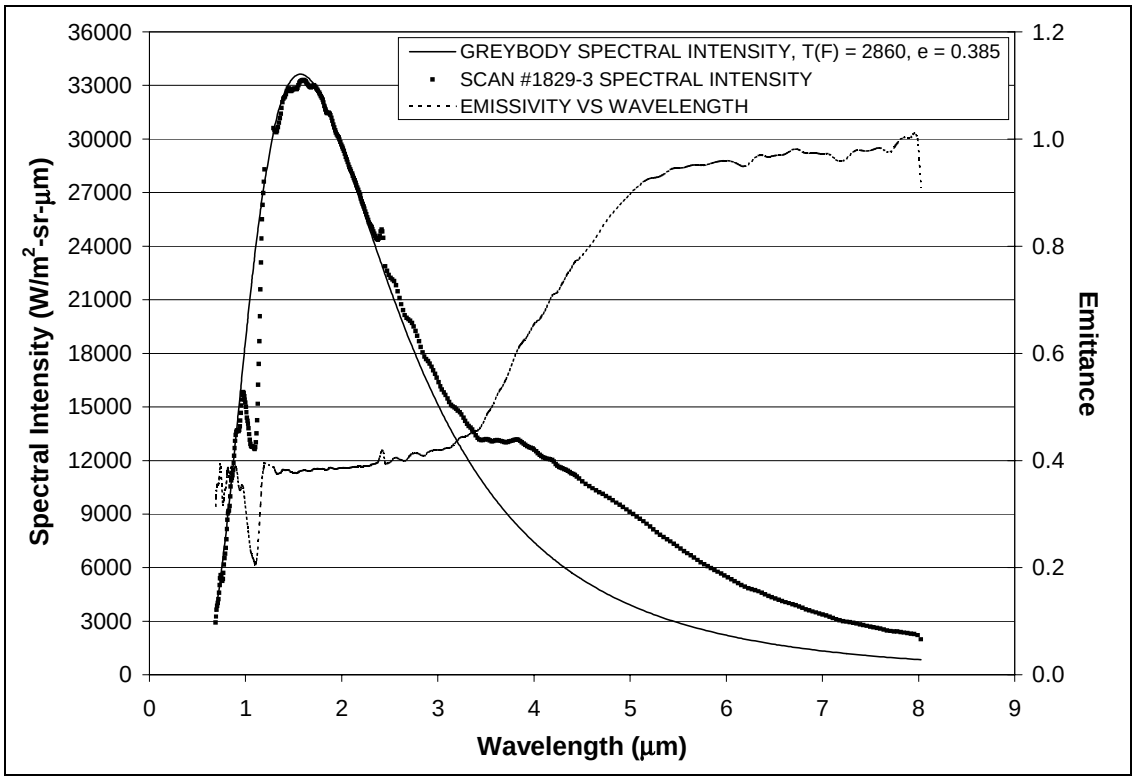

Figure 83: #1829-3, Bare FRCI-12, 2300°F Condition, 5in Nozzle

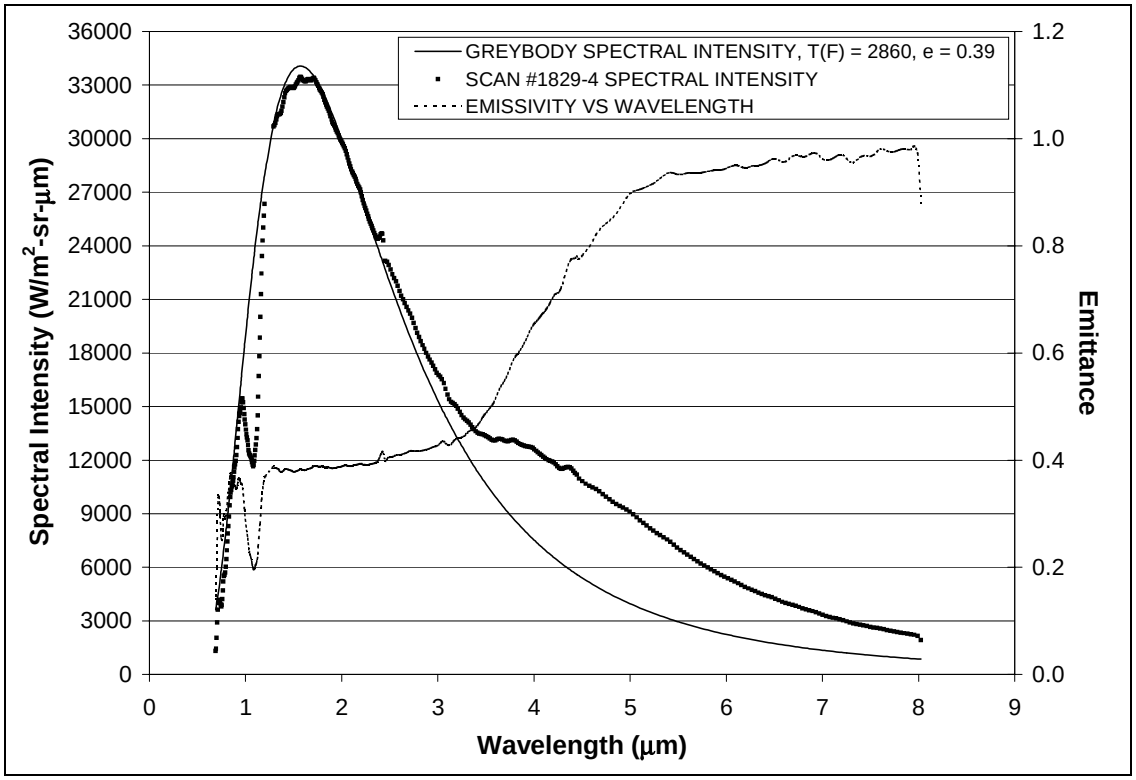

Figure 84: #1829-4, Bare FRCI-12, 2300°F Condition, 5in Nozzle

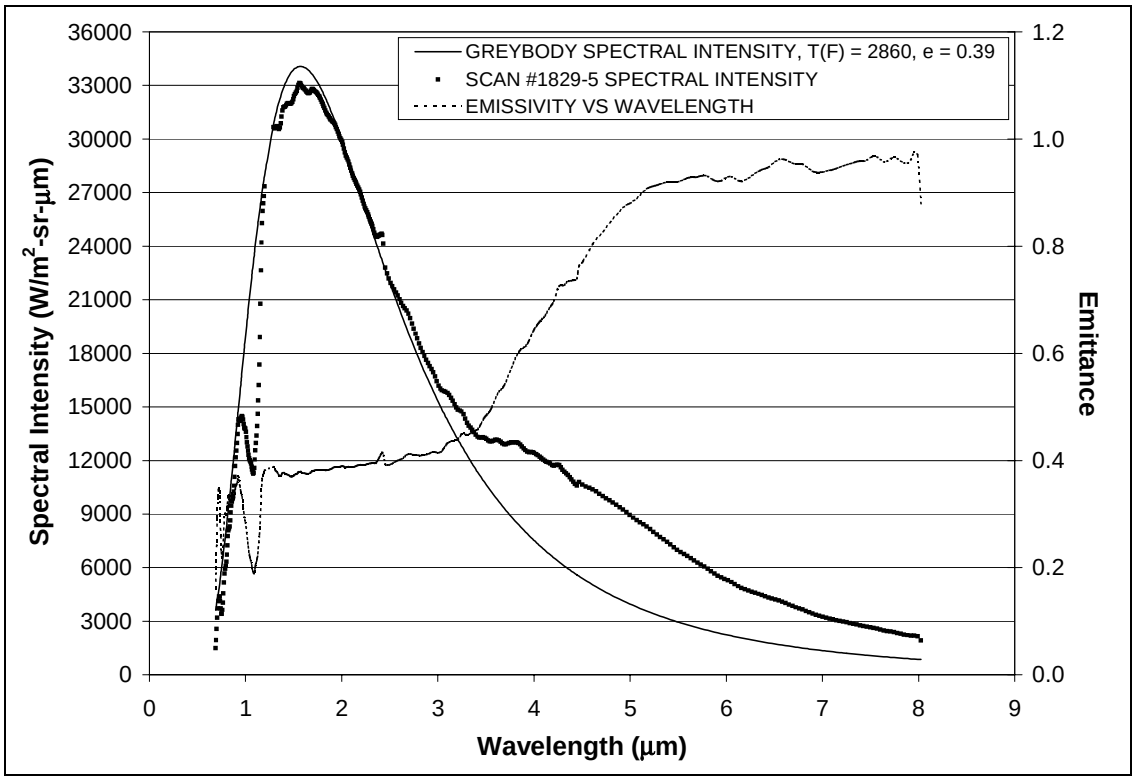

Figure 85: #1829-5, Bare FRCI-12, 2300°F Condition, 5in Nozzle

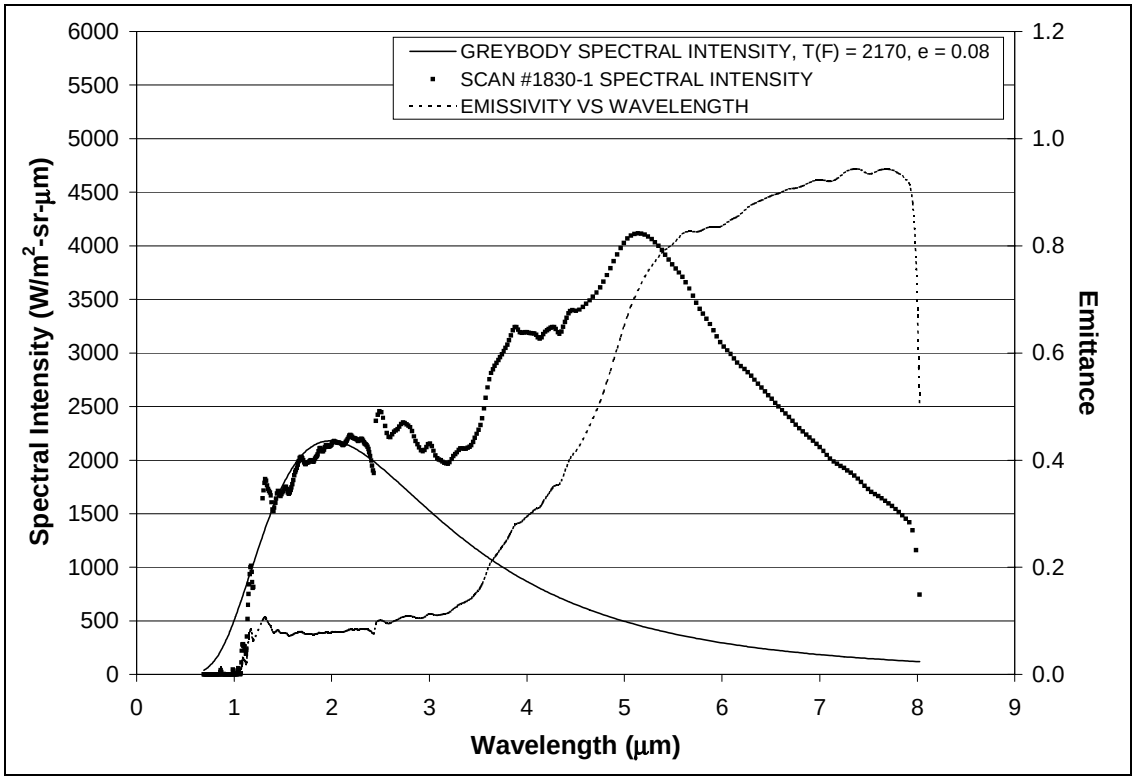

Figure 86: #1830-1, Bare FRCI-12, 1600°F Condition, 15in Nozzle

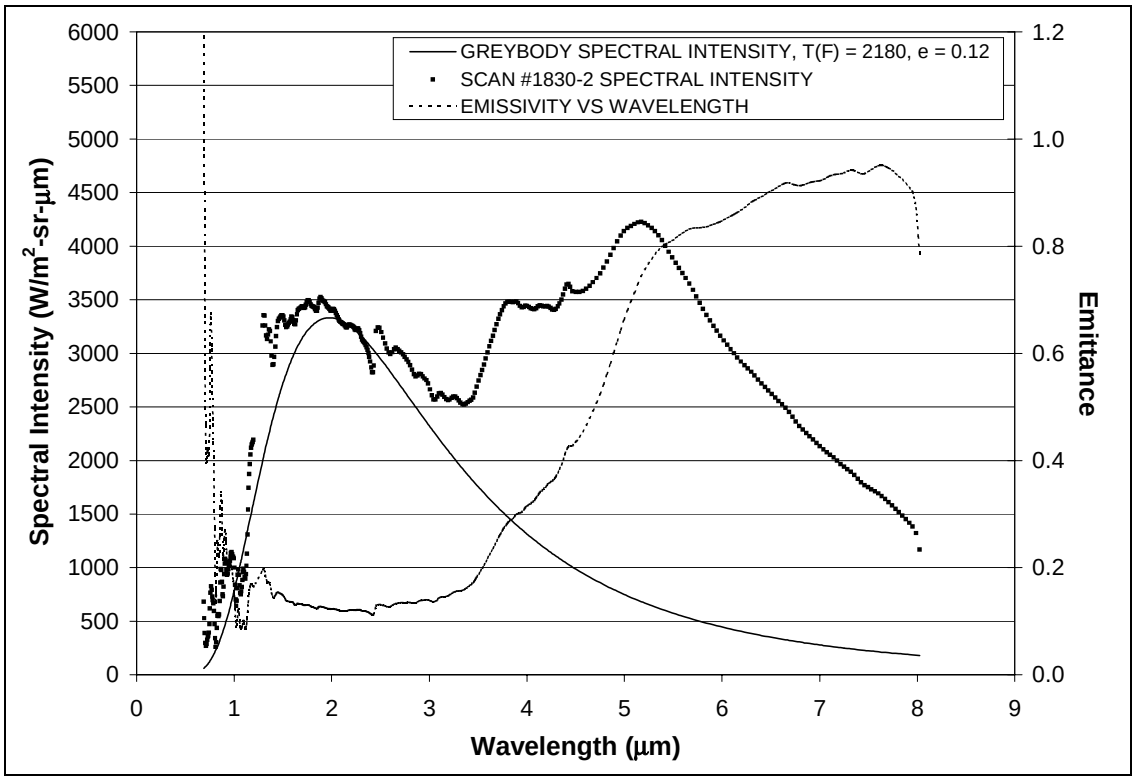

Figure 87: #1830-2, Bare FRCI-12, 1600°F Condition, 15in Nozzle

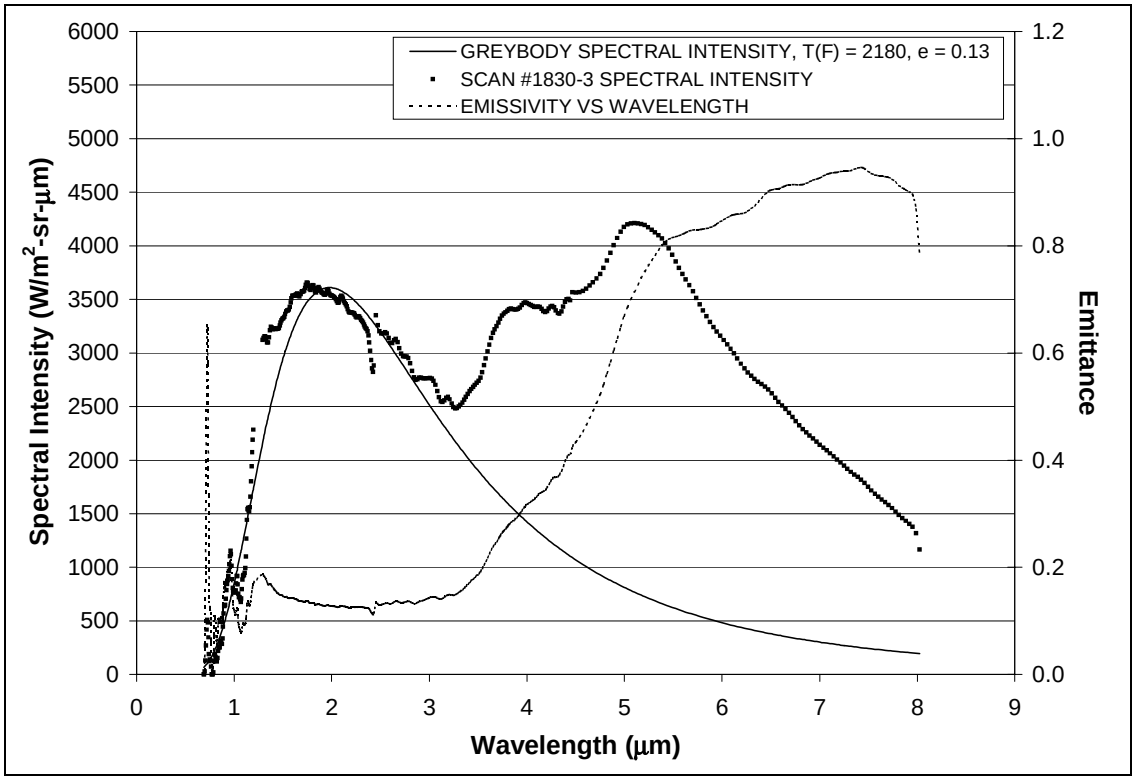

Figure 88: #1830-3, Bare FRCI-12, 1600°F Condition, 15in Nozzle

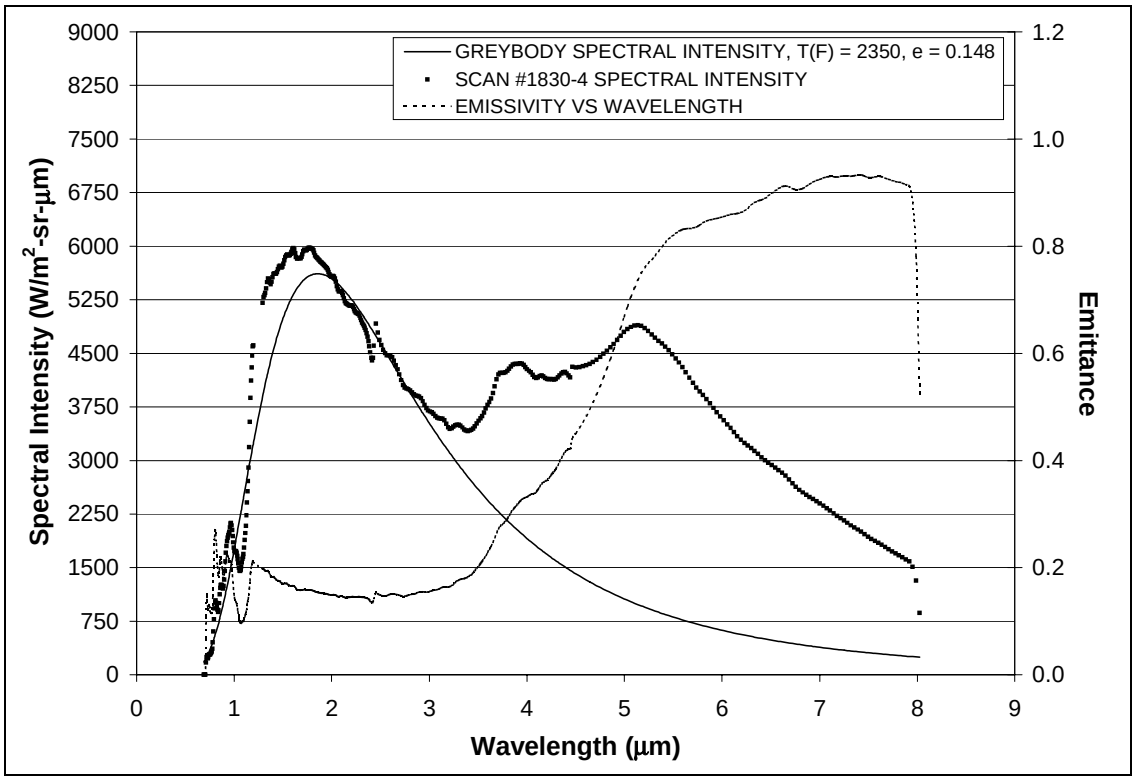

Figure 89: #1830-4, Bare FRCI-12, 1700°F Condition, 15in Nozzle

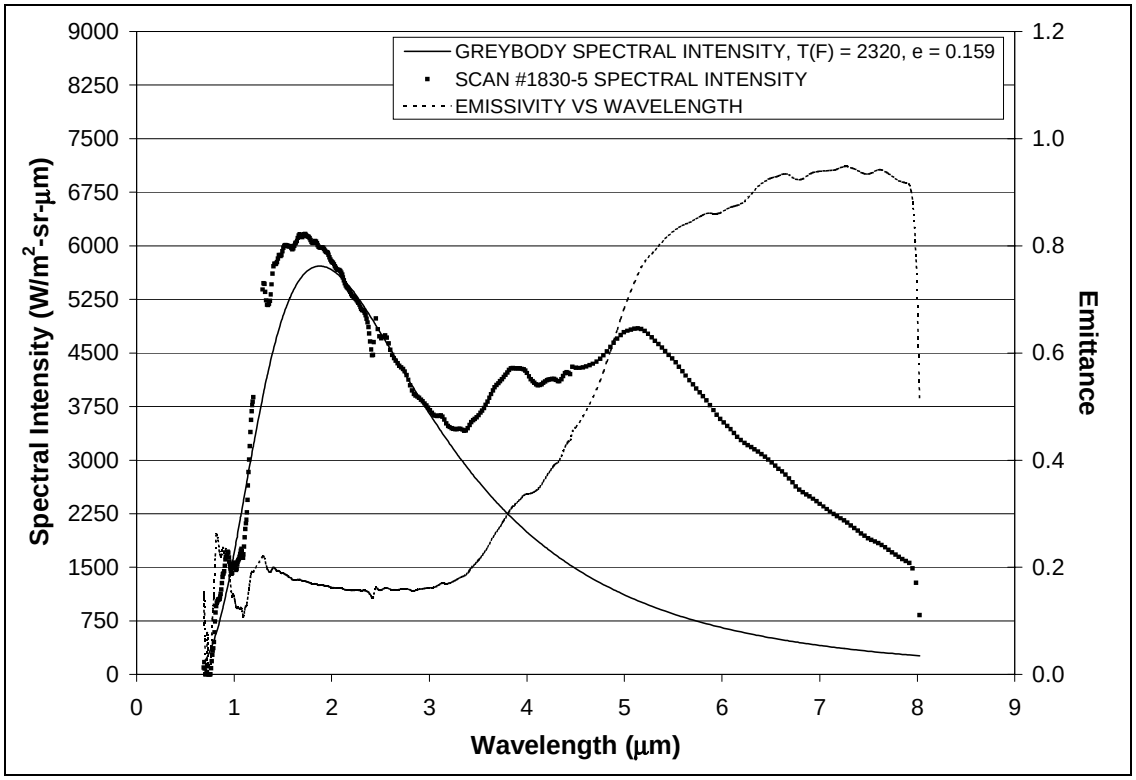

Figure 90: #1830-5, Bare FRCI-12, 1700°F Condition, 15in Nozzle

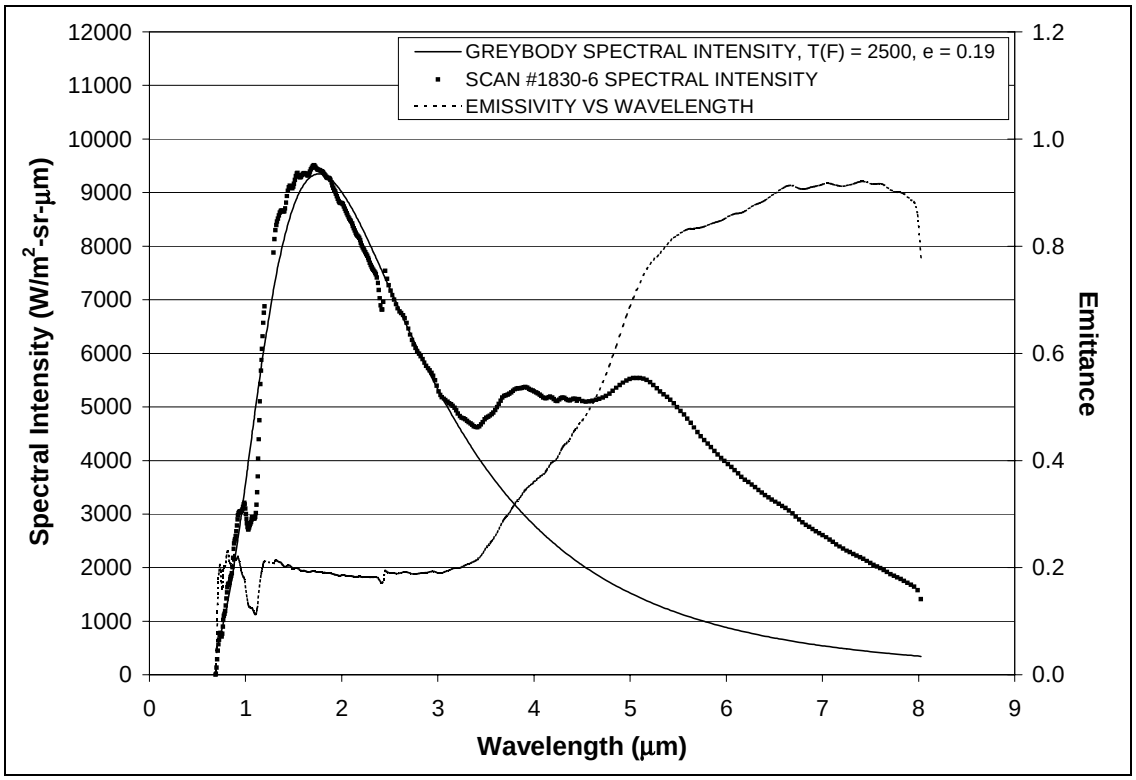

Figure 91: #1830-6, Bare FRCI-12, 1800°F Condition, 15in Nozzle

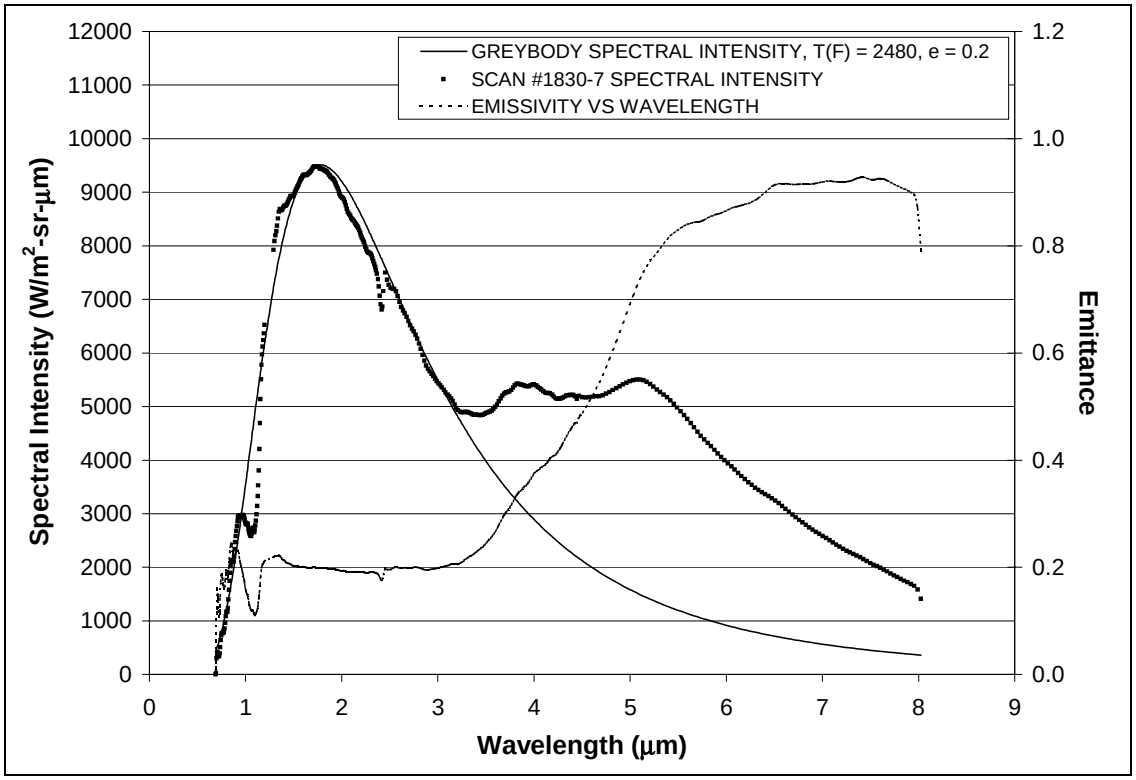

Figure 92: #1830-7, Bare FRCI-12, 1800°F Condition, 15in Nozzle

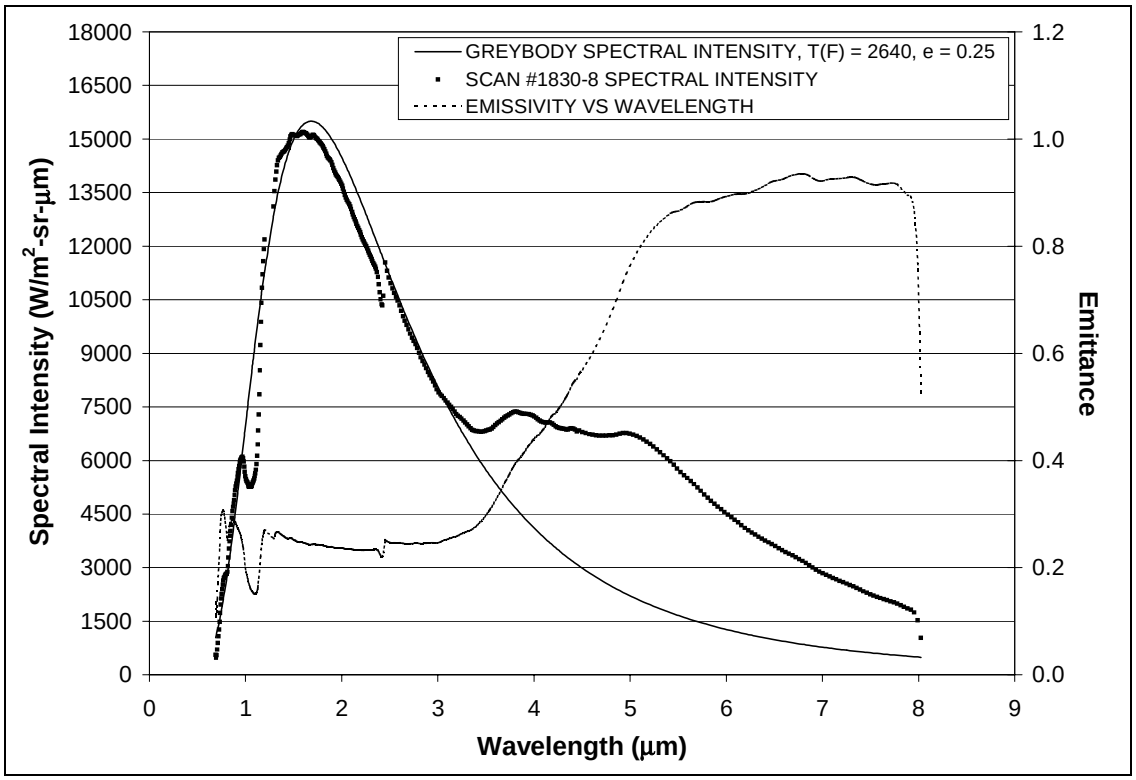

Figure 93: #1830-8, Bare FRCI-12, 2000°F Condition, 15in Nozzle

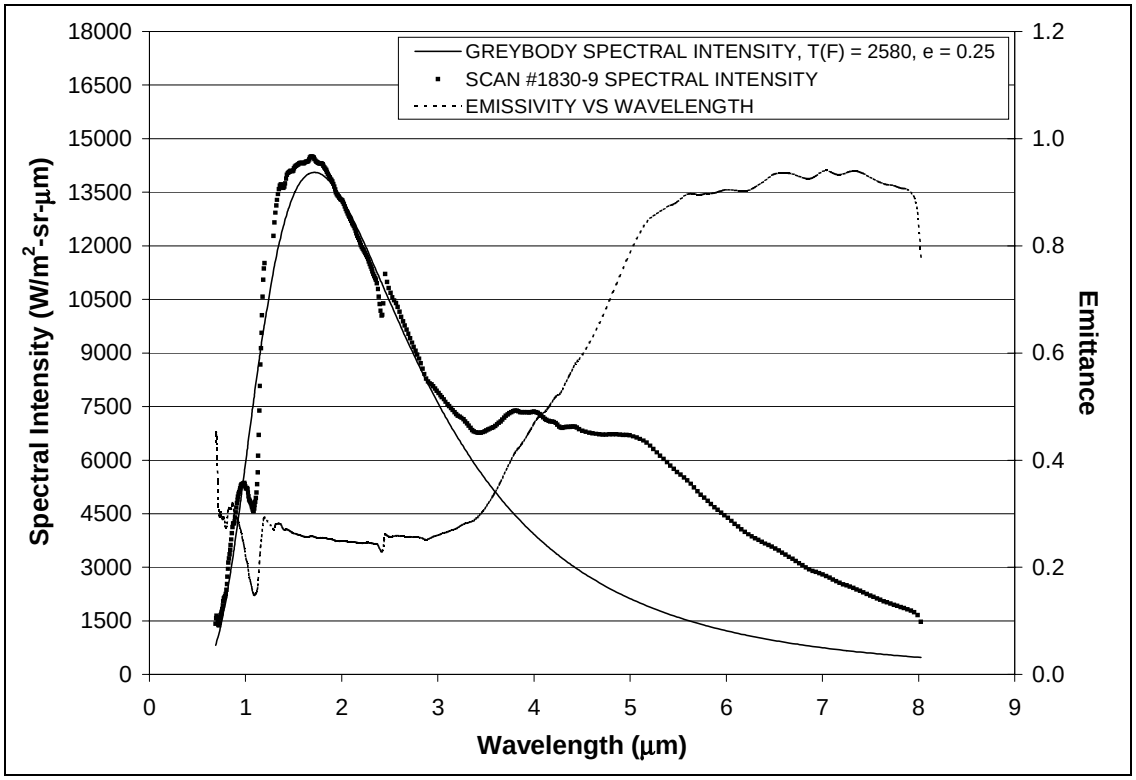

Figure 94: #1830-9, Bare FRCI-12, 2000°F Condition, 15in Nozzle

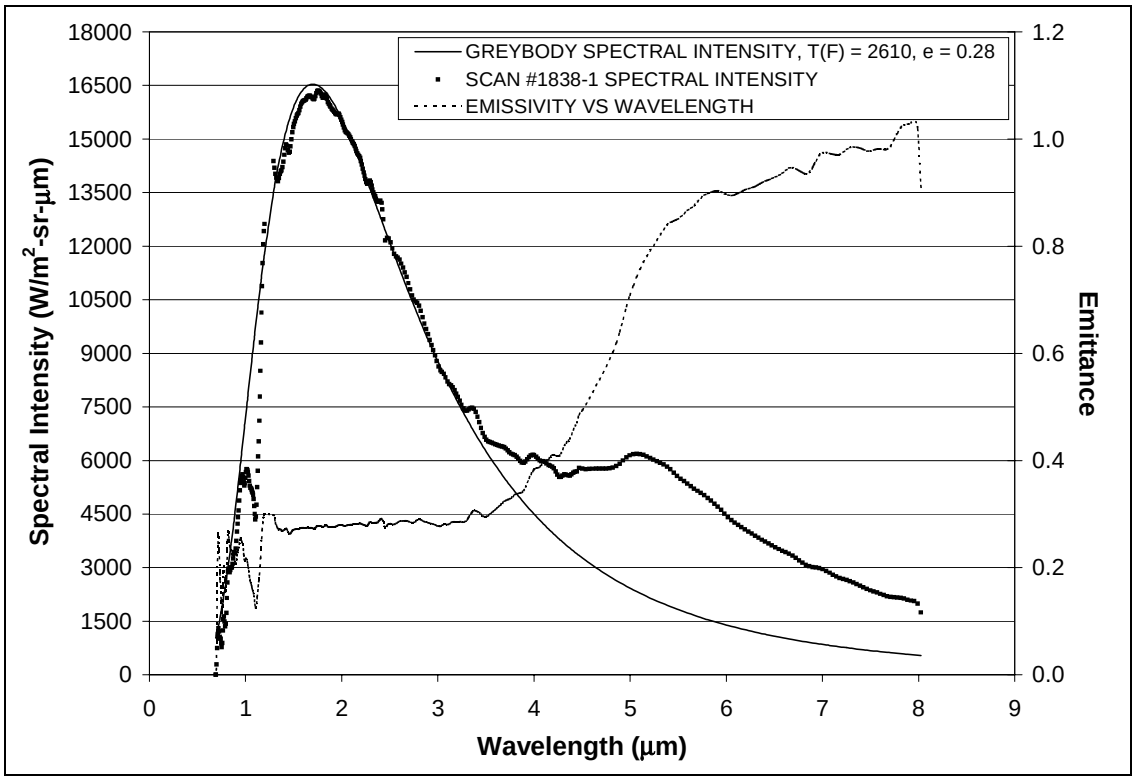

Figure 95: #1838-1, Bare LI-2200, 2000°F Condition, 5in Nozzle

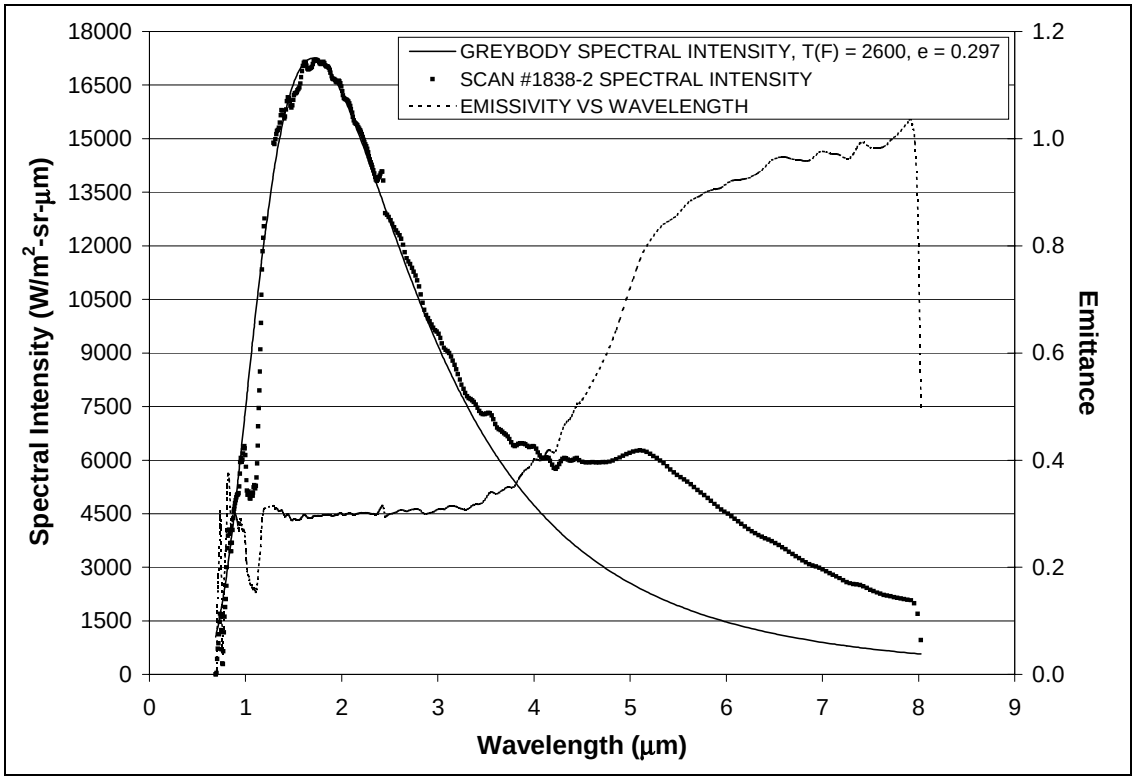

Figure 96: #1838-2, Bare LI-2200, 2000°F Condition, 5in Nozzle

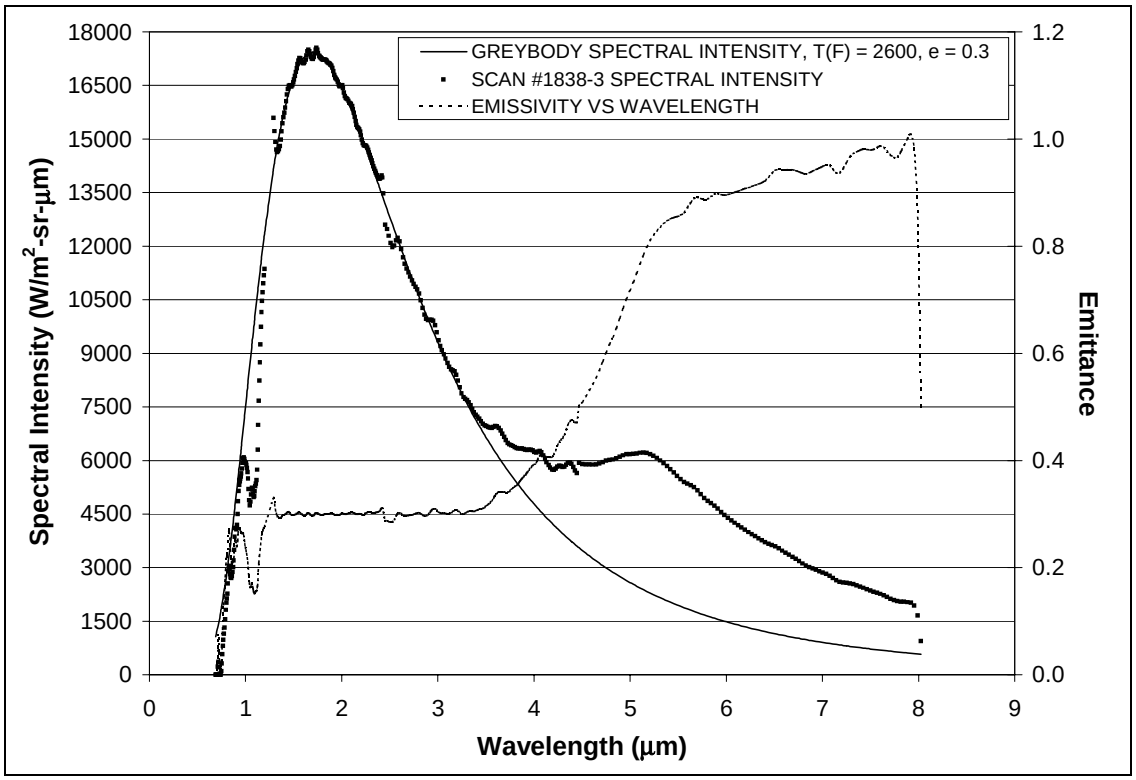

Figure 97: #1838-3, Bare LI-2200, 2000°F Condition, 5in Nozzle

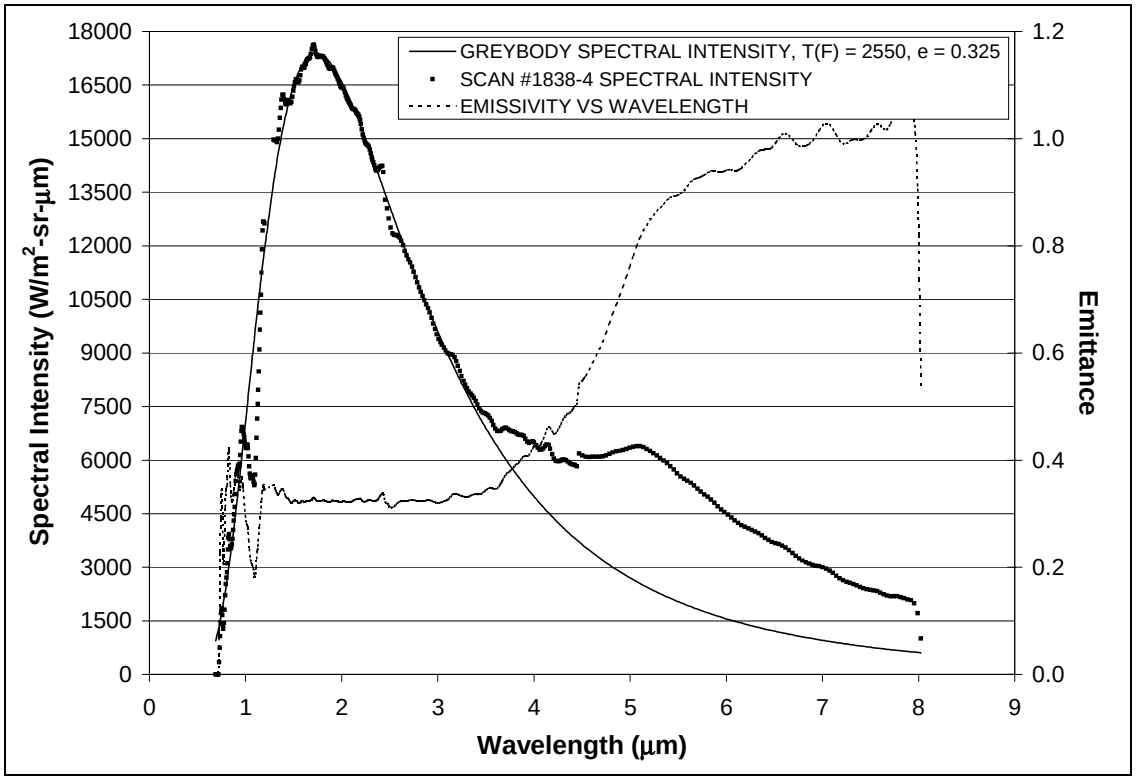

Figure 98: #1838-4, Bare LI-2200, 2000°F Condition, 5in Nozzle

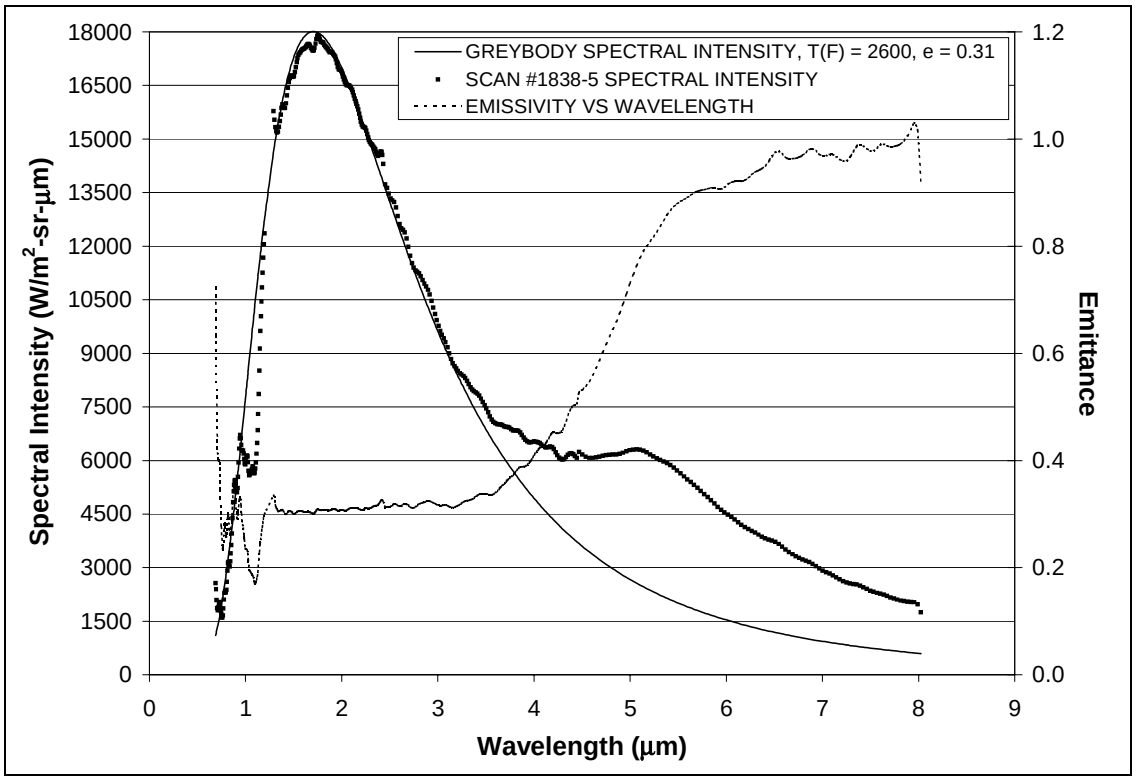

Figure 99: #1838-5, Bare LI-2200, 2000°F Condition, 5in Nozzle

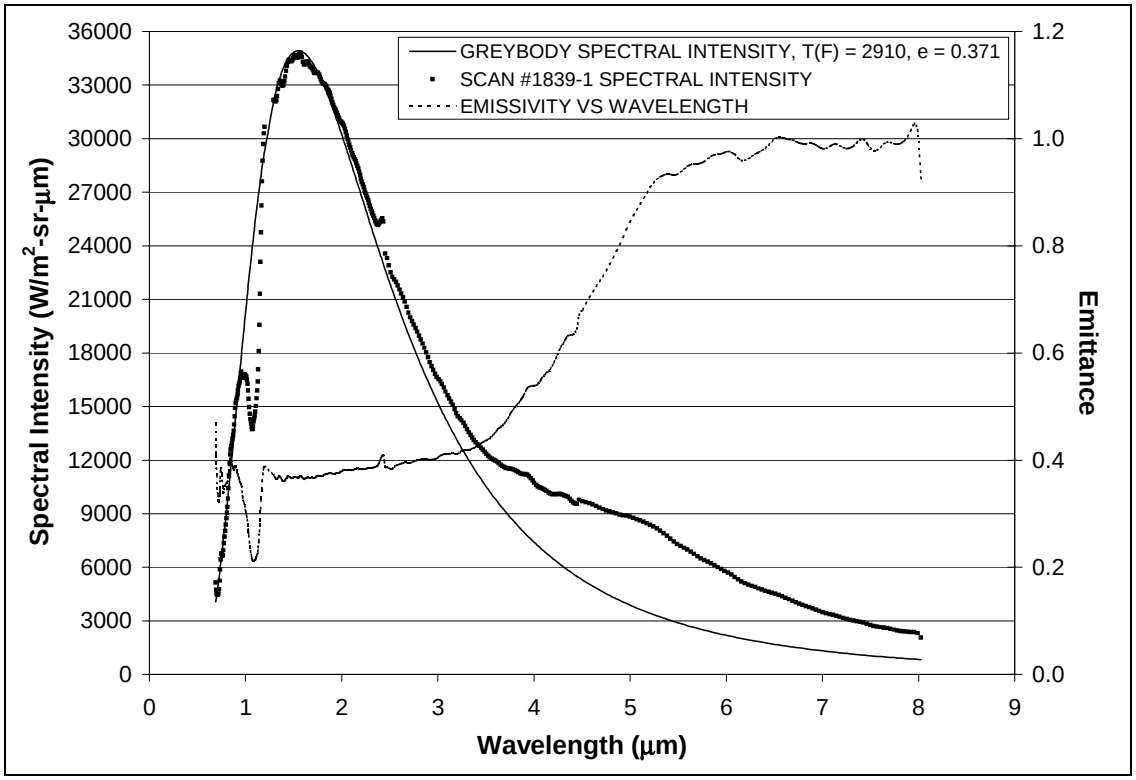

Figure 100: #1839-1, Bare LI-2200, 2300°F Condition, 5in Nozzle

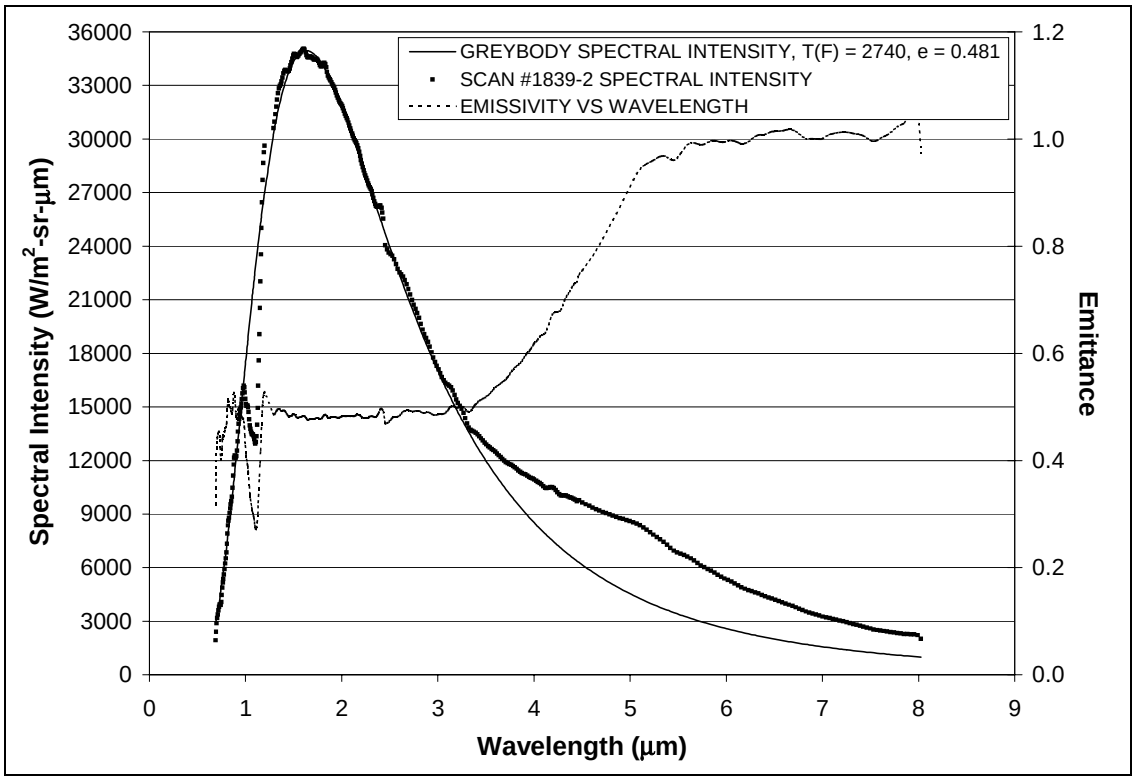

Figure 101: #1839-2, Bare LI-2200, 2300°F Condition, 5in Nozzle

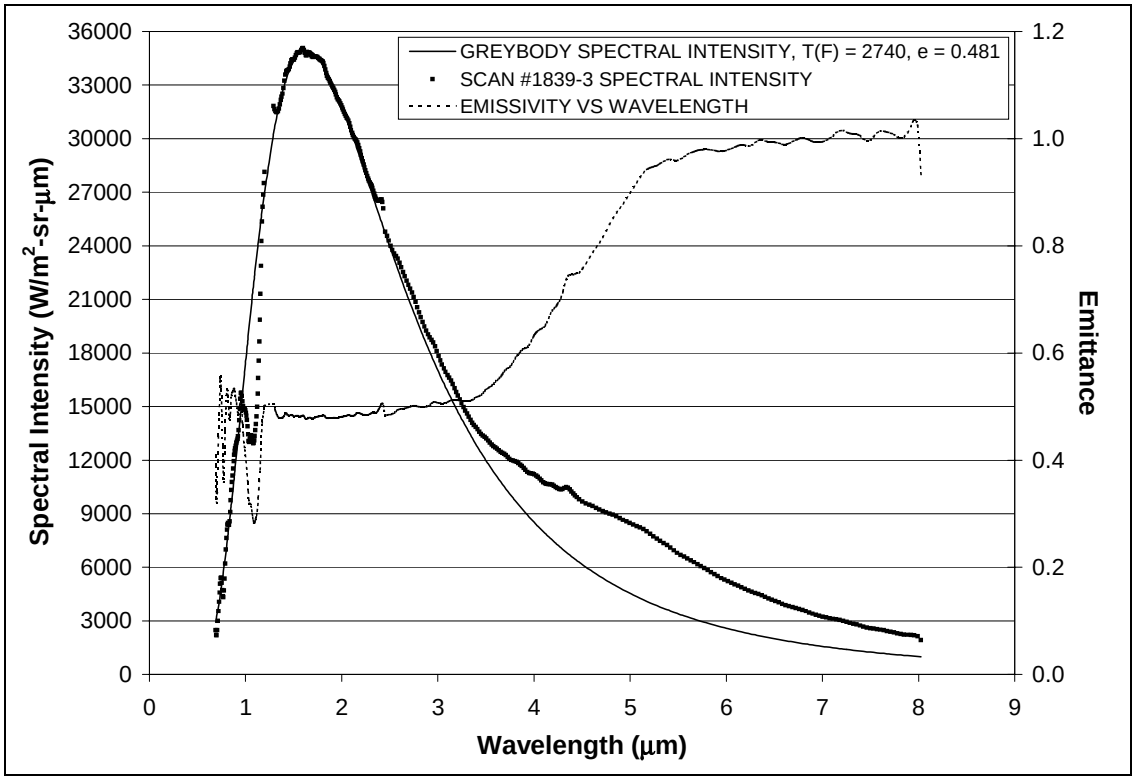

Figure 102: #1839-3, Bare LI-2200, 2300°F Condition, 5in Nozzle

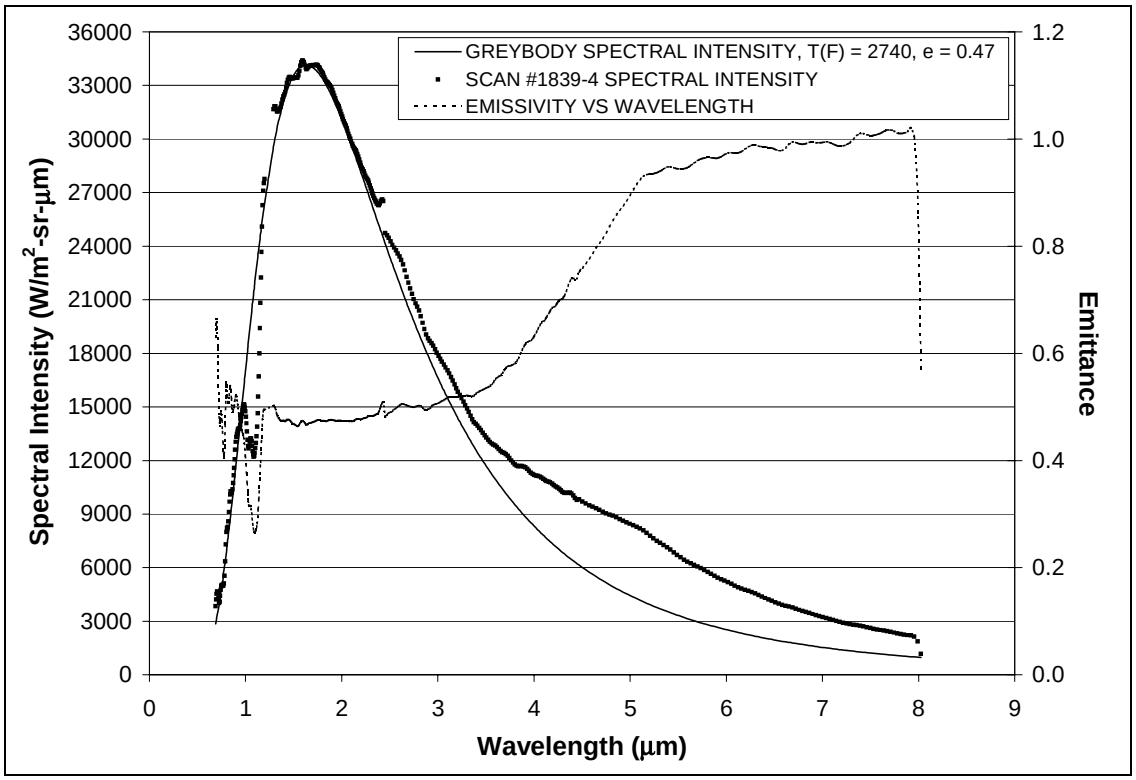

Figure 103: #1839-4, Bare LI-2200, 2300°F Condition, 5in Nozzle

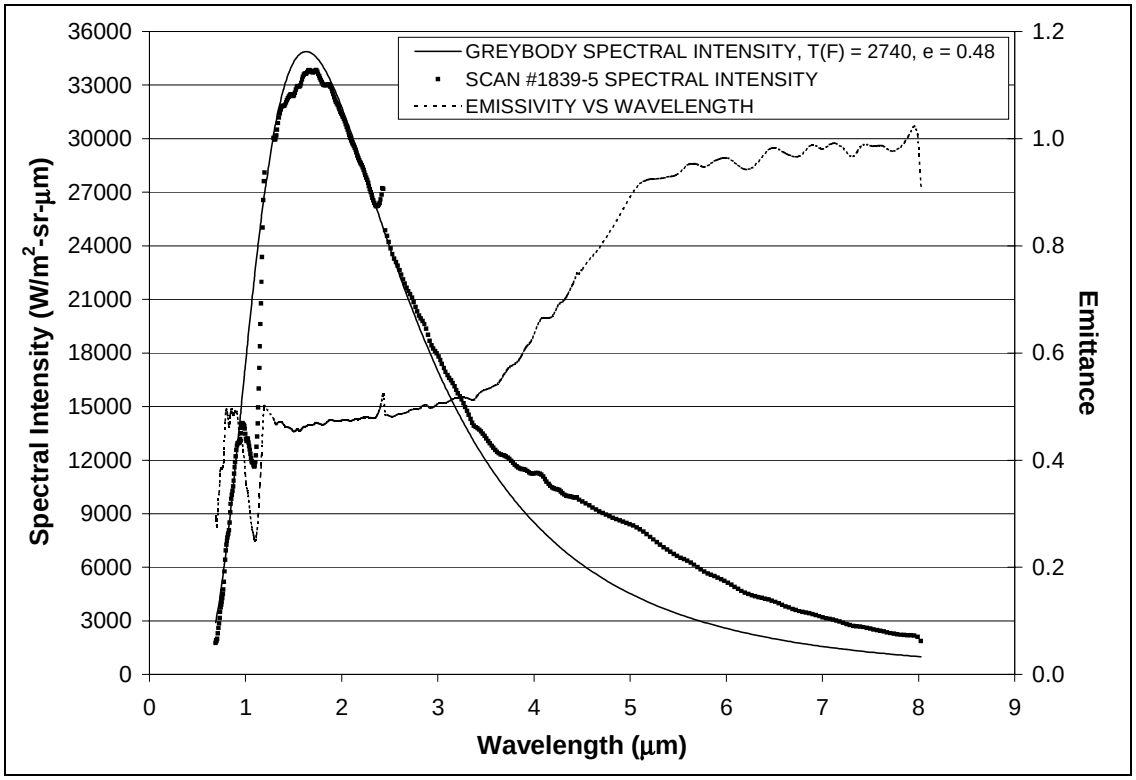

Figure 104: #1839-5, Bare LI-2200, 2300°F Condition, 5in Nozzle

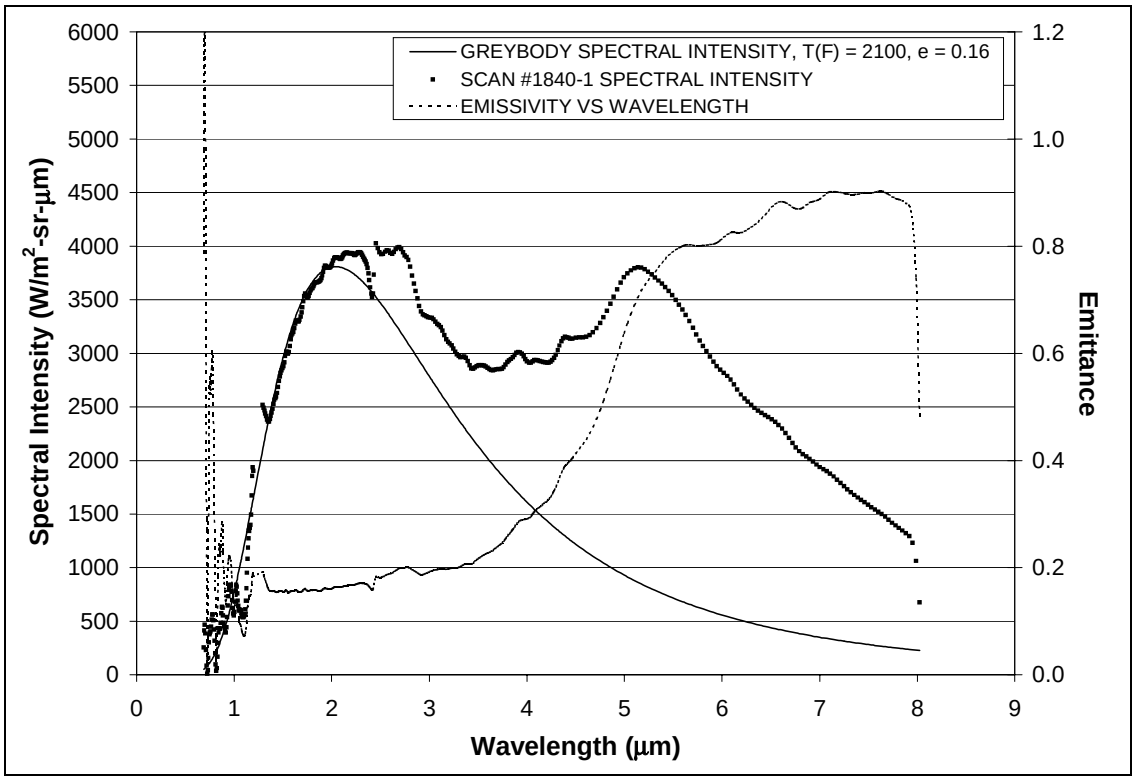

Figure 105: #1840-1, Bare LI-2200, 1600°F Condition, 15in Nozzle

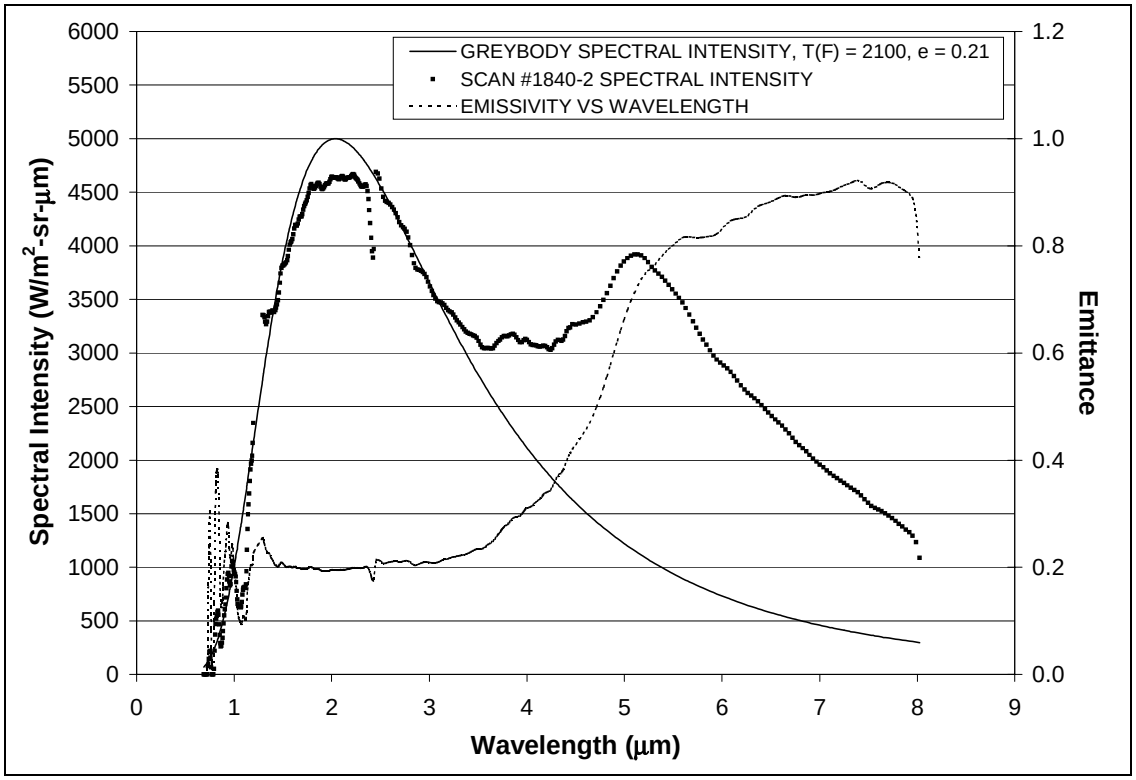

Figure 106: #1840-2, Bare LI-2200, 1600°F Condition, 15in Nozzle

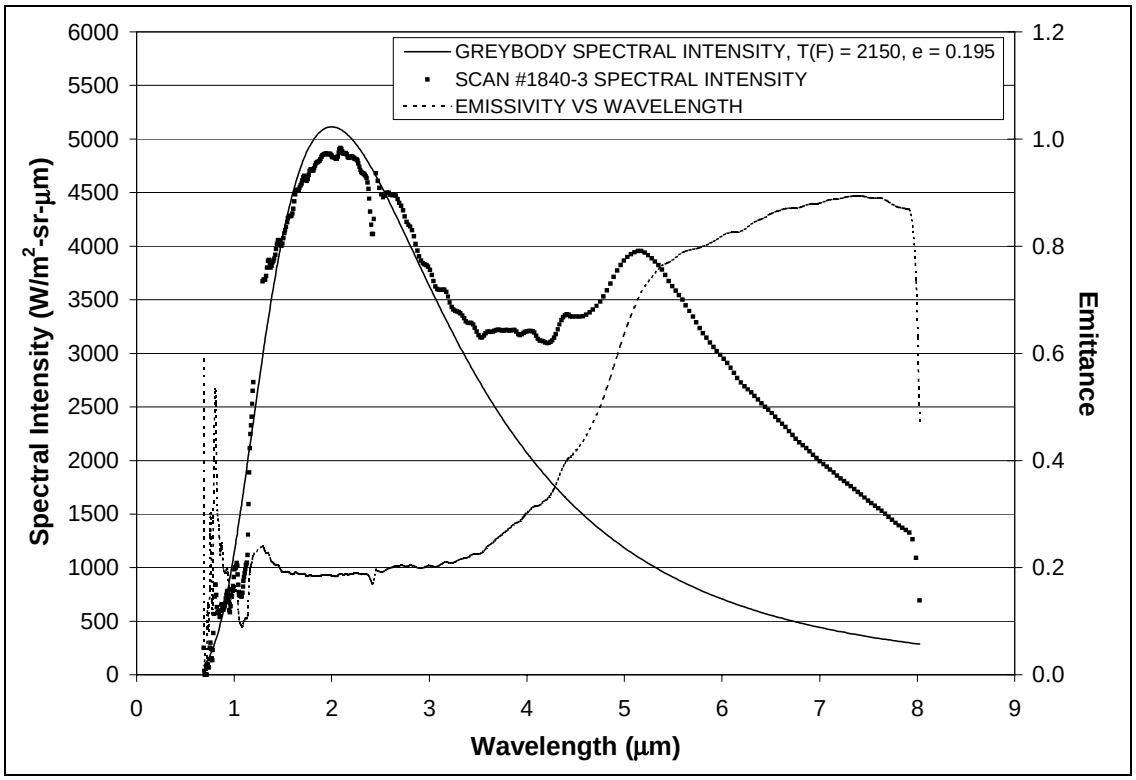

Figure 107: #1840-3, Bare LI-2200, 1600°F Condition, 15in Nozzle

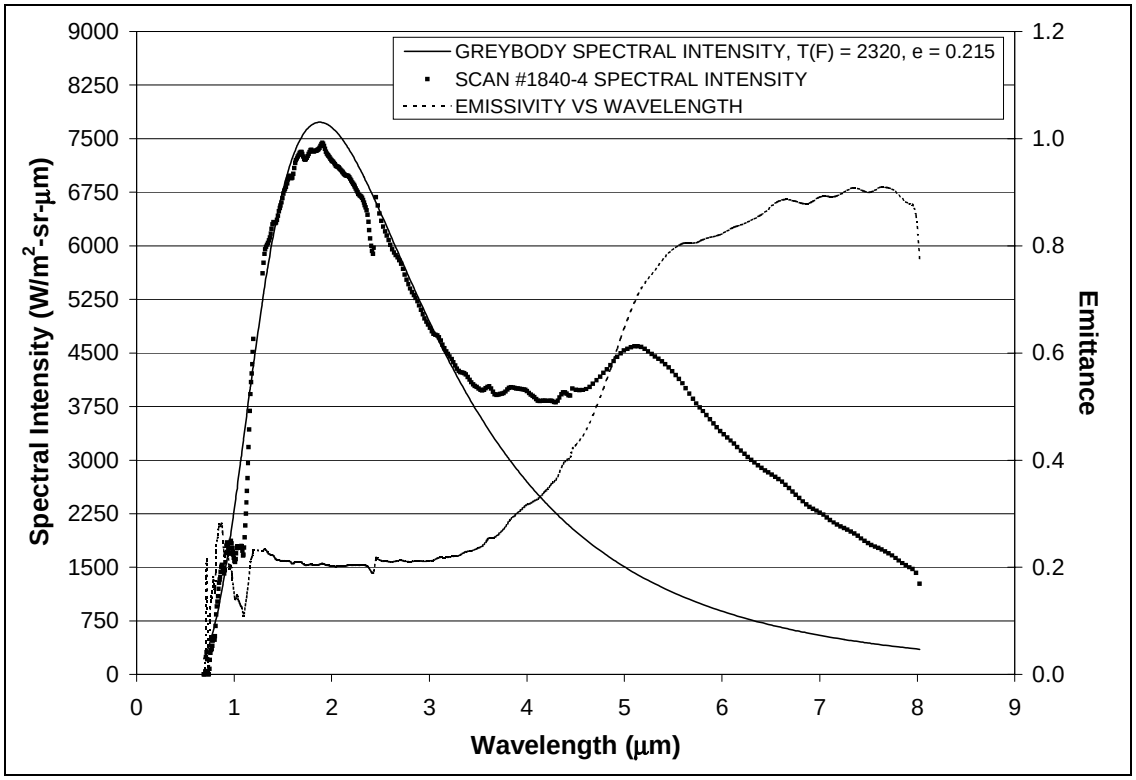

Figure 108: #1840-4, Bare LI-2200, 1700°F Condition, 15in Nozzle

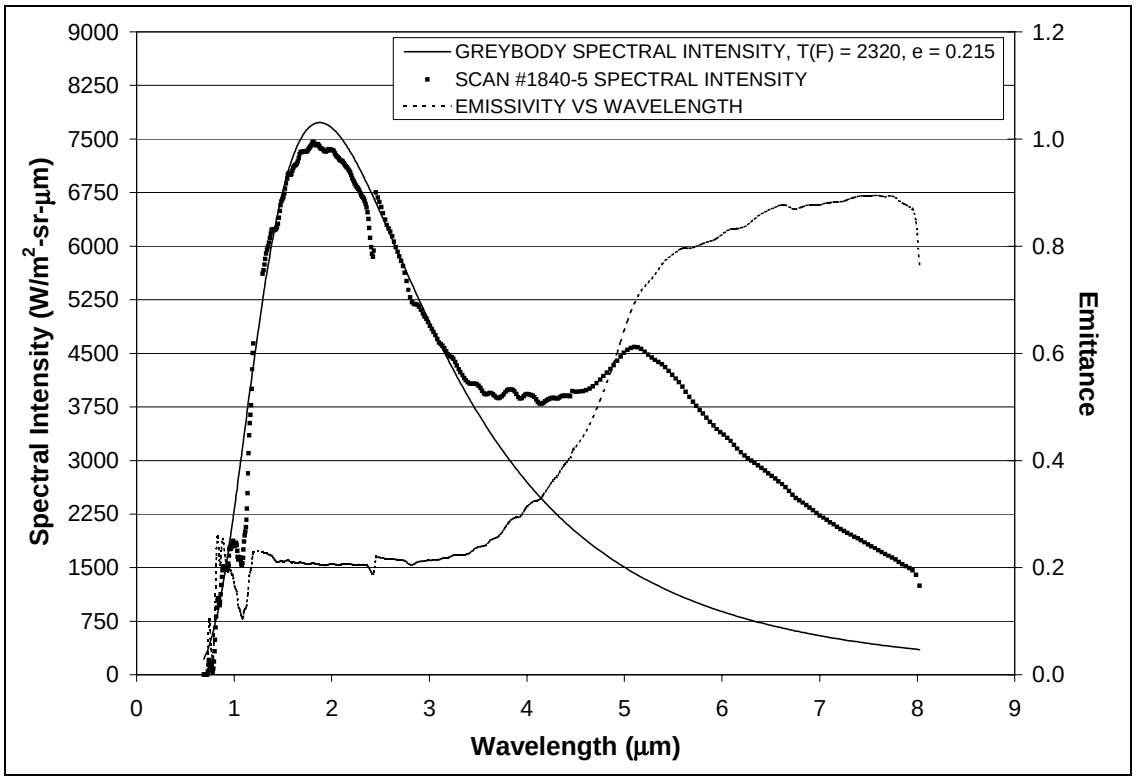

Figure 109: #1840-5, Bare LI-2200, 1700°F Condition, 15in Nozzle

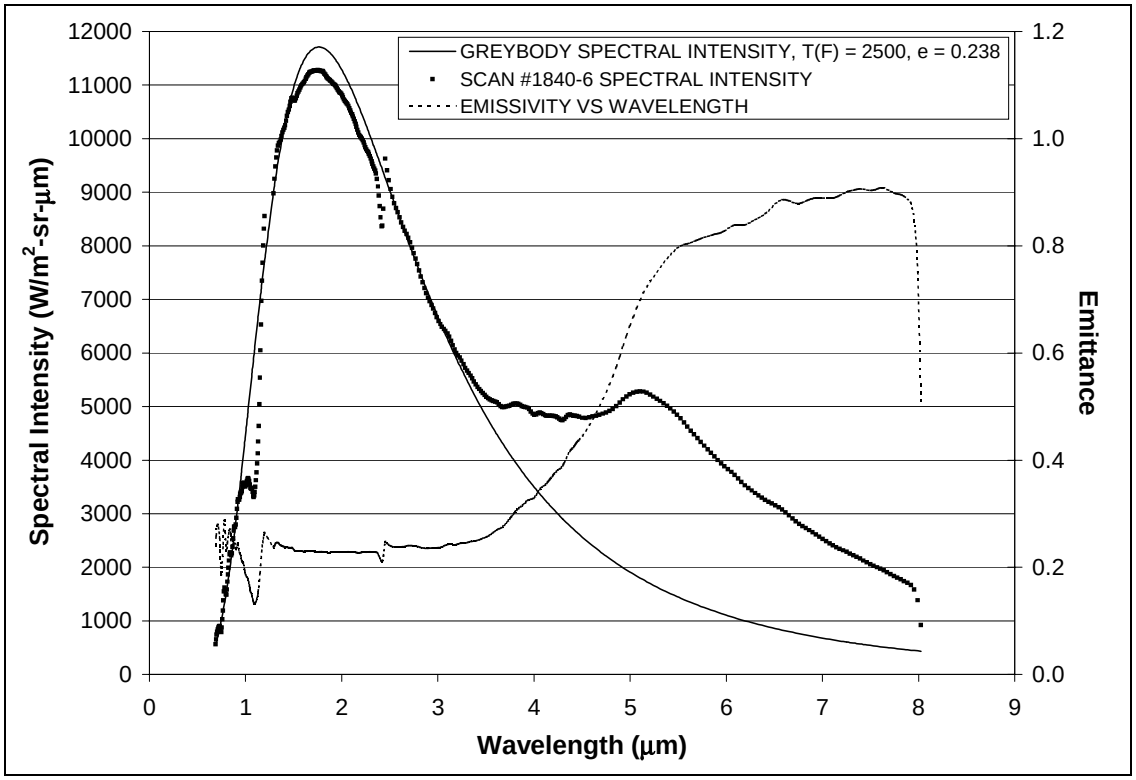

Figure 110: #1840-6, Bare LI-2200, 1800°F Condition, 15in Nozzle

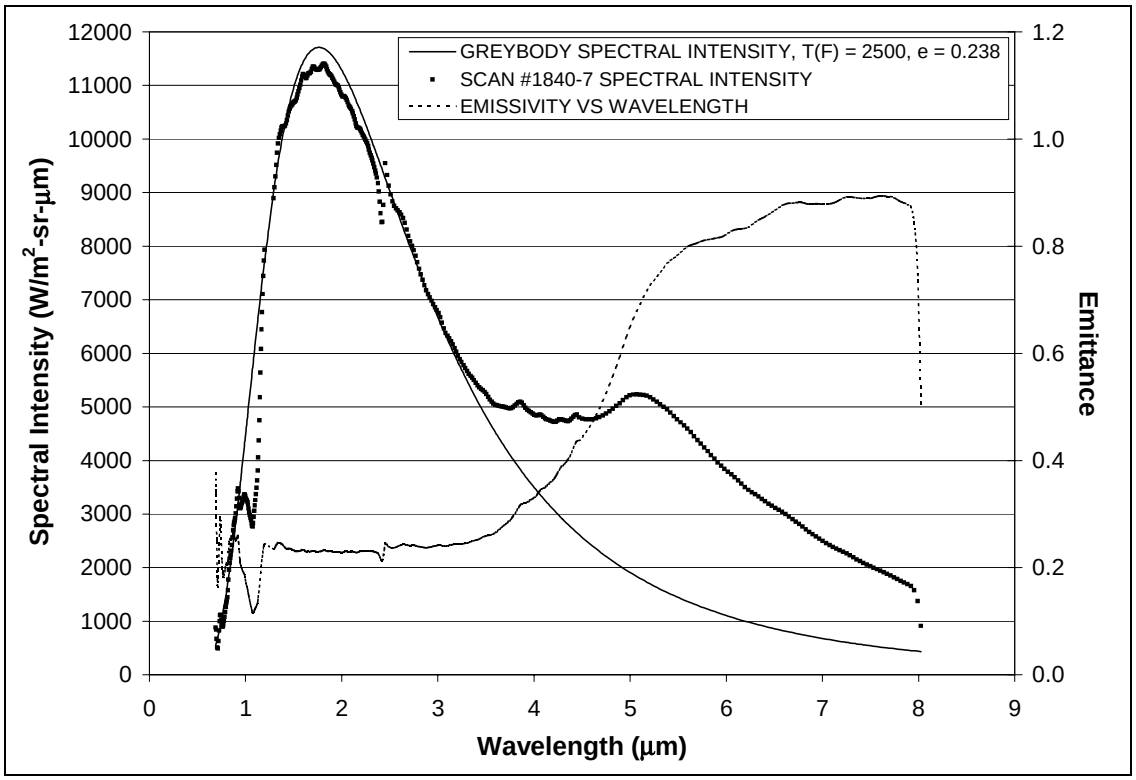

Figure 111: #1840-7, Bare LI-2200, 1800°F Condition, 15in Nozzle

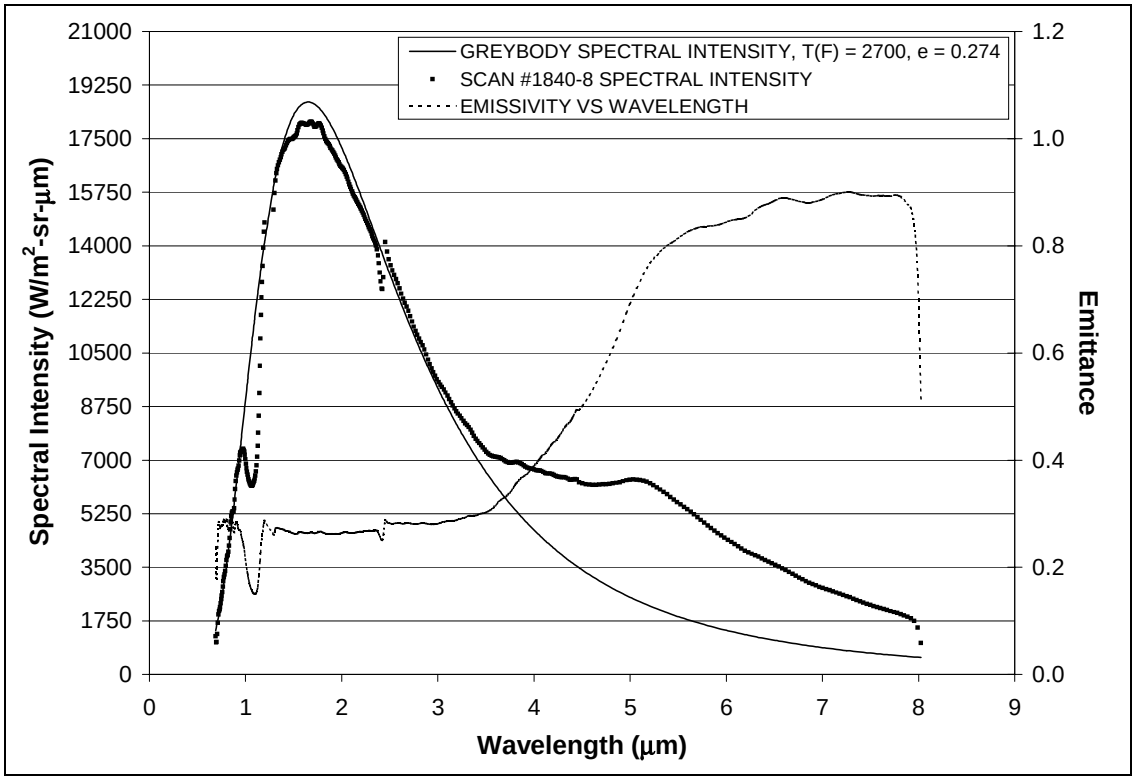

Figure 112: #1840-8, Bare LI-2200, 2000°F Condition, 15in Nozzle

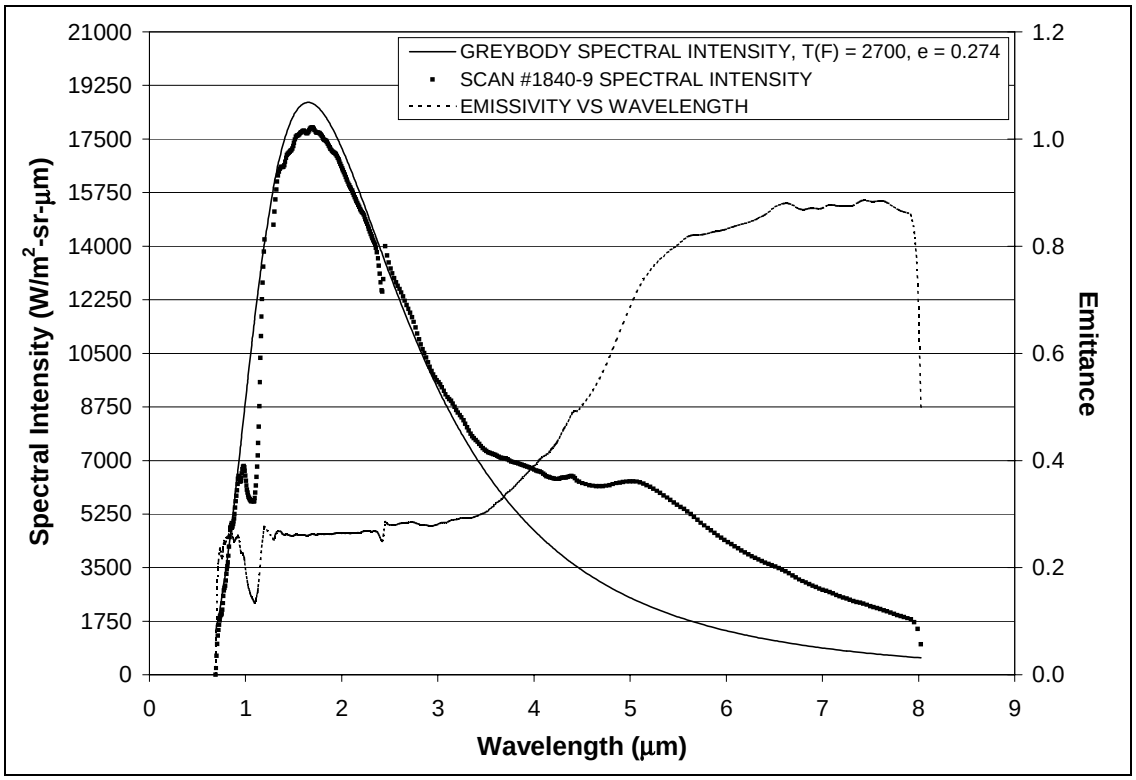

Figure 113: #1840-9, Bare LI-2200, 2000°F Condition, 15in Nozzle

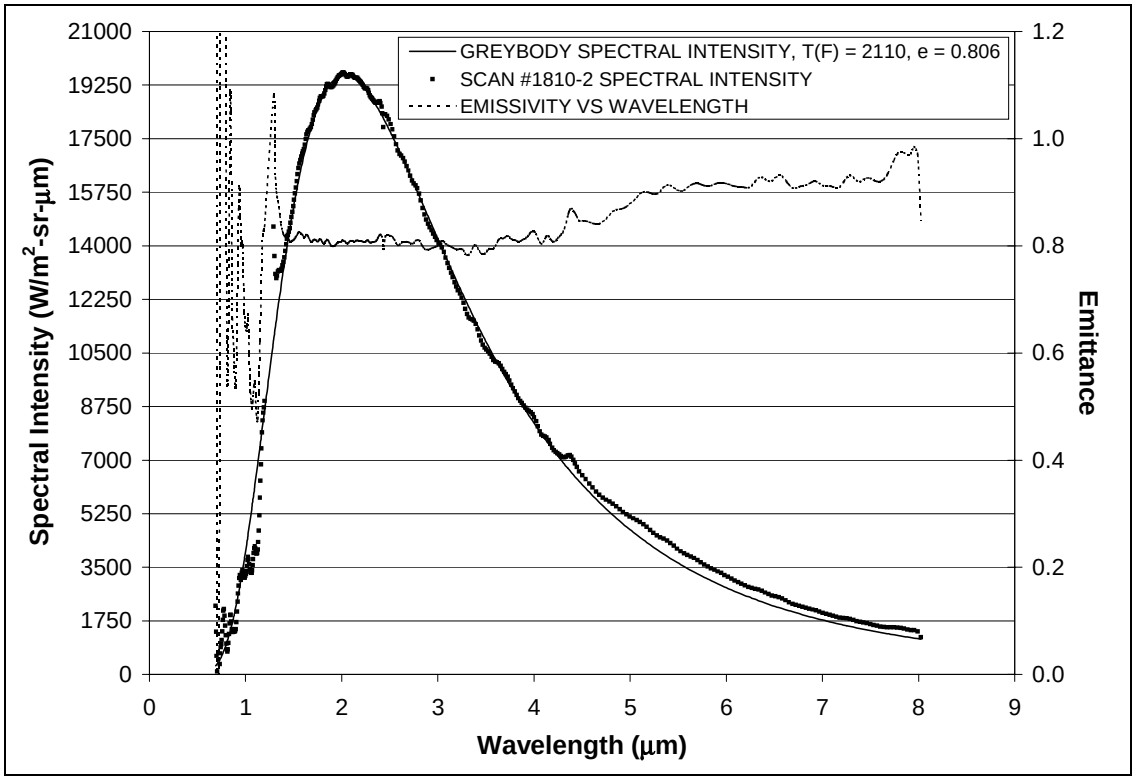

Figure 114: #1810-2, MA-25S, 2000°F Condition, 5in Nozzle

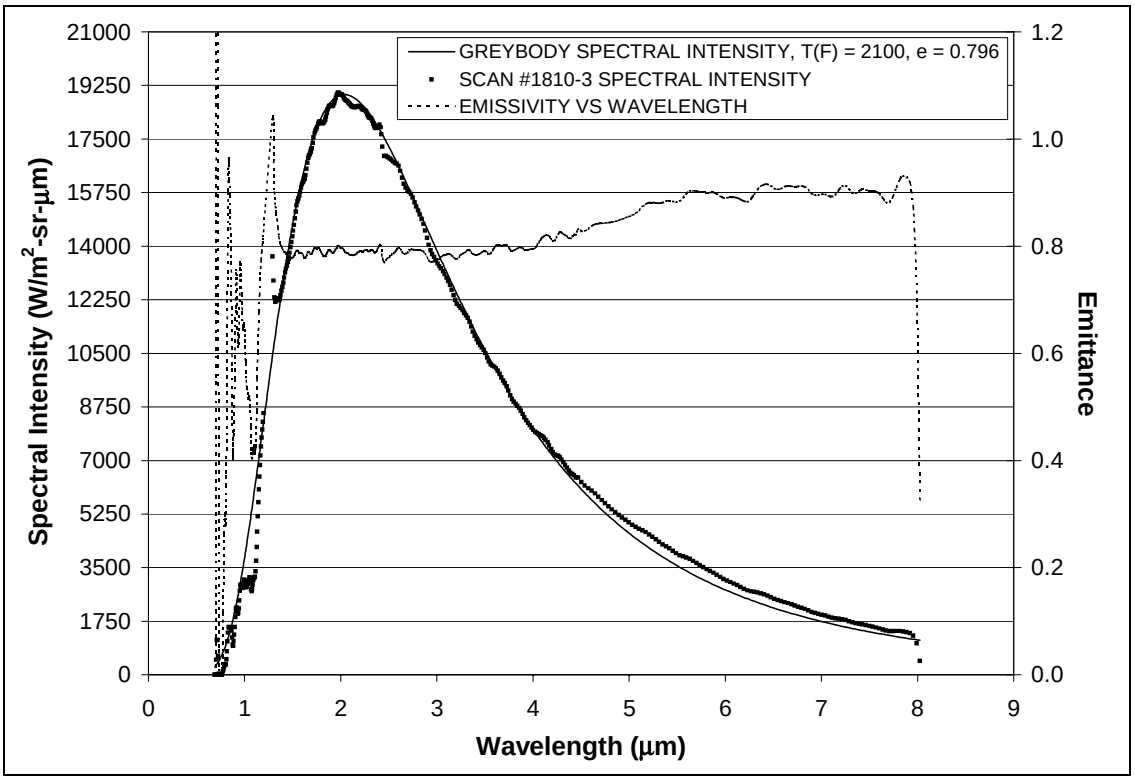

Figure 115: #1810-3, MA-25S, 2000°F Condition, 5in Nozzle

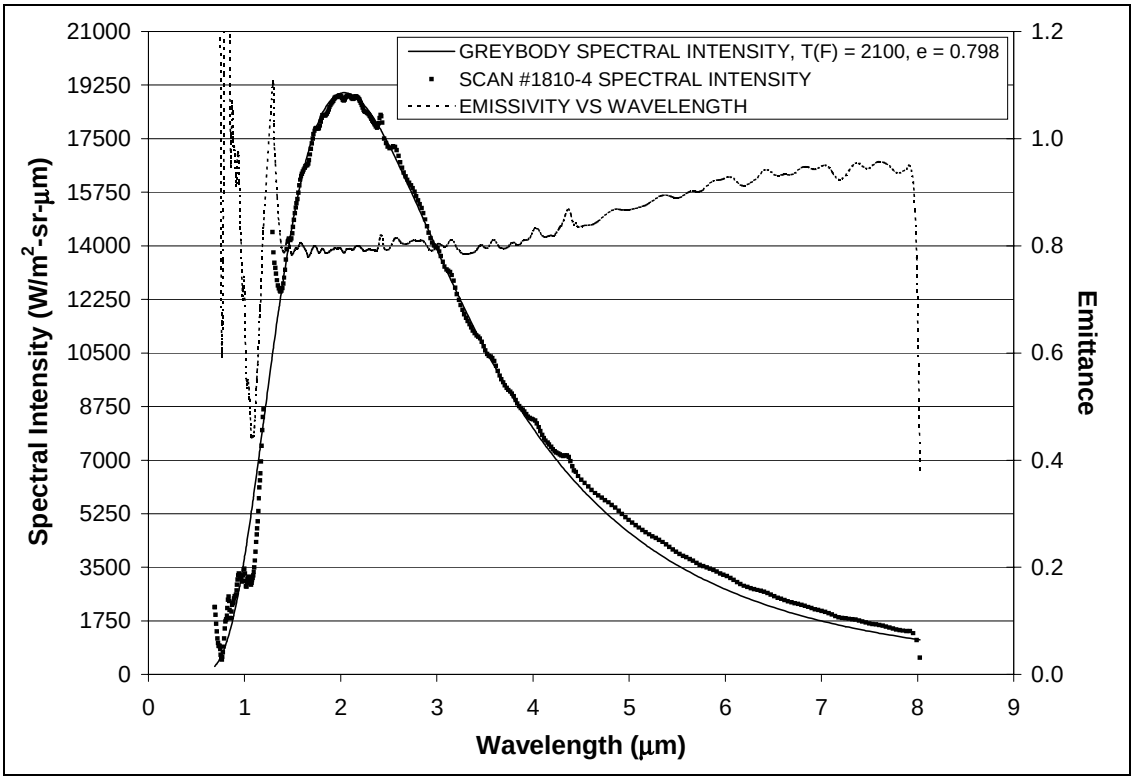

Figure 116: #1810-4, MA-25S, 2000°F Condition, 5in Nozzle

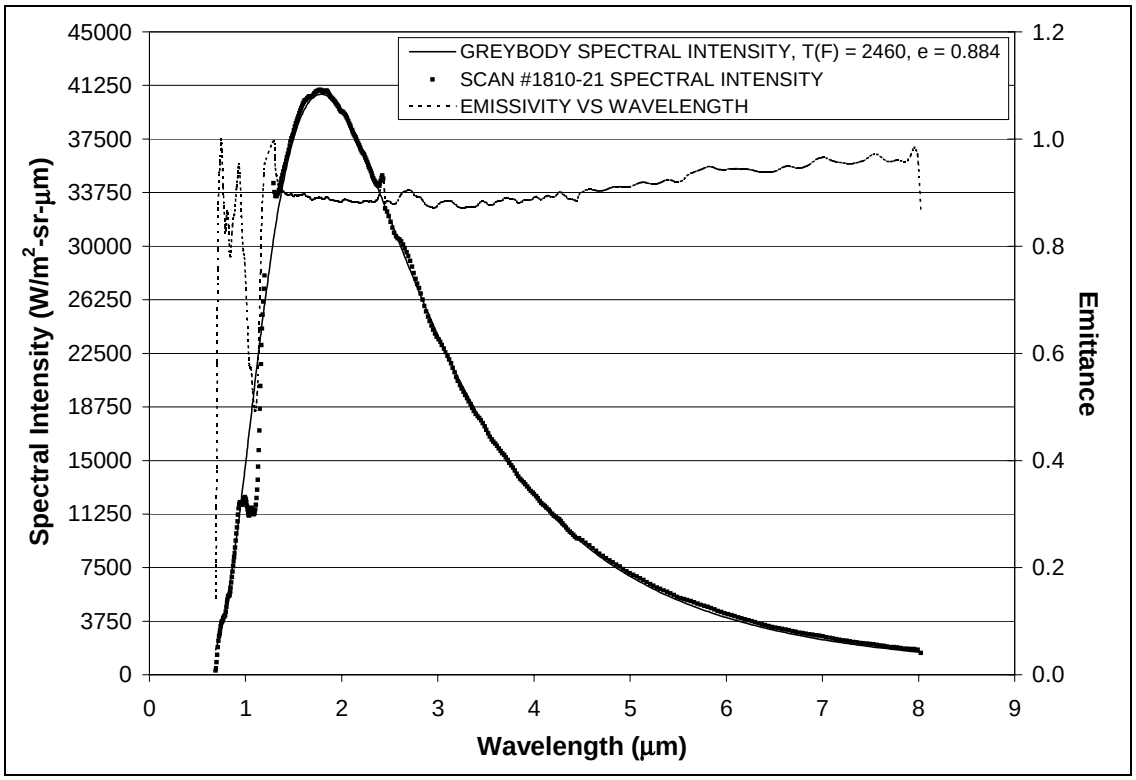

Figure 117: #1810-21, MA-25S, 2300°F Condition, 5in Nozzle

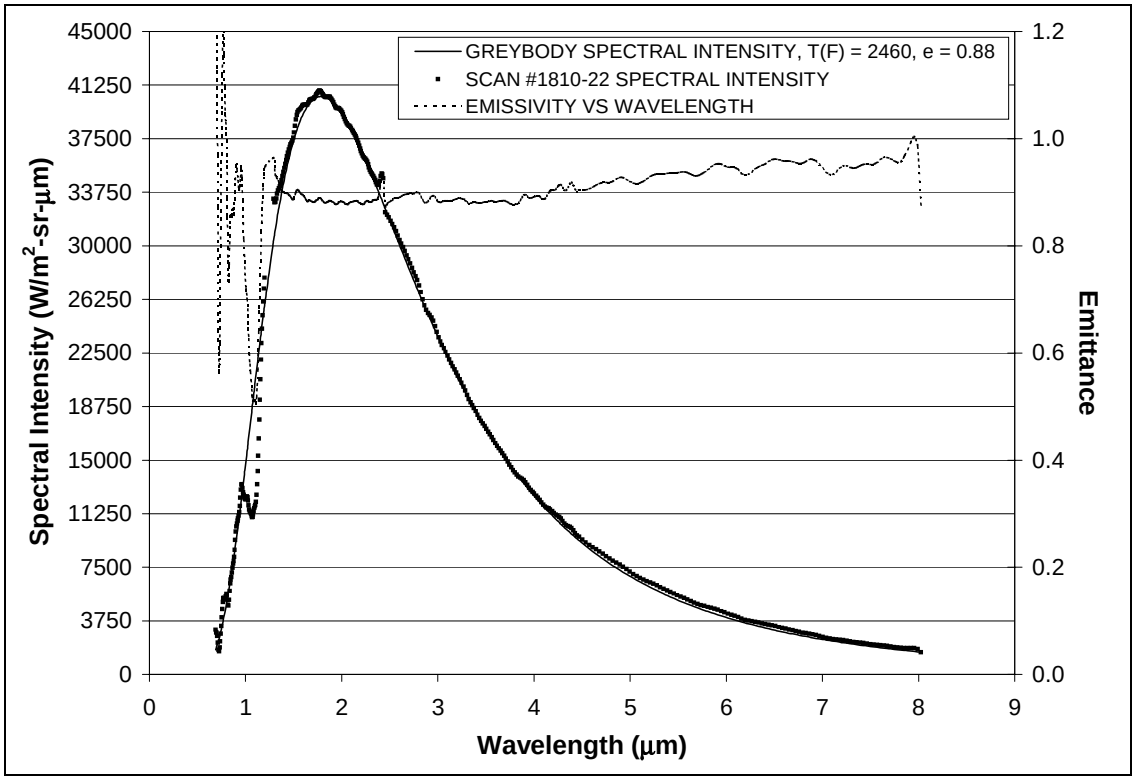

Figure 118: #1810-22, MA-25S, 2300°F Condition, 5in Nozzle

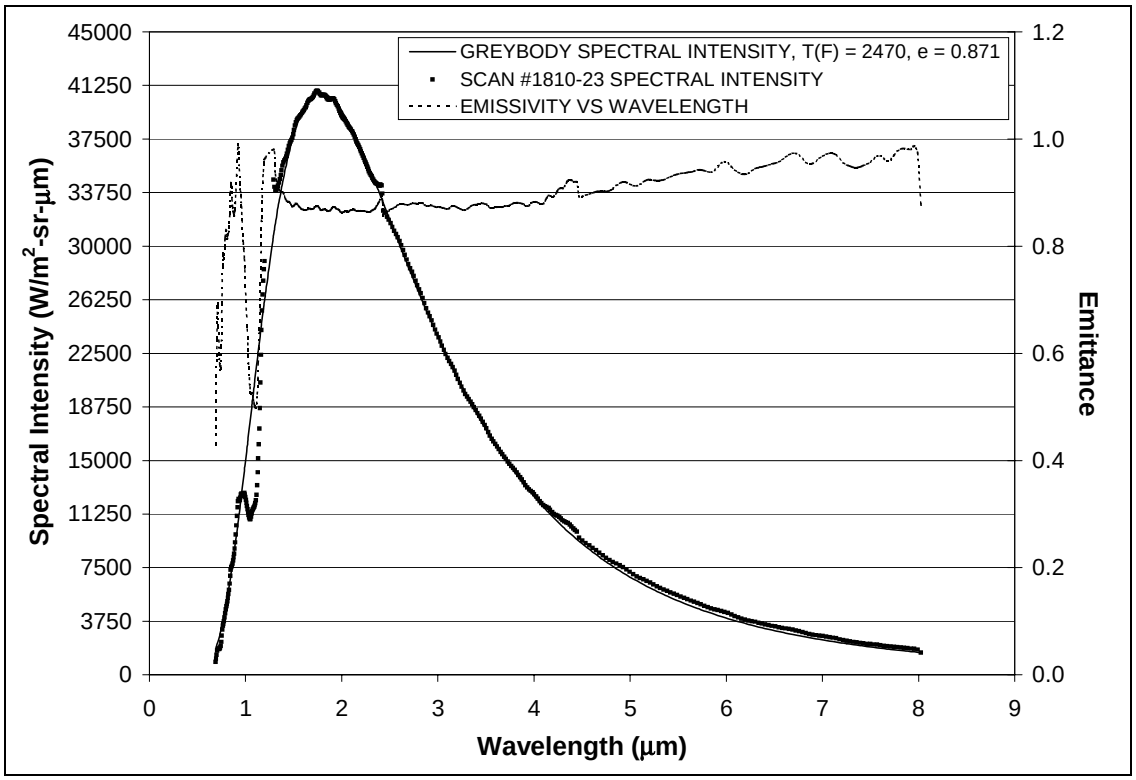

Figure 119: #1810-23, MA-25S, 2300°F Condition, 5in Nozzle

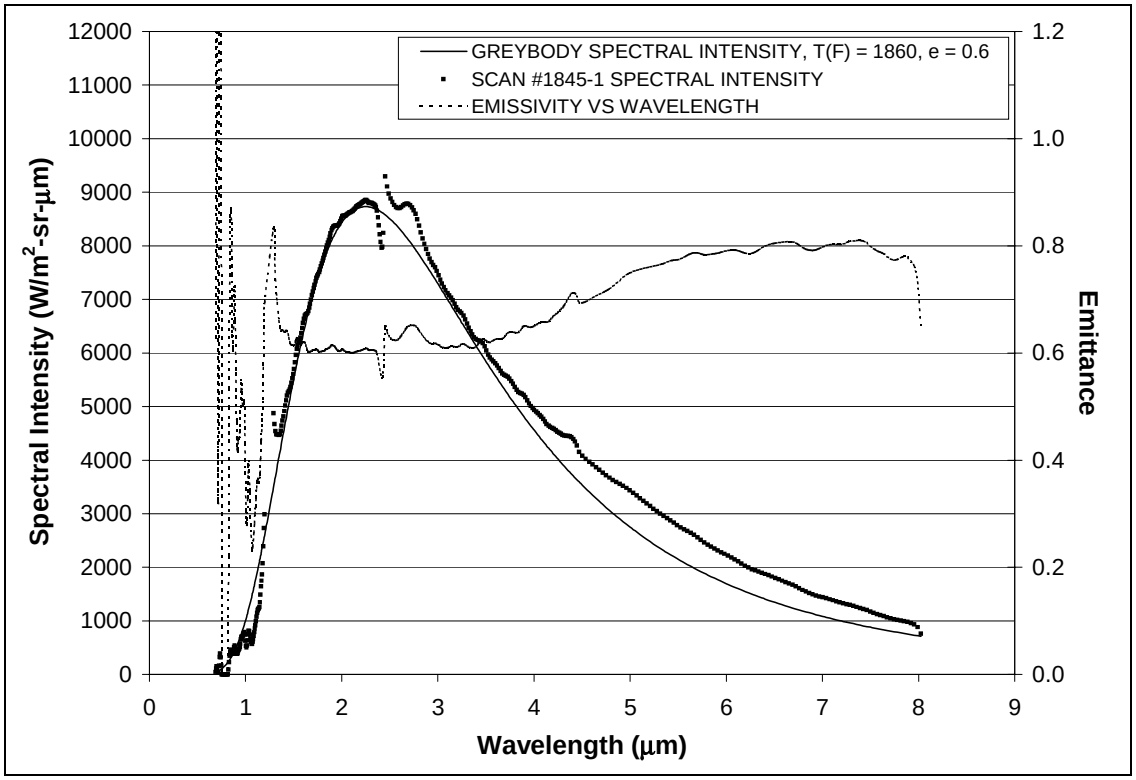

Figure 120: #1845-1, MA-25S, 1600°F Condition, 15in Nozzle

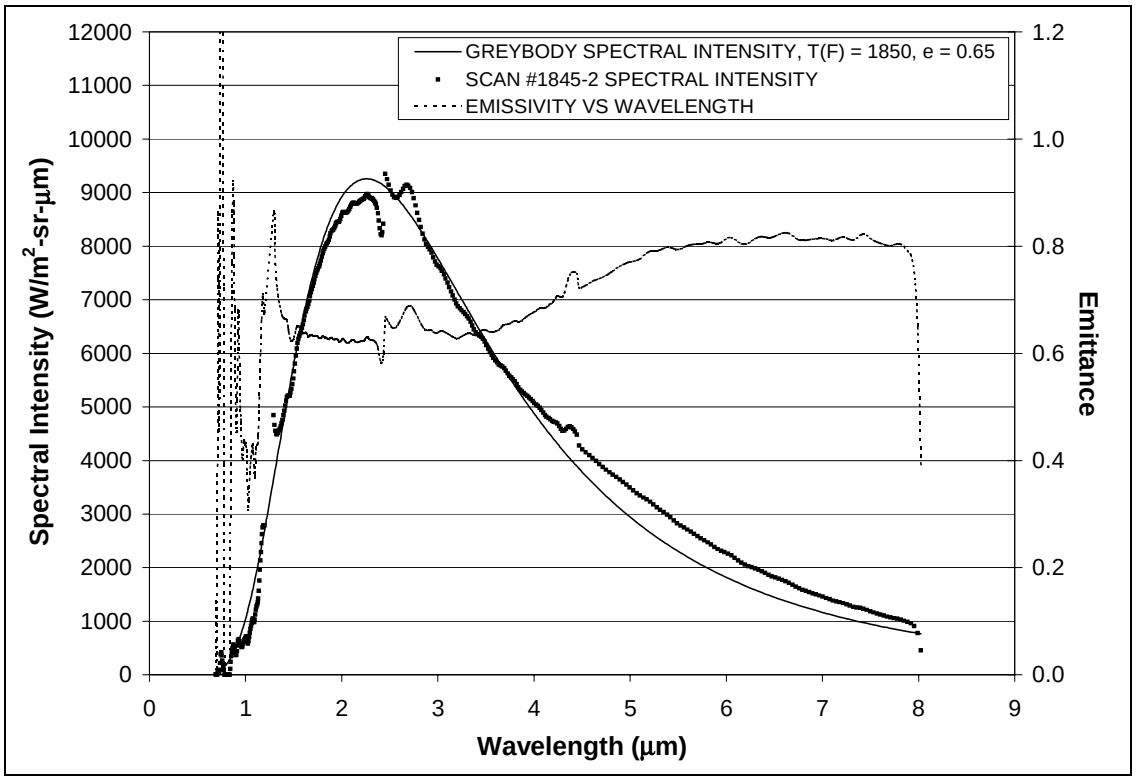

Figure 121: #1845-2, MA-25S, 1600°F Condition, 15in Nozzle

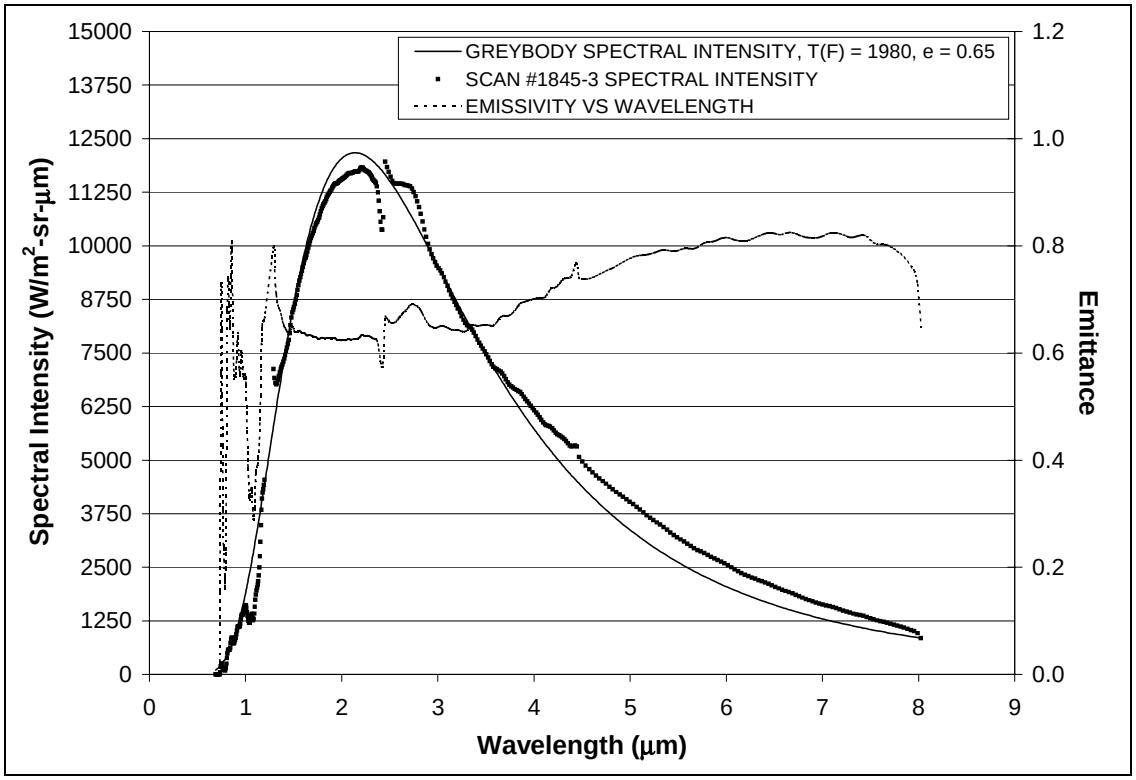

Figure 122: #1845-3, MA-25S, 1700°F Condition, 15in Nozzle

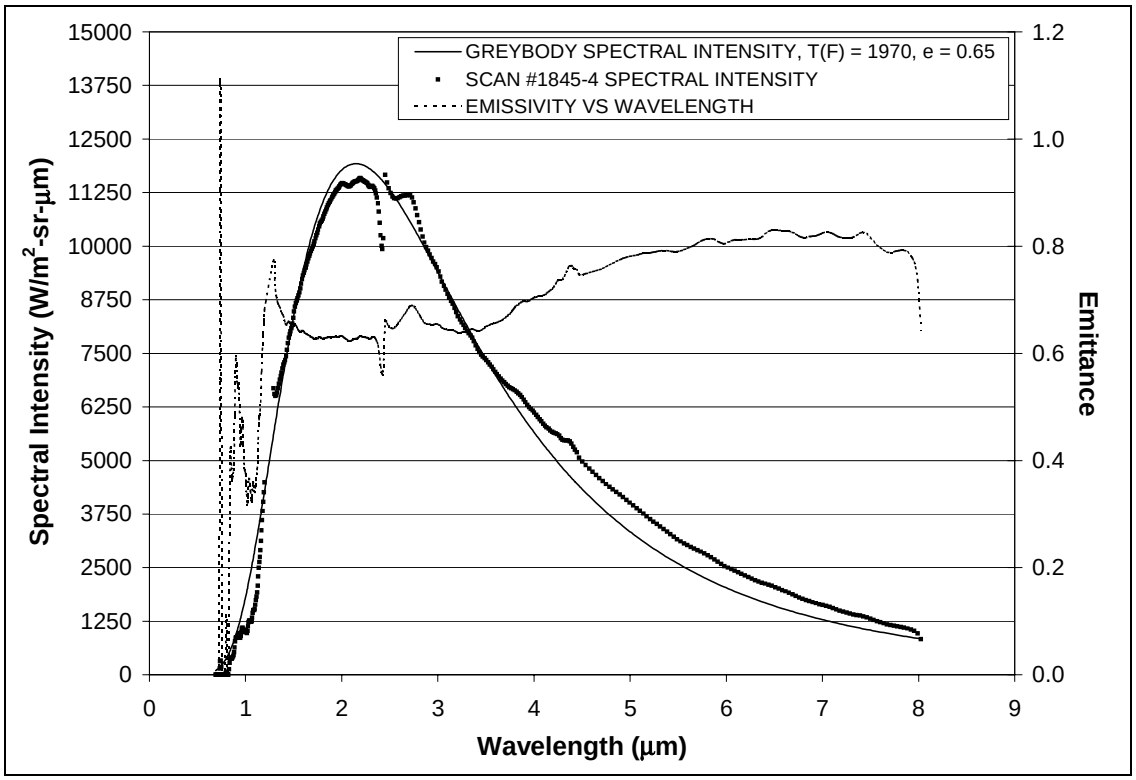

Figure 123: #1845-4, MA-25S, 1700°F Condition, 15in Nozzle

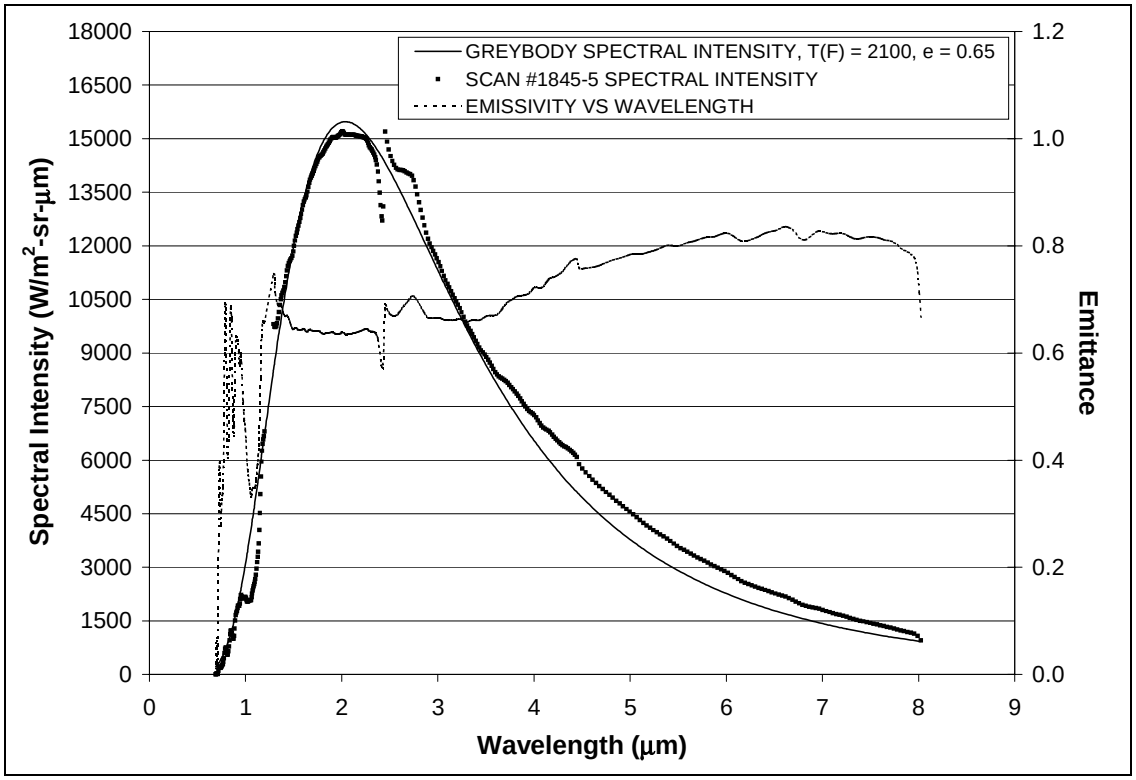

Figure 124: #1845-5, MA-25S, 1800°F Condition, 15in Nozzle

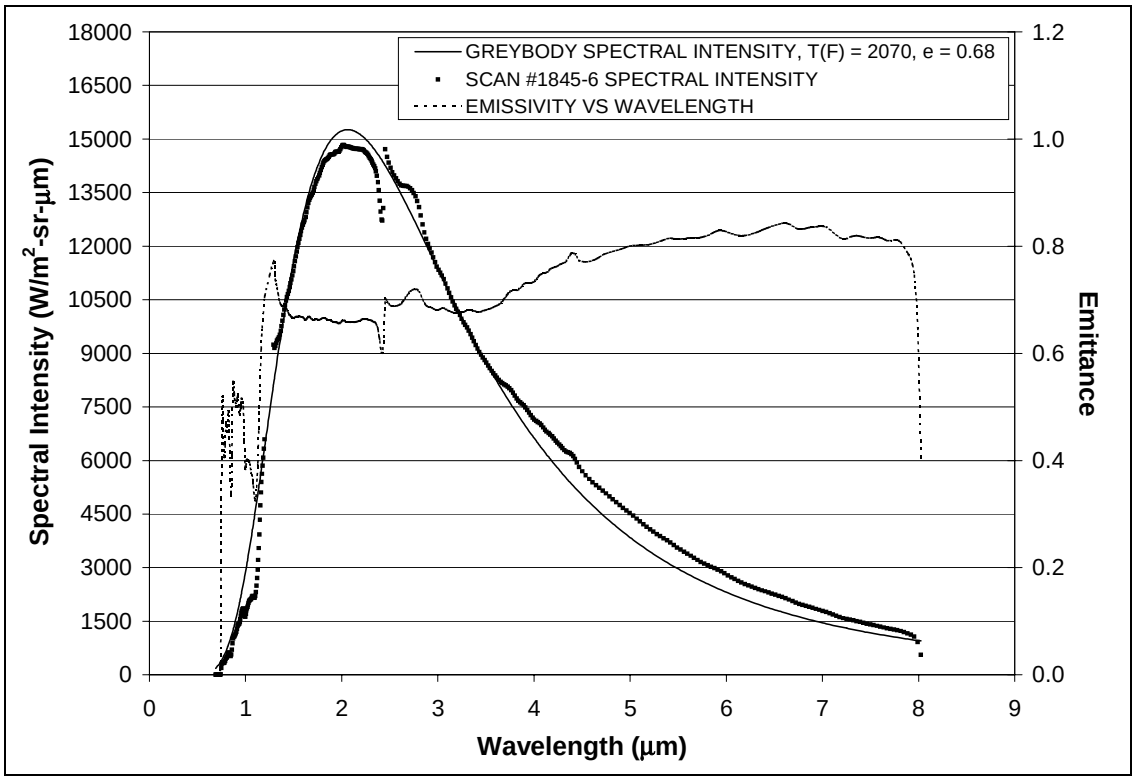

Figure 125: #1845-6, MA-25S, 1800°F Condition, 15in Nozzle

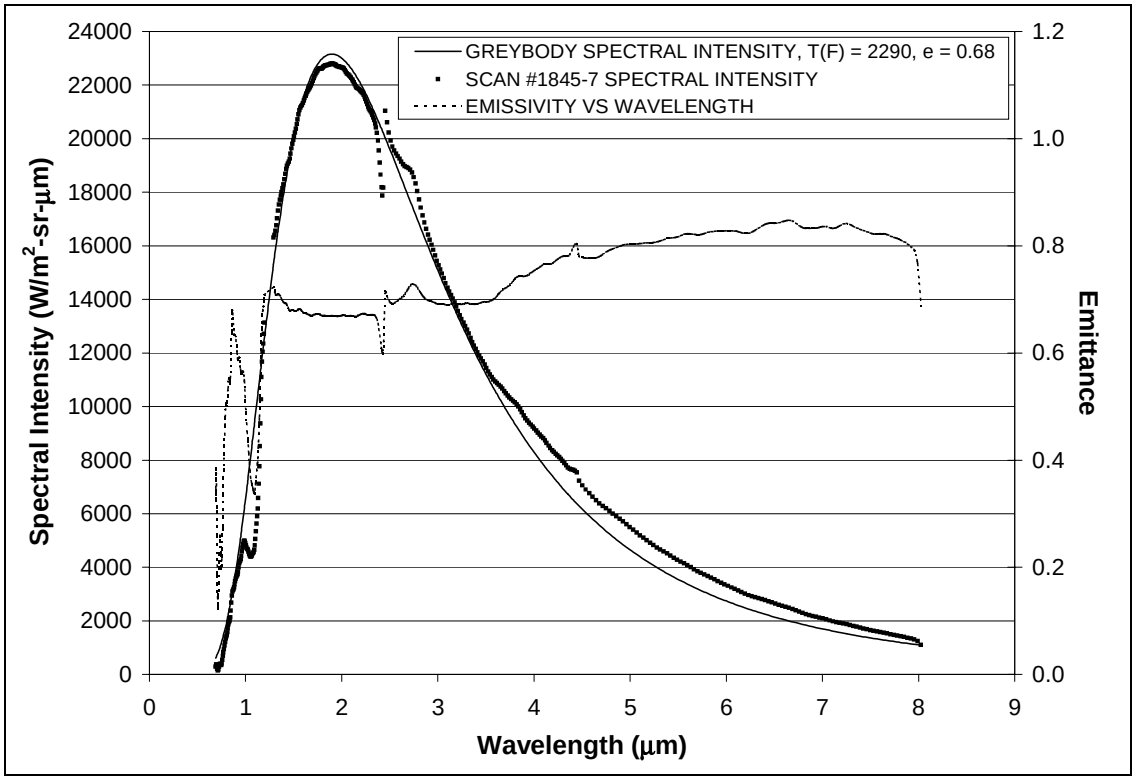

Figure 126: #1845-7, MA-25S, 2000°F Condition, 15in Nozzle

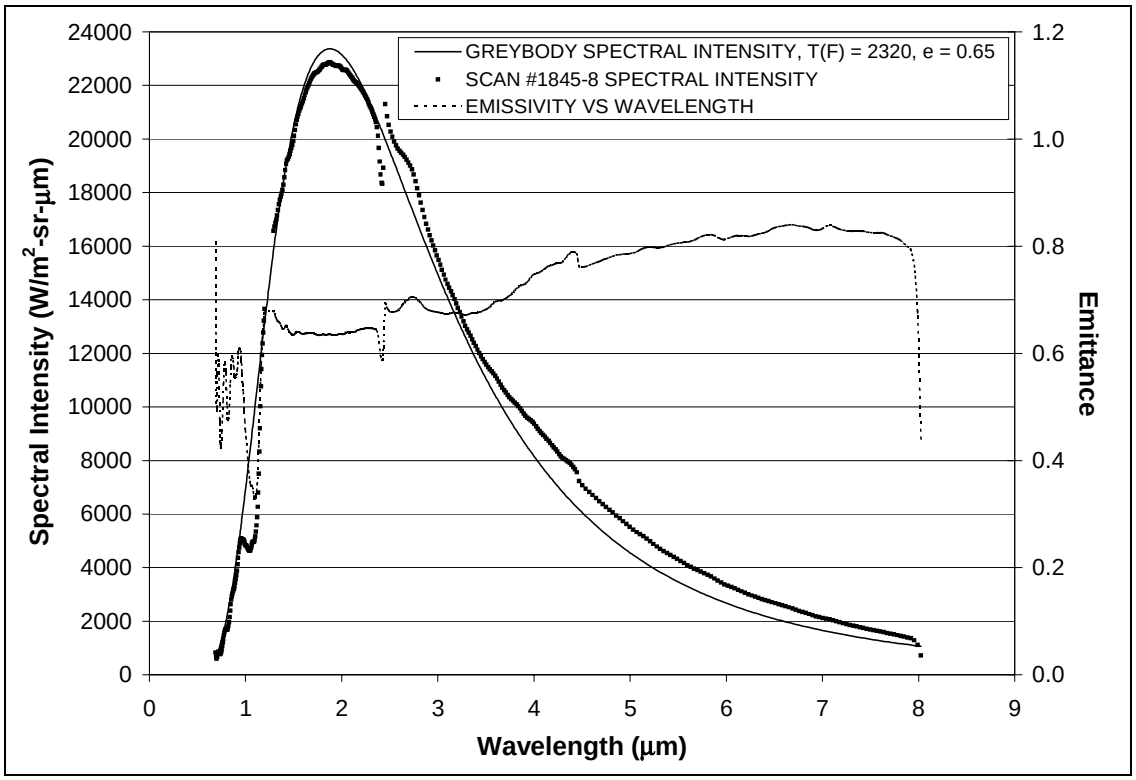

Figure 127: #1845-8, MA-25S, 2000°F Condition, 15in Nozzle

APPENDIX C – PRE- AND POST TEST PHOTOGRAPHS

JSC Photo ID	Model ID	View	Pre/Post
JSC2003E46974	1805	Front	Pre
JSC2003E46975	1805	Back	Pre
JSC2003E46979	**1805**	**Front Oblique**	**Pre**
JSC2003E46680	1805	Front	Post
JSC2003E46681	1805	Back	Post
JSC2003E46691	**1805**	**Front Oblique**	**Post**
JSC2003E44508	1806	Front	Pre
JSC2003E44509	1806	Back	Pre
JSC2003E44510	**1806**	**Front Oblique**	**Pre**
JSC2003E46672	1806	Front	Post
JSC2003E46673	1806	Back	Post
JSC2003E46674	**1806**	**Front Oblique**	**Post**
JSC2003E46976	1807	Front	Pre
JSC2003E46977	1807	Back	Pre
JSC2003E46978	**1807**	**Front Oblique**	**Pre**
JSC2003E46670	1807	Front	Post
JSC2003E46671	1807	Back	Post
JSC2003E46686	**1807**	**Front Oblique**	**Post**
JSC2003E44511	1808	Front	Pre
JSC2003E44512	1808	Back	Pre
JSC2003E44513	1808	Back Oblique	Pre
JSC2003E44514	**1809**	**Front**	**Pre**
JSC2003E44515	1809	Back	Pre
JSC2003E44516	1809	Back Oblique	Pre
JSC2003E46682	1809	Front	Post
JSC2003E46683	1809	Back	Post
JSC2003E46684	**1809**	**Front Oblique**	**Post**
JSC2003E44517	**1810**	**Front**	**Pre**
JSC2003E44518	1810	Back	Pre
JSC2003E44519	1810	Back Oblique	Pre
JSC2003E51353	1810	Front	Post
JSC2003E51354	1810	Back	Post
JSC2003E51355	**1810**	**Front Oblique**	**Post**
JSC2003E44520	1811	Front	Pre
JSC2003E44521	1811	Back	Pre
JSC2003E44522	1811	Back Oblique	Pre
JSC2003E44523	**1812**	**Front**	**Pre**
JSC2003E44524	1812	Back	Pre
JSC2003E44525	1812	Back Oblique	Pre
JSC2003E46668	1812	Front	Post
JSC2003E46669	1812	Back	Post
JSC2003E46687	**1812**	**Front Oblique**	**Post**
JSC2003E44526	1813	Front	Pre
JSC2003E44527	1813	Back	Pre
JSC2003E44528	1813	Back Oblique	Pre

JSC Photo ID	Model ID	View	Pre/Post
JSC2003E44529	1814	Front	Pre
JSC2003E44530	1814	Back	Pre
JSC2003E44531	1814	Back Oblique	Pre
JSC2003E44532	1815	Back	Pre
JSC2003E44533	1815	Front	Pre
JSC2003E44534	**1815**	**Front Oblique**	**Pre**
JSC2003E46678	1815	Front	Post
JSC2003E46679	1815	Back	Post
JSC2003E46685	**1815**	**Front Oblique**	**Post**
JSC2003E44535	**1816**	**Front**	**Pre**
JSC2003E44536	1816	Back	Pre
JSC2003E44537	1816	Back Oblique	Pre
JSC2003E46675	1816	Front	Post
JSC2003E46676	1816	Back	Post
JSC2003E46677	**1816**	**Front Oblique**	**Post**
JSC2003E46664	1817	Front	Pre
JSC2003E46665	1817	Back	Pre
JSC2003E46689	**1817**	**Front Oblique**	**Pre**
JSC2003E46804	1817	Front	Post
JSC2003E46805	1817	Back	Post
JSC2003E46806	**1817**	**Front Oblique**	**Post**
JSC2003E46666	1818	Front	Pre
JSC2003E46667	1818	Back	Pre
JSC2003E46688	**1818**	**Front Oblique**	**Pre**
JSC2003E46807	1818	Front	Post
JSC2003E46808	1818	Back	Post
JSC2003E46809	**1818**	**Front Oblique**	**Post**
JSC2003E46662	1821	Front	Pre
JSC2003E46663	1821	Back	Pre
JSC2003E46690	**1821**	**Front Oblique**	**Pre**
JSC2003E47268	1821	Front	Post
JSC2003E47269	1821	Back	Post
JSC2003E47270	**1821**	**Front Oblique**	**Post**
JSC2003E53981	1845	Front	Pre
JSC2003E53982	1845	Back	Pre
JSC2003E53983	**1845**	**Front Oblique**	**Pre**
JSC2003E54527	1845	Front Oblique In Holder	Post
JSC2003E54528	1845	Front In Holder	Post
JSC2003E54540	1845	Front	Post
JSC2003E54541	**1845**	**Front Oblique**	**Post**
JSC2003E54542	1845	Back	Post
JSC2003E53984	1846	Front	Pre
JSC2003E53985	1846	Back	Pre
JSC2003E53986	1846	Front Oblique	Pre

***Photos in bold are included in this test report**

Table 7: Tile Repair Concepts Photo List

JSC Photo ID	Model ID	View	Pre/Post
JSC2003E49554	**1828**	**Front In Holder**	**Pre**
JSC2003E51344	**1828**	**Front Oblique**	**Post**
JSC2003E51345	1828	Front	Post
JSC2003E51346	1828	Back	Post
JSC2003E49556	1829	Front	Pre
JSC2003E49557	1829	Back	Pre
JSC2003E49558	**1829**	**Front Oblique**	**Pre**
JSC2003E51350	1829	Front	Post
JSC2003E51351	1829	Back	Post
JSC2003E51352	**1829**	**Front Oblique**	**Post**
JSC2003E49559	**1830**	**Front Oblique**	**Pre**
JSC2003E49560	1830	Front	Pre
JSC2003E49561	1830	Back	Pre
JSC2003E54529	**1830**	**Front**	**Post**
JSC2003E54530	1830	Back	Post
JSC2003E49562	1831	Front	Pre
JSC2003E49563	1831	Back	Pre
JSC2003E49564	1831	Front Oblique	Pre
JSC2003E49565	1832	Front Oblique	Pre
JSC2003E49566	1832	Front	Pre
JSC2003E49567	1832	Back	Pre
JSC2003E50259	1833	Front	Post
JSC2003E50260	1833	Back	Post
JSC2003E50261	**1833**	**Front Oblique**	**Post**
JSC2003E49568	1834	Front	Pre
JSC2003E49569	1834	Back	Pre
JSC2003E49570	**1834**	**Front Oblique**	**Pre**
JSC2003E50265	1834	In Chamber	Post
JSC2003E50266	1834	In Chamber	Post
JSC2003E50267	1834	Front In Holder	Post
JSC2003E50268	1834	Front Oblique In Holder	Post
JSC2003E50269	1834	Front Oblique In Holder	Post
JSC2003E51531	1834	Front	Post
JSC2003E51532	1834	Back	Post
JSC2003E51533	**1834**	**Front Oblique**	**Post**
JSC2003E49571	**1835**	**Front Oblique**	**Pre**
JSC2003E49572	1835	Front	Pre
JSC2003E49573	1835	Back	Pre
JSC2003E51341	1835	Front	Post
JSC2003E51342	1835	Back	Post
JSC2003E51343	**1835**	**Front Oblique**	**Post**
JSC2003E49574	**1836**	**Front Oblique**	**Pre**
JSC2003E49575	1836	Front	Pre
JSC2003E49576	1836	Back	Pre
JSC2003E54520	1836	Front In Holder	Post
JSC2003E54521	1836	Front Oblique In Holder	Post

JSC Photo ID	Model ID	View	Pre/Post
JSC2003E54522	1836	Front	Post
JSC2003E54523	1836	Back	Post
JSC2003E54524	**1836**	**Front Oblique**	**Post**
JSC2003E54525	1836	Front In Holder	Post
JSC2003E54526	1836	Front Oblique In Holder	Post
JSC2003E54537	1836	Front Oblique	Post
JSC2003E54538	1836	Front	Post
JSC2003E54539	1836	Back	Post
JSC2003E49577	1837	Front	Pre
JSC2003E49578	1837	Back	Pre
JSC2003E49579	**1837**	**Front Oblique**	**Pre**
JSC2003E55037	1837	Front In Holder	Post
JSC2003E55038	1837	Front Oblique In Holder	Post
JSC2003E55041	**1837**	**Front Oblique**	**Post**
JSC2003E55042	1837	Front	Post
JSC2003E55043	1837	Back	Post
JSC2003E49555	**1838**	**Front In Holder**	**Pre**
JSC2003E50262	1838	Front	Post
JSC2003E50263	1838	Back	Post
JSC2003E50264	**1838**	**Front Oblique**	**Post**
JSC2003E49580	**1839**	**Front Oblique**	**Pre**
JSC2003E49581	1839	Front	Pre
JSC2003E49582	1839	Back	Pre
JSC2003E51347	1839	Front	Post
JSC2003E51348	1839	Back	Post
JSC2003E51349	**1839**	**Front Oblique**	**Post**
JSC2003E49583	1840	Front	Pre
JSC2003E49584	1840	Back	Pre
JSC2003E49585	**1840**	**Front Oblique**	**Pre**
JSC2003E54531	**1840**	**Front Oblique**	**Post**
JSC2003E54532	1840	Front	Post
JSC2003E54533	1840	Back	Post
JSC2003E49586	1841	Front Oblique	Pre
JSC2003E49587	1841	Front	Pre
JSC2003E49588	1841	Back	Pre
JSC2003E49589	1842	Front	Pre
JSC2003E49590	1842	Back	Pre
JSC2003E49591	1842	Front Oblique	Pre
JSC2003E54534	1835A	Front	Pre
JSC2003E54535	1835A	Back	Pre
JSC2003E54536	**1835A**	**Front Oblique**	**Pre**
JSC2003E55039	1835A	Front Oblique In Holder	Post
JSC2003E55040	1835A	Front In Holder	Post
JSC2003E55044	1835A	Front	Post
JSC2003E55045	1835A	Back	Post
JSC2003E55046	**1835A**	**Front Oblique**	**Post**

***Photos in bold are included in this test report**

Table 8: Uncoated RSI Photo List

JSC2003E46979 – Model #1805, Pre-Test, Front Oblique View

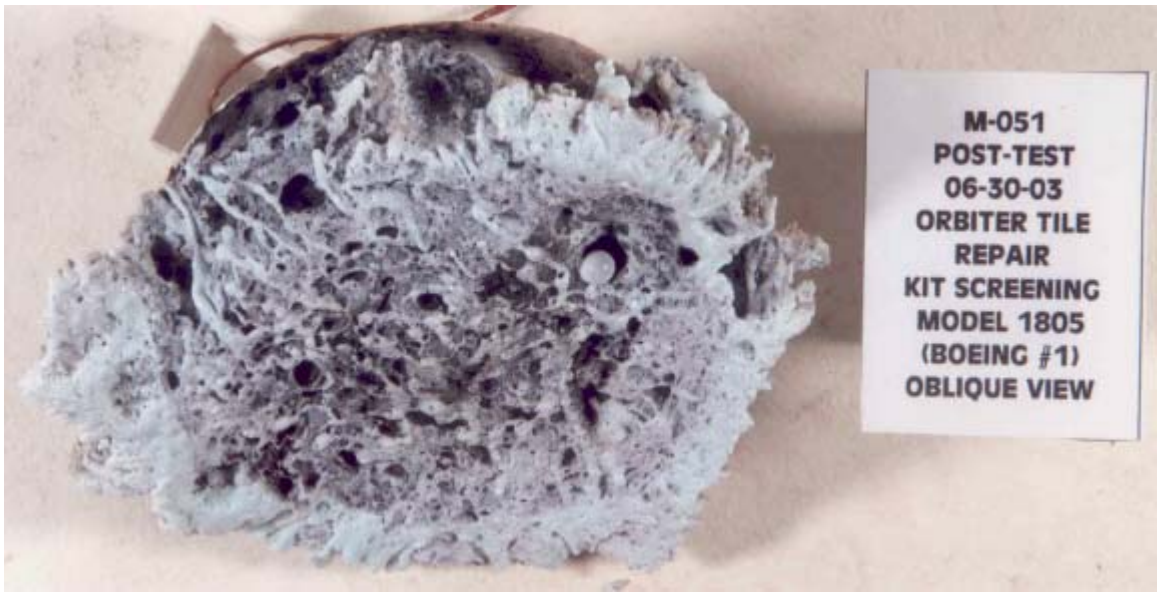

JSC2003E46691 – Model #1805, Post-Test, Front Oblique View

JSC2003E44510 – Model #1806, Pre-Test, Front Oblique View

JSC2003E46674 – Model #1806, Post-Test, Front Oblique View

JSC2003E46978 – Model #1807, Pre-Test, Front Oblique View

JSC2003E46686 – Model #1807, Post-Test, Front Oblique View

JSC2003E44514 – Model #1809, Pre-Test, Front View

JSC2003E46684 – Model #1809, Post-Test, Front Oblique View

JSC2003E44517 – Model #1810, Pre-Test, Front View

JSC2003E51355 – Model #1810, Post-Test, Front Oblique View

JSC2003E44523 – Model #1812, Pre-Test, Front View

JSC2003E46687 – Model #1812, Post-Test, Front Oblique View

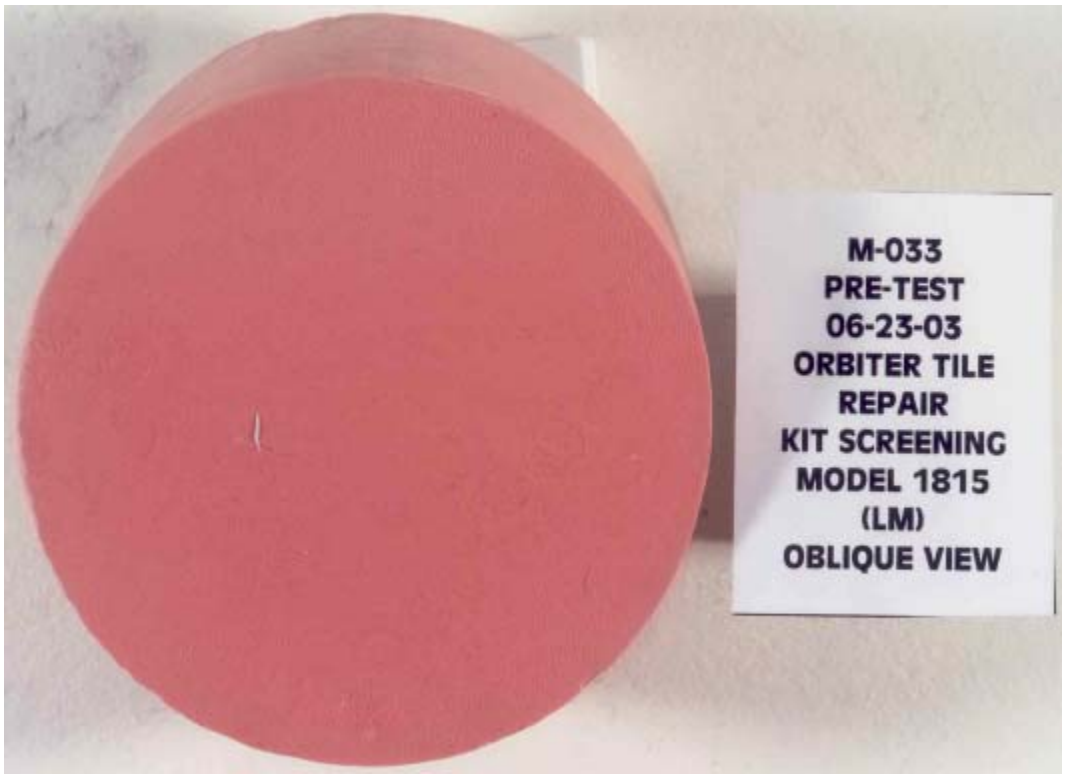

JSC2003E44534 – Model #1815, Pre-Test, Front Oblique View

JSC2003E46685 – Model #1815, Post-Test, Front Oblique View

JSC2003E44535 – Model #1816, Pre-Test, Front View

JSC2003E46677 – Model #1816, Post-Test, Front Oblique View

JSC2003E46689 – Model #1817, Pre-Test, Front Oblique View

JSC2003E46806 – Model #1817, Post-Test, Front Oblique View

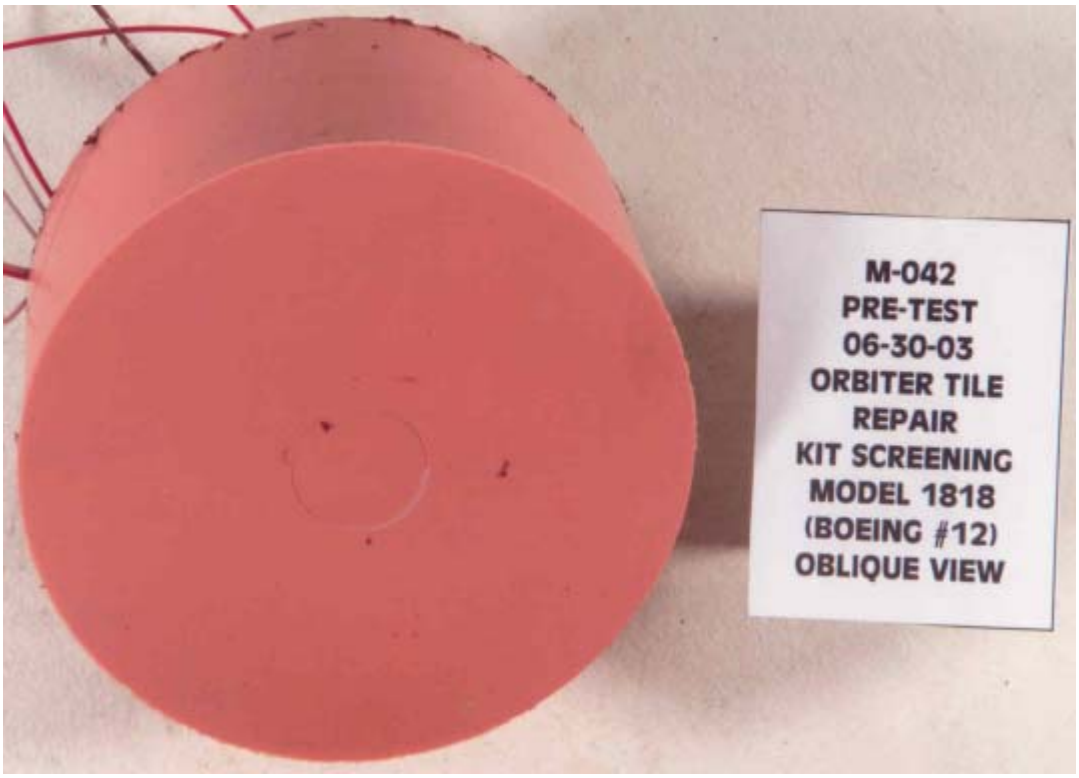

JSC2003E46688 – Model #1818, Pre-Test, Front Oblique View

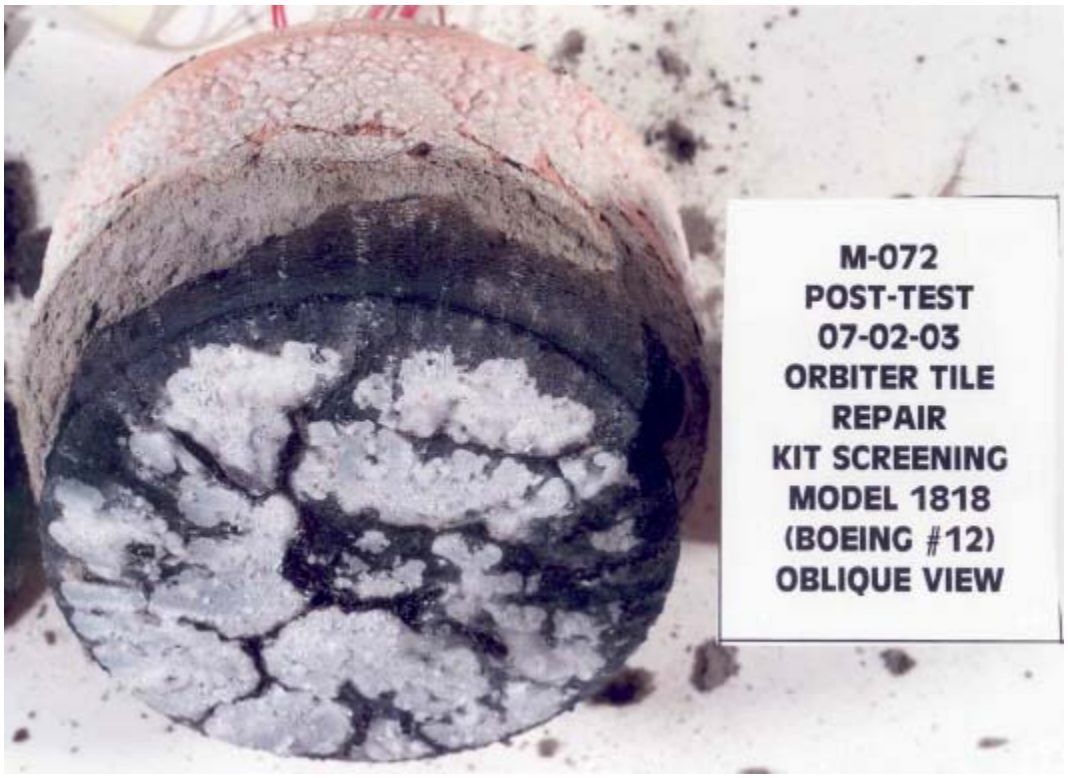

JSC2003E46809 – Model #1818, Post-Test, Front Oblique View

JSC2003E46690 – Model #1821, Pre-Test, Front Oblique View

JSC2003E47270 – Model #1821, Post-Test, Front Oblique View

JSC2003E53983 – Model #1845, Pre-Test, Front Oblique View

JSC2003E54541 – Model #1845, Post-Test, Front Oblique View

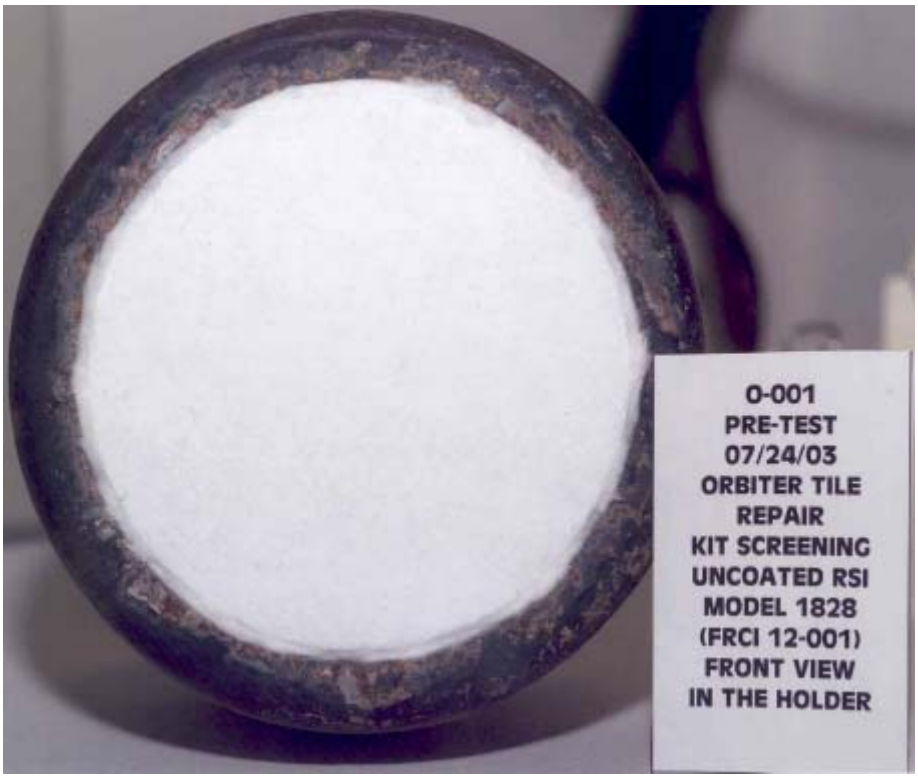

JSC2003E49554 – Model #1828, Pre-Test, Front View in Holder

JSC2003E51344 – Model #1828, Post-Test, Front Oblique View

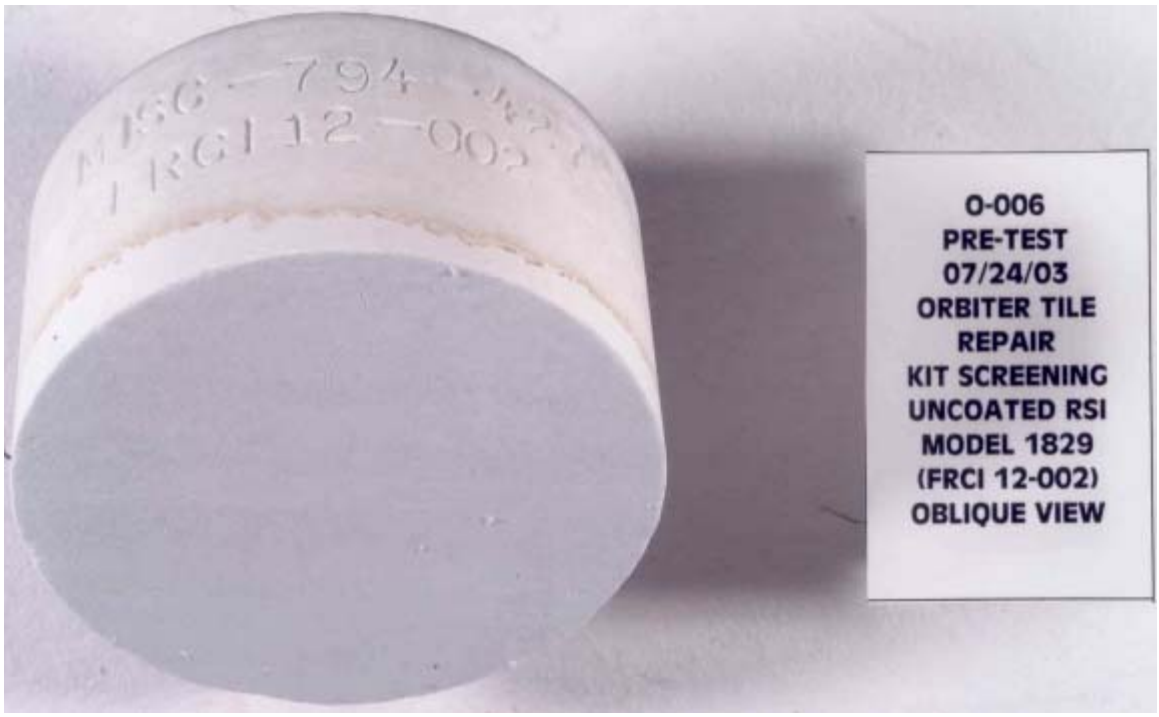

JSC2003E49558 – Model #1829, Pre-Test, Front Oblique View

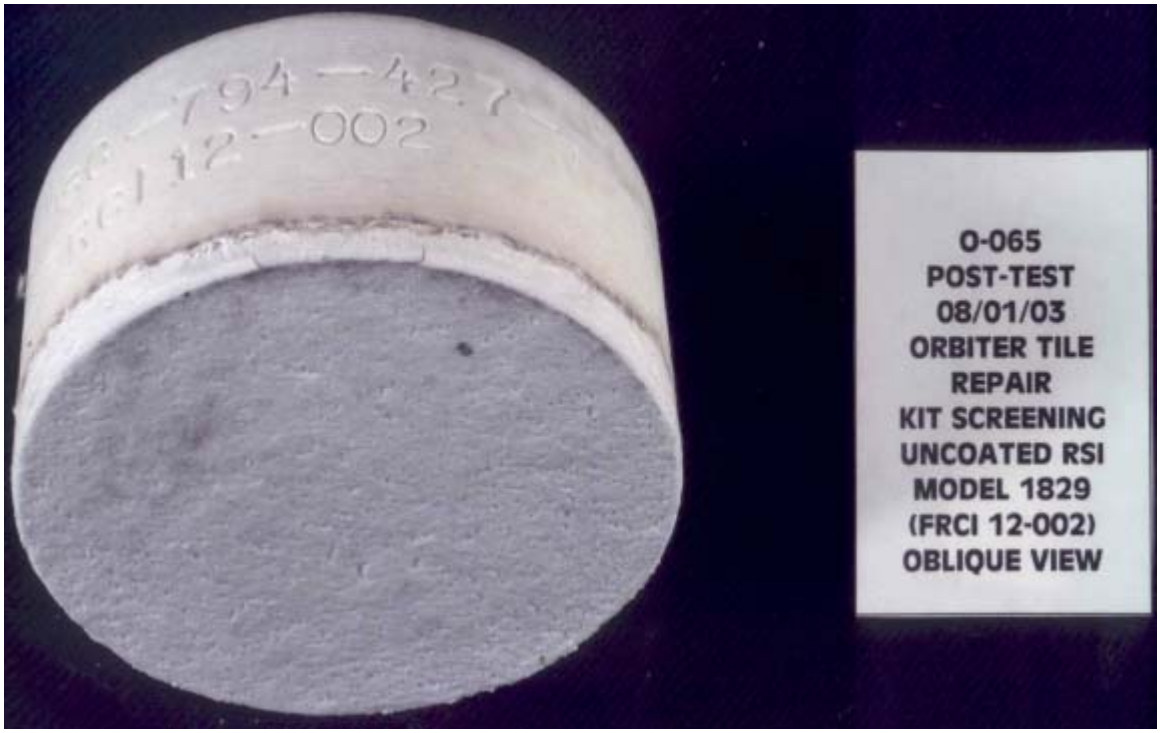

JSC2003E51352 – Model #1829, Post-Test, Front Oblique View

JSC2003E49559 – Model #1830, Pre-Test, Front Oblique View

JSC2003E54529 – Model #1830, Post-Test, Front View

PHOTO NOT AVAILABLE

Model #1833, Pre-Test

JSC2003E50261 – Model #1833, Post-Test, Front Oblique View

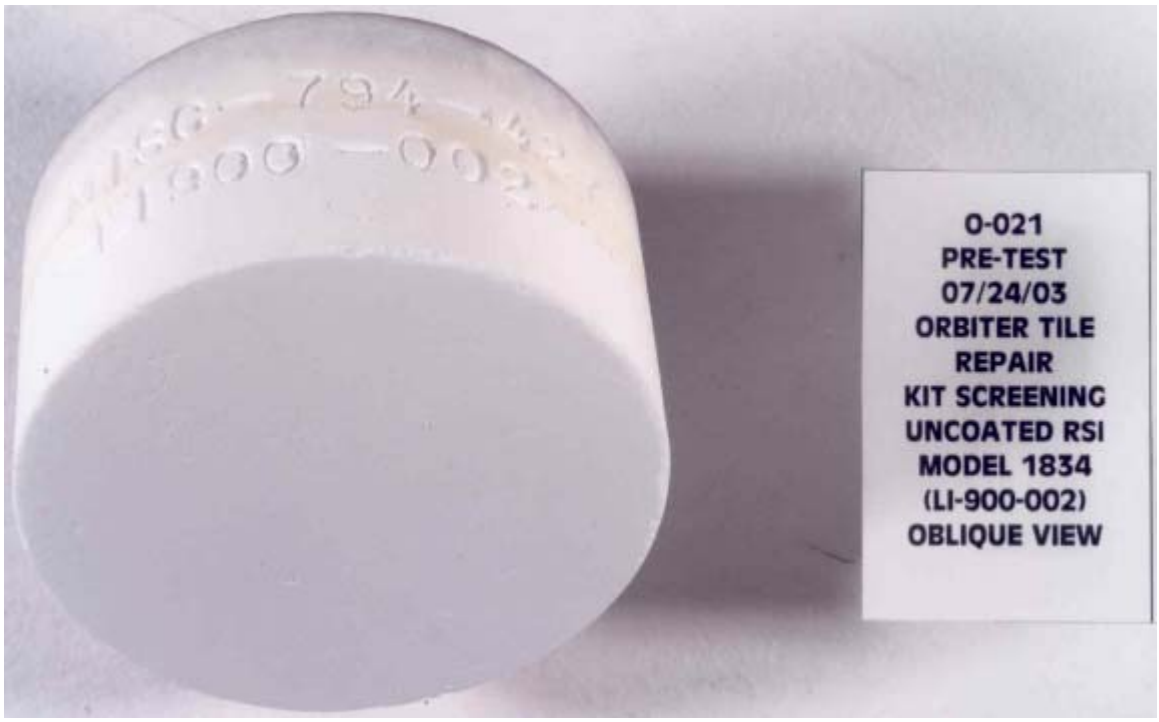

JSC2003E49570 – Model #1834, Pre-Test, Front Oblique View

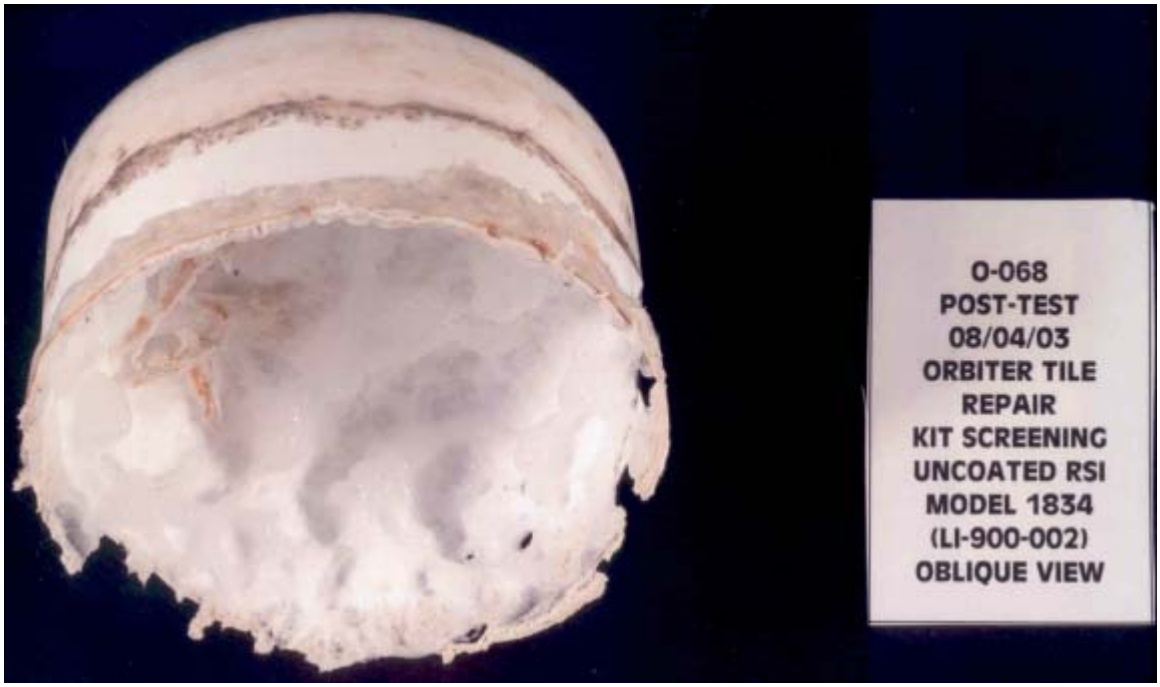

JSC2003E51533 – Model #1834, Post-Test, Front Oblique View

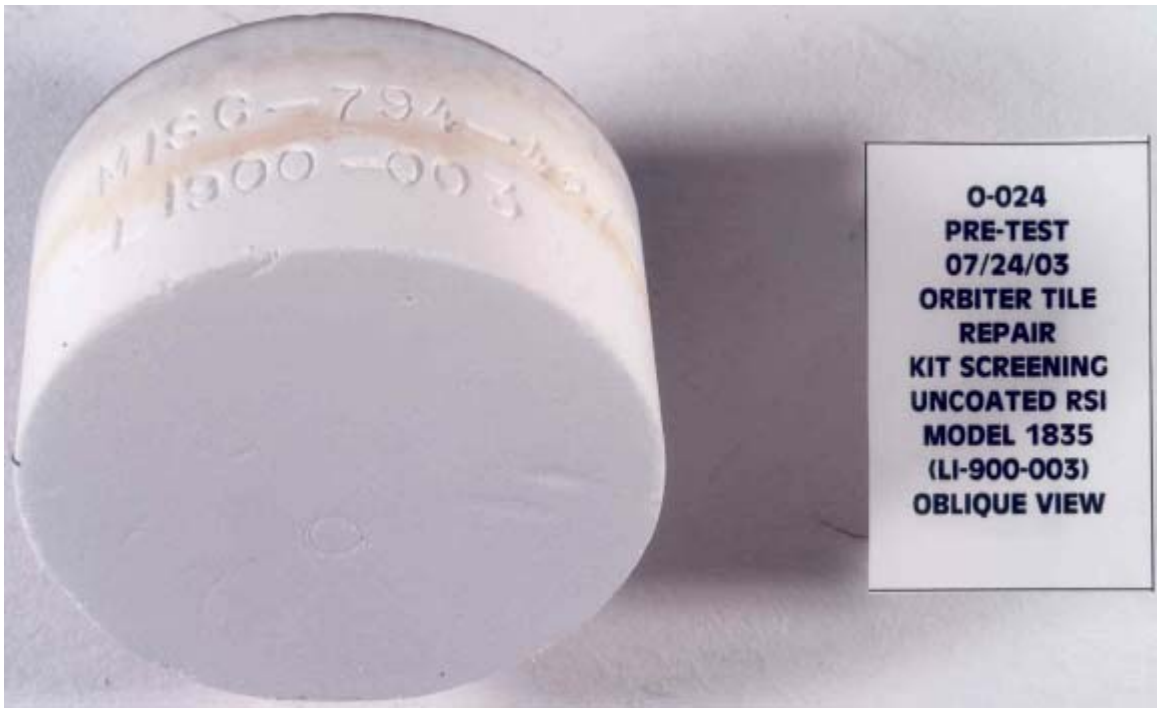

JSC2003E49571 – Model #1835, Pre-Test, Front Oblique View

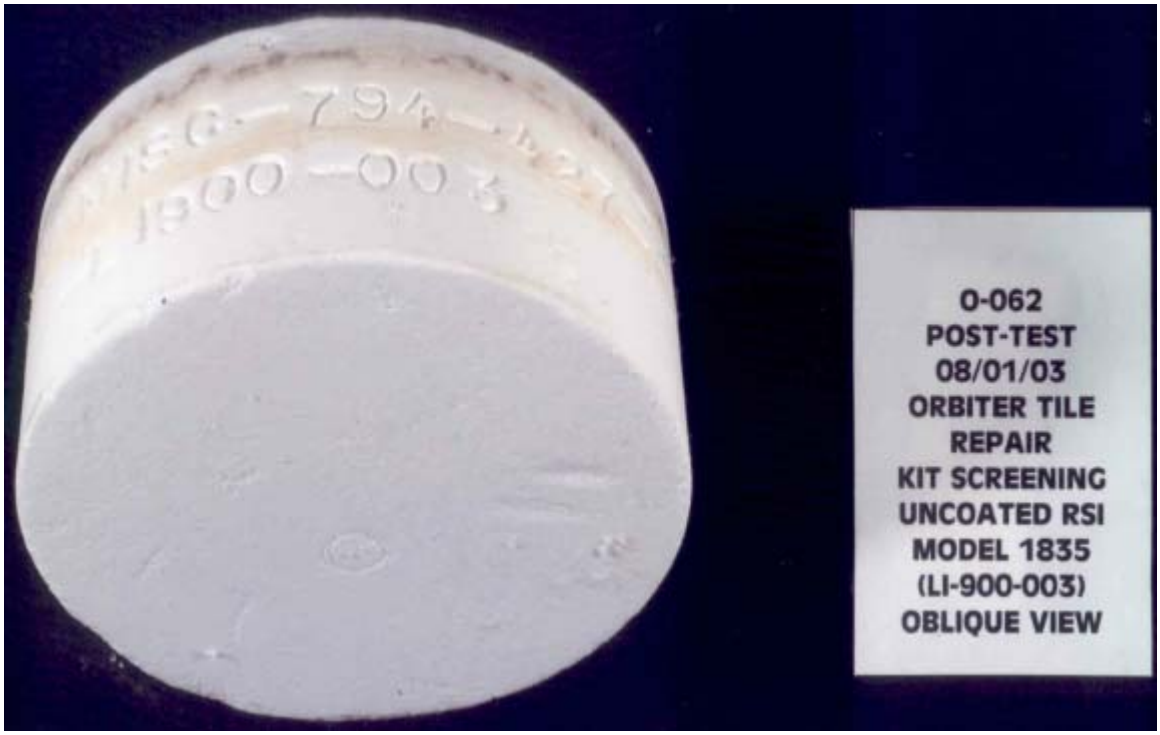

JSC2003E51343 – Model #1835, Post-Test, Front Oblique View

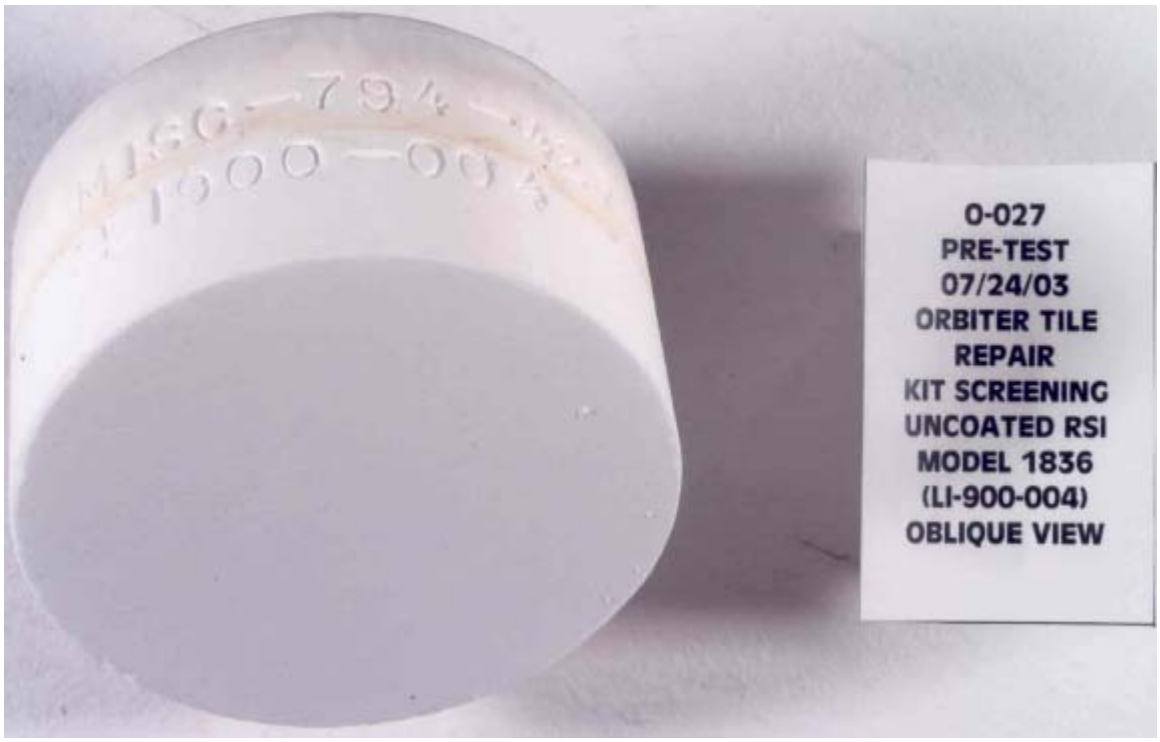

JSC2003E49574 – Model #1836, Pre-Test, Front Oblique View

JSC2003E54524 – Model #1836, Post-Test, Front Oblique View

JSC2003E49579 – Model #1837, Pre-Test, Front Oblique View

JSC2003E55041 – Model #1837, Post-Test, Front Oblique View

JSC2003E49555 – Model #1838, Pre-Test, Front View in Holder

JSC2003E50264 – Model #1838, Post-Test, Front Oblique View

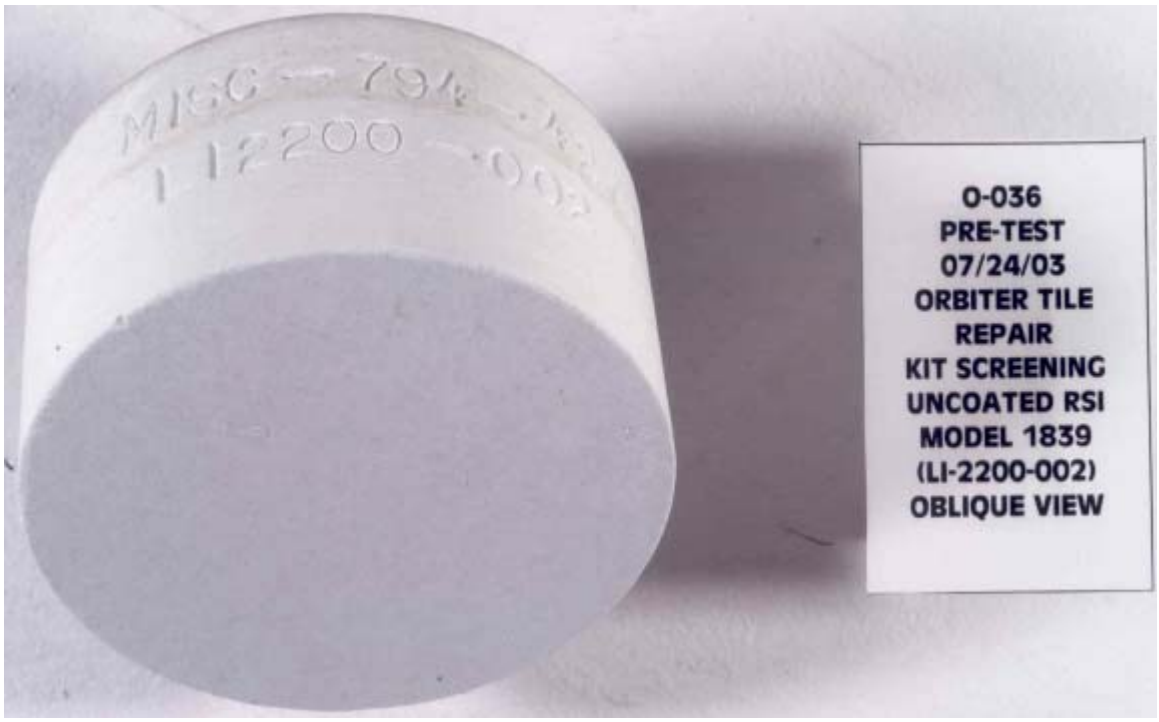

JSC2003E49580 – Model #1839, Pre-Test, Front Oblique View

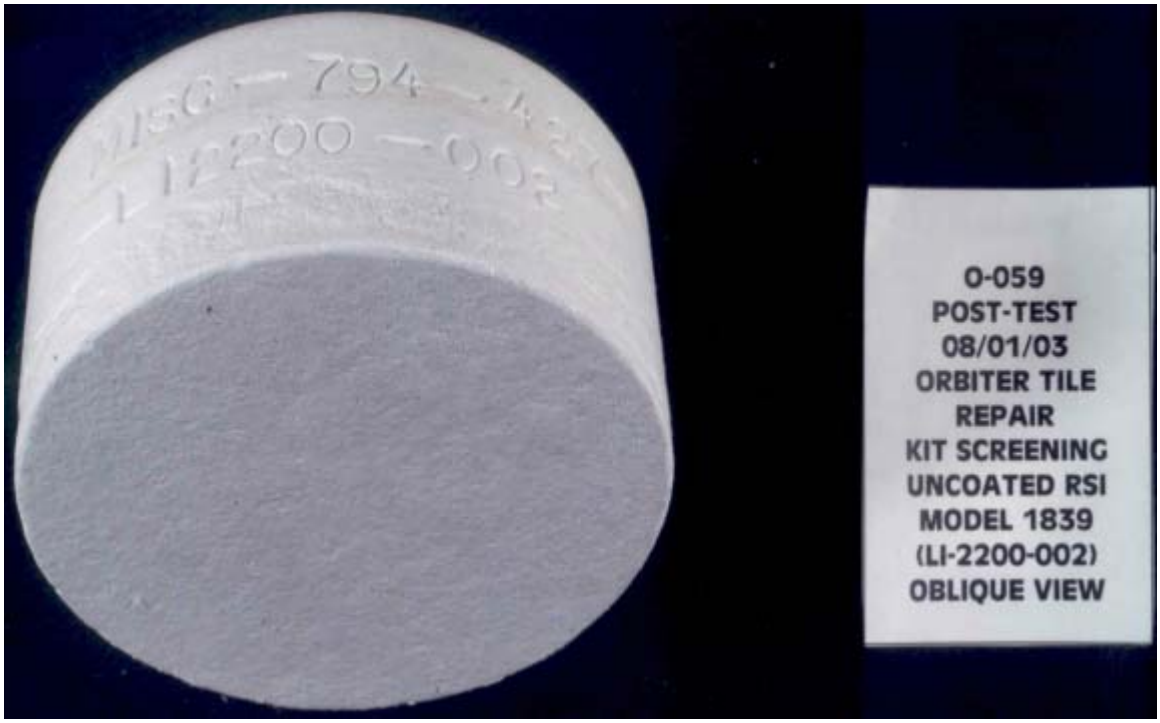

JSC2003E51349 – Model #1839, Post-Test, Front Oblique View

JSC2003E49585 – Model #1840, Pre-Test, Front Oblique View

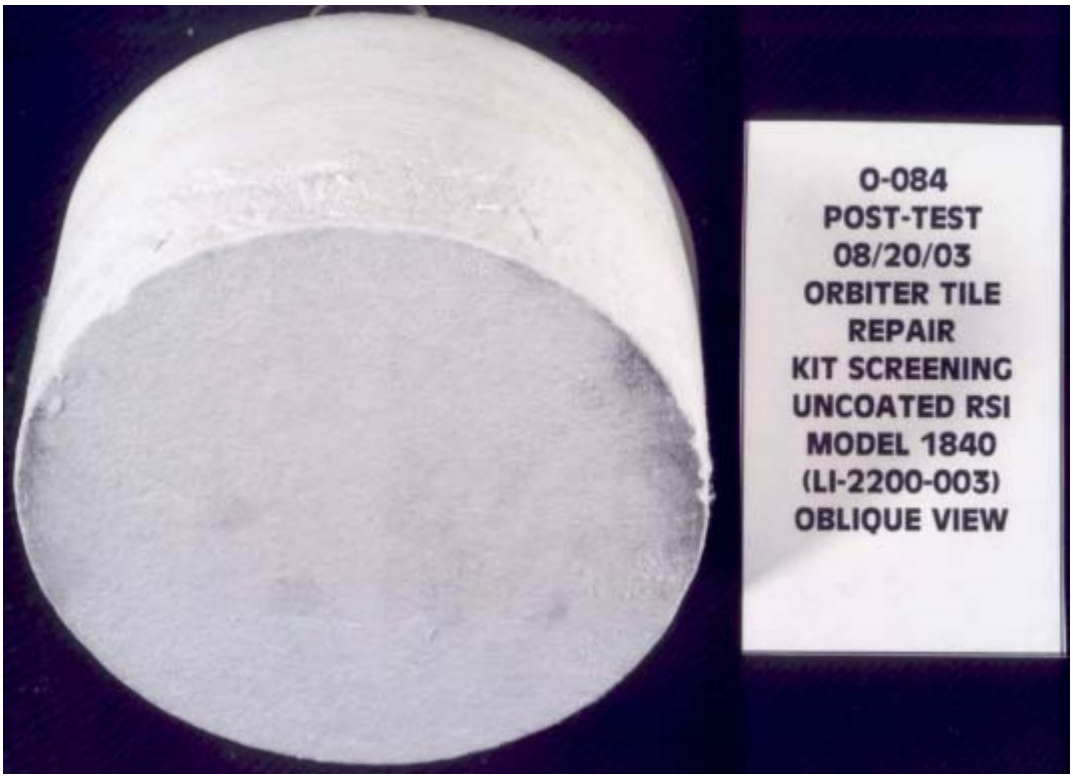

JSC2003E54531 – Model #1840, Post-Test, Front Oblique View

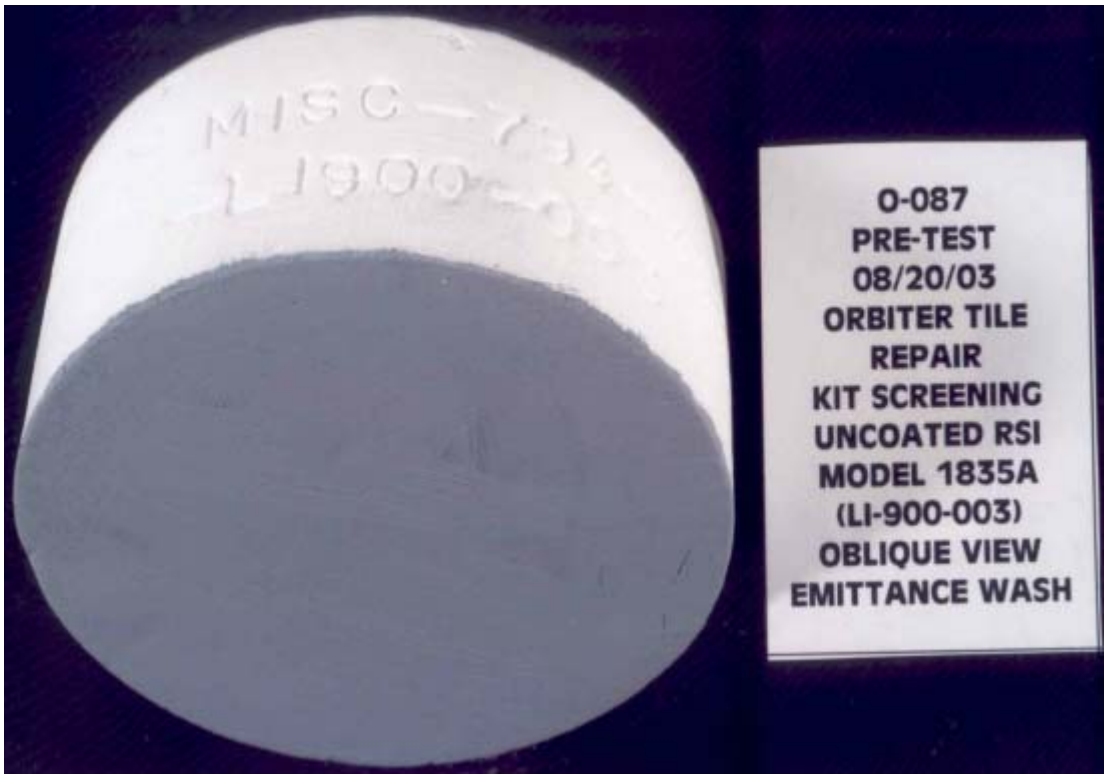

JSC2003E54536 – Model #1835A, Pre-Test, Front Oblique View

JSC2003E55046 – Model #1835A, Post-Test, Front Oblique View

APPENDIX D – BOUSLOG, S., "CATALYTIC EFFECTS ON HEATING TO A 5-INCH FLAT-FACED CYLINDER IN THE ARC-JET"

Introduction

Reaction Cured Glass (RCG) coated and uncoated LI-900 samples were tested as stagnation models in the NASA JSC arc-jet. The test samples were mounted into the front face of a water-cooled model holder that had a front-face diameter of 5.0 inches. A scanning radiometer was focused on the samples during the test with the intent to use the intensity measurements to obtain an emissivity of the samples. In analyzing the data from these tests, a question arose as to the potential difference in heating to the different samples even though they had been exposed to the same arc-jet conditions. The catalytic nature of the RCG coating is fairly well defined but the catalytic nature of the bare, uncoated LI-900 is unknown. Therefore, a short study was undertaken to obtain an estimate of the potential difference in heating associated with differences in the surface catalycity between the two materials.

Approach

The BLIMP code (Ref. 1) was chosen to compute the stagnation heat flux to the models in the arc-jet. BLIMP requires as input the freestream total enthalpy and the stagnation pressure acting on the model. The total enthalpy in the arc-jet plume core was estimated to be twice the bulk enthalpy measured for the arc-jet run. The stagnation pressure was computed using the NATA code (Ref. 2). The arc-jet mass flow rate and bulk enthalpy values were input into NATA and the conical nozzle geometry consistent with a 2.25-inch diameter throat and a 5-inch or 15-inch diameter nozzle-exit was used. The arc-jet test conditions for two test runs and the BLIMP inputs are provided in the following table:

Test Date	7/23/2003	8/20/2003
Run #	2-2551-3	2-2564-3
Throat Diameter (inches)	2.25	2.25
Nozzle Diameter (inches)	5	15
Z distance (inches)	15	20
Bulk Enthalpy (Btu/lbm)	2500	3520
Mass Flow (lbm/sec)	0.13	0.25
Current (amps)	220	500
BLIMP Inputs		
Total Enthalpy (Btu/lbm)	5000	7040
Model Stag. Pressure (psf)	40.2	24.8

The geometry inputs to BLIMP include the wetted surface distance, the streamline spreading metric, the pressure distribution, and the effective nose radius. These values were computed assuming that the nose effective radius was 3.3 times the cylindrical radius of 2.5 inches (0.6875 ft). The streamline spreading metric was based on an axisymmetric geometry and Newtonian pressures were used.

For each of the two test conditions, the BLIMP code was used to compute the stagnation point heat flux for three levels of surface catalycity – 1) fully catalytic; 2) non-catalytic; and 3) RCG catalycity. The ratio of the fully and non-catalytic heat flux to the RCG value was provided as output. The four-temperature range RCG catalycity model developed by Stewart (Ref. 3) was implemented into BLIMP for computation of the RCG heat fluxes. The fully and non-catalytic heat fluxes were obtained by setting the surface reaction rates in BLIMP to $1x10^{+6}$ and $1x10^{-6}$, respectively.

Results

Radiation equilibrium heat fluxes were computed using BLIMP for three surface catalycity assumptions and for two arc-jet test conditions. For the RCG and fully catalytic surfaces, a constant surface emissivity of 0.8 was assumed. For the non-catalytic computations, emittances of both 0.8 and 0.2 were used. The following table summarizes the computed radiation equilibrium stagnation point heat fluxes:

Radiation Equilibrium Heat Fluxes	**Test Run # 2-2551-3**	**Test Run # 2-2564-3**
Fully Catalytic Heat Flux (Btu/ft^2-sec)	30.7	35.3
RCG Catalytic Heat Flux (Btu/ft^2-sec)	19.3	16.5
Non-catalytic Heat Flux (Btu/ft^2-sec) (emittance=0.8)	12.8	11.3
Non-catalytic Heat Flux (Btu/ft^2-sec) (emittance=0.2)	11.0	9.8

In order to estimate the potential increase or decrease in the heat flux relative to a model with an RCG coating, heat flux ratios were computed and are summarized in the following table:

6.4 Heat Flux Ratios	**Test Run # 2-2551-3**	**Test Run # 2-2564-3**
$q_{NonCat}(e=0.8)/q_{RCG}$	0.663	0.685
$q_{NonCat}(e=0.2)/q_{RCG}$	0.570	0.594
$q_{FullCat}/q_{RCG}$	1.591	2.139

Conclusions

This analysis indicates that for this size model and these arc-jet test conditions, the stagnation point heat flux for a non-catalytic surface can be as low as 30 to 40% of the RCG-coated model heat flux. For a fully catalytic surface, the heating could be expected to be as much as 60 to 110% higher than the RCG value. Since the LI-900 intensity measurements indicate that the emittance of the bare LI-900 is closer to 0.2 and since it is believed that the LI-900 catalycity is closer to non-catalytic then fully catalytic, this study estimates that the heat flux to the bare LI-900 could be as much as 40% less than the heating to the RCG coated model.

References

1. Murray, A., “Further Enhancements of the BLIMP Computer Code and User’s Guide” AFWAL-TR-88-3010, June 1988.
2. Bade, W.L. and Yos, J.M., “The NATA Code – User’s Manual, Volume II,” NASA CR-141743, April 1976.
3. Stewart, D.A., “Surface Catalysis and Characterization of Proposed Candidate TPS for Access-to-Space Vehicles,” NASA TM 112206, July 1997.

BLIMP Input File
RCG Catalycity Case

```
 5-inch Flat Face in Arc-jet
$GR01
 KRI(1)=1,0,5,0,0,0,0,0,2,2,0,8,0,0,0,0,0,0,0,0,
$END
$GR02
 NSP=5, NS=10,
 KS(1)=1,1,1,1,1,1,1,1,1,1,1,1,1,1,1,1,1,1,1,1,
$END
$GR03
 NTIME=1,
 IDISC(1)=61*0,
  TIME(1)= -1.,
 S(1)=
 0.0,0.023998,0.059996,0.119991,0.179987,0.239983,0.359974,
 0.479966,0.599957,0.719948,
$END
$GR04
 NETA=13,
 KAPPA=11, CBAR=0.95,
 ETA(1)=0., 0.01, 0.04, 0.08, 0.12, 0.2, 0.32, 0.48, 0.8,
      1.4, 2.0, 3.2, 5.0,
 KONRFT=1,  NPOINT=5, RATLIM = 0.0,
 F2FIX(1)= 0., .05,.1,.15,.2,.3,.4,.5,.6,.8,.95,.99,1.0,
$END
$GR05
 rnose=0.6875,
 ROKAP(1)=
 0.0,0.023993,0.05992,0.119383,0.177938,0.235139,0.34375,0.441916,
 0.526656,0.595392,
$END
$GR07
  PTET(1)=  0.019,
  GE(1)=5000.,
 RADFL(1)=0.0,
$END
$GR09
 GW=567.,
SPFG(1)=.0001,
        .0001, .00001, .21,
$END
 5                                                                    500.
 7NITROGEN    14.008   -.765000
 8OXYGEN      16.0     -.235000
11NI-OXIDE    30.008   -1.00-10
10OXYGEN2     32.0     -1.00-10
 9NITROGEN2   28.016   -1.00-10
 1  7  0  0  0  0  0  0  0  0  0  0  0  0                              2 N
112899+6 134276+5 495056+1 143999-4 188481+3 480829+2   50. 3000.1   0.N
112899+6 134276+5 251170+1 562754-3 714438+7 480829+2 3000. 6000.1   0.N
 1  8  0  0  0  0  0  0  0  0  0  0  0  0                              3 O
595147+5 110486+5 547199+1-839628-3 281492+4 488399+2   50.  500.1   0.O
595147+5 135126+5 494018+1 158694-4 341909+5 500875+2  500. 3000.1   0.O
595147+5 135126+5 454603+1 127034-3 580070+6 500875+2 3000. 6000.1   0.O
 1 11           0  0  0  0  0  0  0  0  0JANAF TAPE 7/71  6/63       3 NO
215659+5 245632+5 654256+1 154125-2 105512+5 696340+2   50.  900.1   0.NO
215659+5 226834+5 866653+1 123447-3-676279+6 688280+2  900. 3000.1   0.NO
215659+5 226842+5 887804+1 556305-4-786411+6 688279+2 3000. 6000.1   0.NO
 1 10  0  0  0  0  0  0  0  0  0  0  0  0JANAF TAPE 7/71 **/61       3 O2
     0+0 254779+5 646891+1 179368-2 310933+4 687932+2   50.  500.1   0.O2
```

```
      0+0 234153+5 806128+1 502466-3-233580+6 679581+2  500. 3000.1   0.O2
      0+0 234103+5 850590+1 340796-3 139692+6 679444+2 3000. 6000.1   0.O2
  1  9  0  0  0  0  0  0  0  0  0  0  0JANAF TAPE 7/71 **/61       4 N2
      0+0 220436+5 664927+1 915790-3 226414+4 635833+2   50.  700.1   0.N2
      0+0 223977+5 759046+1 579254-3-343486+6 638454+2  700. 1800.1   0.N2
      0+0 221451+5 881533+1 602095-4-137243+7 637468+2 1800. 4000.1   0.N2
      0+0 221290+5 863699+1 838839-4-342376+5 637419+2 4000. 6000.1   0.N2
  1  7  1  8     0  0  0  0  0  0  0  0  0JANAF TAPE 7/71  6/63       3 NOS
 215659+5 245632+5 654256+1 154125-2 105512+5 696340+2   50.  900.1   0.NOS
 215659+5 226834+5 866653+1 123447-3-676279+6 688280+2  900. 3000.1   0.NOS
 215659+5 226842+5 887804+1 556305-4-786411+6 688279+2 3000. 6000.1   0.NOS
  2  8  0  0  0  0  0  0  0  0  0  0  0JANAF TAPE 7/71 **/61       3 O2S
      0+0 254779+5 646891+1 179368-2 310933+4 687932+2   50.  500.1   0.O2S
      0+0 234153+5 806128+1 502466-3-233580+6 679581+2  500. 3000.1   0.O2S
      0+0 234103+5 850590+1 340796-3 139692+6 679444+2 3000. 6000.1   0.O2S
  2  7  0  0  0  0  0  0  0  0  0  0  0JANAF TAPE 7/71 **/61       4 N2S
      0+0 220436+5 664927+1 915790-3 226414+4 635833+2   50.  700.1   0.N2S
      0+0 223977+5 759046+1 579254-3-343486+6 638454+2  700. 1800.1   0.N2S
      0+0 221451+5 881533+1 602095-4-137243+7 637468+2 1800. 4000.1   0.N2S
      0+0 221290+5 863699+1 838839-4-342376+5 637419+2 4000. 6000.1   0.N2S

  3  6
                          1.0  O       == 0.5 O2
 1.137E-01 -.5        794.4     502.
 3.638E-03 -.5       -2633.     978.
 1.182E+02 -.5       17546.    1617.
 8.870E-07 -.5      -42520.
                          1.0  N       == 0.5 N2
 1.215E-02  0.       0.0        465.
 4.861E-04 -.5      -2979.      905.
 2.431E+02 -.5      20575.     1575.
 1.507E-04 -.5      -24031.
                           2.0 NO      == 1.0 N2      1.0  O2
 1.000E-06  0.       0.0
             1.0  THBD    1.0  O2      == 2.0 O
N         NO        O         O2        N2
3.61      3.61      90.25     32.5      7.22
   1.00E18  -1.0    59400.0
             1.0  THBD    1.0  N2      == 2.0 N
O         O2        NO        N2
1.92      1.92      1.92      4.80
   1.00E17   -0.5   113100.0
             1.0  N2      1.0  N       == 3.0 N
   4.15E22  -1.5    113100.0
             1.0  THBD    1.0  NO      == 1.0 N       1.0  O
O2        N2        N         O         NO
3.97      3.97      79.4      79.4      79.4
   1.00E20  -1.5    76500.0
             1.0  NO      1.0  O       == 1.0 O2      1.0  N
   3.18E09  1.0     19700.0
             1.0  N2      1.0  O       == 1.0 NO      1.0  N
   6.75E13  0.0     37500.0

 $GR15
  PRE(1)=
  1.0,0.998782,0.992404,0.969846,0.933013,0.883022,0.75,0.586824,
  0.413176,0.25,
 $END
 $GR16
   TW(1)=10*2000.,
   ITW= 0,
   NEMISW=2,
   TEMISW(1)=0.,5000.,
```

```
  EMISW(1)=2*.80,
  QRAD(1)=100*0.,
  IITRS=1,
  IQRFLG=0,
  TTOL(1)=100*2.,
  CNR=.4,
  DELNR=.1,
  JPRTNR=1,
 $END
.
```

REPORT DOCUMENTATION PAGE

Form Approved
OMB No. 0704-0188

1. AGENCY USE ONLY *(Leave Blank)*	2. REPORT DATE	3. REPORT TYPE AND DATES COVERED
	April 2005	NASA Technical Paper

4. TITLE AND SUBTITLE
ARC JET SCREENING OF PHASE 1 ORBITER TILE REPAIR MATERIALS AND UNCOATED RSI HIGH TEMPERATURE EMITTANCE MEASUREMENTS

5. FUNDING NUMBERS

6. AUTHOR(S)
Steven V. Del Papa

7. PERFORMING ORGANIZATION NAME(S) AND ADDRESS(ES)
Lyndon B. Johnson Space Center
Houston, Texas 77058

8. PERFORMING ORGANIZATION REPORT NUMBERS
S-943

9. SPONSORING/MONITORING AGENCY NAME(S) AND ADDRESS(ES)
National Aeronautics and Space Administration
Washington, DC 20546-0001

10. SPONSORING/MONITORING AGENCY REPORT NUMBER
TP-2005-213150

11. SUPPLEMENTARY NOTES

12a. DISTRIBUTION/AVAILABILITY STATEMENT
Unclassified/Unlimited
Available from the NASA Center for AeroSpace Information (CASI)
7121 Standard
Hanover, MD 21076-1320 Subject Category 34

12b. DISTRIBUTION CODE

13. ABSTRACT *(Maximum 200 words)*

Arc jet tests of candidate tile repair materials and baseline Orbiter uncoated reusable surface insulation (RSI) were performed in the Johnson Space Center's (JSC) Atmospheric Reentry Materials and Structures Evaluation Facility (ARMSEF) from June 23, 2003, through August 19, 2003. These tests were performed to screen candidate tile repair materials by verifying the high temperature performance and determining the thermal stability. In addition, tests to determine the surface emissivity at high temperatures and the geometric shrinkage of bare RSI were performed. In addition, tests were performed to determine the surface emissivity at high temperatures and the geometric shrinkage of uncoated RSI.arc

14. SUBJECT TERMS	15. NUMBER OF PAGES	16. PRICE CODE
arc jet engines, atmospheric entry, structural analysis, tiles, silicon rectifiers, spacecraft maintenance, emissivity, thermal stability, shrinkage.	126	

17. SECURITY CLASSIFICATION OF REPORT	18. SECURITY CLASSIFICATION OF THIS PAGE	19. SECURITY CLASSIFICATION OF ABSTRACT	20. LIMITATION OF ABSTRACT
Unclassified	Unclassified	Unclassified	Unlimited